UNIVERSITY OF LONDON

IMPERIAL COLLEGE OF SCIENCE AND TECHNOLOGY

DEPARTMENT OF ELECTRICAL ENGINEERING

UNCHARACTERISTIC HARMONICS IN CONVERTERS AND THEIR MINIMIZATION THROUGH FIRING ANGLE MODULATION

by

FELIX ALBERTO FARRET

B.Sc., M.Sc.

Thesis submitted for the degree of

Doctor of Philosophy

in the Faculty of Engineering

London, July 1984

To my family,

to the Hilliard family

and to Geraldine

ABSTRACT

Converter instability due to feedback control of the direct current can be analysed through the Describing Function Technique (d.f.). A previously written off-line digital computer program to evaluate the d.f. of 6-pulse converters was extended to analyse also 12-pulse converters and to include the effects of transformer saturation. The d.f. was obtained from harmonic analysis of the total d.c.-side and total a.c.-side currents associated with a valve firing angle modulating signal (m.s.). The results from this program can be used to predict oscillations synchronized with the a.c. system voltage.

Such studies using d.f. techniques have shown that a m.s. applied to the control voltage has a profound effect on the d.c.- and a.c.-side uncharacteristic harmonic currents. These studies have also shown that presence of harmonic distortion in the a.c. busbar voltage causes distortion on the d.c. line current ripple and therefore affects the nature of the d.f. . One reason for such distortions is the valve assymmetrical firing pattern caused by the closed loop nature of constant current control. A second reason is that the d.c. current ripple is related to the a.c.-side harmonics even if no closed loop current control is prescribed.

A method of harmonic minimization based on approximate linear relationships between uncharacteristic harmonics and the m.s. was developed and implemented on a converter model.

A circuit to select, adjust and inject the m.s. into the control voltage connected to the output of the injection circuit

inhibits the m.s. injection during transients. This control feature is important because: a) it allows fast transient response of the control and b) it does not contribute to oscillatory behavior. A full set of analytical predictions and model tests using the injection circuit described above for m.s. of 50Hz, 100Hz and 150Hz are presented.

ACKNOWLEDGEMENTS

The work described in this thesis was carried out in the Electrical Engineering Department of the Imperial College of Science and Technology under the supervision of Dr L.L. Freris, M.Sc.(Eng.), Ph.D., D.I.C., MIEE, Reader in Electrical Engineering, whose encouragement, guidance and patience throughout the research are gratefully acknowledged.

The author would like to express his appreciation to his friends and colleagues of the Power System Laboratory with special mention of Dr. M. Shafik.

The author is grateful to the British Council for the financial support and to the Universidade Federal de Santa Maria for granting leave of absence to carry out the work.

Special thanks are due to Mrs. D. Abeysekera for typing this thesis and to Mrs. L. Modak for the drawings.

LIST OF ACRONYMS

d.f.	describing function
DFT	discrete Fourier transform
E.P.U.	error processing unit
i.p.c.	individual phase control
m.s.	modulating signal
PFC	pulse frequency control
PPC	pulse phase control
SCC	short circuit capacity
SCR	short circuit ratio
v.c.o.	voltage controlled oscillator

LIST OF SYMBOLS

a	pulse width
a_k	coefficient "k" of a polynomial representation
A	average cross-sectional area of transformer core
A_k	phase "a" harmonic amplitude of order "k"
A_0	Fourier d.c. component
B_i	magnetic flux density at instant "i"
B_k	phase "b" harmonic amplitude of order "k"
c	capacitance
c_0	d.c. line resonant capacitance
C_∞	d.c. line antiresonant capacitance
D	percentual harmonic distortion

LIST OF SYMBOLS

e_i	input voltage signal
e_0	output voltage signal
E_n	a.c. supply phase voltage
f_0	d.c. line input resonant frequency
f_∞	d.c. line input antiresonant frequency
G	controller transfer function
H	voltage transfer function
H_i	magnetic intensity at instant "i"
I_1	transformer primary current
I_2	transfer secondary current
i_{ak}	phase "a" current (harmonic order k)
I_{ak}	amplitude of phase "a" current
I_B	effective value of phase "B" current
i_{bk}	phase "b" current (harmonic order k)
I_{bk}	amplitude of phase "b" current
i_{ck}	phase "c" current (harmonic order k)
I_{ck}	amplitude of phase "c" current
I_{dc}	d.c. current
I_{dk}	d.c. line harmonic current of order "k"
I_R	effective value of phase "R" current
I_{ref}	reference d.c. current
I_Y	effective value of phase "Y" current
k	harmonic order
K	ramp slope of the sawtooth generator voltage
K_1	d.c. current transducer gain
K_2	E.P.U. gain
k'	resistance ratio
k"	capacitance ratio

LIST OF SYMBOLS

L	d.c. line + reactors total inductance
L_ℓ	d.c. line total inductance
L_n	smoothing reactor inductance
n	integer number
N	describing function (d.f.)
N_1	transformer primary number of turns
N_2	transformer secondary number of turns
n_ℓ	number of repetitive d.f. loops
p	number of pulses
P_{ac}	a.c. power
P_{dc}	d.c. transmitted power
q	integer number as a function of the harmonic order
R	resistance
R_1	frequency adjustment potentiometer
s	Laplace variable
T	steady state interfiring period
T_1	d.c. current transducer time constant
T_2	E.P.U. time constant
t_{OFF}	interval during which m.s. is not applied
V	nominal positive sequen e voltage
ΔV	imbalance voltage
V_0	offset level at the start of the voltage ramp
V_1	amplitude of the voltage pulses due to overlap angle
V_2	amplitude of the voltage pulses due to commutation jump of voltage
V_{ak}	a.c.-side harmonic voltage of order "k"
V_c	control voltage (steady state level)
ΔV_c	control voltage step change

LIST OF SYMBOLS

V_{co}	control voltage difference corresponding to a steady state interfiring period
V_{cl}	lower level voltage at the ramp reset instant
V_c'	control voltage before summing point
V_{dk}	d.c.-side harmonic voltage of order "k"
V_{ϕ}	phase voltage
V_{ℓ}	phase voltage difference of order "ℓ"
V_m	m.s. amplitude
v_{mk}	instant value of the m.s.
$\bar{V}_{mk}$	m.s. phasor of order "k"
V_{nm}	voltage difference between any two generic phases "m" and "n"
V_{sq}	square wave voltage amplitude
x	generic angle ordinate
X	input signal amplitude
x_i	generic ordinate of a point P_i
Y_1	output signal amplitude
Z	impedance
Z_{fn}	filter harmonic impedance of order "n"
Z_i	d.c.-line input impedance
Z_{ℓ}	ℓ-th harmonic impedance seen from the rectifier terminals
Z_n	Norton's equivalent harmonic impedance of the a.c. system

LIST OF GREEK LETTERS

α	firing angle
α_{max}	maximum firing angle
α_{min}	minimum firing angle
$\Delta\alpha$	firing angle variation
$\Delta\theta$	phase imbalance
ϕ	m.s. phase
ϕ_a	phase "a" angle
ϕ_{ac}	a.c. magnetic flux
ϕ_c	phase "c" angle
ϕ_d	difference phase
ϕ_{dc}	d.c. magnetic flux
ϕ_i	core flux at instant "i"
ϕ_ℓ	phase angle of phasor $\bar{V}_\ell$
ϕ_s	sum phase
μ	commutating angle
ζ	filter damping factor
θ	phase angle ($=\omega_0 t$)
θ_1	secondary phase shift due to shifted currents
θ_2	secondary-to-primary phase shift
ω	angular frequency
ω_0	fundamental angular frequency

TABLE OF CONTENTS

CHAPTER 1

INTRODUCTION

1.1 General

The direct current control feedback system used at present in h.v.d.c. converters could be the cause of oscillations which may or may not be synchronized to the a.c. system frequency[1]. Synchronized oscillations result from a.c. system imperfections magnified by the feedback nature of the d.c. current loop. As a consequence, firing pulse variations occurs which in return cause magnification of the related a.c.-side and d.c.-side harmonics (1 to 6).

Power systems are intended to supply the consumers an acceptable sinusoidal voltage. Ideally, the voltage should be perfectly sinusoidal of constant amplitude and frequency. In practice, non-linear loads on the system cause various deviations from the ideal, notably on the waveform. Such distortions occur mainly at the "non-linear consumer" terminals due to harmonic voltage drops in the source impedance. Other consumers in the vicinity of the non-linear load may also be adversely affected.

A distorted current or voltage waveform can be represented under steady-state operation as a sum of a fundamental and a set of harmonic components. In power systems, opening or closure of linear or non-linear loads, cause often changes in the operating conditions, so that the harmonic analysis becomes restricted to conditions which should persist for a reasonable length of time [5]. Among the

causes of harmonic generation are:

1) Transformer saturation or loads containing saturated iron cores;
2) Rectifying loads;
3) A.c. regulators.

Iron saturation causes large components of third and fifth harmonics[27,28]. Rectifying loads contain a large second and fourth harmonic component and even harmonics in general [9,14,37,53].

Harmonic voltages may reach high levels if the harmonic currents pass through a parallel or series resonant circuit. Such harmonic magnifications may happen anywhere in the system depending on the network parameters [13,53].

Harmonic distortion have undesirable consequences such as:

a) reduction of the life of power capacitors due to an increased current through the capacitors;
b) maloperation of protective devices [35,45];
c) extra losses in a.c. motors [46];
d) maloperation of electronic equipment based on the voltage or current crossover of the supply voltage;
e) interference in telephone system [2,15];
f) misleading readings of kWh meters.

Due to the seriousness of the problem, national and international recommendations have been established that indicate the permissible levels of harmonic injection by consumers [40,50,54].

When non-linear loads likely to inject large levels of harmonic currents are installed, filters tuned to the "characteristic" harmonic frequencies are invariably installed as well. However, because of system imperfections uncharacteristic harmonics are also likely to be generated for which filters are not usually provided. Because of this, uncharacteristic harmonic generation could be a serious problem in terms of a.c. voltage distortion and possible converter instability.

1.2 Converter stability and uncharacteristic harmonics - review of literature

Hunting of a rectifier supplying a converter through a transmission line under constant current control was first dealt by Busemann[29] who, in 1948, under some restrictive assumptions found that hunting occurred at half the firing frequency. A formula was derived for the critical equivalent resistance of the rectifier under current control leading to instability.

Bjaresten[30] and Fallside[31,32] modelled the rectifier as a pure sampler and were able to derive respectively a closed form and an infinite series for the critical gain of the closed-loop system leading to instability at half the firing frequency. Fallside used the describing function to extend the instability studies for large disturbances at other subharmonics of the firing frequency using zero commutation angle and an infinite a.c.-busbar.

With the exception of Busemann, the other researchers

viewed the controlled rectifier as a fast static amplifier rather than the main piece of equipment for h.v.d.c. transmission.

Representation of the converter for stability studies, involves important details such as the non-zero commutation time, the non-zero a.c. network impedance and the non infinite d.c.-line reactor (1,38,39,55).

Sucena Paiva and Freris[34] developed a linearized discrete model of the converter to represent the intermitent control action of a converter with a finite commutation angle and infinite busbar. The stability boundaries predicted by the model which used the Z-transform method of analysis, were successfully confirmed on a h.v.d.c. simulator. For high cut-off frequency of the control loop, this model predicts harmonic instability at half the firing frequency and fails to predict low frequency oscillations unrelated to the firing frequency when the control cut-off frequency is low. These non synchronized frequencies may be developed under certain conditions and be sustained at values of the loop gain less then the critical value due to the non-linear properties of the converter, and therefore cannot be predicted by a linearized model[1]. Simulator tests using infinite busbar showed that other modes of harmonic instability not predicted by the linearized model may also happen.

A more detailed representation of the converter is then necessary to represent the a.c. busbar voltage as a dependent variable. Parallel resonances and antiresonances may occur due to the high quality factor of the filters connected to the converter busbar and certain frequencies will be reduced or magnified according to the harmonic impedance value encountered by the corresponding harmonic currents[1,3].

Interaction between a.c.- and d.c.-side quantities and modulation and demodulation converter processes are other important aspects of harmonic interaction [5,6,48,51].

Sucena Paiva and Freris [7,34,36] used sinusoidal carrier functions as an approximation of the full computational requirements to calculate the transfer function of a converter taking into account the effect of filter plus a.c. system impedance. Using this method, only the onset of instability can be predicted since frequency domain techniques are used with linearized models.

The decribing function was also used by Sakurai et al [56] to analyse a particular mode of harmonic instability detected on the Shin-Shinano frequency converter. A fundamental frequency oscillation on the d.c.-side and a second harmonic in the a.c.-side were observed. This mode is likely to occur under d.c.-side resonance near to the fundamental frequency under a combined a.c.-side antiresonance between the 2nd and 3rd harmonic.

Jotten et al [49] studying the influence of resonances on the d.c.-side and anti-resonances on the a.c.-side on the current controller, concluded that if the d.c. resonance and a.c. anti-resonance frequencies are related by the modulating process controlled-loop, instability may occur with high gain and wide bandwidth controllers. The resulting oscillation would be close to one of the lowest harmonic orders.

Ferreira [1] developed a converter model capable of predicting oscillations synchronized with the a.c. system voltage for 6-pulse converters. The Describing Function (d.f.) technique was used to evaluate the frequency response of the current control loop. An off-line digital computer program was developed to perform the harmonic analysis of the a.c.- and d.c.-side currents. The resulting

d.f. locus together with the frequency response of the linear elements of the control loop were used to predict oscillations synchronized with the a.c. system voltage. Extensive number of test results on a h.v.d.c. simulator were compared with the theoretical predictions and a satisfactory accuracy was obtained in nearly all cases. Transformer saturation and 12-pulse operation were not dealt in Ferreira's work.

1.3 Harmonics in h.v.d.c. converters - review of literature

Low commutating reactance with respect to the d.c. smoothing reactance, makes the converter act as a source of harmonic current from the a.c. point of view and as a source of harmonic voltage from the d.c. point of view. Reduction of some of these harmonics at the converter busbar may be achieved through a) increased number of pulses, b) harmonic filters and c) harmonic injection.

The pulse number is determined by the number of phases available at the secondary of the converter transformer. For a balanced steady-state condition, the a.c.-side harmonics are of order "qp±1" (characteristic harmonics) where "q" is an integer and "p" is the pulse number whilst d.c.-side characteristic harmonics are of order "qp". In h.v.d.c. the pulse number is limited to 12 by a) problems of insulating the transformers to withstand the higher alternating voltages combined with the high direct voltages (2,9); b)economical costs (2); c) presence of abnormal harmonics (6) and d) complexity of the circuitry.

Harmonic filters connected to the a.c. system have in general two functions: 1)harmonic minimization and 2) provision of reactive power.

Filters may be connected either on the primary or on the tertiary winding of the converter transformer but not normally on the secondary. The connection may be series or parallel. A series filter carries the full current from the source and must be throughout insulated to ground for full voltage. A shunt filter is usually grounded at one end and carries only the tuned harmonic current and partially some fundamental current. Therefore, shunt filters are cheaper than series filters and have the advantage of supplying reactive power rather than consuming it as in the case of series filters.

Filters in h.v.d.c. are in general of three types :

1) Single tuned filter
2) Double tuned filter
3) Highpass damped filter

Tuned filters (high Q) are sharply tuned to one or two of the lower characteristic frequencies, e.g. the fifth and seventh. The highpass filters (low Q), if shunt connected, offer a low impedance over a wide range of frequencies above certain order, e.g. the seventeenth [2].

In 12-pulse converters, the filtering system may be simplified either by using a single filter of the damped type for 2 pairs of characteristic harmonics, e.g. the 11-th and the 13-th, or for harmonics above a certain order which usually is the 12-th. The quality factor, Q, for the first case ranges between 20 to 50 while the second case has a much lower Q(2 to 4) [15,40,52].

On the d.c.-side, the basic filtering principle is similar to that of the a.c.-side[14]. But component ratings are considerably different since the harmonic current is largely reduced by the d.c. smoothing reactor and the capacitor bank usually has to fully withstand the d.c-side voltage.

Increased pulse number or filtering are costly methods of harmonic minimization and are used to minimize only characteristic harmonics.

Several methods of harmonic injection are presented in the literature to minimize harmonics. These methods can be broadly classified into three groups:

1) a.c.-side harmonic injection
2) d.c.-side harmonic injection
3) control injection

1.3.1 a.c.-side harmonic injection

On the a.c.-side, a method of magnetic flux compensation is proposed by Sasaki[16]. A current transformer is used to detect the harmonic components from the non-linear load and these are fed through a pulse amplifier into the tertiary winding of a transformer in such a way as to cause cancellation of the harmonic currents. Practicability and cost seem to be the strongest objection to this method. The system involves the amplifier output coupling to the

tertiary winding of the converter transformer to prevent the fundamental current from damaging the amplifier and a rather critical transformer connection becomes necessary. For harmonics of lower orders, very high power amplifiers become necessary with a consequent increase in costs. A positive point of this scheme is its ability to minimize uncharacteristic harmonics such as the third and ninth.

Another harmonic injection method is proposed by Bird [17] and later developed by Ametani[18]. The method is based on the use of the triplen harmonics from an external source which are added to the line current rectangular blocks of current . The main advantage of this system over filtering is that the system impedance is not part of the injection circuit impedance which can then be independently designed. The disadvantages are a) ineffective dissipation of the triplen harmonic power; b) difficulties in adjusting the amplitude and phase of the injected harmonic to suit each practical operating condition; c) compensates only one harmonic at a time; d) needs a triplen harmonic generator with the necessary locking to the a.c.-side voltage.

Several papers[12,20,21,23,26,43] present different arrangements of sequentially switched RLC circuits using SCR's to generate pulses of current to compenate the reactive and distortive components of the converter current. Therefore, the reactive power becomes controllable and the selected harmonics, minimized. An optimal equipment design can reduce the harmonic level while compensating reactive power[24,25]. Mechanical switching of a capacitor bank may introduce transients owing to the inaccurate timing of the contact closure.

1.3.2 d.c.-side harmonic injection

On the d.c.-side, the d.c. voltage ripple can be used as a source of harmonics to be injected back into d.c.-side[19]. The principle is based on the same phase relationship that each d.c. pole has with respect to the common mode d.c. ripple voltage. The period of this frequency is 1/3T, i.e. a triplen frequency voltage. Therefore, the transformer must be star-connected on the rectifier side and must have either a delta primary or tertiary winding. The primary winding of a single-phase transformer is connected to the common mode d.c. ripple voltage. This transformer provides the commutating voltage for a fullwave rectifier connected to the secondary winding (called "feedback converter") whose output is connected in series with the d.c. output. The result is that the original 6-pulse converter configuration has been converted into a 12-pulse converter system seen from the a.c./d.c. harmonic point of view. This arrangement seems to be efficient with respect to harmonic reduction point of view but the high ratings of this additional h.v. equipment makes such arrangement very costly.

Mahmoud et al[22] use a re-injection of the d.c. voltage ripple to modify the current waveforms through the d.c.-side transformer winding by adjusting the injection magnitude and frequency. This method seems suitable for 3rd harmonic suppression.

The difficulties related to the implementation of the harmonic minimization methods so far presented in the literature are:

a) high costs;

b) purpose designed h.v. equipment;

c) major modifications in h.v. equipment.

1.3.3 Control injection

Ferreira[1] suggests a d.c.-side harmonic minimization controller to be used in conjunction with microcomputers. To obtain the control voltage frequency spectrum, a Discrete Fourier Transform (DFT) is suggested from which an auxiliary signal could be selected. Ferreira's suggestion is based on open-loop tests using a signal generator as source of the auxiliary signal whose adjustment of frequency, amplitude and phase depends on the influence upon a) the control voltage or b) the d.c.-side harmonics.

1.4 Objectives of this Thesis

1) Generalization of a computer program to obtain 6- and 12-pulse converter describing functions;
2) Analytical studies of uncharacteristic harmonics related to control voltage modulation;
3) Development and implementation of a new harmonic minimization method based on control voltage modulation.

1.5 Organization of the chapters

A general literature review about converter stability and

harmonic minimization is presented in Chapter 1.

A computer program to obtain 6- and 12-pulse converter describing functions is described in Chapter 2. Comparison between 6- and 12-pulse converter describing functions are presented for the most relevant cases. Transformer saturation effects are also taken into consideration and numerous examples showing the differences between describing function with and without transformer saturation are presented.

In Chapter 3, the derivation of approximate relationships between modelling signal and uncharacteristic harmonics, is made. An approximate proportionality between small amplitude of those two quantities is established by using sinusoidal modulating signals imposed on the control voltage.

The circuitry to inject modulating signals into the control voltage of the IC-h.v.d.c. simulator is fully described in Chapter 4 with several examples of application. In Chapter 5, a harmonic minimization method based on control voltage modulation is described. Furthermore, practical and theoretical tests are shown to confirm the predictions established in Chapter 3.

A summary of the relevant conclusions of each chapter is presented in Chapter 6 with a list of the original contributions contained in this thesis and suggestions for further development in the field.

CHAPTER 2

CONTROL VOLTAGE MODULATION AND CONVERTER STABILITY

2.1 Introduction

A number of different quantities may be controlled in h.v.d.c. converters. In practice, the direct current and the extinction angle are most frequently the parameters under control.

Usually, h.v.d.c. transmission systems operate with constant current (CC) control in the rectifier side and constant extinction angle (CEA) in the inverter side. Such control functions are performed through the firing control system and involve :

1) measurement of the controlled quantity
2) comparison with a reference value
3) processing of the error
4) modification of the ignition angle to reduce the error.

Appropriate error processing and modification of the ignition angle play a key role in the stability of converters under closed-loop control.

Operation under constant current control can be detrimental with respect to abnormal harmonic generation mainly because the d.c. current ripple is fed back into the controller. Such ripple although filtered, may be sufficient to cause firing angle irregularity and precipitate harmonic magnification.

In reference (1), the describing function technique (d.f.) is proposed to determine the conditions of occurrence of harmonic instability

for 6-pulse converters. The d.f. is evaluated by a computer program based on a steady-state non-linear model of the converter valid for large perturbations. In the program, the control voltage is modulated by a signal of a selected frequency and the component of same frequency present in the direct current is calculated. The complex ratio between the two quantities yields the describing function.

This chapter deals with converter stability under control voltage modulation. Basically, the d.f. studies for a 6-pulse converter presented in reference (1), are extended to cover 12-pulse converters and transformer saturation. However, as an introduction to the d.f. method, a brief revision of firing systems used in h.v.d.c. converters is first presented. In Chapter 3, an approximate expression of the d.f. as well as some approximate theoretical expressions of the uncharacteristic harmonics caused by control voltage modulation are described.

2.2 Firing system

The firing system provides the pulses necessary to initiate conduction of the valves so that the chosen quantity is regulated, e.g. d.c. current. Firing systems vary widely but can be classified into two general categories

1) Individual phase control (i.p.c.)
2) Equally spaced firing pulses using a voltage controlled oscillator (v.c.o.)

2.2.1 Individual phase control

In this firing system, the zero crossing points of the commutating voltages are determined and a delay, α, is added in order to determine the firing pulse instants.

The instant at which the valve starts conducting in such systems, depends critically on the a.c. network voltages. Disturbances in the firing angle or in the d.c. current produce a.c. current variations which through the a.c. system impedance result in voltage distortions at the converter busbar. These distortions, in turn, affect the firing pulses. In general, instability occurs at frequencies which are multiples of the a.c. system fundamental frequency, resulting in a stationary distortion of the voltage waveforms. This type of firing system suffers from marked disadvantage mainly when the a.c. system short-circuit ratio, SCR (as defined in Appendix A), is low and for this reason is not used in recent h.v.d.c. systems.

2.2.2 Equally Spaced Firing Pulses

This system is based on a voltage controlled oscillator (v.c.o.) which produces equally spaced firing pulses, irrespective of imbalances and distortions on the a.c. supply voltage. In steady-state, the pulses are accurately spaced by 60^{o} and each pulse occurs within a range defined between α_{min} and α_{max}. Therefore, the frequency of the firing pulses in steady-state must be an exact multiple of the a.c. supply.

Since, for h.v.d.c. the individual phase control has been abandoned, only v.c.o. based systems are considered in the next sections.

2.3 Types of control systems

2.3.1 Pulse Frequency Control (PFC)

In principle a voltage controlled oscillator converts an input d.c. voltage into a train of pulses whose frequency is proportional to the input. A change in the phase of the firing pulses causes however a change on the d.c. current a fact which is used to control this current. A change in phase can be achieved by changing transiently the frequency of the oscillator and making it return to the steady-state value after the desired d.c. current level has been achieved. This is known as Pulse Frequency Control and it is represented in Fig. 2.1.

In analogue controllers the sawtooth generator represented in figure 2.1(a) is an integrator while in microcomputer based controller the sawtooth generator is a counter. Whenever the control voltage, V_c, equals the ramp voltage from the sawtooth generator a pulse is produced at the output of a monostable. The monostable output shifts the firing ring counter and at the same time resets the sawtooth generator voltage to zero.

A step change in the control voltage, V_c, (Figs 2.1(b) and (c)) will result in a continuous frequency change of the firing pulses and cumulatively increasing phase angle [6]. The interfiring period is proportional to the control voltage :

$$T_o = \frac{V_c}{K\omega_0}$$

where K is the slope of the ramp voltage from the sawtooth generator.

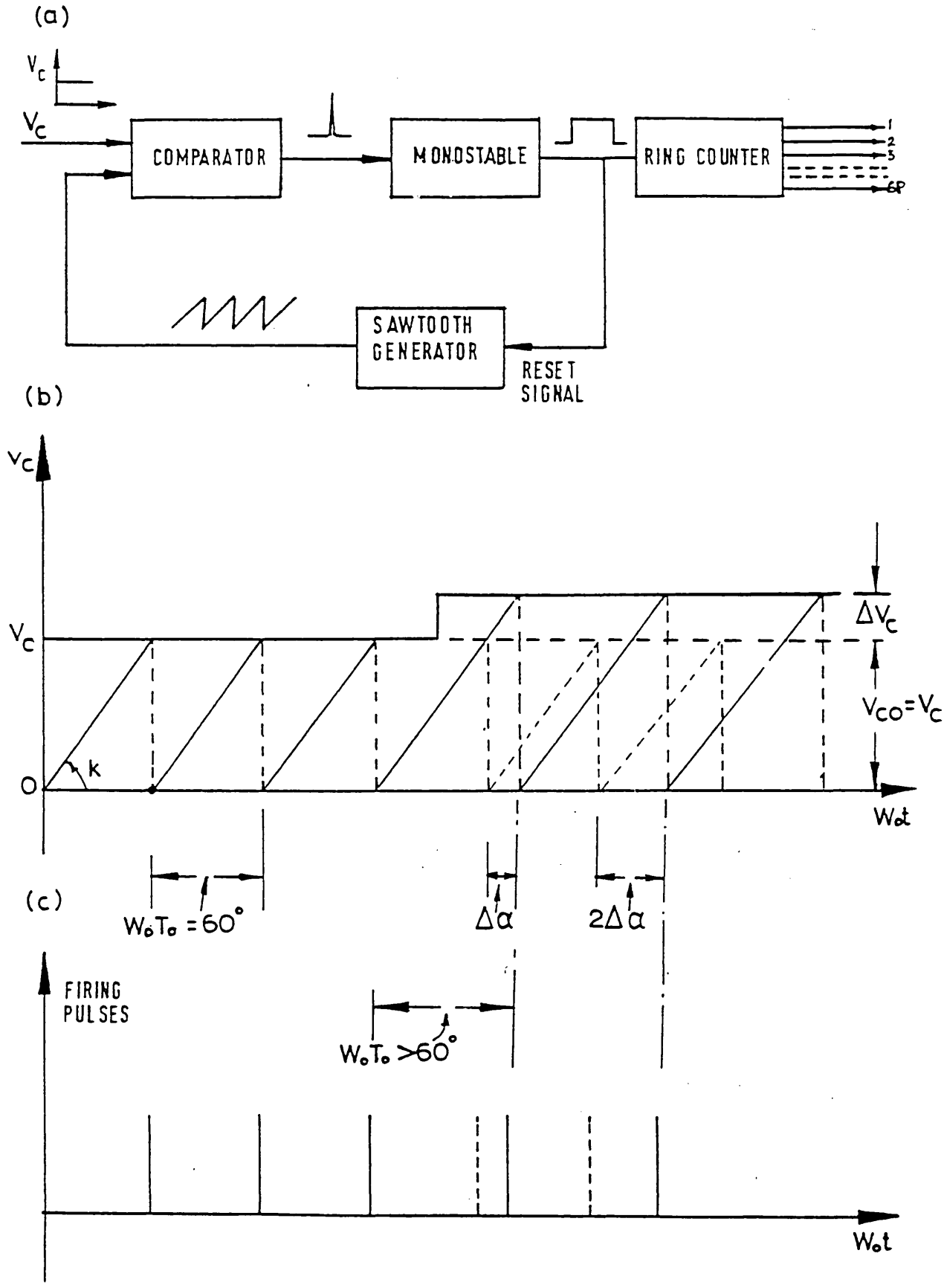

Fig. 2.1 - PULSE FREQUENCY CONTROL (PFC)

(a) Functional Block Diagram
(b) Comparator Inputs
(c) Firing Pulse Instants

As long as the control voltage remains at a steady level, equidistant firing pulses are generated. A step increase or decrease, ΔV_c, on the control voltage, will produce a corresponding change, $K\Delta V_c$, in the interfiring period and the firing pulse phase will change linearly with time. After "n" firing pulses since the beginning of the step change, the total firing pulse phase is :

$$\Delta\alpha_n = n\ K\Delta V_c \quad .$$

An integral relationship, therefore, exists between firing pulse phase and control voltage. Synchronization of the firing pulses with the a.c. system can be implemented through a measurement of d.c. current, firing angle or extinction angle, depending on the chosen converter control mode.

2.3.2 Pulse Phase Control (P.P.C.)

In this type of control the firing pulse train phase rather than its frequency is modified and the firing angle is proportional to the control voltage.

One way of achieving this phase change is by controlling the voltage level at the beginning and the end of the ramp voltage, V_{c1}, as in Fig. 2.2. Here, the ramp voltage of the sawtooth generator is not reset to zero but to V_{c1}. In analogue controllers, V_{c1} is stored as a a capacitor charge immediately after each firing pulse.

As V_{co} is a constant, any increase in V_c by a small amount, ΔV_c, will produce an identical increase in V_{c1}. As a consequence,

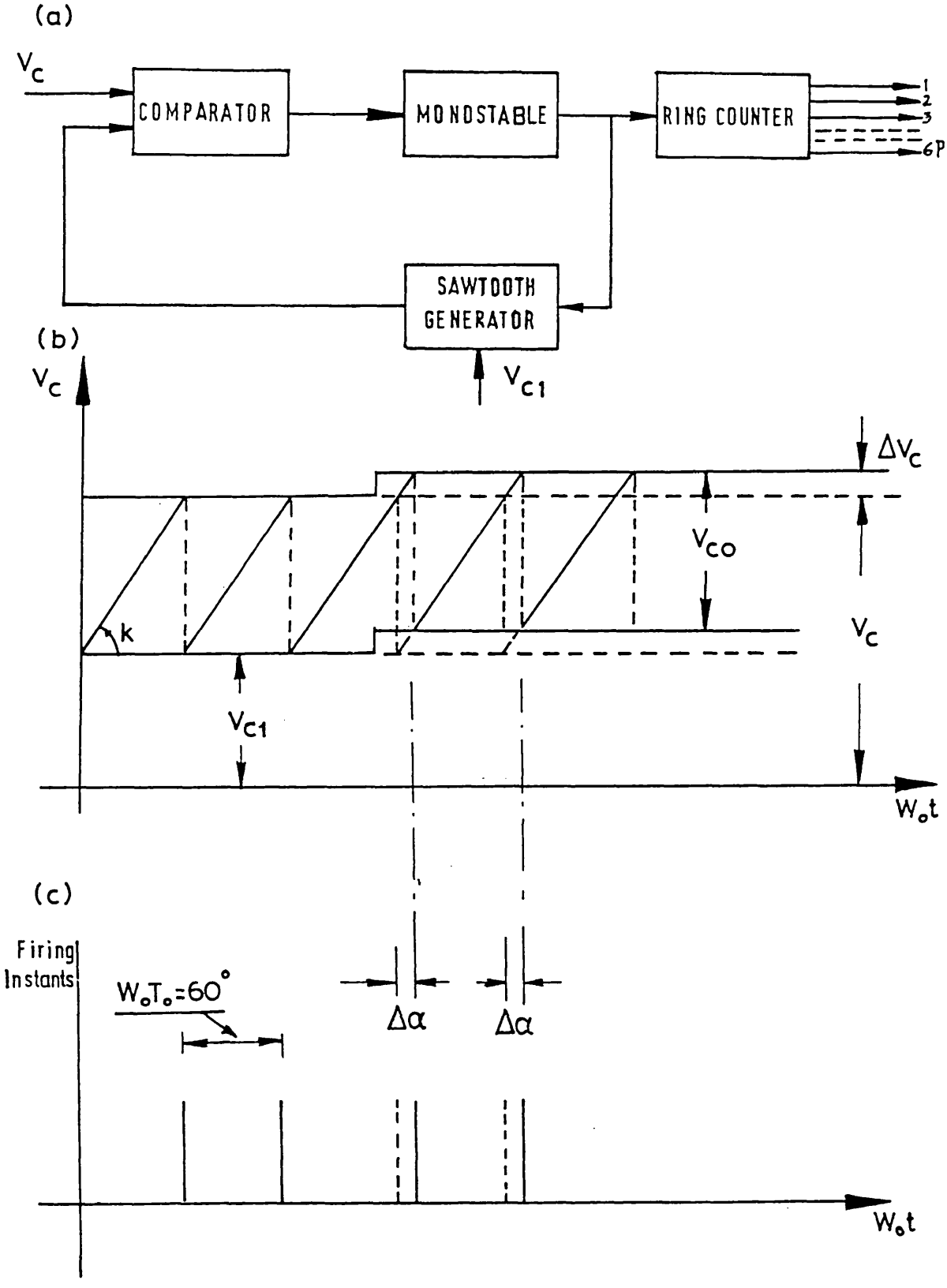

Fig. 2.2 - PULSE PHASE CONTROL (PPC)

(a) Functional Block Diagram
(b) Comparator Inputs
(c) Firing Pulse Instants

the frequency of the firing pulse train remains unchanged although its phase is varied by an angle $\Delta\alpha$ so that

$$\Delta\alpha = K\Delta V_c .$$

The PPC system possesses the following advantages over the PFC system :

a) The proportional characteristic results in a larger stability margin;

b) Operation with constant firing angle is implemented simply by setting a constant control voltage;

c) The converter gain, V_d/V_c, can be made independent of the converter control angle, α , by introducing an "inverse cosine" current between the "error processing unit" and the firing control system.

2.4 h.v.d.c. system stability

Stability in h.v.d.c. systems is conditioned by the presence of several closed-loop control systems. Abnormal harmonics accompanied by firing-pulse imbalance, have been reported in several cases (New Zealand, Cross-Channel) sometimes causing excessive interference which has necessitated adding expensive special filters. Such instabilities give rise to abnormal harmonic currents which are injected into the a.c. network resulting in unacceptable voltage distortion levels.

There are two possible instability modes:

- oscillations synchronized with the a.c. system (harmonic instability);
- oscillations unsynchronized with the a.c. system

Linearized discrete models of converters have been developed which enable the prediction of the onset of instability [7]. The main limitation of such modes is that they are incapable of

a) predicting limit cycles synchronized with the a.c. system voltage;

b) taking into account a.c. system imperfections and firing angle irregulatities.

Stability studies of h.v.d.c. converters are important for two main reasons:

1) It is vital to understand the mechanism of the occurrence of limit cycle oscillations (sustained oscillations) established under circumstances such as :

a) resonances in a.c. and/or d.c. system;

b) imbalance/distortion in a.c. voltage;

c) unbalanced transformer reactances;

d) transformer saturation;

e) firing angle irregularities.

2) It is required to design robust controllers which minimize uncharacteristic harmonic generation.

Phenomena present in non-linear systems such as limit cycle and sub-harmonic oscillations, can be studied through the describing function technique (also known as "Method of Harmonic Balance"). This technique is especially useful because :

a) it is simple and reliable;

b) it is a natural extension of frequency response methods used in linear stability analysis.

2.5 Systems with non-linear feedback and the describing function

In general, systems with non-linear feedback can be represented by a lumped linear element and a lumped non-linear element. The linear element is represented by its transfer function, G(s), while the non-linear element is given by its describing function, N.

The d.f. is defined as the ratio of the input-signal frequency component of the output of a non-linear system to the amplitude of the input signal. If the input to a non-linear element is a sinusoidal signal of "fundamental" frequency, the d.f. method assumes that the output is a periodic signal of the same fundamental frequency. The analysis below, therefore, assumes that only the amplitude of the "fundamental" harmonic is non-negligible and that any other harmonic and d.c. component are sufficiently small or sufficiently attenuated by the low-pass characteristic of the linear element that may be neglected.

Fig. 2.3 is the block diagram of a typical non-linear system represented by its linear and non-linear elements. The input to the non-linear element is given by :

$$x(\omega t) = X \sin \omega t.$$

The steady-state output y can be given by the series :

$$y(\omega t) = \sum_{k=1}^{\infty} Y_k \sin (k\omega t + \phi_k) .$$

As a consequence, if the input and the output of the non-linear element are represented by phasors, the d.f. will be, by definition, given by the complex ratio between output and input signals :

$$N(X,\omega) = \frac{Y_1(X,\omega)}{X} \; e^{j\phi_1(X,\omega)} \quad . \tag{2.1}$$

Eqn 2.1 is a function of the amplitude and the frequency of the input signal. Therefore, the non-linear element is considered to have variable gain and pulses which are functions of the amplitude and frequency of the input signal.

The conditions for the existence of a limit cycle are defined by the solution, (X_0,ω_0), of the identity [10]:

$$G(j\omega) = -\frac{1}{N(X,\omega)} \; . \tag{2.2}$$

Nichols diagrams and gain-phase plots are the most widely used techniques for stability analysis when using d.f.'s. As shown in Fig. 2.4, a possible solution of eqn 2.2 is provided by the intersection between the two loci $G(j\omega)$ and $-1/N(X,\omega)$. The solution of eqn 2.2 gives information about magnitude, X_0, and frequency, ω_0, of the sustained oscillation.

The limit cycle itself can be classified as stable or unstable according to the nature of the perturbations around the point (X_0,ω_0). Stability of a limit cycle oscillation can be established from the Nyquist or Nichols diagram as follows [10]. A positive direction is taken to be the one in which the linear locus, $G(j\omega)$, is pointing towards increasing frequency while the non-linear locus, $-1/N$, is pointing towards increasing amplitude. For the gain-phase plot, a stable limit cycle occurs when the $-1/N$ locus appears to an observer stationed on the linear locus and facing its positive direction, to cross from left to right in its positive direction. If a polar plot is used instead, the

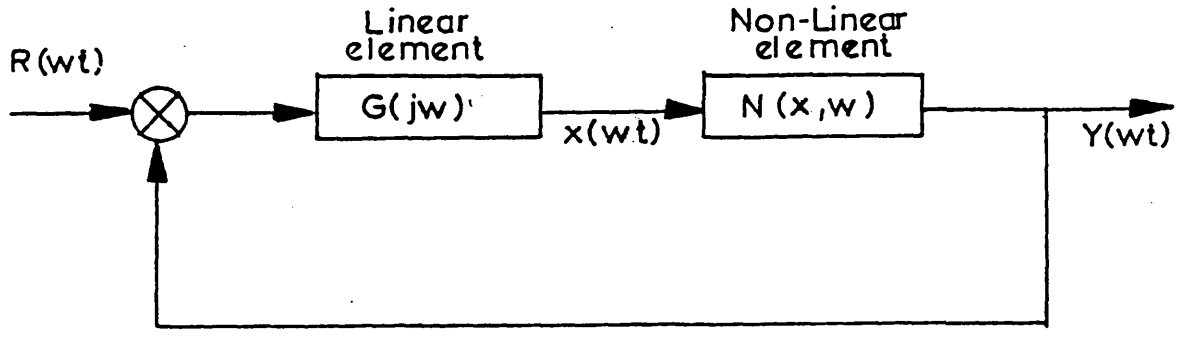

Fig. 2.3 - SYSTEM WITH A NON-LINEAR FEEDBACK

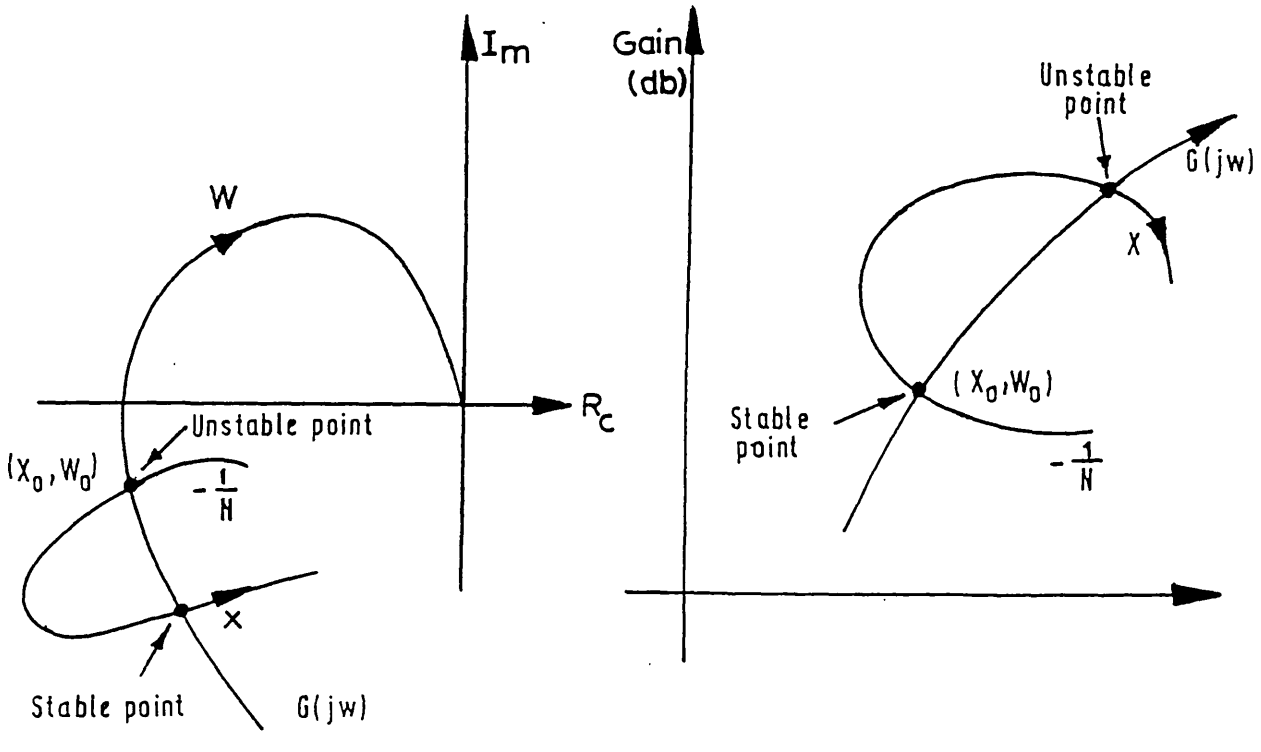

a) Polar plot (NYQUIST)

b) Gain-phase plot (NICHOLS)

Fig. 2.4 - CONDITIONS FOR EXISTENCE OF A LIMIT CYCLE

non-linear locus should cross the linear locus from right to left in the direction of increasing amplitude, as illustrated in Fig. 2.4.

2.6 Theoretical and Experimental d.f. for 6-pulse converters

Fig. 2.5 shows the block diagram of a h.v.d.c. system operating under constant current control, the linear and non-linear elements being separated by a hatched line. The blocks represented inside the hatched line can be lumped into a single non-linear element which includes the converter a.c. system, d.c. system and valve firing system. The d.f. for this lumped non-linear element is defined by :

$$\bar{N} = \frac{\bar{I}_{dk}}{\bar{V}_{mk}} \qquad (2.3)$$

where:

$\bar{I}_{dk}$: d.c. harmonic of order k.

$\bar{V}_{mk}$: modulating signal (input signal) of frequency $k\omega_o$

To evaluate the d.f., the steady-state control voltage, V_c, is modulated by an input signal, $\bar{V}_{mk}$, expressed by :

$$v_{mk} = V_m \sin(k\omega_0 t + \phi) \quad . \qquad (2.4)$$

Excited by $\bar{V}_{mk}$ the d.c.-side current will contain a term which can be defined as :

$$i_{dk} = I_{dk} \sin(k\omega_0 t + \phi_{dk}) \qquad (2.5)$$

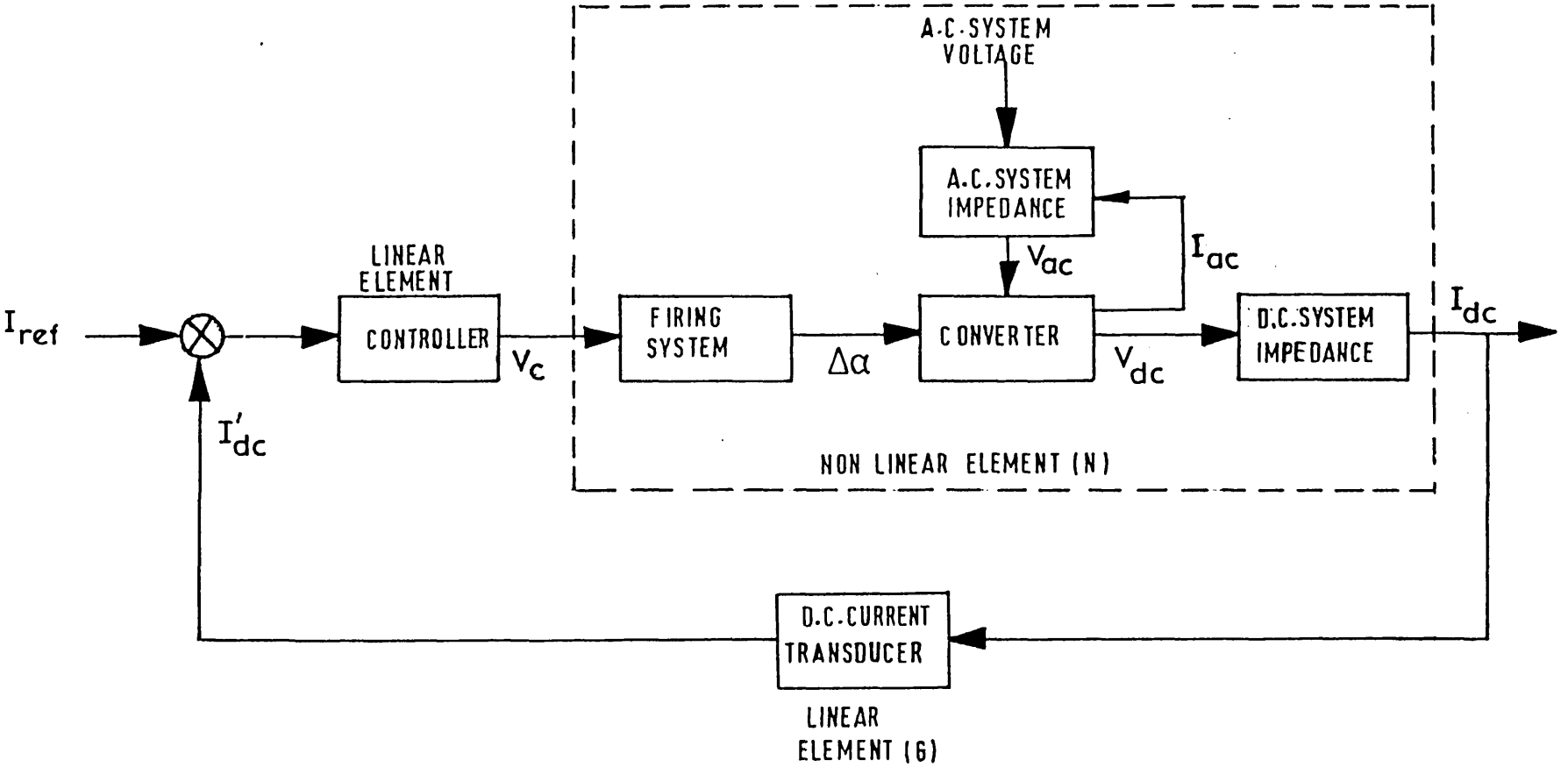

Fig. 2.5 - h.v.d.c. AS A NON-LINEAR FEEDBACK SYSTEM

Either amplitude or phase of $\bar{V}_{mk}$ can be used as the control parameter to obtain the d.f. at a given frequency. Letting $\emptyset$ vary from 0^{o} to 360^{o}, a closed curve must result. Several theoretical and experimental loci of d.f.'s using the definition above are presented in reference [1]. In this reference, the theoretical d.f.'s were obtained through a computer program capable of analysing the mechanism of harmonic generation by 6-pulse converters in the presence of imperfections in the a.c. voltage, converter transformer and firing system. The flowchart of such computer program is presented in Fig. 2.6. The program performs a detailed steady-state calculation of a complete h.v.d.c. link, yielding all the a.c.- and d.c.-side harmonic voltages and currents up to the 30th order.

The experimental d.f's were obtained through a digital transfer function analyser. The built-in function generator provides the modulating signal and a built-in correlator with a frequency range identical to the function generator, performs the measurement of the relevant d.c. side harmonic current. All tests were performed under open-loop current control.

The experimental determination of the d.f. obtained in reference[1] showed fair agreement with the theoretical results predicted by the computer program in nearly all cases examined. Difficulties in establishing the exact input data to the computer program to match the test conditions explain the discrepancies. A typical comparison between practical and theoretical results is depicted in Fig. 2.7 which was taken from reference [1]. Fig. 2.7(a) shows a d.f. obtained from the computer program and from practical tests on the IC-h.v.d.c. simulator under similar conditions. In Fig. 2.7(b) the gain-phase plot predicts a theoretical 50Hz limit cycle oscillation for a gain 23.2. Under similar conditions,

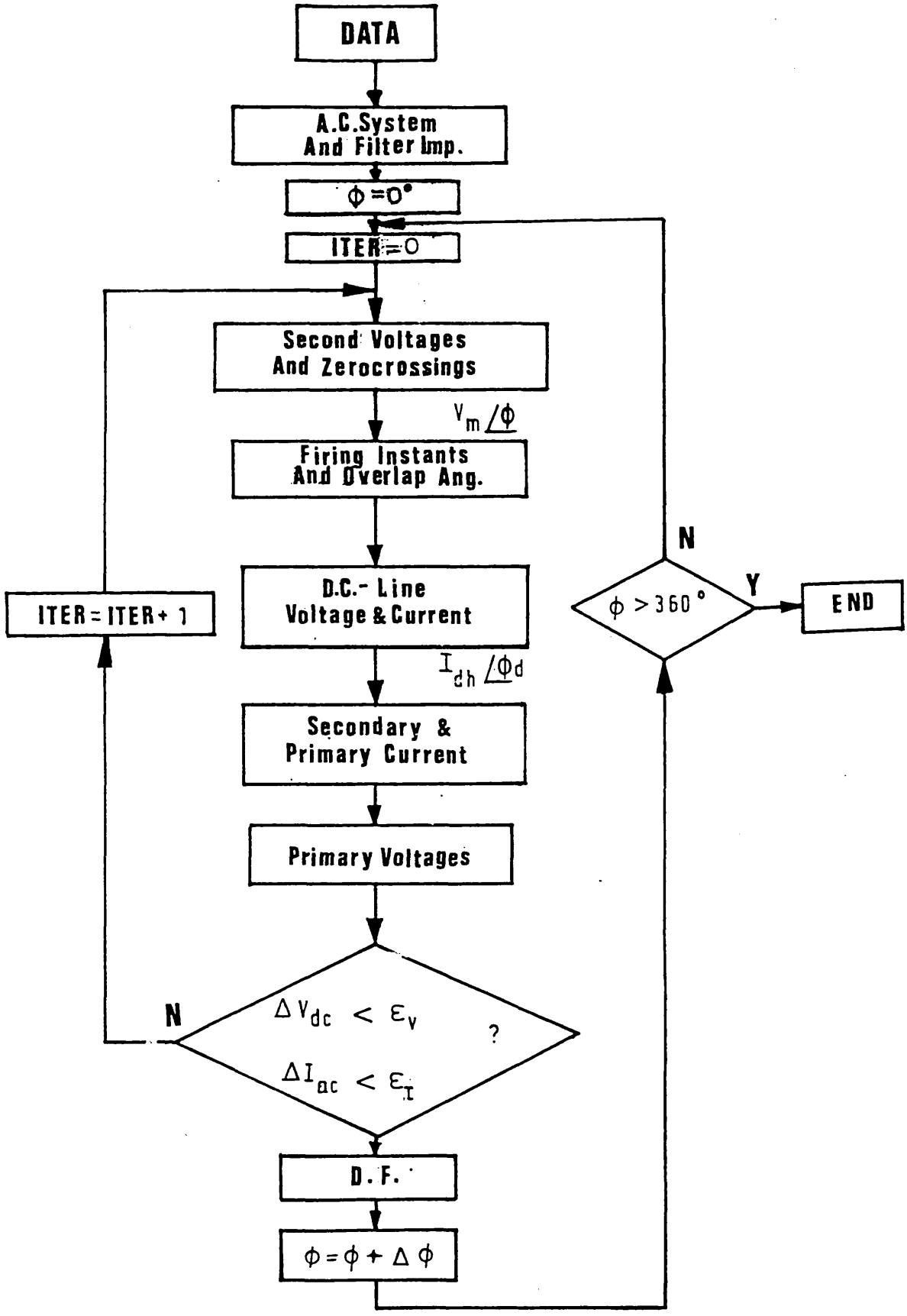

Fig. 2.6 - FLOWCHART TO DERIVE D.F.'s FOR 6-PULSE OPERATION

f = 50 Hz

α^{o} = 15.2

$\Delta\alpha$ = 14.6

"Unbalanced transformer reactances"

SCR = ∞

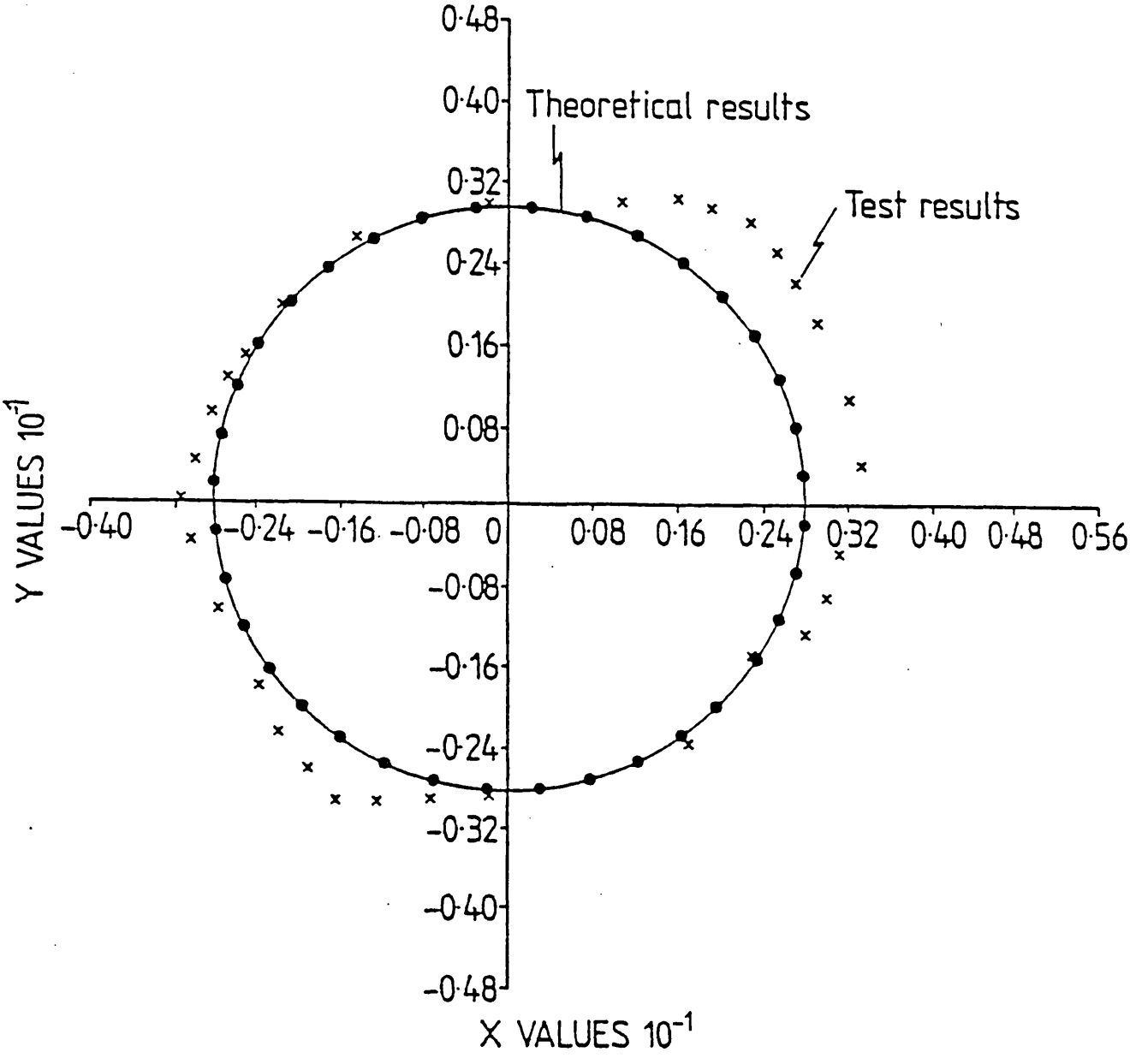

Fig. 2.7(a) - DESCRIBING FUNCTION:COMPARISON BETWEEN THEORETICAL AND TEST RESULTS

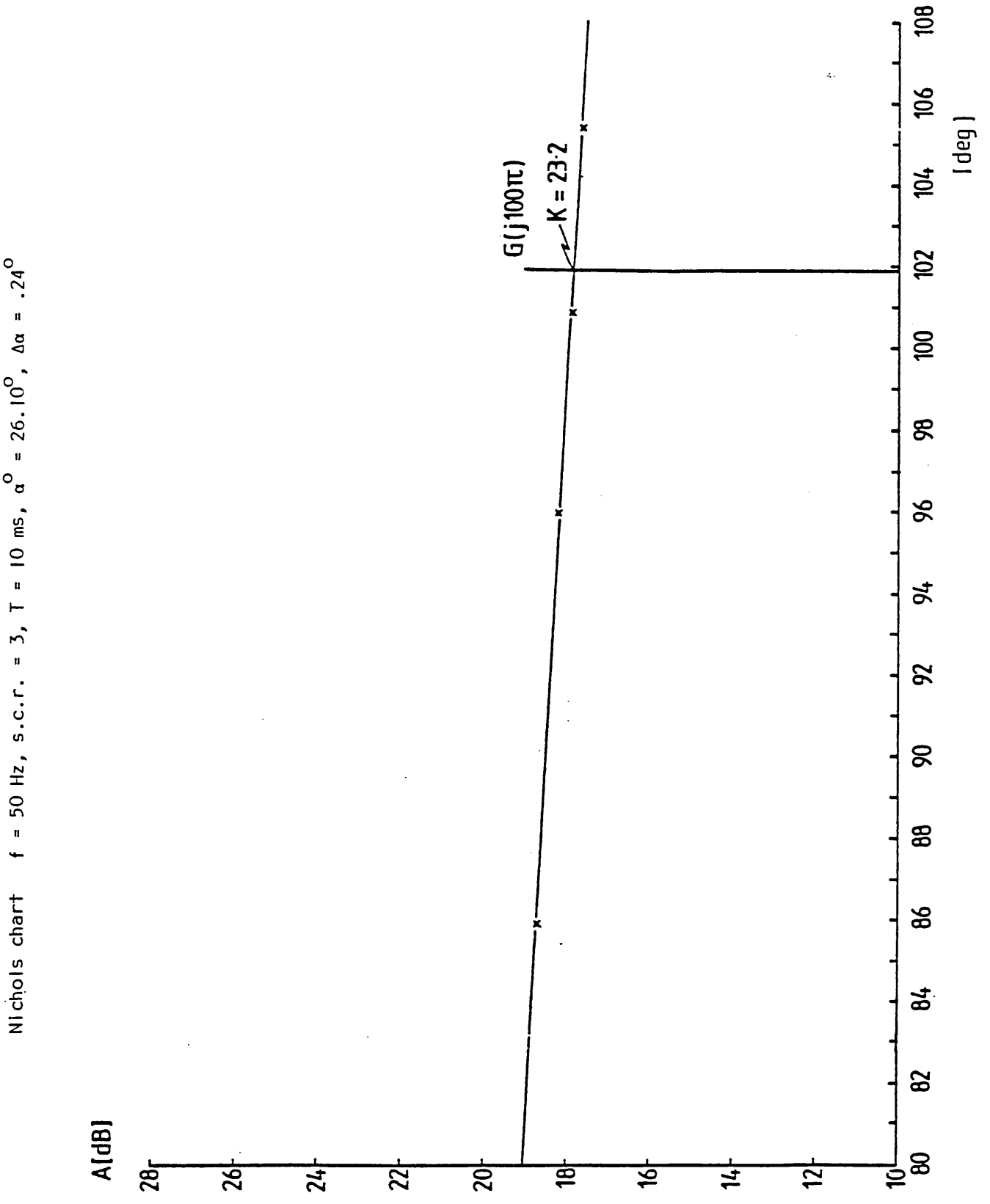

Fig. 2.7(b) – CONVERTER STABILITY USING NICHOLS CHART

on the h.v.d.c. simulator the oscillation occurred for a gain 20.0.

2.7 Describing functions for 12-pulse converter

Twelve pulse operation is achieved from two bridge converters connected to the a.c. supply through a star-star and a star-delta transformer. The 30^{o} phase shift introduced cancels some d.c. voltage and some a.c. current harmonics compared to 6-pulse operation.

To analyse harmonics and derive describing functions for 12-pulse operation, the 6-pulse program presented in Figure 2.6 can be used with certain modifications.

Three basic modifications of the 6-pulse models are necessary to simulate 12-pulse operation, namely : doubling of firing pulses, determination of total d.c. voltage and determination of total a.c. current.

The number of pulses from a v.c.o. based valve firing circuit can be easily doubled by reducing by half the d.c. level bias which in conjunction with a sawtooth waveform, generates the pulsing instants.

The total d.c. voltage in a 12-pulse system can be determined through the addition of the individual contributions of each bridge. This includes both, the constant term and each harmonic present.

The total a.c. current in a 12-pulse system can be similarly determined through the separate phasorial addition of the fundamental and of each harmonic contribution from the two 6-pulse bridges.

The overall iterative simulation program for either 6- or 12-pulse operation is shown in Figure 2.8 .

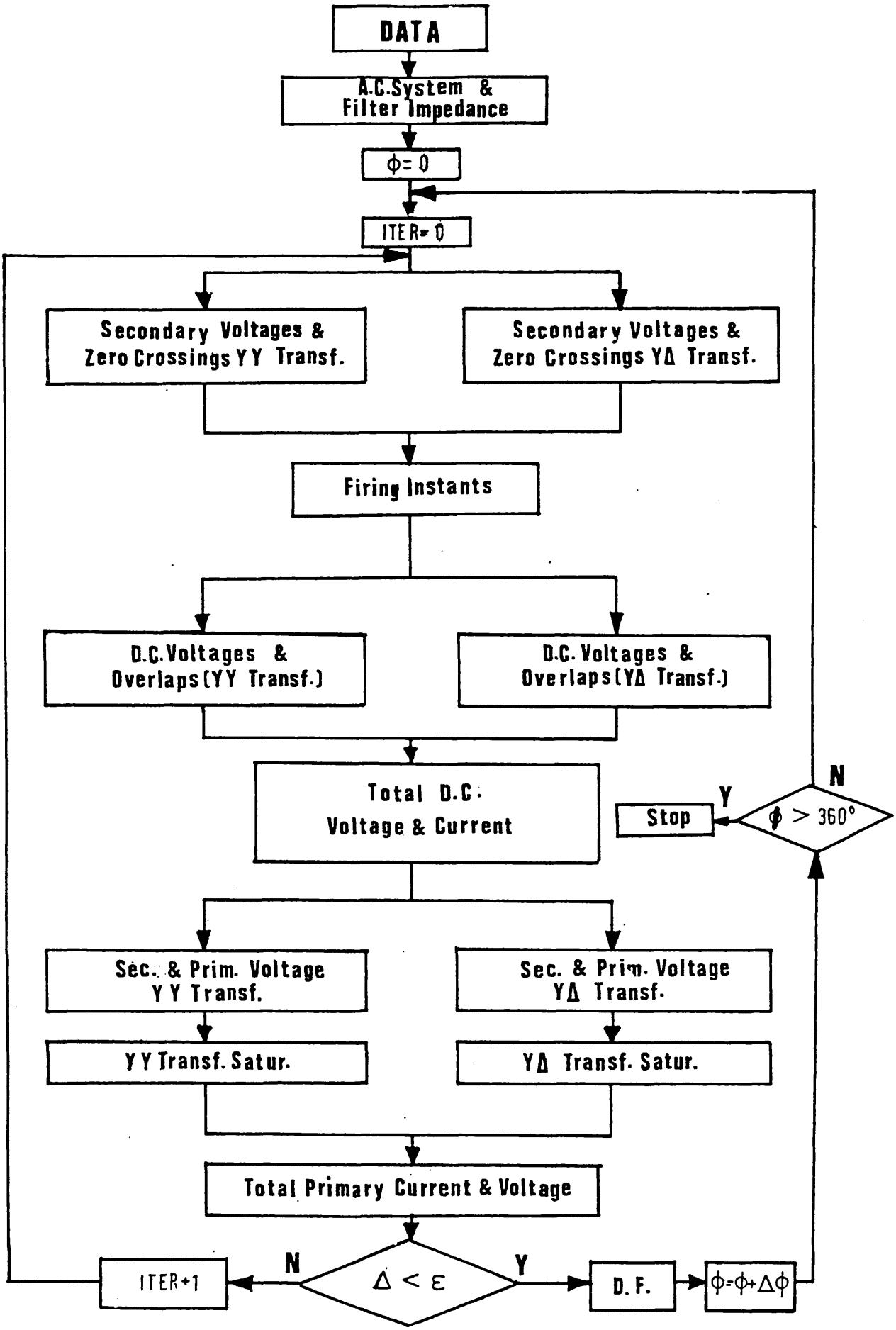

Fig. 2.8 - FLOWCHART TO DERIVE D.F.'s FOR 12-PULSE OPERATION

2.8 Comparison between 6- and 12-pulse d.f.'s

It is shown in reference [1] that the d.f.'s are not equally sensitive to all types of possible distortion on the a.c. system. Table 2.1 indicates the cases for which this sensitivity is most pronounced

TABLE 2.1

MOST SENSITIVE DESCRIBING FUNCTIONS

M.S. FREQ.	PRIMARY DISTORTION	
	FREQ.	SEQUENCE
50Hz	100Hz	+
100Hz	50Hz	
150Hz	100Hz	-

To identify any differences between 6- and 12-pulses d.f.'s, similar studies were carried out using 6- and 12-pulse converters under identical per unit conditions. The data used in the calculations for 12-pulse d.f.'s are :

Converter rated output	
d.c. voltage per bridge	250kV
d.c. current	2kA
Converter transformer	
rating	2×295.5 MVA
copper loss	2500kW
voltage ratio	400±15%/209kV
Control setting	
nominal firing angle	15°
nominal extinction angle	18°
Smoothing inductor (per station)	
resistance	0.325Ω
inductance	0.5 H
D.C. transmission line	
length	800km
resistance	10Ω
inductance	0.48H
capacitance	up to 40 μF

Typical case of the most sensitive d.f.'s are presented in Figs. 2.9 to 2.11.

Figure 2.9 shows the case of a 100Hz harmonic of positive sequence having an amplitude of 1% of the fundamental impressed on the primary of the converter transformer. The total effect on the 50Hz d.f.

is a slight shift of the 12-pulse with respect to the 6- pulse d.f. . This happens probably due to variations in the commutation angles which cause differences in the effective a.c. impedance seen by the converter when changing from 6- to 12- pulse operation. The same applies to tne 150Hz d.f. shown in figure 2.11 where, 2nd harmonic distortion of negative sequence is imposed on the converter busbar.

Figure 2.10 shows the 100Hz d.f. for a 1 % distorted fundamental. This indicates that the elimination of some harmonics with 12-pulse operation results in a circular d.f. .

Extensive studies with 12-pulse converters brought out several interesting aspects on to d.f. loci that were not apparent in the 6-pulse converter studies presented in reference [1]. These aspects are being discussed in the following sections.

2.9 Analysis of resonance and antiresonance effects

With a finite a.c. source impedance, the converter busbar voltage is a function of the current through the converters. A conventional model of the equivalent impedance of the a.c. system and filters is shown in figure 2.12.

The busbar harmonic voltage of order "n" is obtained in Appendix A as

$$V_n = Z_n \left(\frac{E_m}{Z_{sn}} - I_n \right) \qquad (2.6)$$

where

$$Z_n = \frac{Z_{sn} Z_{fn}}{Z_{sn} + Z_{fn}} .$$

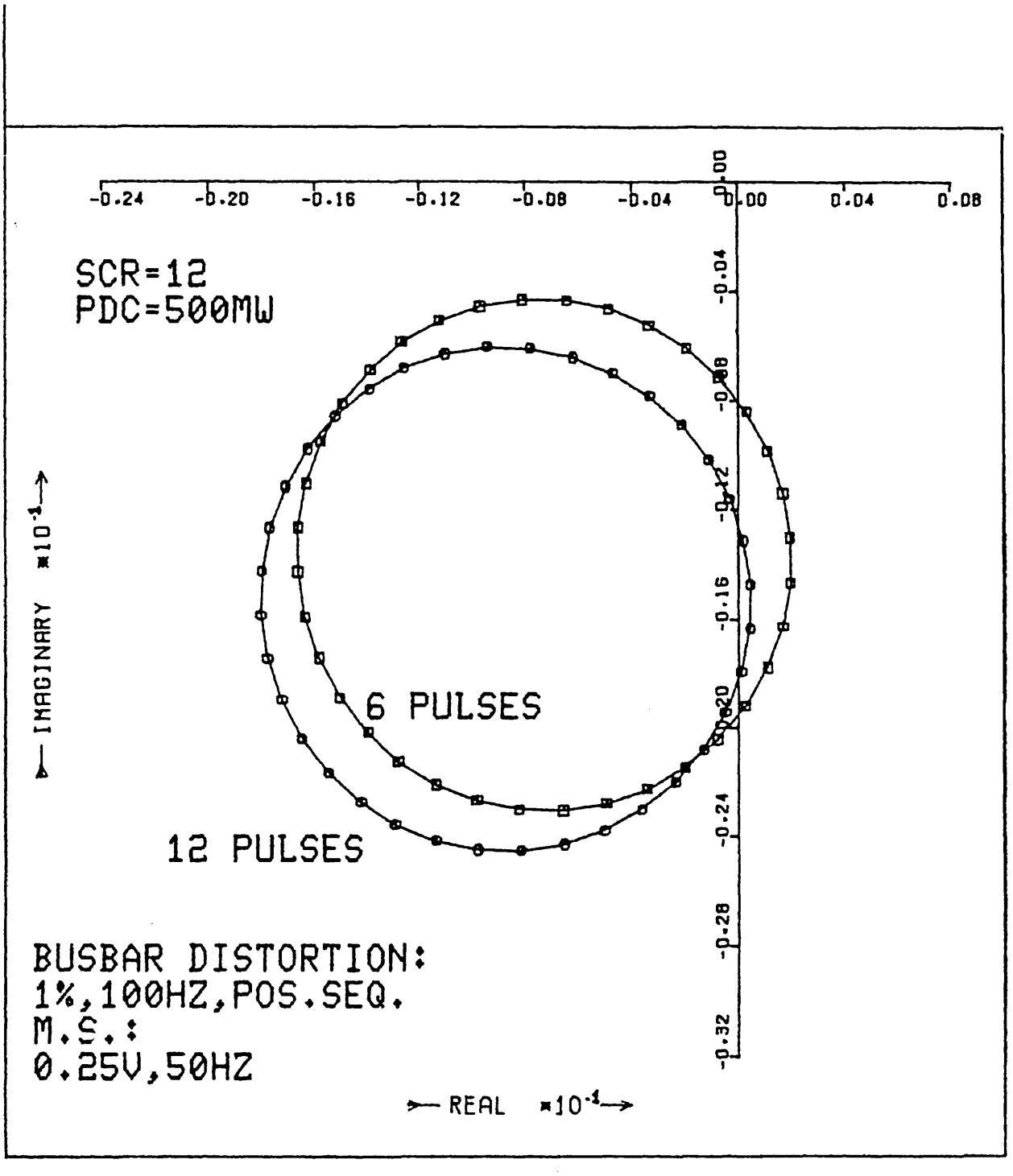

Fig. 2.9 - DF's FOR 6- AND 12-PULSE OPERATION

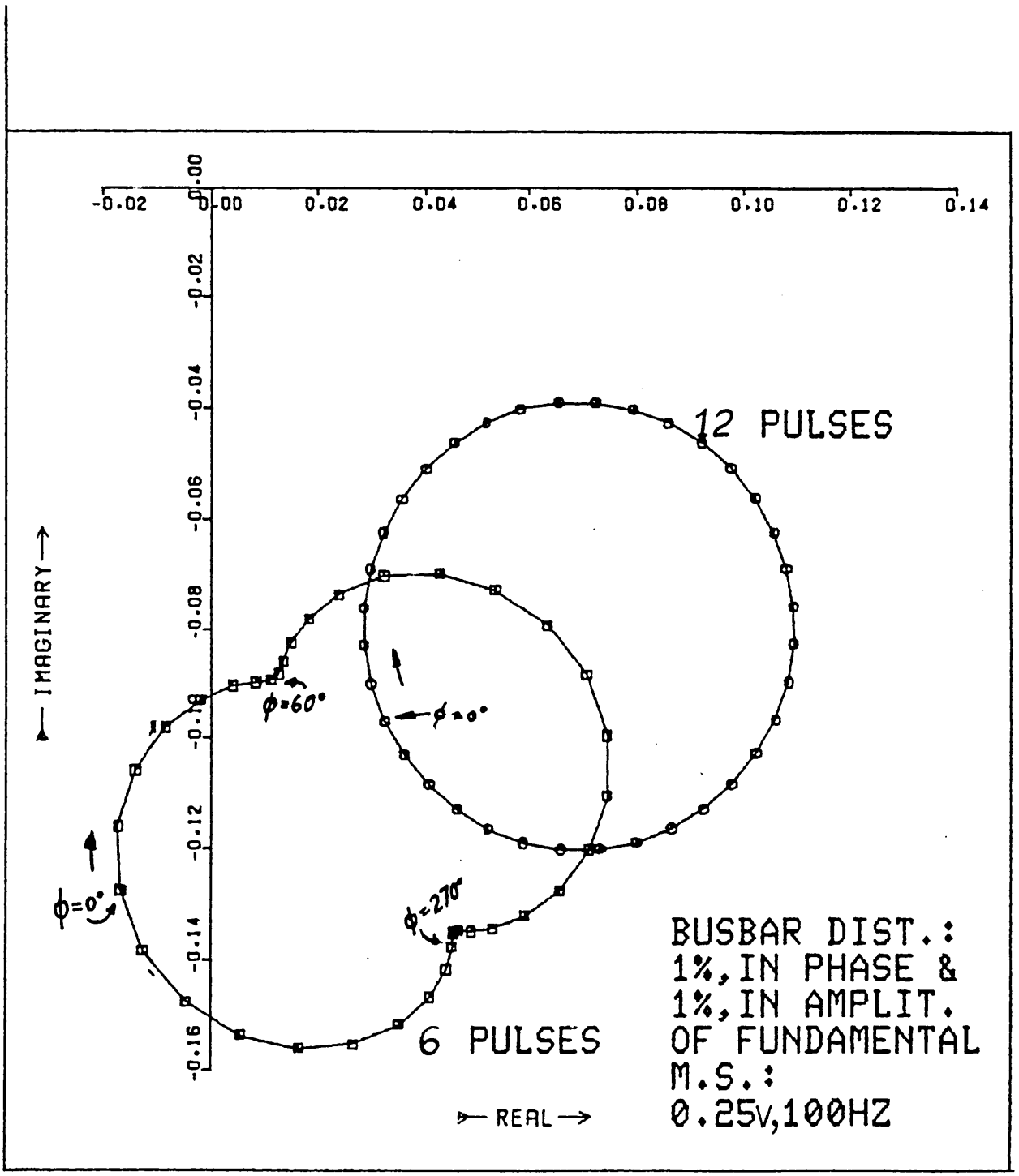

Fig. 2.10 - DF's FOR 6- AND 12-PULSE OPERATION

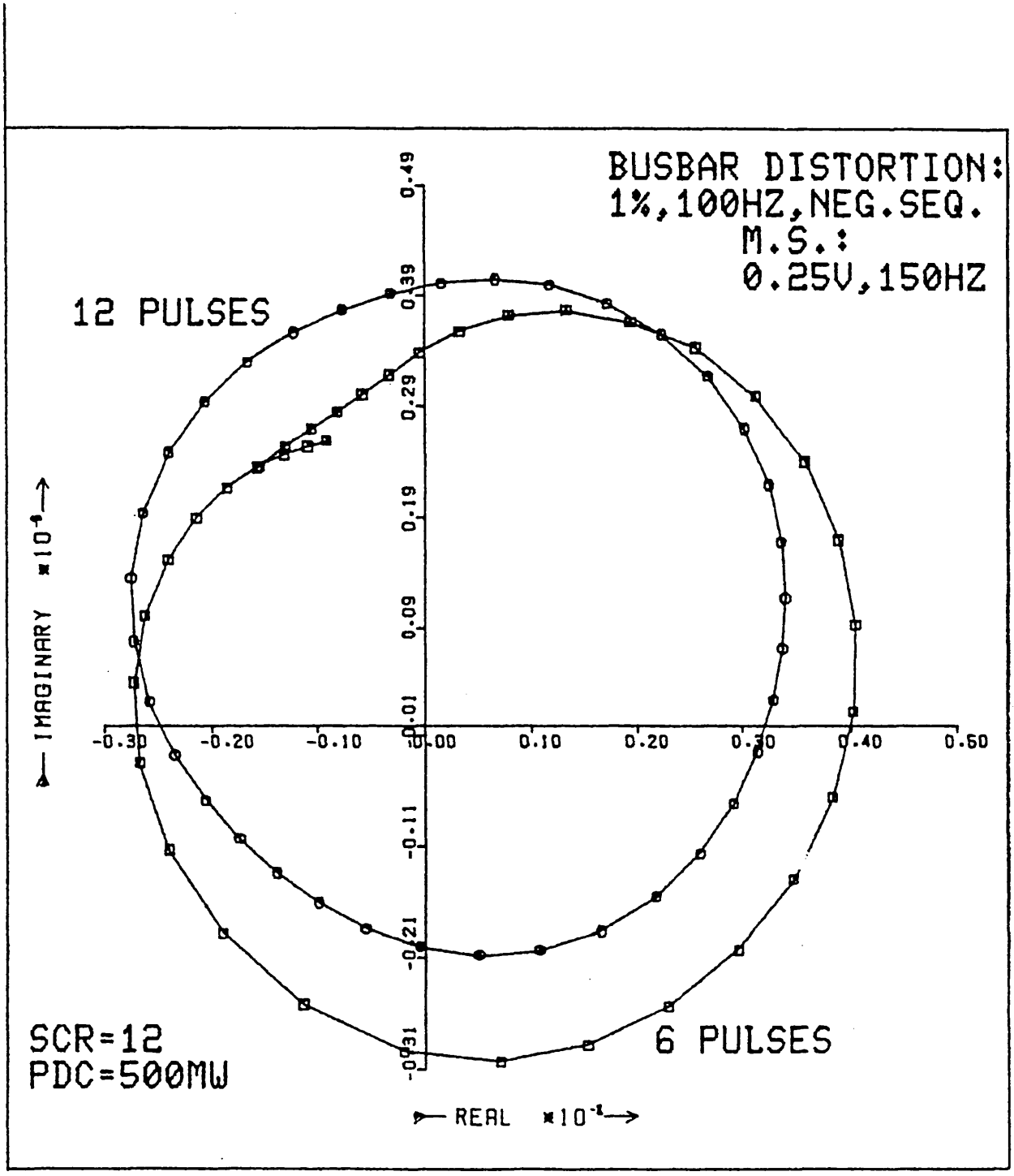

Fig. 2.11 - DF's FOR 6- AND 12-PULSE OPERATION

Norton's equivalent of the circuit shown in Fig. 2.12, is shown in Fig. 2.13.

The resonant frequency of the equivalent impedance gives:

$$Z_n = 0 \ .$$

In such a case, the n-th harmonic from the a.c. system can neither affect nor be affected by the converter. This is an ideal case never met in practice.

The antiresonant frequency gives

$$Z_{fn} = - Z_{sn}$$

where Z_{sn} can be defined in terms of the a.c. parameters by:

$$Z_{sn} = \frac{V^2}{P \times SCR}$$

where : V is the nominal a.c. line voltage

P is the active a.c. power

SCR is defined in Appendix A.

Figure 2.13 can be simplified to an ideal current source if the source impedance is at its anti-resonant value ($Z_n \rightarrow \infty$). Voltage V_n is then determined by an impedance which is a function of the converter operating point. Under this condition a steady-state solution might be difficult.

In practice, the impedance source is not infinite and V_n may be obtained by equation 2.6. Table 2.2 presents two examples of non convergence when SCR = 3 and 12 for 12-pulse operation.

TABLE 2.2

CASES OF NON CONVERGENCE

SOURCE IMPEDANCE (Ω)			MOD. SIGNAL		P	SCR
50Hz	100Hz	150Hz	V_m(V)	F(Hz)	MW	
321.	123.	70.	0.5	100.	500.	2
2000	150.	76.	0.5	50.	500.	12

A simplified model of the d.c. line is shown in figure 2.14.

If the inverter is considered as a short-circuit for all harmonics and if R is negligible (Appendix A), the impedance seen by the rectifier is :

$$Z_\ell = j\omega L \frac{2 - \omega^2 LC}{1 - \omega^2 LC} \quad . \qquad (2.7)$$

The resonant frequency of the line at which $Z_\ell = 0$ is

$$f_0 = \frac{1}{\pi\sqrt{(2L_r + L_\ell)C}}$$

and the antiresonant frequency at which $Z_\ell \to \infty$ is :

$$f_\infty = \frac{f_0}{\sqrt{2}} \quad .$$

As it is demonstrated in Sections 3.9 - 3.11 of Chapter 3, the m.s. of a given frequency usually gives rise to harmonic current of the same frequency in the d.c. circuit. The closer that frequency is to the d.c.-

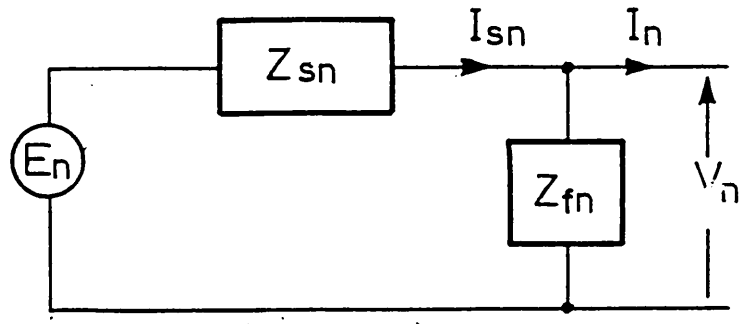

Fig. 2.12 - EQUIVALENT a.c. SYSTEM IMPEDANCE AND FILTERS

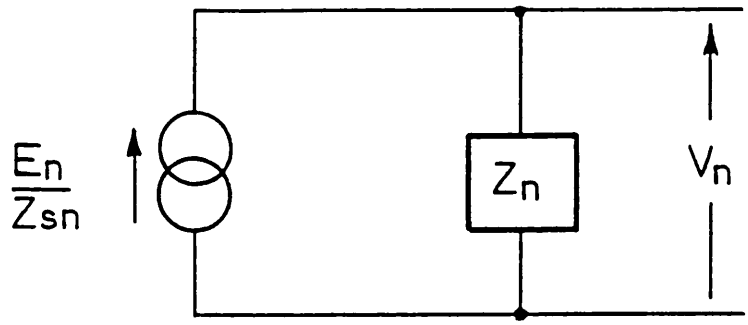

Fig. 2.13 - a.c. SYSTEM NORTON's EQUIVALENT

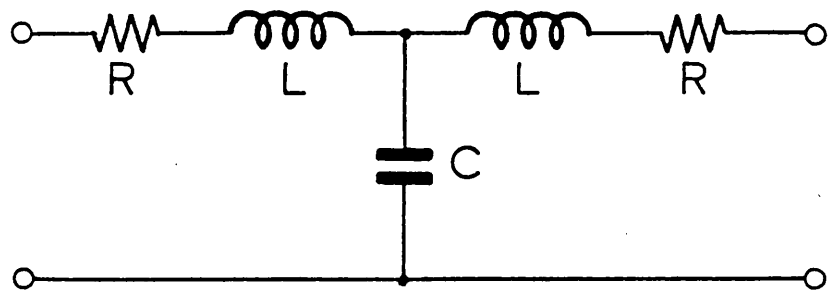

Fig. 2.14 - T-EQUIVALENT OF THE d.c. LINE

line resonant frequency, the larger the corresponding d.c. side harmonic current. Such a current is only limited by the transformer reactance and line reactance and causes enlargement of the d.f. locus. The lower the d.c. line impedance at resonance, the more difficult it is to arrive at a convergent solution. Conversely, the d.c. line antiresonant impedance causes the reverse effect, i.e. zero d.c. line harmonic current and a reduction in the amplitude of the d.f. .

Table 2.3 illustrates the profound effect that line impedance variations has on the value of the d.f. . In this table, the line capacitance, C_{LINE}, was changed from 0.μF to 40.μF.

TABLE 2.3

D.F. FOR DC-LINE RESONANCE AND ANTIRESONANCE
(SCR=3; M.S.:FREQ=150Hz;AMPL.=0.25V)

C_{LINE} (μF)	Z_{LINE} (Ω)	θ_{LINE} (DEG.)	DESCRIBING FUNCTION	NUMBER OF ITER.	OBS
0.0000	2790.	90.	.0376 + j.0084	5	
1.5213	→∞	-	.0000 + j.0000	4	ANTI RESONANCE
2.0000	539.	-90.	-.0346 - j.0056	4	
3.0427	.01	90.	NON CONVERGENCE	-	RESONANCE
5.0000	1145.	90.	.1344 + j.0338	5	
10.0000	1280.	90.	.0921 + j.0217	4	
15.0000	1320.	90.	.0851 + j.0199	5	
>30	1358.	90.	.0786 + j.0182	5	

Using the data given in Section 2.7 and line impedance from eqn 2.7, the capacitances which give the resonant and antiresonant impedances are, respectively :

$$C_0 = 3.0427\mu F$$

$$C_\infty = 1.5213\mu F \ .$$

As C_{LINE} was increased, the impedance given by eq. 2.7 tended to a limit value given by

$$Z_\ell = j\omega L = j\omega(L_r + \frac{L_\ell}{2}).$$

For large values of capacitances ($C_{LINE} > 30\mu F$) the line impedance tends to 1358Ω.

Table 2.3 suggests that the d.c.-line harmonic current is largest for impedance values closer to the resonant value, e.g. note the d.f. amplitude for $C_{LINE} = 5\mu F$. In Section 3.12 of Chapter 3, the approximate expression of the d.f. explains the close relation between d.f. and d.c. line impedance.

It is very difficult to achieve convergence on a computer program for a d.c. line impedance close to resonance and virtually impossible, when the d.c. line resonance is associated with an a.c. source antiresonance

2.10 Periodicity of the d.f. with balanced a.c. source

In the case of balanced a.c. voltages and a "p" pulse bridge, the effect of phase shifting the m.s. to obtain the d.f. is illustrated diagramatically in figure 2.15 for a 100Hz m.s. and p=6. In position (2), the m.s. will distort the d.c. voltage in the same way it did in position (1), except that now this effect occurs 360/p degrees later. As the m.s. has progressed by the same angle, the d.c. voltage distortion will be cyclic.

The total fundamental cycle (360^{o}) contains k×N subintervals therefore, the number of discrete points of the d.f. determined within a 360/p interval is :

$$n = \frac{k \times N}{p} \qquad (2.8)$$

where k is the m.s. harmonic order and N is the total number of discrete positions within the m.s. cycle.

Furthermore, the loops that the d.f.-curve contains for balanced a.c. sources is:

$$n_{\ell} = \frac{N}{n} = \frac{p}{k} \quad .$$

This conclusion is important with regard to computing time especially for p = 12. Only n discrete positions need to be calculated and then repeated n_{ℓ} times.

2.11 Continuity of the d.f.

There is a maximum amplitude of m.s. beyond which the d.f. becomes discontinuous. About this limiting value, the firing pulse system provides no unique solution. This critical value is a function of the sawtooth generator ramp slope, K, as can be seen in Fig. 2.16. The limit is determined by the maximum positive tangent to the m.s. . If the m.s. is given by eqn 2.4 then:

$$\frac{dv_{mk}}{d(\omega_0 t)} = kV_m \cos(k\omega_0 t + \emptyset) \quad .$$

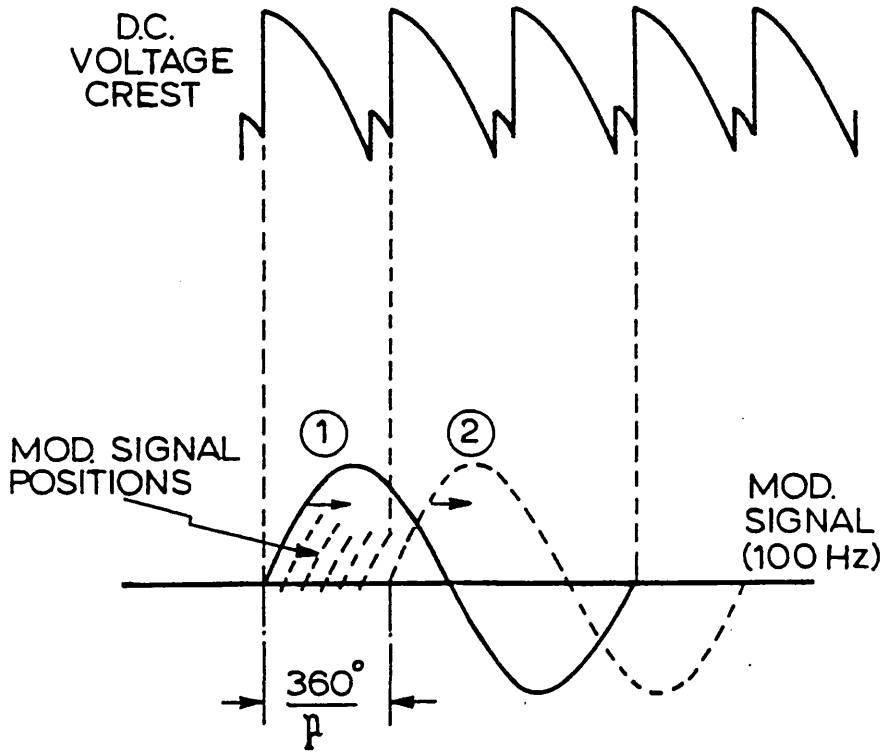

Fig. 2.15 - PERIODICITY OF THE D.F.

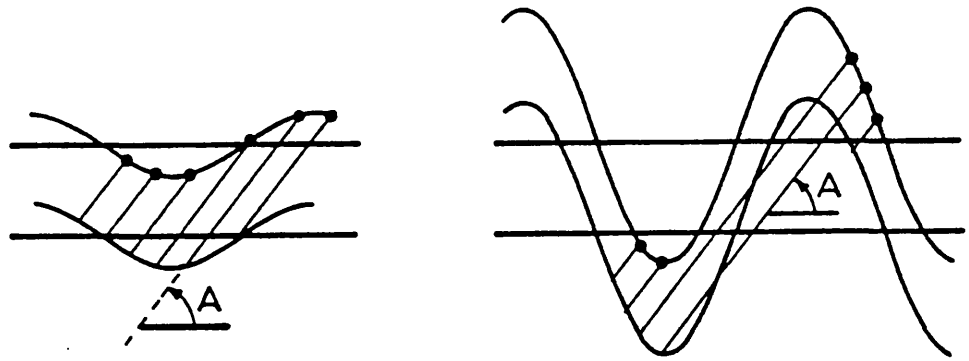

Fig. 2.16 - CONTINUITY OF THE D.F.

The maximum positive slope is :

$$\left.\frac{dv_{mk}}{d(\omega_0 t)}\right|_{max} = kV_m \quad .$$

Therefore, if :

$$kV_m \geq K \tag{2.9}$$

the d.f. is expected to be discontinuous.

Example :

- ramp slope

$$K = \frac{1.5V}{30^o}$$

- modulating signal

$$f = 150Hz$$

V_m to be estimated.

For a continuous d.f. it is necessary that :

$$V_m < \frac{K}{k} = 1.4324V \quad .$$

Describing function loci derived confirm the presence of discontinuity at the limits indicated by eqn 2.7. Furthermore, problems of convergence have occurred in the proximity of the limits within a range of 10%. Figs 2.17 and 2.18 show a d.f. of a 12-pulse converter with

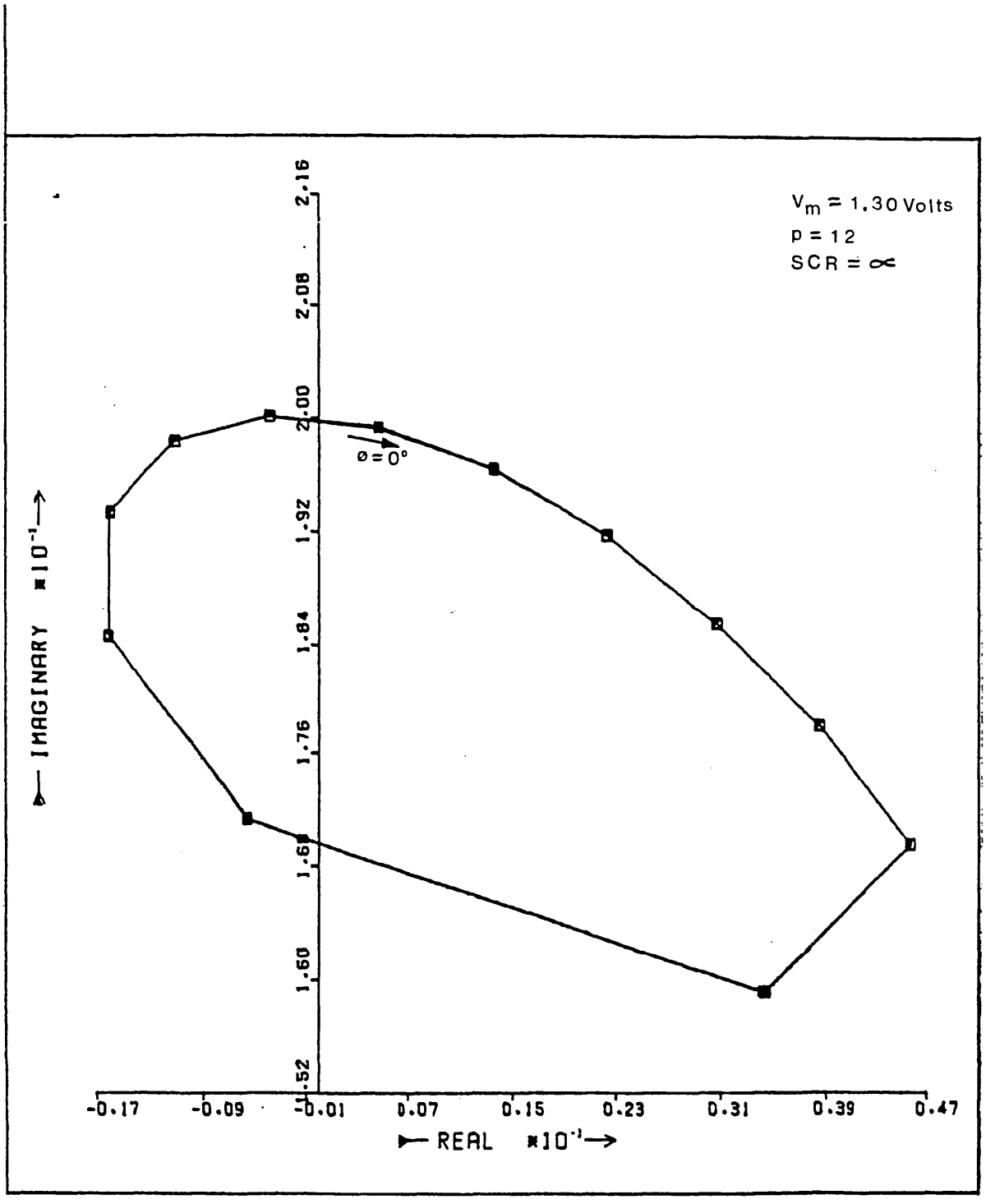

Fig. 2.17 - D.F. FOR 100Hz m.s.

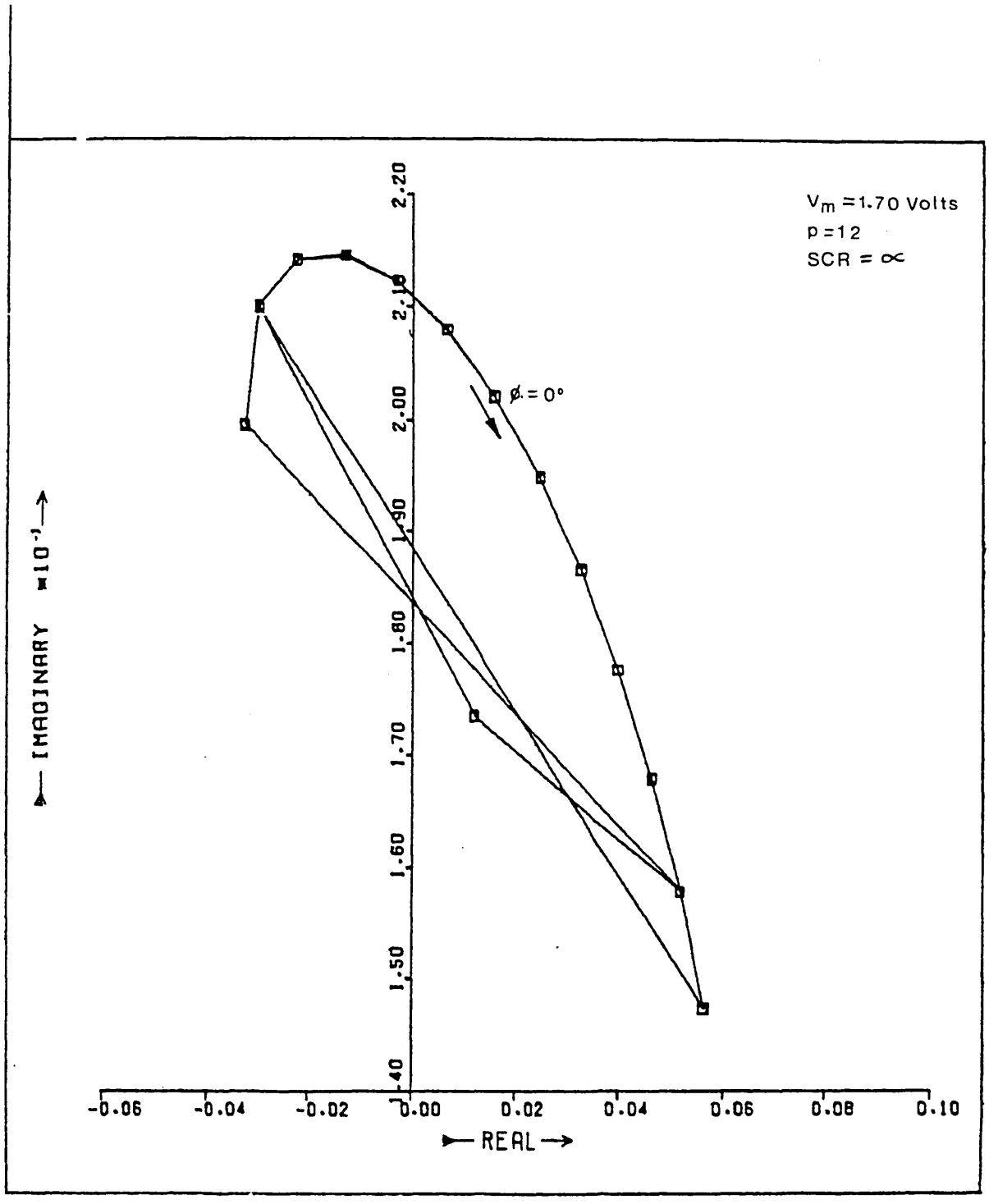

Fig. 2.18 - D.F. FOR 100Hz m.s.

100Hz m.s. and with amplitude lower and higher than the maximum, respectively.

Table 2.4 gives the m.s. limiting values, for all cases studied in this chapter.

TABLE 2.4

M.S. LIMITING VALUES FOR $K=9/\pi^{rd}/SEC$

M.S. FREQ. (Hz)	50	100	150
M.S. MAX. AMPL. (V)	2.86	1.43	0.95
$\Delta\alpha$ MAX. (DEGREES)	57.2	28.6	19.0

2.12 Some observations on d.f. properties

The d.c.-side harmonic currents are intimately dependent on (a) the a.c. voltage waveshape; (b) control voltage disturbances; and (c) unbalanced a.c. system impedances When pulse phase control (PPC) is used, then the calculation of the interfiring period depends normally on the I_{ref}, the actual d.c. current level, the m.s. and the amplifier gain, K. The ignition angle, α, will vary with the m.s. and, for small α's and large amplitudes of m.s., the variation may be greater than α itself. To prevent such possibility, a minimum ignition angle, called α_{min}, is necessary to ensure a certain voltage across the valve before firing it. However, in a most general case, the a.c.-side harmonics can modify the instant of initiation and ending of the overlap angle as well as the harmonic content along all conduction period. Under these circumstances the d.c.-side harmonic currents could be thought of as having two

approximately independent sources : (a) the a.c. supply waveform and (b) control voltage disturbances. This is dealt with in Chapter 3.

The following examples of d.f. seem to confirm the above deductions. In Fig. 2.19, the 50Hz d.f. of a 12-pulse converter supplied from an a.c. source with a phase imbalance, is shown.. It can be seen that 2% distortion gives twice as much d.f. expansion than 1%. The center of the circle (0,%) remains the same for all loci. Similar observations can be made with respect to Fig. 2.20 for a 100Hz d.f. and amplitude imbalance of 1% and 2%.

Fig. 2.21 suggests a vector representation for the d.f. based on the observations of figures 2.19 and 2.20. Vector n_1 determines the center of the family of d.f. curves and is approximately constant and possibly mostly dependent on the d.c. line impedance and m.s. amplitude. Vector n_2 rotates p/k times within a fundamental cycle and is possibly mostly dependent on the d.c. voltage ripple. Vector n_3 rotates at the harmonic frequency imposed at the converter busbar and is possibly mostly dependent on the harmonic distortion at the converter busbar. Vectors n_1 and n_2 could be obtained from the balanced a.c. source case. This is discussed in more detail in Chapter 3.

2.13 Saturation of the Converter Transformer

A transformer connected to a linear or non-linear load and excited by a sinusoidal voltage, absorbs in general symmetrical excitation current. This current contains only odd harmonics provided that the load does not absorb a direct component of current. If it does , the magnetic flux has no positive-negative symmetry with respect to amplitude and an average

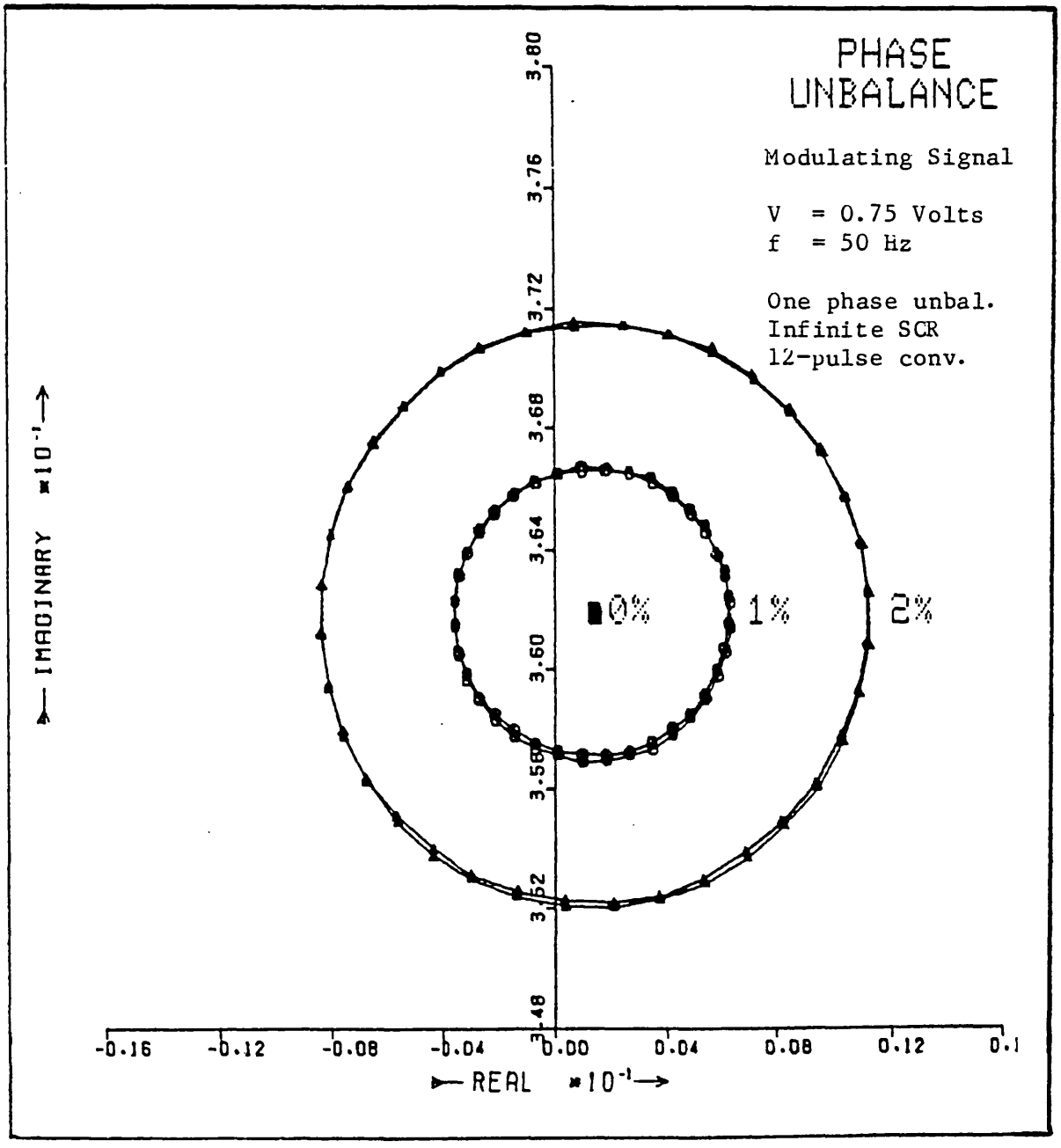

Fig. 2.19 - D.F. FOR 50 Hz M.S.

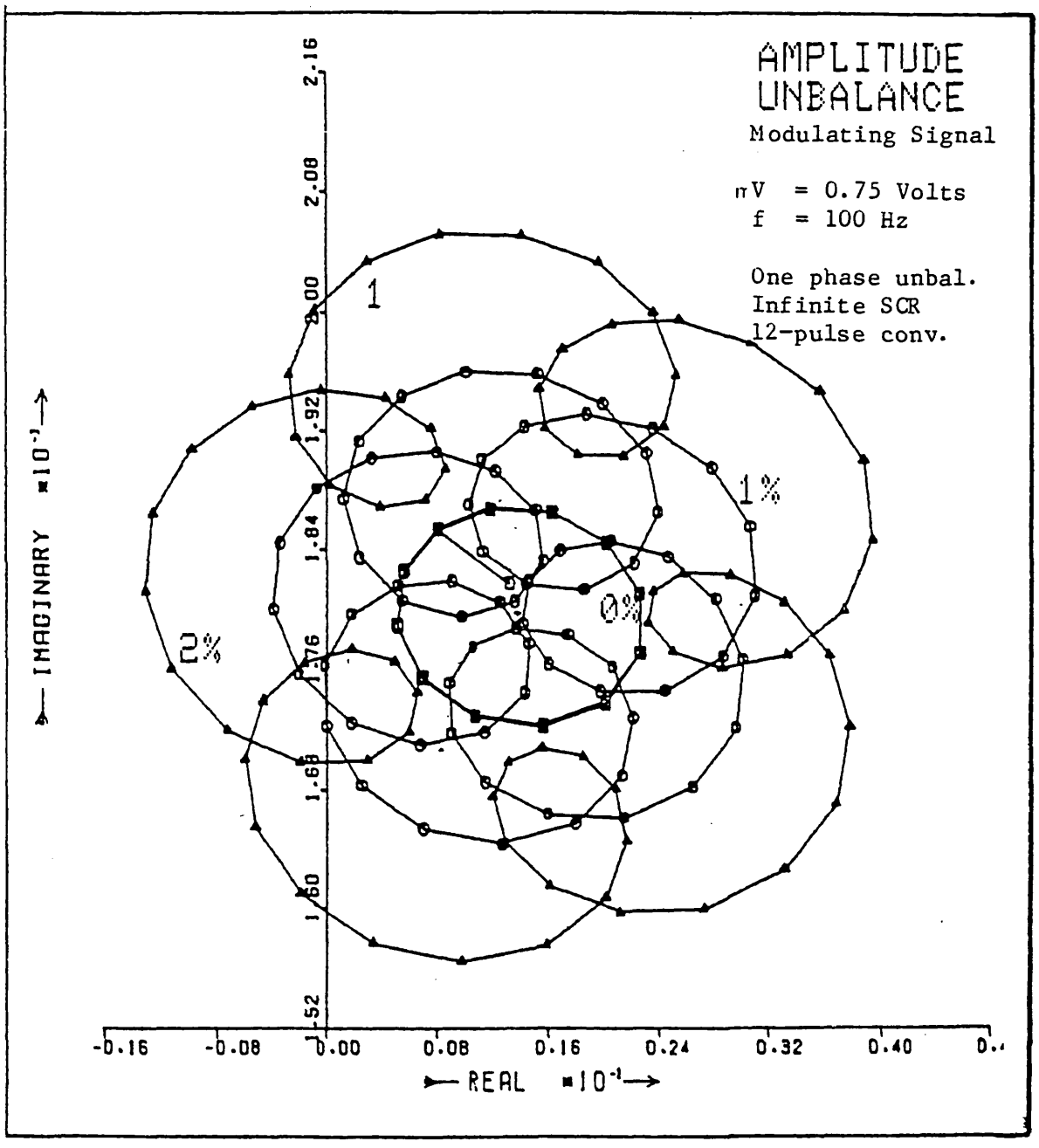

Fig. 2.20 - D.F. FOR 100 Hz M.S.

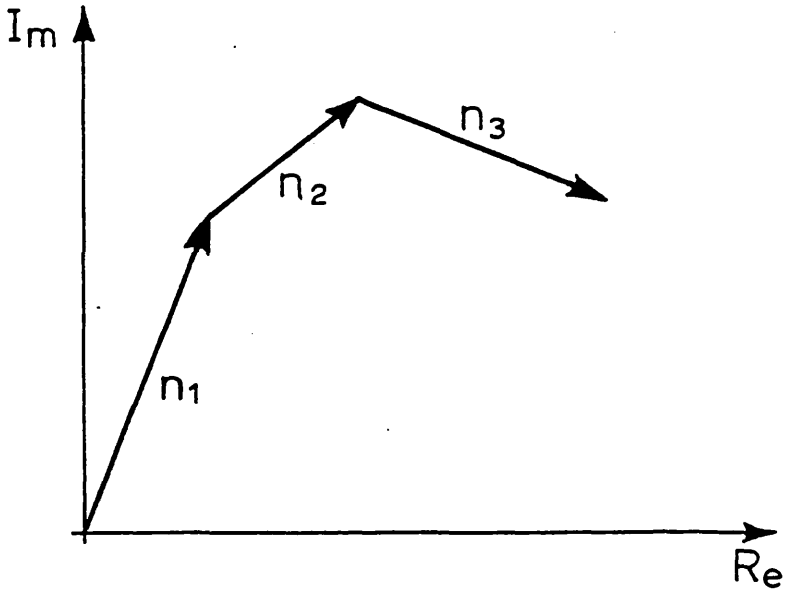

Fig. 2.21 - VECTOR REPRESENTATION OF THE D.F.

flux, ϕ_{dc}, different from zero exists. This in turn requires the existence of a direct component of excitation current and every harmonic order should be expected at the converter busbar [3]. Fig. 2.22 shows a simplified representation of the saturated primary current waveshape in a single phase transformer excited by a pure sinusoidal voltage.

If the postulated infinite busbar supplies only a.c. components under steady-state condition, there is no direct component of current through the primary winding of the converter transformer. However, if there exists a direct current through the secondary winding, it must be supplied somehow by the a.c. source. The problem may be solved by shifting the primary current reference as shown in Fig. 2.22(b). The secondary d.c. current is referred to the primary in such a way that Ampère's Law is satisfied:

$$\int H d\ell = N_1 I_1 = N_2 I_{dc}$$

where:

N_1, N_2 : primary and secondary number of turns, respectively

I_1 : reflected primary current

I_{dc} : average secondary current .

For analysis purposes, the primary current may be split into two components:

a) a current which is a function of the secondary load current including the direct component;

b) an excitation current which contains a direct component equal and opposite to the direct level of the referred load current.

It is assumed that any harmonic component which may be present in the secondary current is transferred to the primary but causes no

change in the core magnetization. The total core flux at instant "i" can then be given by :

$$\phi_i = \phi_{ac} + \phi_{dc}$$

where :

ϕ_{ac} : a.c. magnetic flux

ϕ_{dc} : d.c. magnetic flux.

Except in the case of severe resonance, the harmonic voltages cause second order effects on the total core flux [3] and ϕ_{ac} can be written as :

$$\phi_{ac} = \phi_m \sin(\omega_0 t + \theta)$$

where:

ϕ_m : maximum a.c. magnetic flux

ω_0 : fundamental frequency

θ : phase angle.

The maximum flux, ϕ_m, is related to the maximum phase voltage, V_m, by:

$$\phi_m = \frac{V_m}{N_1 \omega_0} .$$

The d.c. flux is related to the d.c. current by:

$$\phi_{dc} = \frac{LI_{dc}}{N_2} .$$

The magnetic flux density at instant "i" may be obtained from

$$B_i = \frac{\phi_i}{A}$$

where A is the average cross-sectional area of the transformer core.

The magnetizing force may be obtained from the iron core saturation curves, as shown in Fig. 2.23.

The BH curve shown in Fig. 2.23 may be approximated by some function :

$$H_i = f(B_i) \quad . \tag{2.10}$$

In a polynomial representation, eqn 2.10 becomes :

$$H_i = \sum_{k=0}^{n} a_k B_i^k \quad .$$

The current at instant "i" is determined by :

$$I_i = \frac{H_i \ell}{N_1}$$

where ℓ is the average magnetic path.

The current waveshape can be decomposed into its Fourier components.

It is shown in reference [3], that there exists an approximate linear relationship between lower order harmonics and the direct current. Under constant d.c. level, these harmonics do not disappear even if the transformer is underloaded.

The harmonic distortion may be defined as [2]

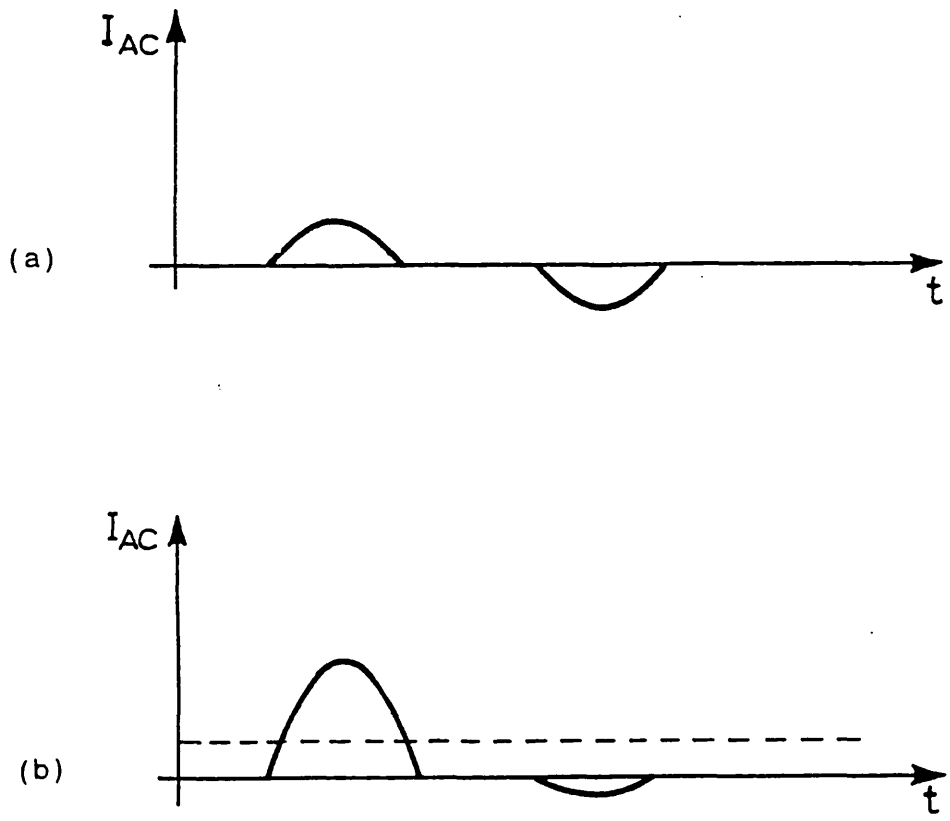

Fig. 2.22 - SATURATED CURRENT

(a) Saturated excitation current
(b) Effects of d.c. Flux Offset on the saturated excitation current

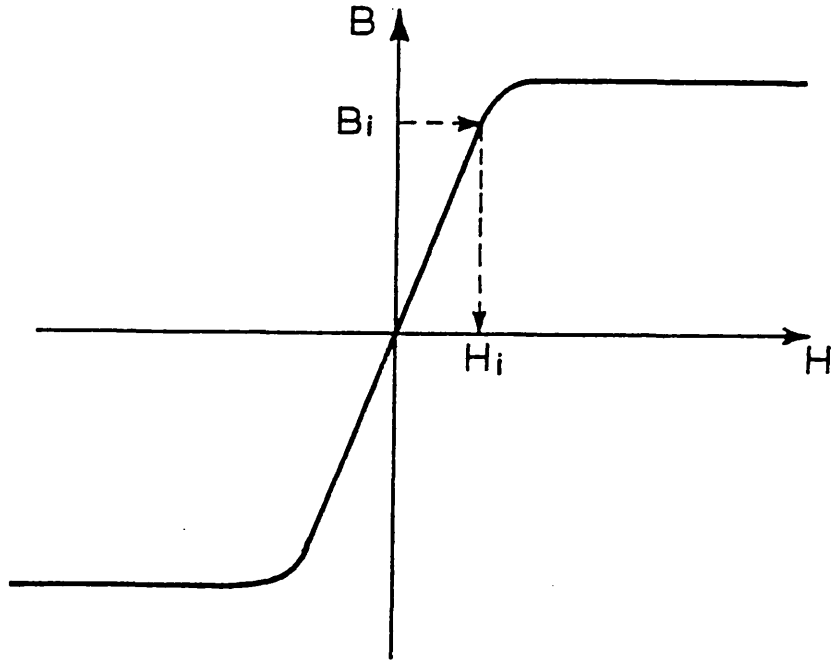

Fig. 2.23 - SATURATION CURVE (B×H)

$$D(\%) = \frac{\sqrt{\sum_{n=2}^{\infty} I_n^2}}{I_1}$$

where I_n is the harmonic current of order "n".

2.14 Effects on YY and YΔ transformers

The secondary d.c. current cannot be directly referred to the primary in terms of line-to-line values as for a.c. currents. The direct current must be related to the flux offset in phase-to-phase terms. Figs 2.24(a) and (b) show star-star and star-delta transformer connections, respectively with the associated current relationships.

Examples for YΔ transformer

a) $I'_R = - I_Y$

$I'_B = 0$

$Z_R = Z_Y = Z_B = R$.

Then: $I_R = - \frac{I'_R}{3T}$

$I_Y = + \frac{I'R}{3T}$

$I_B = 0$

b) $I'_Y = I'_B \quad \therefore \quad I'_R = - 2I'_Y$.

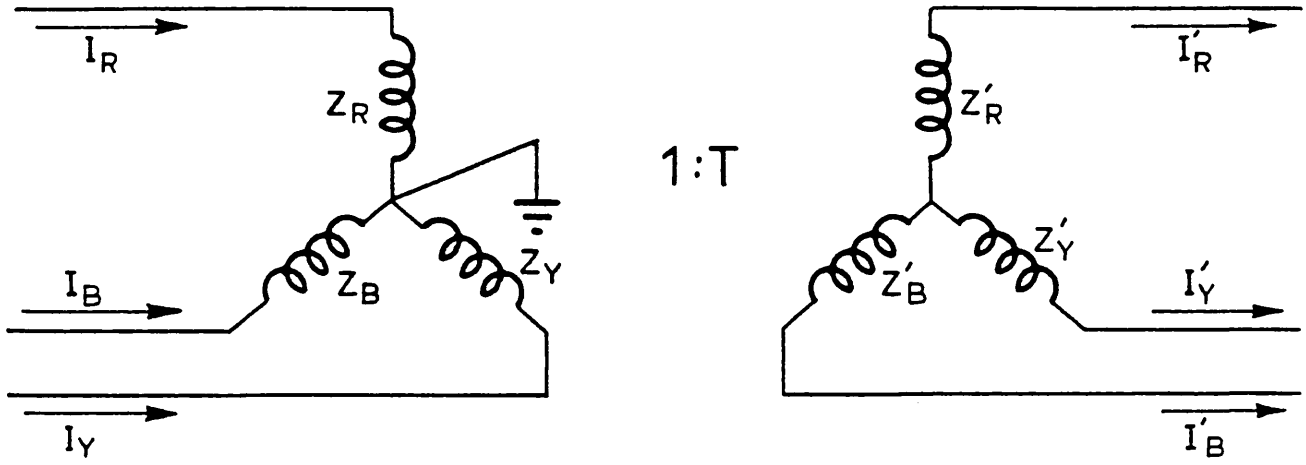

$$I_R = \frac{I'_R}{T} \qquad I_Y = \frac{I'_Y}{T} \qquad I_B = \frac{I'_B}{T}$$

$$T = \frac{V_1}{V_2} = \frac{N_1}{N_2} = \frac{I_2}{I_1}$$

Fig. 2.24 - YY-TRANSFORMER CONNECTION

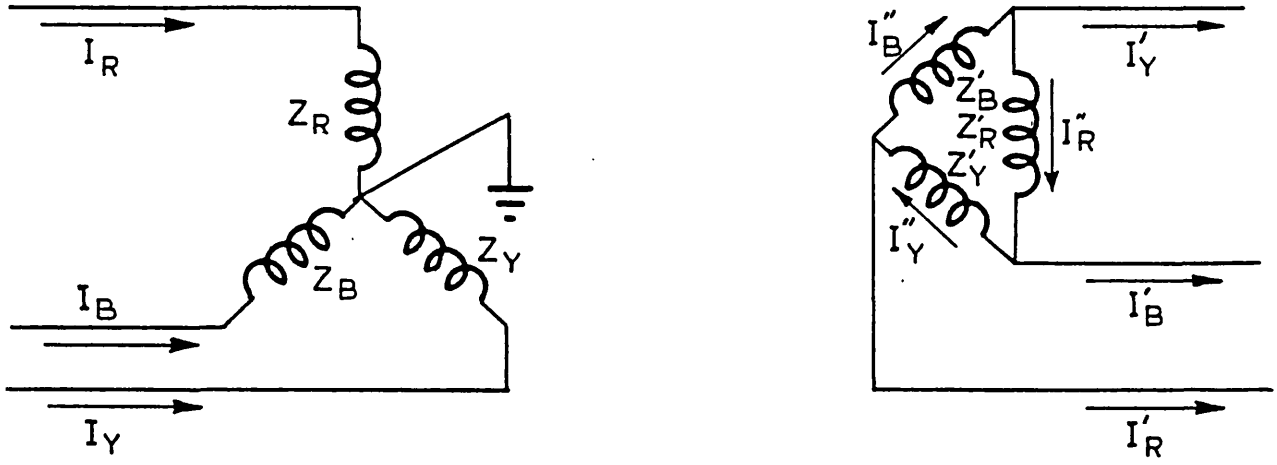

$$I_R = \frac{I''_R}{T} = \frac{I'_B Z'_Y - I'_Y Z'_B}{T(Z'_R + Z'_B + Z'_C)}$$

$$I_Y = \frac{I''_Y}{T} \quad \frac{I'_R Z'_R - I'_B Z'_R}{T(Z'_R + Z'_B + Z'_C)}$$

$$I_B = \frac{I''_B}{T} \quad \frac{I'_Y Z'_R - I'_R Z'_Y}{T(Z'_R + Z'_Y + Z'_B)}$$

Fig 2.24(b) - YΔ-TRANSFORMER CONNECTION

Then: $I_R = 0$

$$I_Y = \frac{I'_R}{T}$$

$$I_B = \frac{I'_R}{T} \quad .$$

From these examples it is clear that a transformer may be saturated or nonsaturated by the presence of d.c. current.

The block diagram of Fig. 2.25 describes the computer subroutine developed to include saturation effects in the iterative process used to solve the non-linear relationship between ϕ_{dc} and I_{dc}.

2.15 Saturation and Harmonic Generation

2.15.1 a.c./d.c. data

In order to study the effect of transformer saturation on the d.f., the following data were used:

a) a.c.-side

Line voltage = 100kV

SCR = 12

θ = 87.8 (source impedance angle)

b) Transformer characteristics

The a.c. power was supplied through 3 identical single-phase transformers connected in YY configuration:

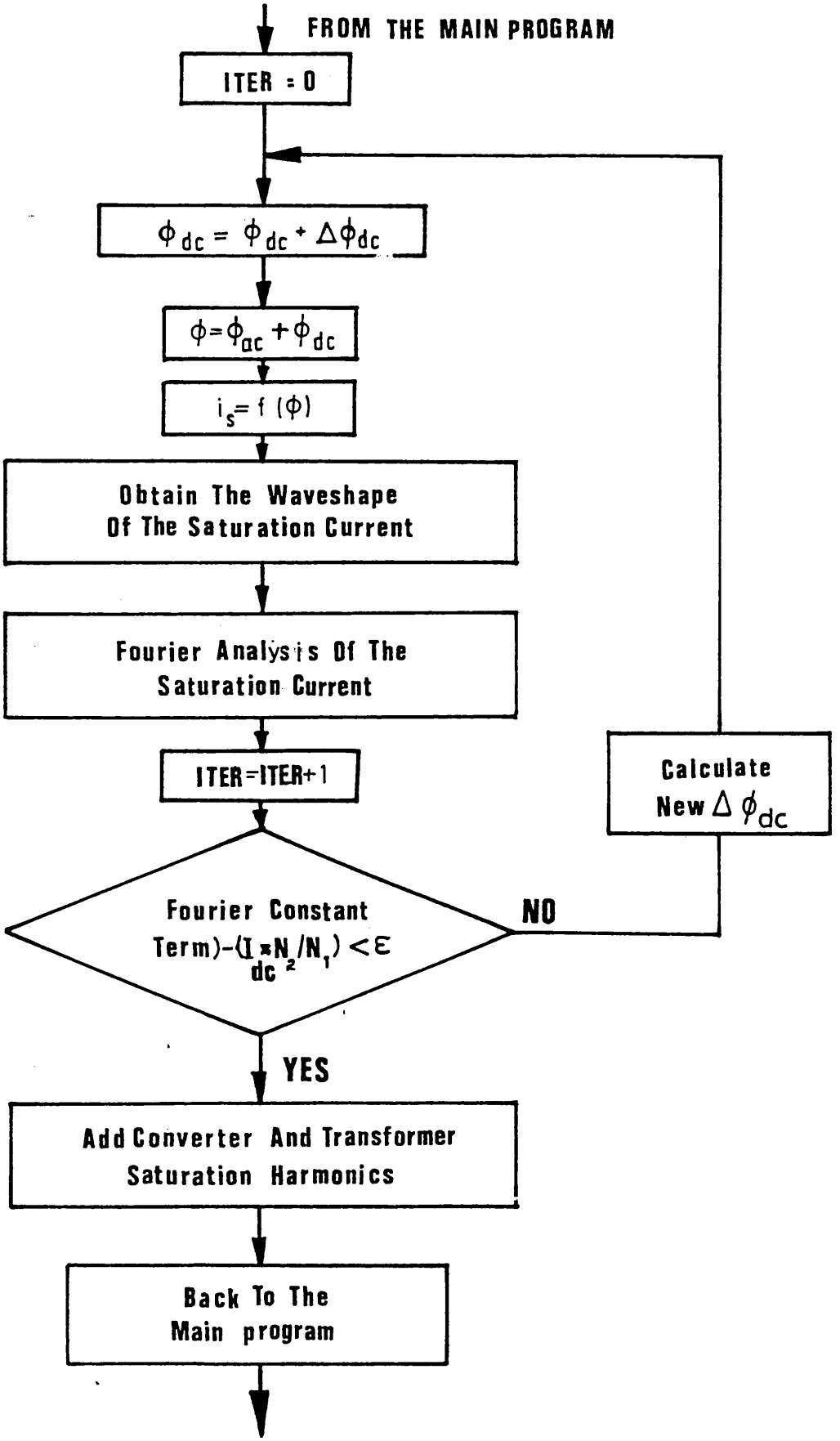

Fig. 2.25 - SUBROUTINE TO DERIVE TRANSFORMER SATURATION EFFECTS

Power (per transformer)	185MVA
Av. core length	2.71m
Av. core section	$0.64m^2$
Transformer ratio	160/58
Primary turns	2154
Core material	NUMETAL

Saturation curve given by four polynomial sections the coefficients of which are given in Table 2.5.

c) d.c.-side

d.c. transmission line

reactor

rectifier side : R = 1.6Ω; L = 0.3H

inverter side : R = 1.6Ω; L = 0.3H

line

R = 1.Ω ; L = .2H

I_{dc} = 2kA

P_{dc} = 500MVA

d) Control

6-pulses

$\alpha = 150°$

$k = 9/\pi \; Vd/V$

$V_m = 0.5V(\Delta\alpha=10°)$

TABLE 2.5

SATURATION CURVE OF NUMETAL IN TERMS OF A POLYNOMIAL

POLYNOMIAL COEFFICIENTS	B LIMITS IN TESLA				
	.0~.001	.001~.2	.2~.6	.6~.74	>.74
a_0	.0	.0	1.5	-61806.2	-76036.0
a_1	.0	22.7	-24.7	366512.2	104174.0
a_2	.0	-506.7	288.9	-810392.7	.0
a_3	.0	8188.8	-1532.7	790974.5	.0
a_4	.0	-95214.6	4315.9	-287071.7	.0
a_5	.0	591183.2	-6200.2	.0	.0
a_6	.0	-1921174.5	3628.3	.0	.0
a_7	.0	2525638.3	.0	.0	.0
a_8	.0	.0	.0	.0	.0
a_9	.0	.0	.0	.0	.0

2.15.2 Results

Figs 2.26 - 2.34 show the computer derived plots of the d.f. with and without transformer saturation. The following symbolic convention was used throughout the figures :

IH : order of the m.s. frequency

HARM1 : order of primary imposed harmonic (2% of the fundamental voltage)

POS.SEQ. : positive sequence of the imposed harmonic

NEG.SEQ. : negative sequence of the imposed harmonic

□ : discrete point of d.f. when transformer saturation is not taken into account

0 : discrete point of d.f. when transformer saturation is taken into account

The figures show that d.c. current through the transformer secondary distorts the d.f. locus. Furthermore, the d.c. current through each transformer phase changes as the m.s. phase varies. Over a complete d.f. cycle, the transformer may pass from a heavily saturated to an unsaturated state. The a.c. current percentage distortion may reach values of over 50% (of the primary fundamental current) in some of the cases studied.

The most prominent effect of saturation on the d.f. occurs when the m.s. frequency is 50Hz and a 2nd harmonic negative sequence distortion is present (Fig. 2.27). Primary a.c. current distortion as high as 50% was noticed due to high level of d.c. current caused by control disturbances. Lower distortions on the 50Hz d.f. were observed with positive or negative sequence 150Hz distortion imposed on the primary voltage (Figs. 2.28 - 2.29). Unbalances in the fundamental may also cause some alteration on the d.f. as observed in Fig. 2.34 plotted for a 2% fundamental distortion. Other combinations between m.s. and primary frequency harmonic distortion seem to have little effect on the d.f.

With a 100Hz m.s. the firing angles of the odd numbered valves are identically delayed by the same angle as the even ones are identically

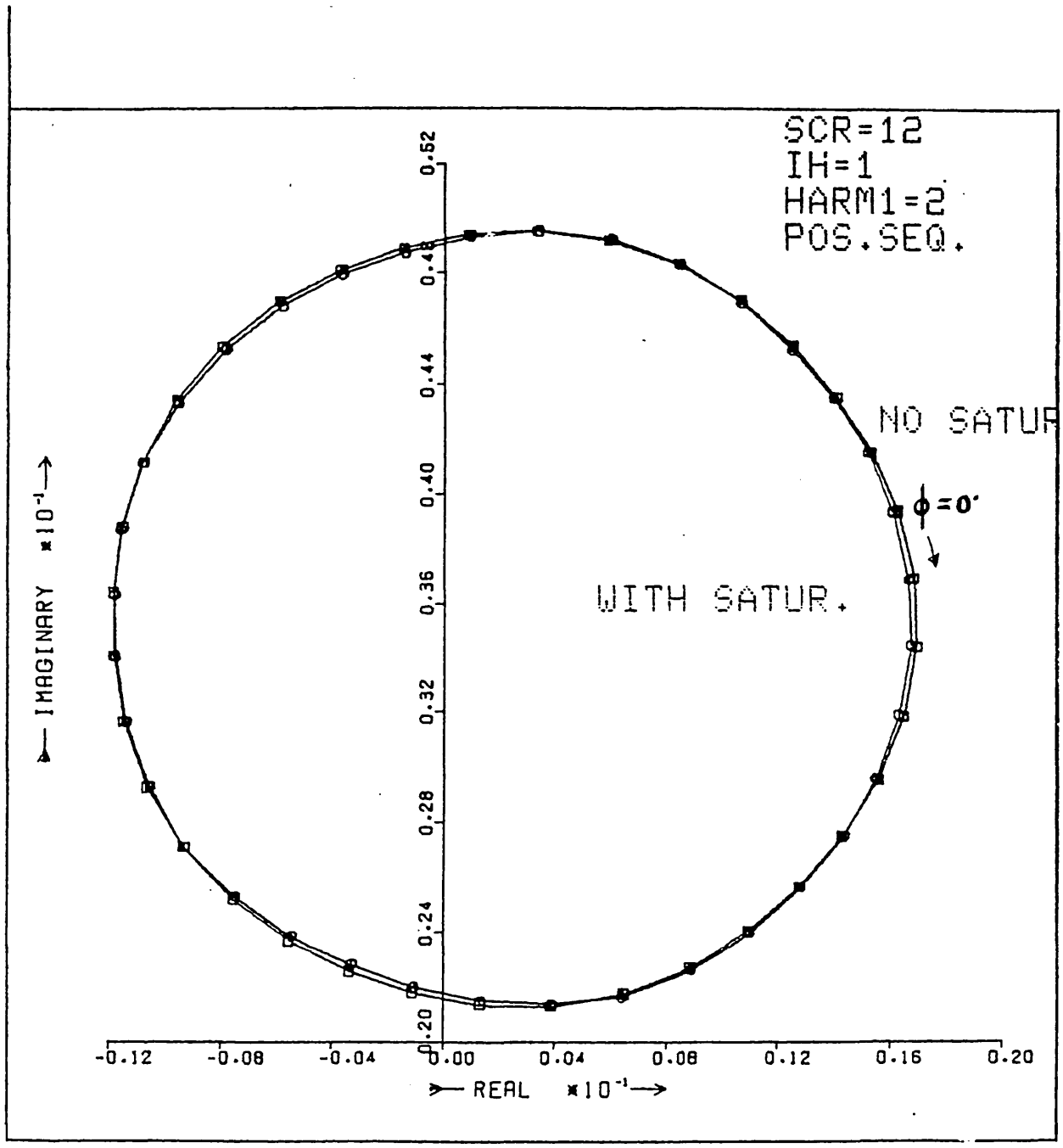
SCR=12
IH=1
HARM1=2
POS.SEQ.
NO SATUR
Φ=0°
WITH SATUR.
IMAGINARY ×10⁻¹
REAL ×10⁻¹
0.52
0.48
0.44
0.40
0.36
0.32
0.28
0.24
0.20
-0.12
-0.08
-0.04
0.00
0.04
0.08
0.12
0.16
0.20

Fig. 2.26

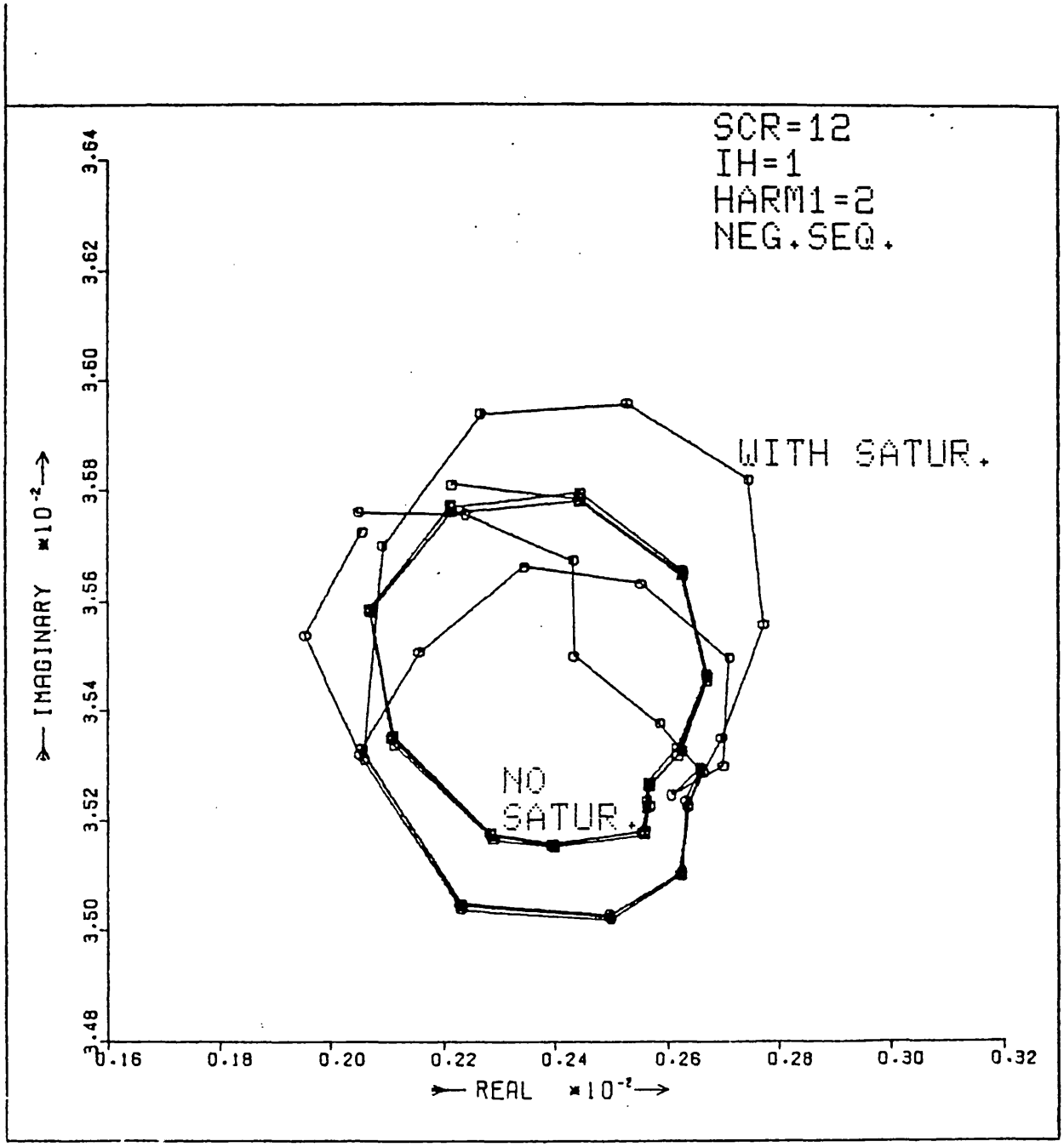
SCR=12
IH=1
HARM1=2
NEG.SEQ.
WITH SATUR.
NO SATUR.
IMAGINARY ×10⁻²
REAL ×10⁻²
3.48
3.50
3.52
3.54
3.56
3.58
3.60
3.62
3.64
0.16
0.18
0.20
0.22
0.24
0.26
0.28
0.30
0.32

Fig. 2.27

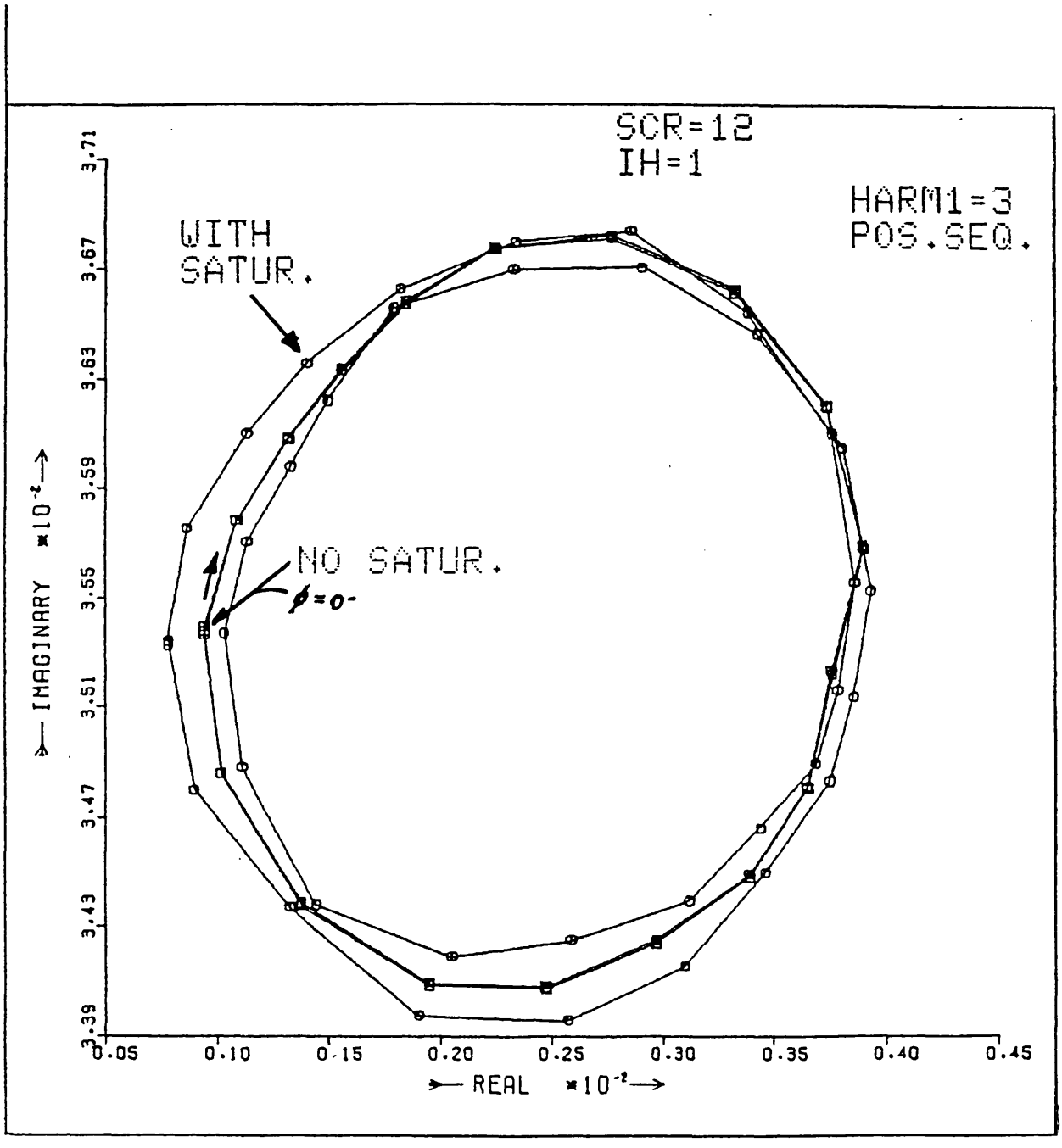
SCR=12
IH=1
HARM1=3
POS.SEQ.
WITH
SATUR.
NO SATUR.
ϕ=0°
IMAGINARY ×10⁻²
REAL ×10⁻²
3.39
3.43
3.47
3.51
3.55
3.59
3.63
3.67
3.71
0.05
0.10
0.15
0.20
0.25
0.30
0.35
0.40
0.45

Fig. 2.28

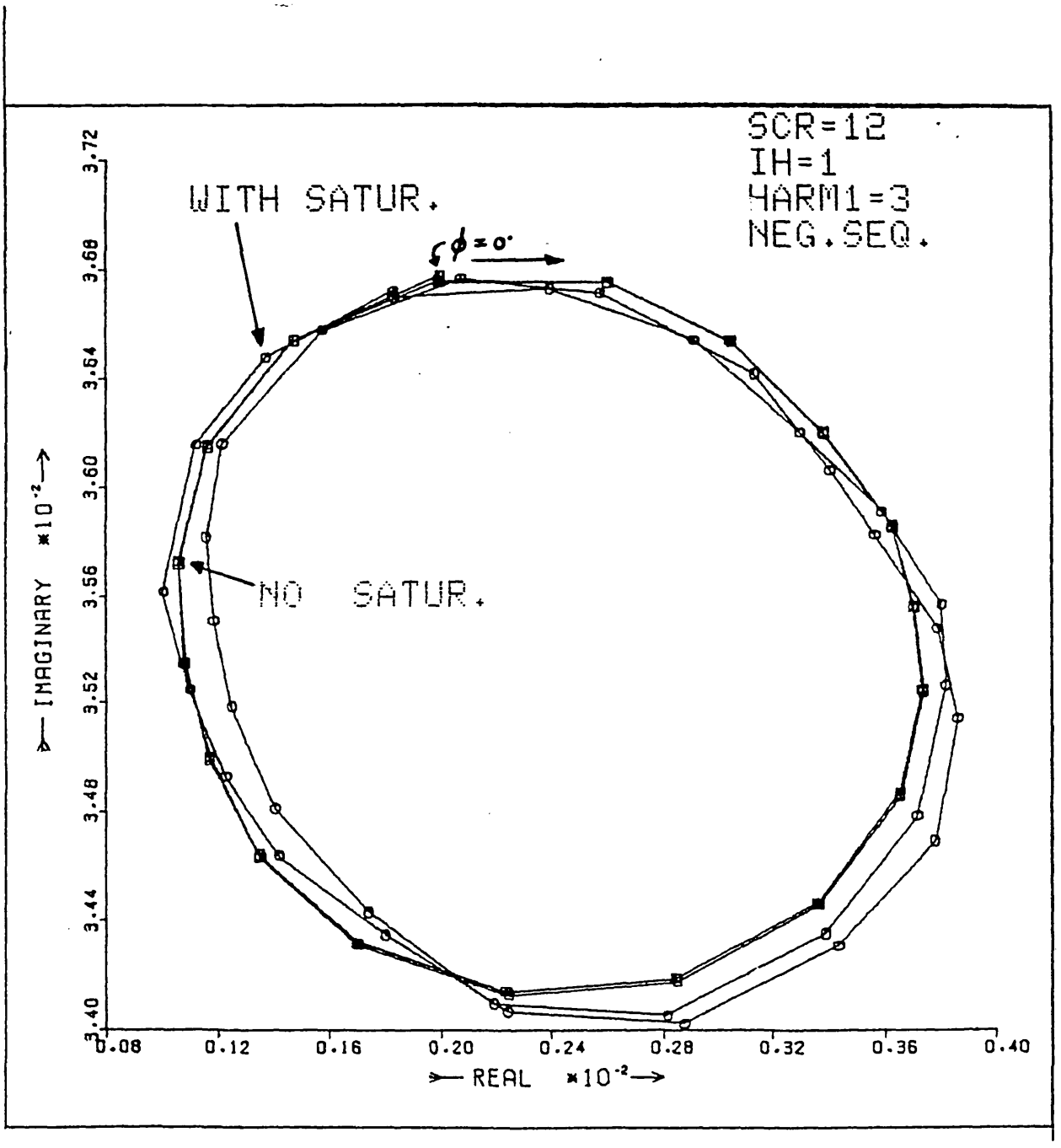
SCR=12
IH=1
HARM1=3
NEG.SEQ.
WITH SATUR.
NO SATUR.
$\phi = 0°$
IMAGINARY $\times 10^{-2}$
REAL $\times 10^{-2}$
3.40
3.44
3.48
3.52
3.56
3.60
3.64
3.68
3.72
0.08
0.12
0.16
0.20
0.24
0.28
0.32
0.36
0.40

Fig. 2.29

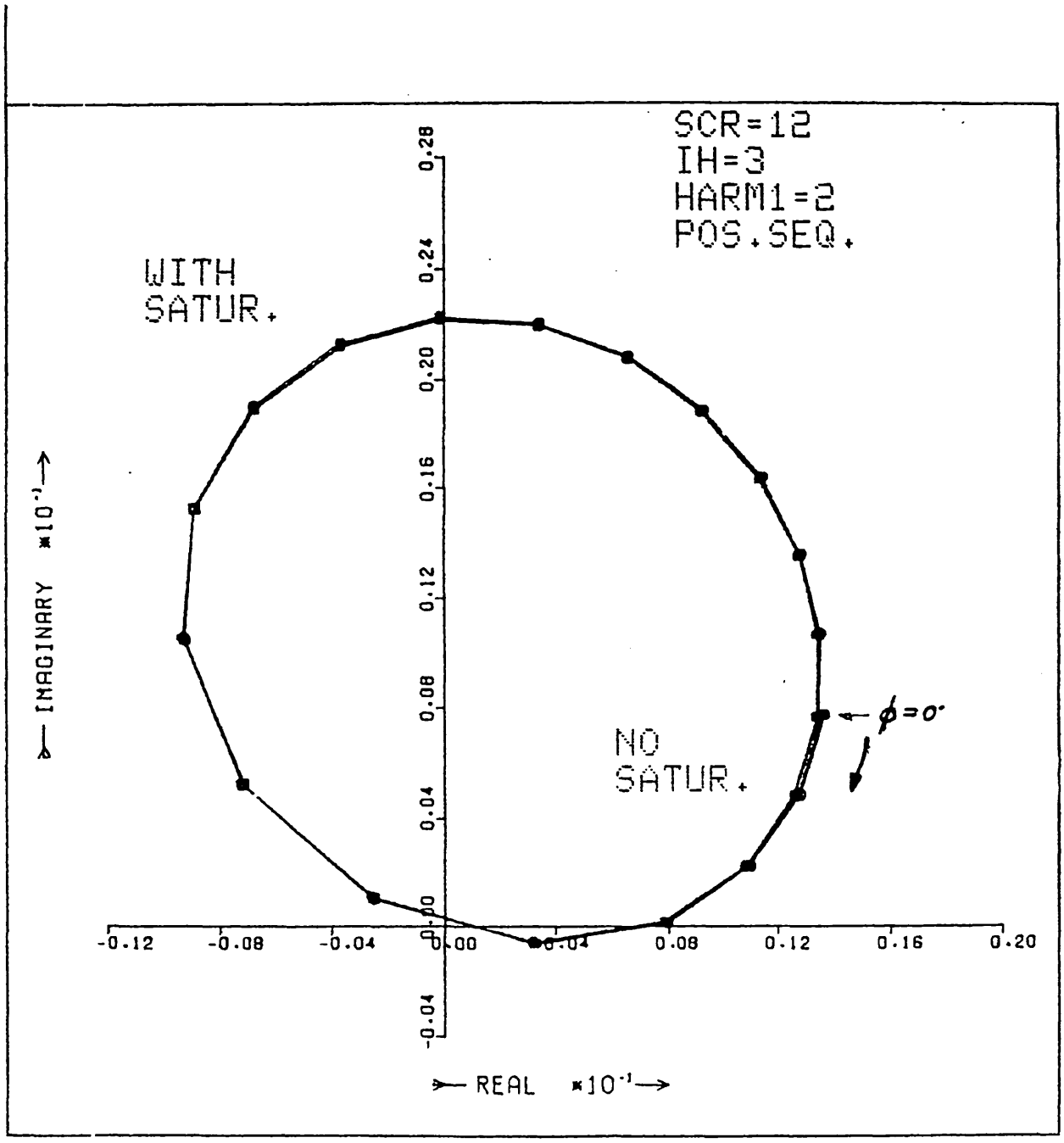
SCR=12
IH=3
HARM1=2
POS.SEQ.
WITH
SATUR.
NO
SATUR.
φ=0°
IMAGINARY ×10⁻¹
REAL ×10⁻¹
0.28
0.24
0.20
0.16
0.12
0.08
0.04
0.00
-0.04
-0.12
-0.08
-0.04
0.00
0.04
0.08
0.12
0.16
0.20

Fig. 2.30

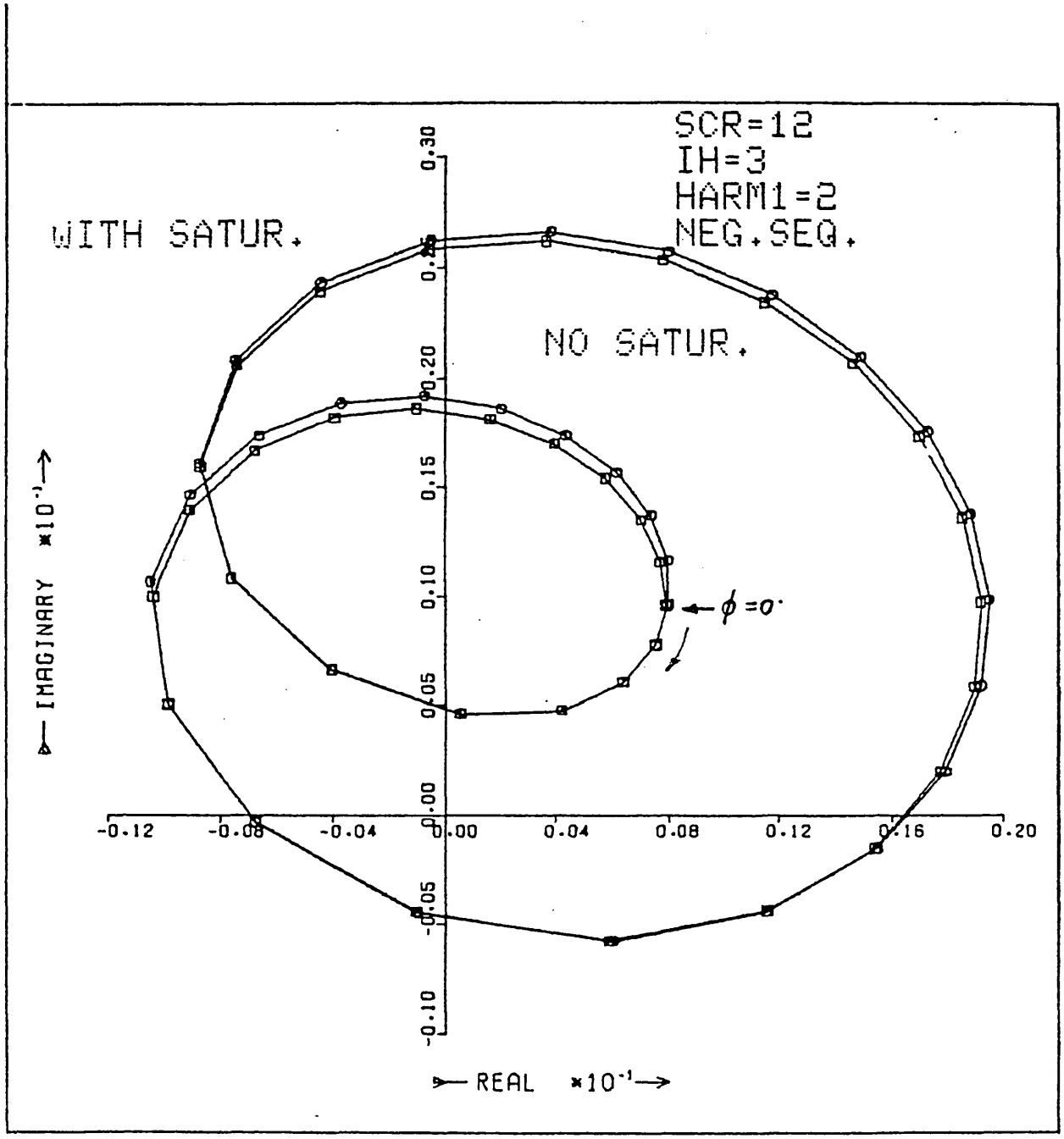
SCR=12
IH=3
HARM1=2
NEG.SEQ.
WITH SATUR.
NO SATUR.
φ =0°
IMAGINARY ×10⁻¹
REAL ×10⁻¹
0.30
0.20
0.15
0.10
0.05
0.00
-0.05
-0.10
-0.12
-0.08
-0.04
0.00
0.04
0.08
0.12
0.16
0.20

Fig. 2.31

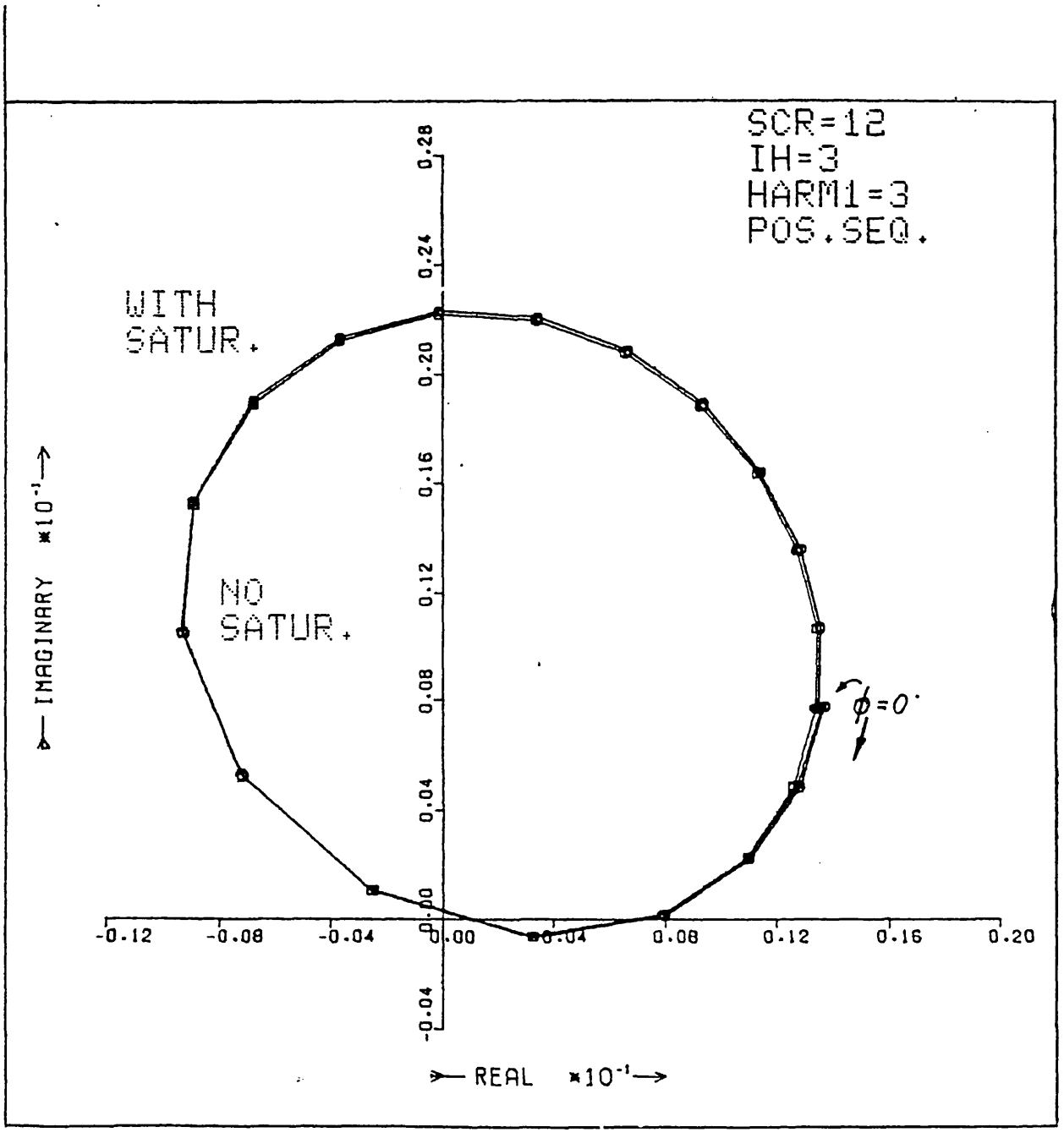
SCR=12
IH=3
HARM1=3
POS.SEQ.
WITH
SATUR.
NO
SATUR.
IMAGINARY ×10⁻¹
REAL ×10⁻¹
φ=0°
0.28
0.24
0.20
0.16
0.12
0.08
0.04
0.00
-0.04
-0.12
-0.08
-0.04
0.00
0.04
0.08
0.12
0.16
0.20

Fig. 2.32

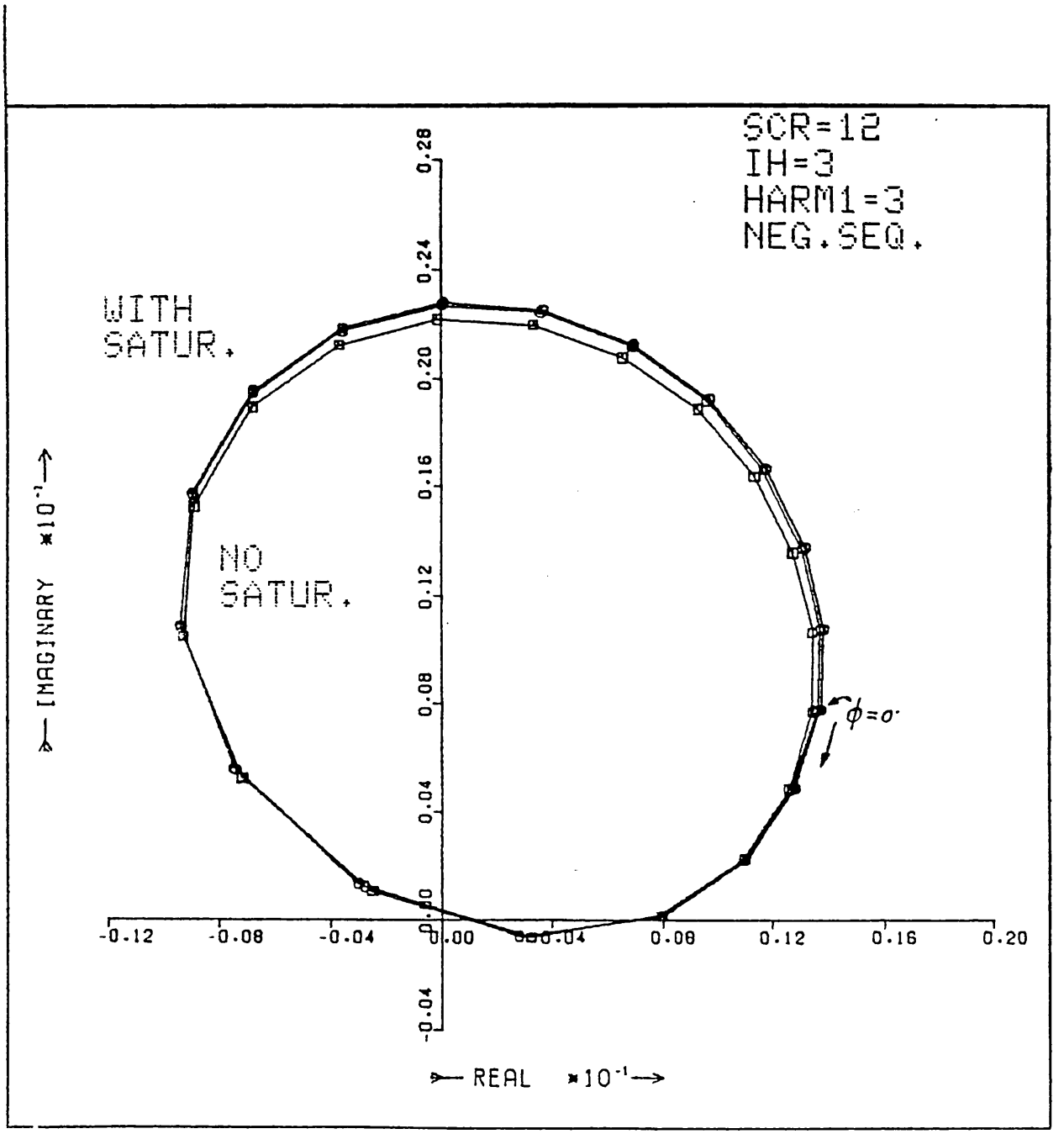
SCR=12
IH=3
HARM1=3
NEG.SEQ.
WITH
SATUR.
NO
SATUR.
IMAGINARY *10⁻¹
REAL *10⁻¹
φ=0°
0.28
0.24
0.20
0.16
0.12
0.08
0.04
0.00
-0.04
-0.12
-0.08
-0.04
0.00
0.04
0.08
0.12
0.16
0.20

Fig. 2.33

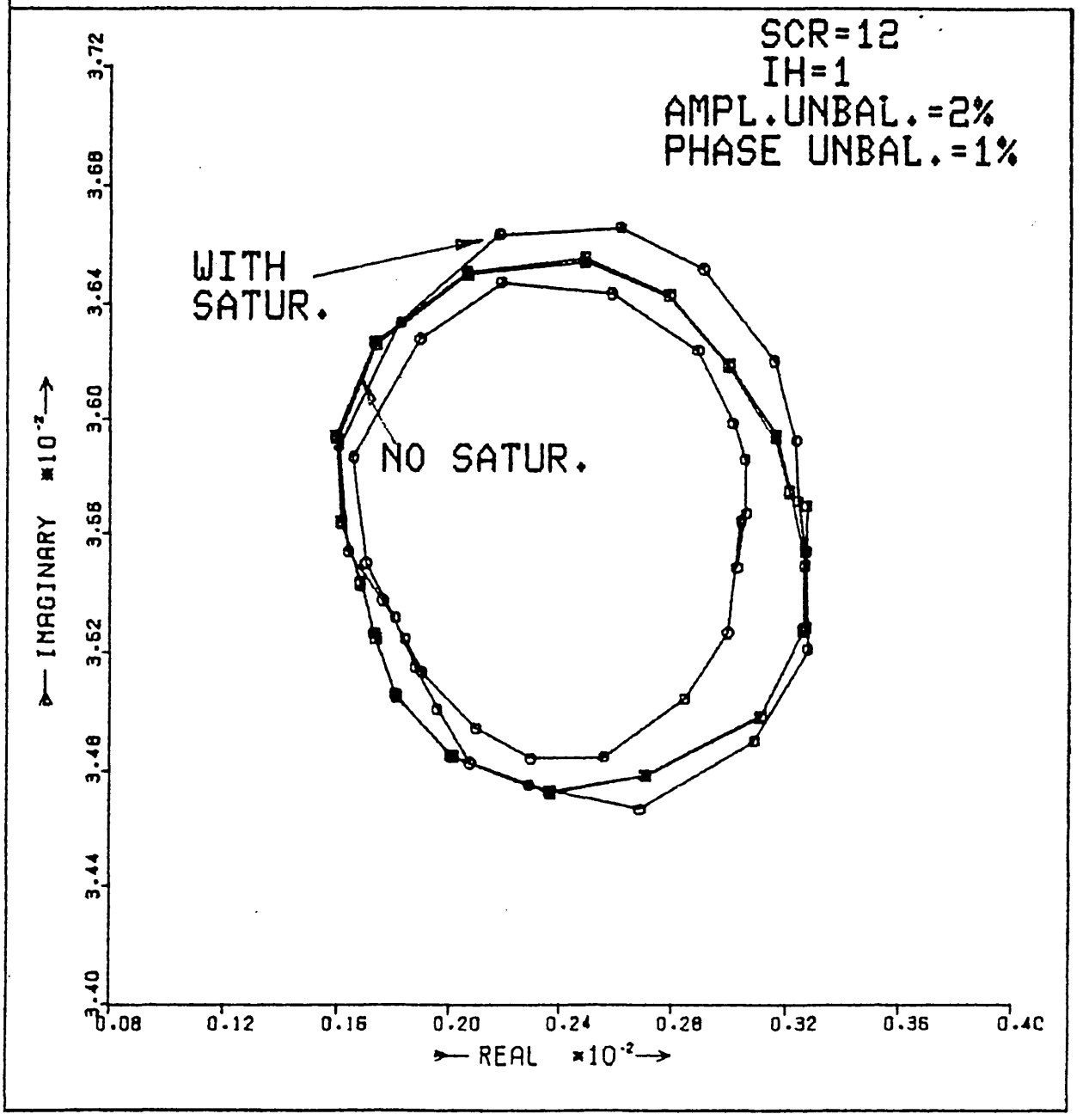
SCR=12
IH=1
AMPL.UNBAL.=2%
PHASE UNBAL.=1%
WITH SATUR.
NO SATUR.
INAGINARY ×10⁻²
REAL ×10⁻²
3.72
3.68
3.64
3.60
3.56
3.52
3.48
3.44
3.40
0.08
0.12
0.16
0.20
0.24
0.28
0.32
0.36
0.40

Fig. 2.34

advanced. The commutation angles follow a similar pattern of change as discussed in Chapter 3. Under these conditions and with balanced undistorted source voltages, the net d.c. current level was negligibly low. As a consequence, transformer saturation has little effect on the 100Hz d.f., even under primary distortions (2nd or 3rd harmonic of positive or negative sequence) or fundamental imbalances.

In general, transformer saturation tends to enlarge the d.f. locus. However, this enlargement is not very pronounced when compared to the effect of other imbalances and/or distortion examined previously.

2.16 Conclusion

Describing functions obtained for both 6- and 12- pulse converters under similar operating conditions, exhibit only slight differences. The most noticeable difference seems to be the one relating to fundamental imbalances on the a.c. source for a 100Hz m.s. . This is possible due to the 6th harmonic elimination in 12-pulse operation.

The study of 12-pulse converters resulted in some interesting observations on converter d.f's. For example, it was established that the d.f. can shift from one quadrant to another through changes in the d.c. line impedance. It was also noticed that the d.f. size decreases as the m.s. frequency gets closer to the d.c. line antiresonant frequency and increases as the m.s. frequency gets closer to the d.c. line resonant frequency.

Imposed harmonics at the primary converter busbar of the same frequency as the m.s. seem not to affect the d.f. . This is especially true for the 3rd harmonic when the phase voltage difference is zero.

It was demonstrated that the maximum m.s. amplitude to preserve continuity of the d.f. locus should not exceed K/k. This is imposed by the maximum positive tangent to the m.s. . It was also established that in the case of balanced a.c. sources the d.f. is periodic.

The d.f. may be represented by the summation of three distinct vectors. This possibility of decomposition was surmised from the shapes of the d.f. loci and from the apparent independence of the effect on these loci of (a) the harmonics on the a.c. system and (b) the m.s. imposed on the control voltage.

When the saturation characteristic of the transformer is simulated, the d.c. current through the secondary winding of the transformer alters the shape of the locus, particularly when the m.s. is 50Hz. These alterations are approximately proportional to the d.c. current.

A 2nd harmonic of negative sequence has the most pronounced effect on the 50Hz d.f. . Third harmonic of positive or negative sequence has little effect on the 50Hz d.f. and virtually no effect on d.f.'s of other frequencies.

The effect on the d.f. of transformer saturation is negligible for m.s. frequencies of order higher than one. Symmetrical transformer saturation (zero offset flux) has similarly a negligible effect on the d.f. of any frequency.

CHAPTER 3

THEORY OF UNCHARACTERISTIC HARMONIC GENERATION

3.1 Introduction

Studies using d.f. techniques have shown that the m.s. applied to the control voltage has a profound effect on the d.c. line uncharacteristic harmonic currents. These studies have also shown that presence of harmonic distortion in the a.c. busbar voltage causes distortion in the d.c. line current ripple and therefore, affects the nature of the d.f. . One reason for such distortions is the valve asymmetrical firing pattern caused by the closed loop nature of constant current control. A second reason is that the d.c.-side harmonics are related to those on the a.c.-side even if no closed loop current control is used.

If uncharacteristic a.c.- and d.c.-side harmonics are interrelated through the m.s. then, any a.c.-side harmonic content can be modified by acting upon the m.s. . It follows that modification of the control voltage could force the converter to generate such uncharacteristic harmonics so that the presence of selected undesired harmonics on the a.c.-side are minimized.

In Chapter 5, a method of harmonic minimization based on control voltage modulation is proposed. The method is based on the approximate linearity existing between a.c.-side and the d.c.-side harmonics generated either by control voltage modulation or by unbalances in the a.c. system.

The relations underlying the harmonic minimization method, are derived in the following sections.

Fig. 3.1 is a "cause and effect" flow chart illustrating the

interactions amongst parameters in a controlled converter connected in an a.c. system of finite source reactance.

The relationships of interest are:

a) firing angle variation, $\Delta\alpha$, and amplitude, V_m, of the m.s.;

b) firing angle variation, $\Delta\alpha$, and a.c. busbar harmonic voltage, V_{ak}, of order k.

c) firing angle variation, $\Delta\alpha$, and d.c.-side harmonic current, I_{dk} of order k.

d) a.c.-side harmonic voltage, V_{ak}, and d.c.-side harmonic voltage, V_{dk}.

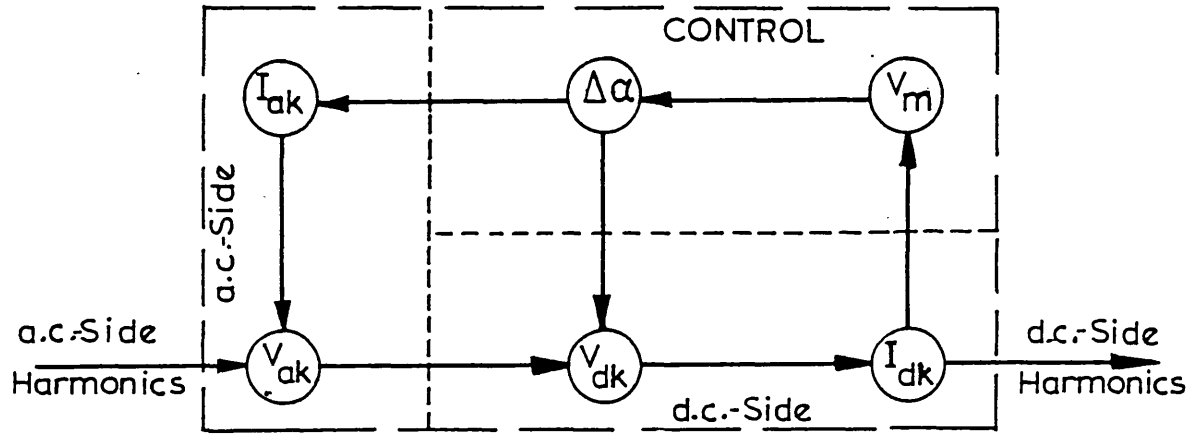

Fig. 3.1 - DIAGRAM OF HARMONIC INTERACTION

In addition, this chapter deals with the

a) generation of uncharacteristic harmonics due to a.c. source unbalances;

b) effect of 6- or 12-pluse operation on characteristic harmonics.

3.2 Control Voltage Modulation due to d.c. Current Ripple

The schematic diagram of a constant current control scheme is shown in Fig. 3.2. (a). It is based on the measurement of the d.c. - line current, I_{dc}, which is transformed into its analogue quantity, I'_{dc}, and compared to a reference value, I_{ref}. The difference is amplified and processed in the Error Processing Unit (E.P.U) the output from which shifts the train of firing pulses in such a way that the error is reduced.

The d.c. current transducer and the E.P.U. have, both, a low-pass characteristic. The d.c. current transducer has a fast time response in comparison with the usual time response encountered in h.v.d.c. controllers. For example, the time response, T_1, of an LEM-type of current monitoring sensor is about 1μs.

In the Imperial College h.v.d.c. converter, a Hall Effect device is used for d.c. current measurements. The time constant of this device plus output amplifier is about $T_1 = 0.18$ms and the transfer function is given by:

$$H_1(s) = \frac{K_1}{1+sT_1} \quad . \qquad (3.1)$$

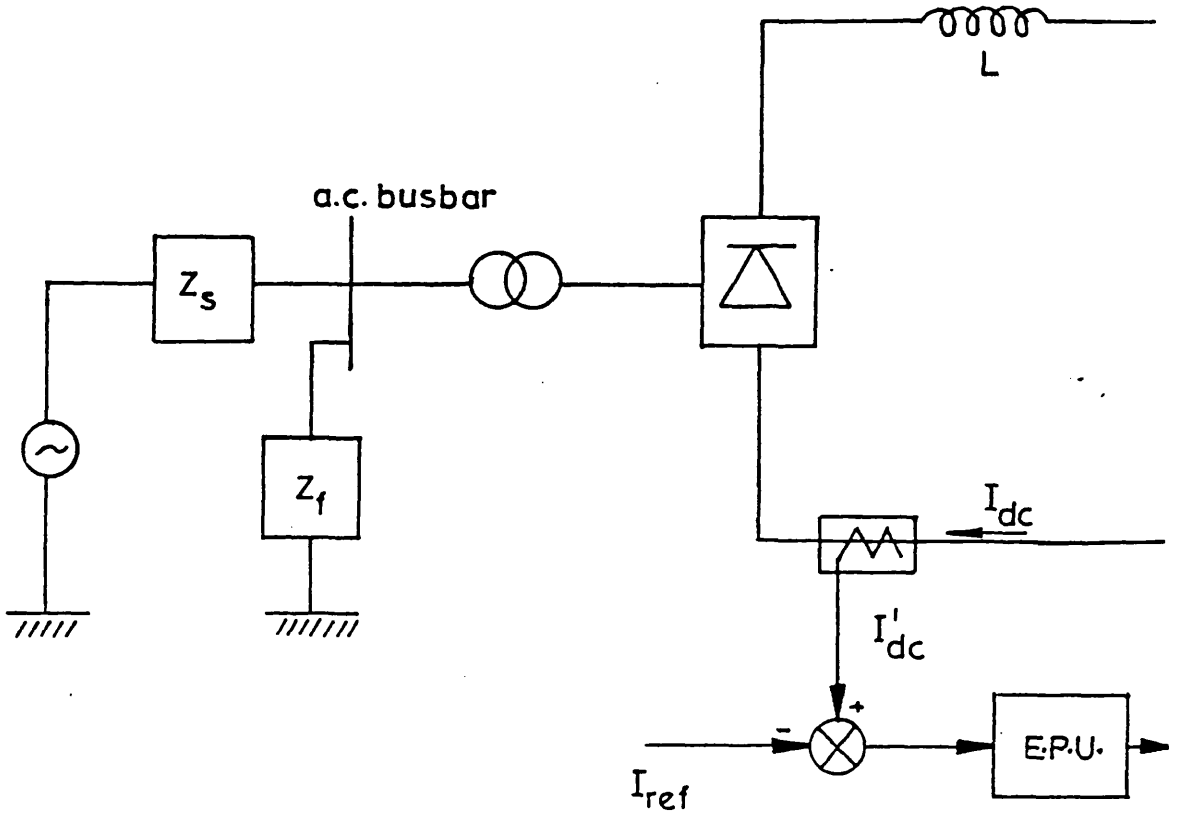

(a) Schematic diagram of a constant current control.

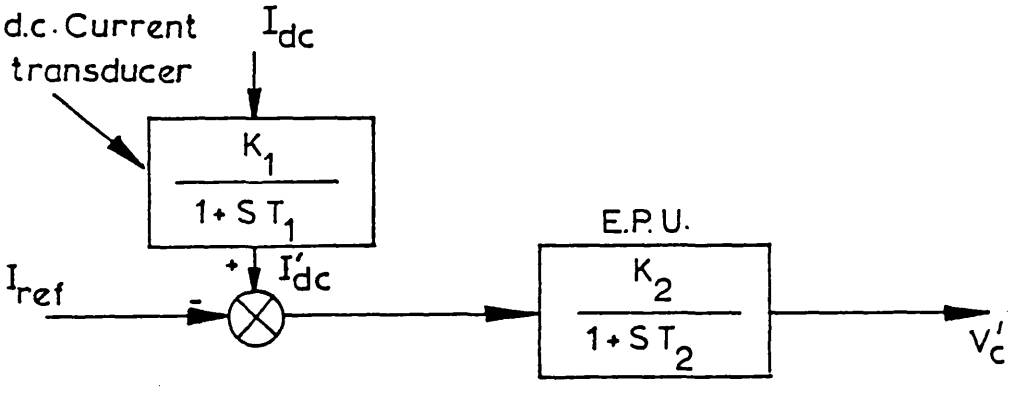

(b) Analog circuit to produce the control voltage.

V'_c Control voltage.

Z_f Filter impedance.

Z_s a.c. System impedance.

E.P.U. Error processing unit.

Fig. 3.2 - CONSTANT CURRENT CONTROL

The E.P.U. is basically a low-pass amplifier whose transfer function is given by:

$$H_2(s) = \frac{K_2}{1+sT_2} \quad . \tag{3.2}$$

The transfer function of the constant current controller of Fig. 3.2(b) is therefore:

$$V'_c = \frac{K_2}{1+sT_2}\left(\frac{K_1}{1+sT_1} I_{dc} - I_{ref}\right) \tag{3.3}$$

Equation 3.3 may be simplified if the reference current, I_{ref}, is assumed to be a ripple free d.c. level. For frequencies different from zero, eqn 3.3 becomes :

$$\frac{V'_c}{I_{dc}} = \frac{K_1K_2}{(1+sT_1)(1+sT_2)} \quad . \tag{3.4}$$

3.3 Linearity between $\Delta\alpha$ and V_m

Operation of modern valve firing systems (equally spaced firing pulses) is based on a voltage-controlled oscillator (V.C.O.) which, in the steady state, operates at p times the a.c. frequency. A firing pulse is produced each time the control voltage equals the ramp voltage. The angle at which this occurs can be obtained from Fig. 3.3 as :

$$Kx_3 = V - V_0 + V_m \sin(x_0 + x_3) \tag{3.5}$$

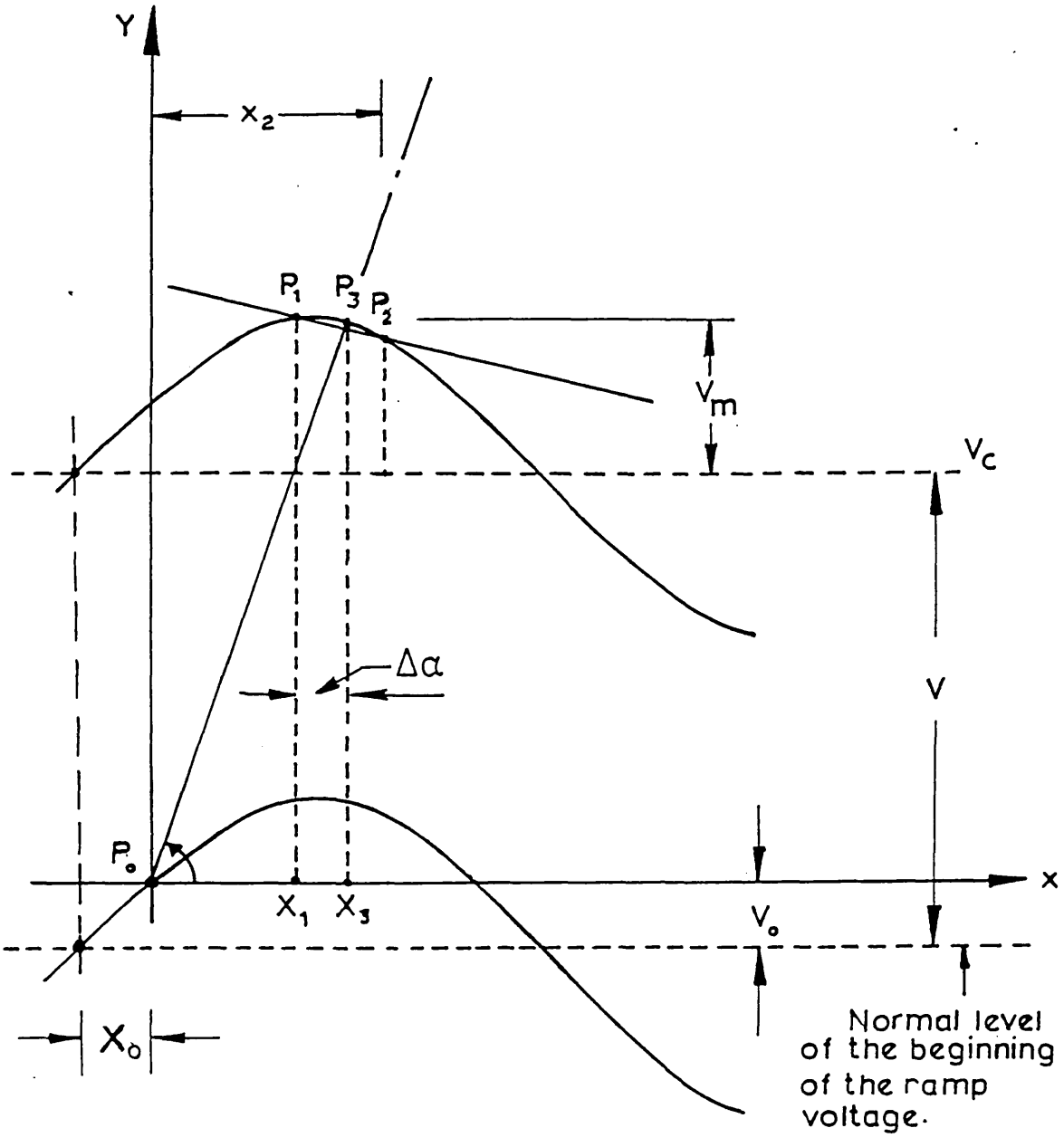

Fig. 3.3 - FIRING ANGLE VARIATION DUE TO A M.S. SUPERIMPOSED ON AN IDEALLY FLAT CONTROL VOLTAGE

where

K - slope of the ramp voltage (V/degrees)

x_3 - interfiring period in degrees.

$$V = \frac{360}{p} K$$

V_0 - offset level at the beginning of the ramp voltage with respect to the ideally flat control voltage.

V_m - modulating signal amplitude

x_0 - phase difference between the instant at which the m.s. goes positive and the instant at which the next firing occurs.

In what follows the time reference is always the instant at which the last firing pulse occurred, e.g. point P_0 in Fig. 3.3. Every firing pulse defines a new reference for the next firing pulse. The offset, V_0, changes at each new reference.

Eqn 3.5 is a transcendental equation and it can be solved by numerical methods [1]. In order to establish an approximate linearity between $\Delta\alpha$ and V_m, an analytical solution is necessary. An approximate formula to relate those two quantities is developed below.

$P_0(x_0,y_0)$ is the instant when the last firing occurred. This is the instant taken as the origin of the coordinate system.

$P_1(x_1,y_1)$ defined by the instant when the ramp voltage would equal the ideally flat level of the control voltage.

$P_2(x_2,y_2)$ obtained by adding to x_1, an angle defined by the maximum limits within which, the solution of eqn 3.6 is acceptable.

$P_3(x_3,y_3)$ coordinates of the exact solution of eqn 3.5.

An approximate solution of eqn 3.5 is the intersection point between line $\overline{P_0\text{-}P_3}$ and line $\overline{P_1\text{-}P_2}$. Line $\overline{P_1\text{-}P_2}$ is expressed analytically by:

$$y - y_1 = \frac{y_2 - y_1}{x_2 - x_1}(x - x_1) \tag{3.6}$$

where:

$$x_1 = \frac{V - V_0}{K} \tag{3.7}$$

$$V_0 = V_m \sin x_0 \tag{3.8}$$

$$y_1 = V - V_0 + V_m \sin(x_0 + x_1) \tag{3.9}$$

$$x_2 = \frac{V_m}{K} \sin(x_0 + x_1) + x_1 \tag{3.10}$$

$$y_2 = V - V_0 + V_m \sin(x_0 + x_2) \tag{3.11}$$

Eqn 3.6 can be written more explicitly as :

$$y - y_1 = K(a-1)(x-x_1) \tag{3.12}$$

where:

$$a = \frac{\sin(x_0+x_2)}{\sin(x_0+x_1)} .$$

Furthermore, line $\overline{P_0 - P_3}$ can be expressed by:

$$y = Kx. \tag{3.13}$$

The intersection between lines $\overline{P_1 - P_2}$ and $\overline{P_0 - P_3}$ is obtained from the simultaneous solution of eqns 3.12 and 3.13. The solution for coordinate "x" is the approximate interfiring period which is given by:

$$x \cong x_3 = \frac{(V-V_0)(2-a) + V_m \sin(x_0+x_1)}{K(2-a)} \qquad (3.14)$$

Table 3.1 gives a comparison between interfiring periods calculated from the solution of eqn 3.5 using the Newton-Raphson method and from eqn 3.14. The largest difference between the two solutions does not exceed 0.1%.

TABLE 3.1 - INTERFIRING PERIOD CALCULATED BY EQNS 3.5 AND 3.14

(V_m = 0.5 Volts; YΔ)

VALVE No.	x_0	NEWTON-RAPHSON	EQN 3.14
1	17.99	66.87	66.88
2	84.87	56.32	56.31
3	141.17	51.52	51.53
4	197.48	53.08	53.09
5	245.79	61.12	61.12
6	306.90	71.09	71.09

The variation $\Delta\alpha$, due to the m.s. is defined as :

$$\Delta\alpha = x_3 - x_1 \quad . \qquad (3.15)$$

Without m.s., $x_1 = 360/p$ and x_1, in eqn 3.10, becomes approximately equal to x_2 for small values of V_m/K (say, for $V_m/K < 10^o$). As a consequence, $a \cong 1$. Furthermore, in eqn 3.7, $V_0 << V$ or $x_1 \cong V/K$. On these basis, eqn 3.15 can be simplified to become:

$$\Delta\alpha = \frac{V_m}{K} \sin(x_0 + \frac{V}{K}) \quad . \tag{3.16}$$

Eqn 3.16 shows that $\Delta\alpha$ varies linearly with, V_m for small values of V_m/K. Eqns 3.15 and 3.16 are plotted in Fig. 3.4 where only negligible error is introduced through the use of the simplified form.

3.4 Effect of the Control Voltage on Characteristic Harmonics

A brief introduction of the basic theory of harmonic analysis in converters[2] is necessary as a preamble to the understanding of the relationship between $\Delta\alpha$ and the amplitude of uncharacteristic harmonics.

Assuming: a) supply voltage perfectly sinusoidal; b) infinite d.c. line reactance; c) equally spaced firing pulses; d) zero commutating impedance and e) infinite a.c.-side short-circuit ratio, converter operation produces only characteristic harmonics, i.e. :

$k = np \pm 1$ for the a.c.-side

$k = np$ for the d.c.-side

where:

k - is the harmonic order

p - number of pulses

n - any integer number.

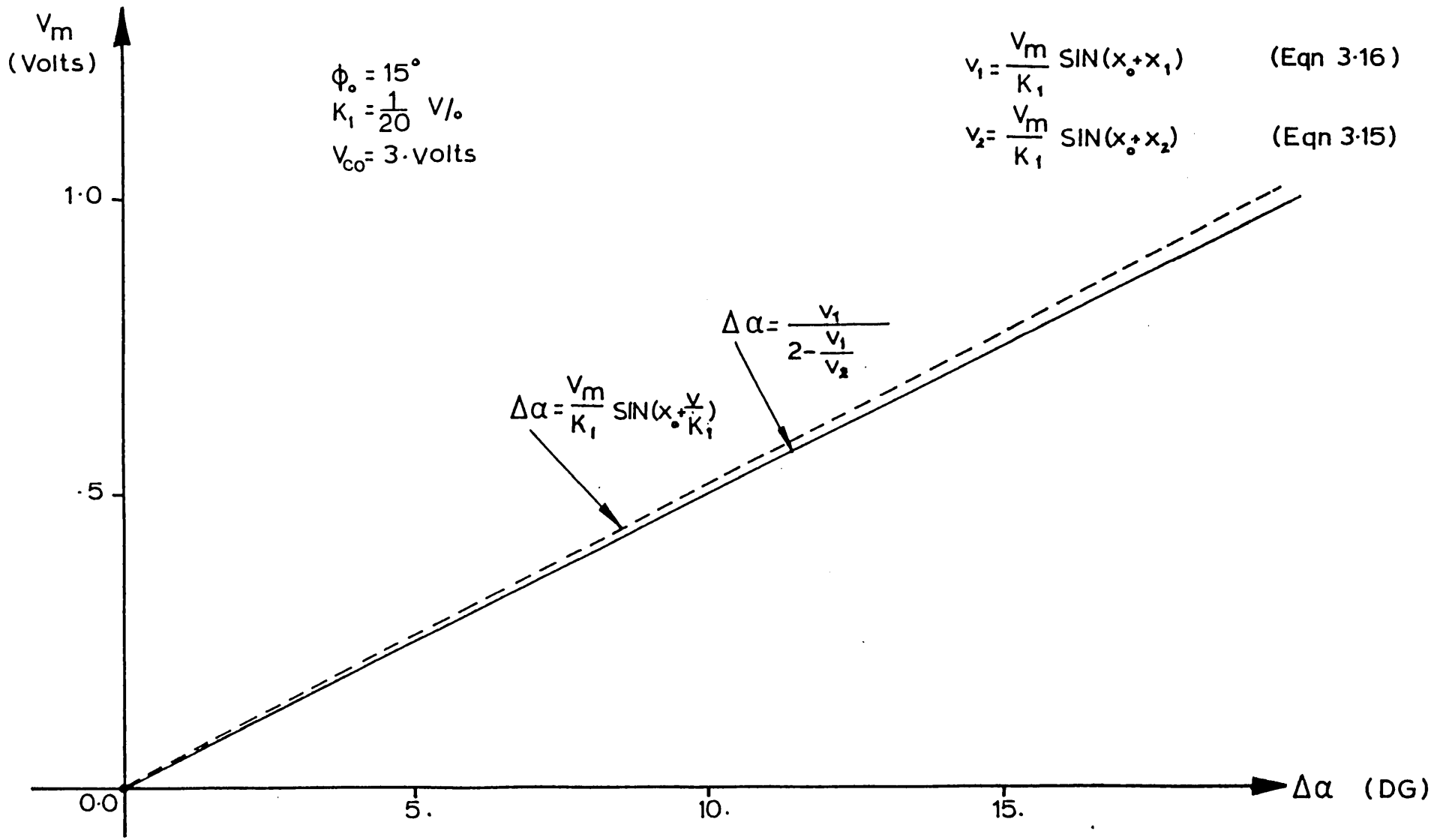

Fig. 3.4 - COMPARISON BETWEEN THE SOLUTIONS GIVEN BY EQN 3.15 AND EQN 3.16

In a 6-pulse converter, the a.c. line currents on the valve side of the transformer , would consist of a series of equally spaced rectangular blocks of current, alternatively positive and negative, as shown in Fig. 3.5(a). Each pulse has a similar pattern except that, the blocks are shifted by multiples of 120^{o}. For this reason, only phase "a" is represented in Fig. 3.5(b). Associated to each block of current, there is one letter (a, b or c) and one number (1, 2, 3, 4, 5 or 6). The letter indicates the a.c. phase to which the valve is connected and, the number indicates the conducting valve.

Fourier analysis may be performed on the current waveforms presented in Fig. 3.5(b) where the angle reference is taken at the middle of a positive block of phase "a".

The series of positive blocks is an even function which is given by:

$$F_{+}(\theta) = \frac{2}{\pi}\left(\frac{a}{\pi} + \sum_{k=1}^{\infty} \frac{1}{k} \sin \frac{ka}{2} \cos k\theta \right) \qquad (3.17)$$

where: "a" is the width of each block, "k" is the harmonic order and

$$\theta = \omega_0 t.$$

The negative series of pulses, $F_{-}(\theta)$, can be obtained from the positive series, $F_{+}(\theta)$, if :

a) the sign of $F_{+}(\theta)$ is reversed;

b) the reference is delayed 180^{o} (that is, by replacing θ by $\theta - 180$).

The resulting series of negative blocks is given by :

(a) Transformer converter line currents.

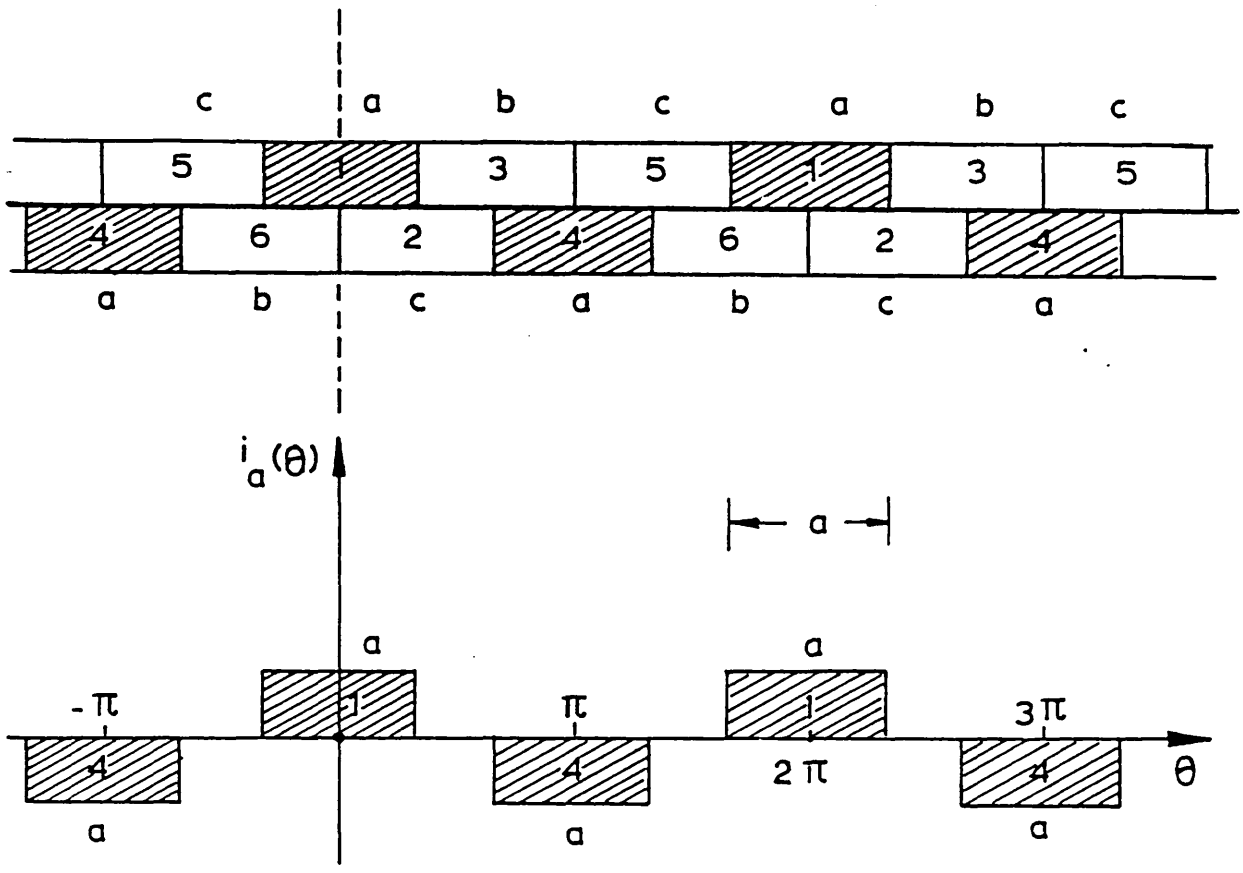

(b) Phase "a" line currents.

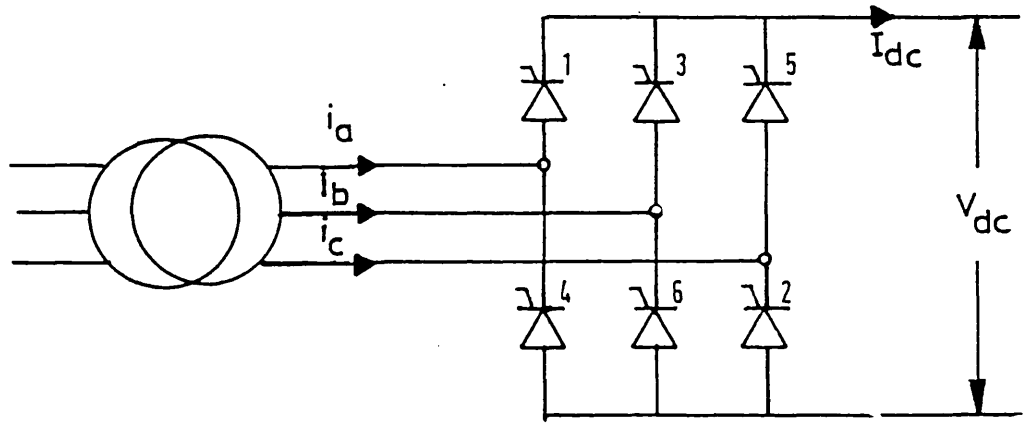

(c) Three phase converter.

Fig. 3.5 - LINE CURRENT OF A 6-PULSE CONVERTER UNDER NO OVERLAP ANGLE

$$F_{-}(\theta) = \frac{2}{\pi}\left[-\frac{a}{4} - \sum_{k=1}^{\infty}(-1)^{k}\frac{1}{k}\sin\frac{ka}{2}\cos k\theta\right] \qquad (3.18)$$

The total secondary phase current can be derived by adding eqns 3.17 and 3.18. It is convenient to give the phase current as a fraction of the d.c. line current and, for the general base case, let:

$$F(\theta) = \frac{i(\theta)}{I_{dc}} \qquad (3.19)$$

and $a = 120^{o}$.

Then, the phase "a" current can be expressed by:

$$i = \frac{2\sqrt{3}}{\pi} I_{dc}\left(\cos\theta - \frac{1}{5}\cos 5\theta + \frac{1}{7}\cos 7\theta - \frac{1}{11}\cos 11\theta + \frac{1}{13}\cos 13\theta - \ldots\right) \qquad (3.20)$$

Eqn 3.20 contains only harmonics of order $6n \pm 1$. These are known as the characteristic harmonics. The amplitude of the fundamental frequency current is :

$$I_{1} = \frac{2\sqrt{3}}{\pi} I_{dc}$$

and, for any other harmonic current of order k, the amplitude is:

$$I_{ak} = \frac{I_{1}}{k} .$$

This harmonic analysis will be referred to in the following sections as "base case".

If the control system does not produce equally spaced firing pulses, i.e. either a $\neq 120^{o}$ or a pulse train occur early or late by some $\Delta\alpha$, then uncharacteristic harmonic currents are generated even if the other assumptions at the beginning of this section are satisfied. Note that the same harmonics are only present if some of the assumptions at the beginning of this section are relaxed, i.e. finite a.c. system and commutating impedances. This case is analysed in the next sections.

3.5 Effect of control voltage modulation on harmonics

As explained in Section 3.2, the control voltage in h.v.d.c. converters with constant current control have always some residual ripple. As a consequence, the firing pulses are not exactly equidistant and not only are the characteristic harmonics slightly changed from their theoretical magnitudes and phases but also uncharacteristic harmonics are produced. In practical non-ideal a.c. systems of low short circuit ratio such uncharacteristic harmonics interact with harmonics originated in the a.c. system itself and, from this interaction, a distorted a.c. busbar voltage results.

A.c.-side and d.c.-side harmonics are considered in this chapter. It is convenient, under the harmonic analysis point of view, to obtain first the a.c.-side harmonic currents and, subsequently the corresponding a.c.-side harmonic voltage as explained in Section 2.6 (Chapter 2). Conversely, on the d.c.-side it is more convenient to obtain initially the harmonic voltage and then, the harmonic current. In this section, a preliminar general description is given of how the a.c. current and the d.c. voltage harmonic analysis is performed.

The harmonics generated by converters can be identified according to

their origin as follows:

a) characteristic harmonics (base case)

b) harmonics due to non-equidistant firing pulses;

c) harmonics due to the overlap angle

d) harmonics due to distortions on the a.c. supply;

e) harmonics from the d.c. line;

d) harmonics due to non-linearities, e.g. transformer saturation.

Characteristic harmonics were analysed earlier in Section 3.4; harmonics due to the overlap angle are only briefly considered later in connection with the d.c. voltage; finally the effect of transformer saturation was dealt within Section 2.12 (Chapter 2). Harmonics due to firing pulse irregularities can be assumed to have their origins in the incremental current difference between line currents generated by converter operation with (a) equidistant and (b) non-equidistant firing pulses. This difference can be represented by a train of current pulses as follows.

In a positive series of blocks, the effects of early firing by $\Delta\alpha$ is represented by a current pulse of width $\Delta\alpha$ added to the beginning of each block of the base case. This incremental current must return through another phase. Therefore, a pulse of identical width is subtracted from the end of the block of another phase started 120^{o} earlier. Conversely, a later firing by $\Delta\alpha$ is represented by a pulse of width $\Delta\alpha$ substracted from the beginning of each block of the base case and by an addition of a pulse $\Delta\alpha$ to the end of the current block of another phase started 120^{o} earlier. This is summarised in Table 3.2.

TABLE 3.2

INCREMENTAL PHASE CURRENT TO ACCOUNT FOR NOT EQUALLY SPACED FIRING PULSES

SERIES OF BLOCKS	FIRING PULSE	POLARITY OF THE PULSE ADDED TO THE BLOCK OF PHASE CURRENT	
		AT THE BEGINNING OF THE BLOCK	AT THE END OF THE BLOCK
POS.	EARLY	+	-
POS.	LATE	-	+
NEG.	EARLY	-	+
NEG.	LATE	+	-

An example of how the firing pulses may be affected by a 50Hz m.s. imposed on the control voltage is given in Fig. 3.6. The negative going crossover of that m.s. coincides with the firing pulse to valve 1. At this particular position, the m.s. causes the phase variation of firing pulse to valve 2 to be the negative variation of firing pulse to valve 6. Similarly, the phase variation of firing pulse to valve 3 is the negative variation of firing pulse to valve 5. This can be explained by geometrical considerations on Fig. 3.6 , which permit to conclude that the portion of the figure limited by the first half cycle of the m.s. is the symmetrical negative of the portion limited by the second half cycle. This makes the firing pulse variations to be symmetrical with respect to firing pulse to valve 4. Similar conclusions can be drawn to any 50Hz, 100Hz or 150Hz m.s. which has one of its crossover instants coinciding with a firing pulse.

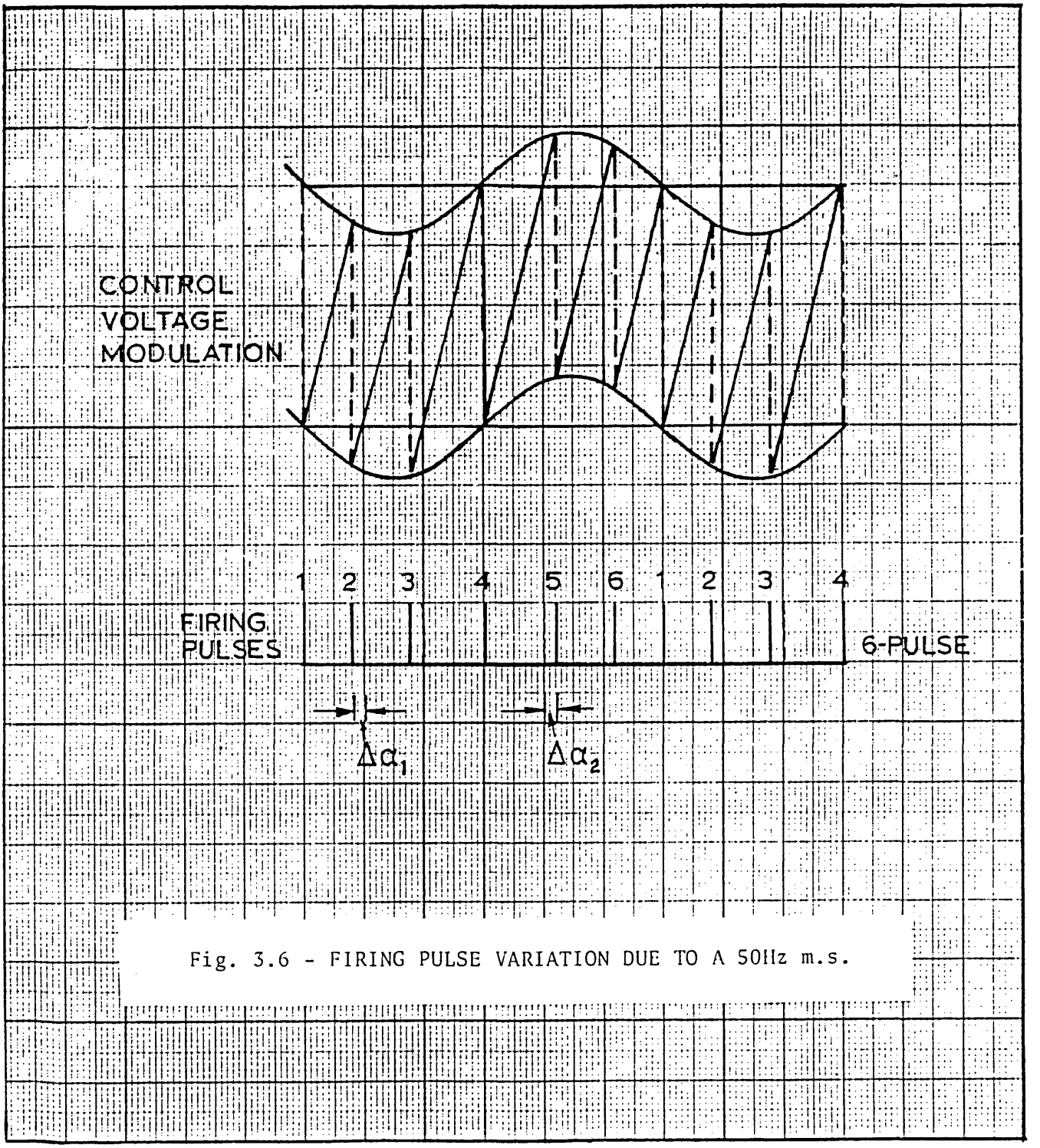

Fig. 3.6 - FIRING PULSE VARIATION DUE TO A 50Hz m.s.

Fig. 3.7 presents an example of how a firing pulse variation may affect the a.c. side currents of a 6-pulse converter. The incremental current differences between the base case and the case in which the firing pulses are not equidistant, are separately represented for phases"a", "b" and "c" in Fig. 3.7.

Non-equidistant firing pulses may be obtained by control voltage modulation. The uncharacteristic harmonics generated by any converter having a modulated control voltage depends on the firing pulse pattern caused by the m.s. .

In Chapter 4 (Section 4) it is explained how a specific firing pulse pattern can be obtained from injection of a modulating signal (m.s.) onto the control voltage. In the following sections, the theoretical harmonics caused by sinusoidal m.s. of 50Hz, 100Hz and 150Hz, are analysed. These frequencies are all multiples of the fundamental frequency therefore in steady-state, the firing pulse for each valve must be identically affected every 360 degrees.

In the incremental a.c.-side harmonic current analysis, the overlap angle is neglected. Inclusion of the overlap angle would have resulted in excessively complex equations. In Chapter 5, test results with finite commutating reactance agree well with results obtained using the simplified theory in which overlap is neglected. The exclusion of overlap angle is therefore justified.

In the case of incremental d.c. line voltages, it is not difficult to include approximately the effects of the overlap angle. This is shown in sections 3.9, 3.10 and 3.11 where a fixed commutation period is assumed. It is also assumed that firing imbalance causes series of voltage pulses of two different amplitudes, V_1 and V_2 which are one overlap angle apart from each other. These pulse amplitudes are obtained as a

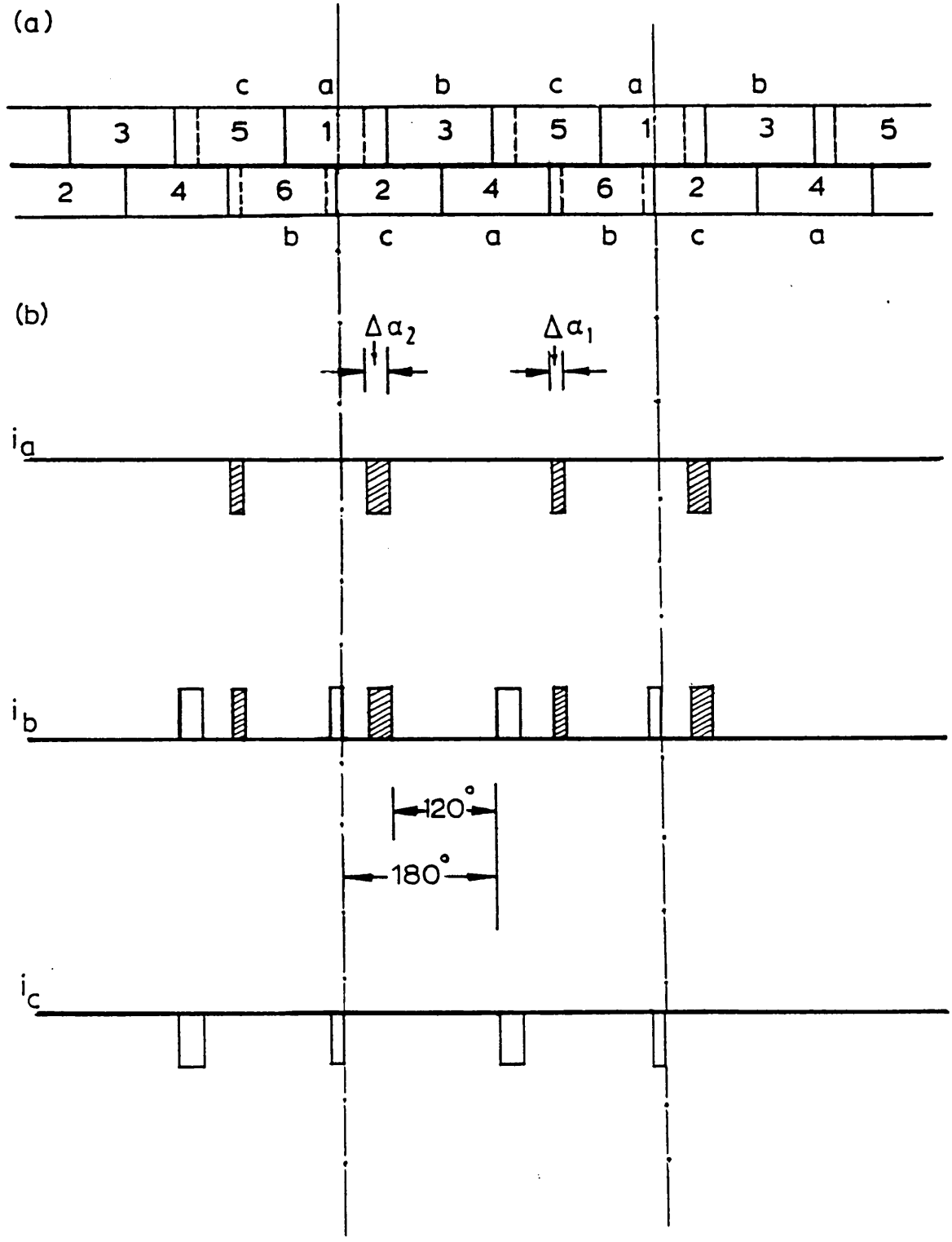

Fig. 3.7 - INCREMENTAL LINE CURRENT CAUSED BY A 50Hz m.s.

(a) Line Currents
(b) Incremental Line Currents

function of the base case amplitudes of phase voltage as follows :

$$V_1 = \frac{E_n}{2}\underline{/\theta_n - \alpha} \quad - \frac{E_m}{2}\underline{/\theta_m - \alpha} \tag{3.21}$$

$$V_2 = \frac{E_n}{2}\underline{/\ \theta_n - \alpha - \mu} \quad - \frac{E_m}{2}\underline{/\theta_m - \alpha - \mu} \tag{3.22}$$

where:

E_n, E_m are the voltage amplitude of any two phases, n and m, respectively,

θ_n is the argument of the voltage phases, $\bar{E}_m$ at the instant of the last voltage zero crossing.

$\theta_m = \theta_n + 240$

α is the firing angle

μ is the overlap angle.

The incremental analysis of the series of d.c. voltage pulses is developed much in the way used to obtain the a.c. - line harmonic currents.

3.6 Effect of a 50Hz m.s. on the a.c.-side Harmonic Currents

Fig. 3.6 shows a 50Hz m.s. superimposed on a flat control voltage. In each cycle of the m.s., three consecutive valves in the firing order are fired early (say, valves 1, 2 and 3) and the other three remaining valves, are fired late (4, 5, 6). As a result, the firing pulse distribution becomes such that, if an even numbered valve in one of the bridge arms (say, arm "a"), is fired $\Delta\alpha_1$ degrees early, then another even numbered valve (say, in the arm "b") will fire late by an approximately equivalent angle

$\Delta\alpha_1$, but of opposite sign. The same happens to the corresponding odd numbered valves of arms "a" and "b", except that by a different angle, $\Delta\alpha_2$. In the third arm (arm "c") one valve fires early and the other fires late by an approximately equivalent angle $\Delta\alpha_2$. If the positive going crossover of the m.s. coincides with any firing pulse, the even numbered valves of arms "b" and "c" experience theoretically the same $|\Delta\alpha|$ as shown in Fig. 3.6. The corresponding odd numbered valves of arms "b" and "c" have also equal variation of firing angles in terms of absolute value. The valves of arm "a" are assumed to fire on time.

Fig. 3.7(a) is based on the case of Fig. 3.6, and shows how valve currents are modified with respect to the base case when a 50Hz m.s. is superimposed on the control voltage. The letters outside of the current blocks indicate the conducting phase while the numbers inside of the current blocks indicate the conducting valve. In Fig. 3.7(b), the incremental current due to the difference between the base case phase currents and the case when a 50Hz m.s. is superimposed on the control voltage, is shown. From this figure, the following conclusions can be drawn:

a) Phases "a" and "b" are made up of alternate pulses of width $\Delta\alpha_1$ and $\Delta\alpha_2$;

b) Phase "c" is leading phase "a" by approximately 120° .

c) Phase "b" is a combination of the currents through phases "a" and "c" (Fig. 3.7(b)) because :

I) the converter transformer secondary has no neutral return

II) valve 1 is assumed to fire on time and therefore, it is not associated with incremental current pulses

d) From a, b and c above can be concluded that the train of pulses, form an approximate balanced 3-phase set of second harmonic currents of positive sequence.

e) There is a net d.c. current level through all phases.

Table 3.3 summarises the firing angle variations for a 50Hz m.s. .

TABLE 3.3

FIRING ANGLE VARIATION, $\Delta\alpha$, DUE TO

A 50Hz M.S.

VALVE	$\Delta\alpha$
1	0
2	$-\Delta\alpha_1$
3	$-\Delta\alpha_2$
4	0
5	$+\Delta\alpha_2$
6	$+\Delta\alpha_1$

Because the first current pulse through phase "c" coincides with the reference, the Fourier analysis of the incremental phase current is started by that phase.

3.6.1 Harmonic Analysis of Phase "c"

The series of current pulses through phase "c" can be divided into two types :

1) Pulses of width $\Delta\alpha_1$

2) Pulses of width $\Delta\alpha_2$.

The same two steps used to obtain eqn 3.18, can be employed in the Fourier analysis of the current pulses of Fig. 3.7. These steps are:

a) sign reversal and b) phase shifting. Sign reversal turns the series of negative pulses into a series of positive pulses. Phase shifting refers the middle of an incremental block of current, to the main angle reference which is fixed at the middle of the positive block of current through valve 1 (Fig. 3.5). These two steps of analysis are performed on the generic summation term of eqn 3.17 which is given below in terms of phase current in connection with eqn 3.19.

$$i_{ck} = \frac{2I_{dc}}{k\pi} \left(\sin \frac{ka}{2} \cos k\theta\right) \qquad (3.23)$$

where subscript "c" indicates phase "c" and subscript "k" indicates harmonic order k.

To describe the two trains of negative pulses of phase "c" as represented in Fig. 3.7, the variables "a" and "θ" in eqn 3.23 are replaced by the values given in Table 3.4. The two expressions are then combined into a single equation.

TABLE 3.4

PHASE "c" PULSE TRAIN PARAMETERS, (50Hz M.S.)

PULSES OF WIDTH	a	θ
$\Delta\alpha_1$	$\Delta\alpha_1$	$\theta + \frac{\Delta\alpha_1}{2}$
$\Delta\alpha_2$	$\Delta\alpha_2$	$\theta - \frac{\Delta\alpha_2}{2} - 180.$

The harmonic current of order k through phase "c" is then given by:

$$i_{ck} = -\frac{2I_{dc}}{k\pi}\left[\sin\frac{k\Delta\alpha_1}{2}\cos k\left(\theta+\frac{\Delta\alpha_1}{2}\right)+\sin\frac{k\Delta\alpha_2}{2}\cos k\left(\theta-\frac{\Delta\alpha_2}{2}-180\right)\right]$$

.....(3.24)

Eqn 3.24 can be simplified through

$$\sin A\cos B = \tfrac{1}{2}[\sin(A-B)+\sin(A+B)]$$

to become

$$i_{ck} = \frac{2I_{dc}}{k\pi}\left[\cos k(\theta-90)\sin k90-\cos k\left(\theta+\frac{\Delta\alpha_1-\Delta\alpha_2}{2}-90\right)x \sin k\left(\frac{\Delta\alpha_1+\Delta\alpha_2}{2}+90\right)\right] \qquad (3.25)$$

Odd and even harmonics can be considered separately.

a) Odd harmonics (odd k)

Introducing the identities

$$\cos(A-90) = \sin A$$

$$\sin(A+90) = \cos A$$

into eqn 3.25 yields

$$i_{ck} = \frac{2I_{dc}}{k\pi}\left[\sin k\theta - \sin k\left(\theta+\frac{\Delta\alpha_1-\Delta\alpha_2}{2}\right)\cos k\left(\frac{\Delta\alpha_1+\Delta\alpha_2}{2}\right)\right] \qquad (3.26)$$

b) Even harmonics (even k)

$$i_{ck} = -\frac{2I_{dc}}{k} \sin k\left(\frac{\Delta\alpha_1+\Delta\alpha_2}{2}\right) \cos k\left(\theta + \frac{\Delta\alpha_1-\Delta\alpha_2}{2}\right) \qquad (3.27)$$

Eqns 3.26 and 3.27 can be rewritten as

$$i_{ck} = I_{ck} \sin k(\theta - \phi_c) \qquad \text{(odd k)} \qquad (3.28)$$

$$i_{ck} = I_{ck} \cos k(\theta + \phi_d) \qquad \text{(even k)} \qquad (3.29)$$

where:

$$I_{ck} = \frac{2I_{dc}}{k\pi} \sqrt{(\cos k\phi_s - \cos k\phi_d)^2 + \sin^2 k\phi_d} \qquad \text{(odd k)} \qquad (3.30)$$

$$I_{ck} = -\frac{2I_{dc}}{k\pi} \sin k\phi_d \qquad \text{(even k)} \qquad (3.31)$$

$$k\phi_c = \text{TAN}^{-1}\left(\frac{\sin k\phi_d \cos k\phi_s}{1 - \cos k\phi_d \cos k\phi_s}\right) \qquad (3.32)$$

$$\phi_s = \frac{\Delta\alpha_1 + \Delta\alpha_2}{2} \qquad (3.33)$$

$$\phi_d = \frac{\Delta\alpha_1 - \Delta\alpha_2}{2} \; . \qquad (3.34)$$

It was noticed that, as in characteristic harmonics, the magnitude of eqns 3.28 and 3.29 are related inversely to the harmonic order. In h.v.d.c. systems under steady-state operation $\Delta\alpha_1$ and $\Delta\alpha_2$ would be very

small ($< 5^{o}$). An approximation of eqns 3.30 and 3.31 can then be made for low harmonic orders (small k) and small values of $\Delta\alpha_1$ and $\Delta\alpha_2$ as shown in Appendix B by equations B.8 and B.10 for odd harmonics and equations B.13 and B.14 for even harmonics. Those equations are presented below:

a) For odd harmonics :

$$I_{ck} \cong \frac{kI_{dc}}{8\pi} (\Delta\alpha_1 + \Delta\alpha_2)^2 \qquad (3.35)$$

$$k\phi_c \cong 0 \qquad (3.36)$$

b) For even harmonics :

$$I_{ck} \cong - \frac{I_{dc}}{\pi} (\Delta\alpha_1 + \Delta\alpha_2) \qquad (3.37)$$

$$k\phi_d \cong 0. \qquad (3.38)$$

For small values of $\Delta\alpha_1$ and $\Delta\alpha_2$, the squared term in eqn 3.35 and therefore, the magnitudes of odd harmonics are negligible. On the other hand, the amplitude of current of low even harmonic orders given by eqn 3.37 are approximately proportional to the firing angle variation.

3.6.2 Harmonic Analysis of Phase "a"

Values of "a" and "θ" to represent the harmonic currents through phase "a" according to the generic term of eqn 3.23, are shown in

Table 3.4. This Table is compiled with values obtained from Fig. 3.7.

TABLE 3.5

PHASE "a" PULSE TRAIN PARAMETERS

(50Hz M.S.)

PULSE OF WIDTH	a	θ
$\Delta\alpha_1$	$\Delta\alpha_1$	$\theta + 120 - \frac{\Delta\alpha_1}{2}$
$\Delta\alpha_2$	$\Delta\alpha_2$	$\theta - 60 + \frac{\Delta\alpha_2}{2}$

The procedure used to obtain the harmonic current follows the same lines as in the previous sub-section and is shown in Section B.3 of Appendix B. The results of this analysis are summarised below:

a) For odd harmonics

$$i_{ak} = I_{ak} \sin k(\theta + \phi_a + 120) \tag{3.39}$$

where

$$I_{ak} = \frac{2I_{dc}}{k\pi}\sqrt{(\cos^2 k\phi_s - \cos^2 k\phi_d)^2 + \sin^2 k\phi_d} \tag{3.40}$$

$$k\phi_a = k\phi_c \tag{3.41}$$

b) Even harmonics

$$i_{ak} = I_{ak} \cos k(\theta - \phi_a + 120) \tag{3.42}$$

where

$$I_{ak} = - \frac{2I_{dc}}{k\pi} \sin k\phi_s \tag{3.43}$$

$$\phi_a = \phi_d \quad . \tag{3.44}$$

3.6.3 Harmonic Analysis of Phase "b"

As pointed out at the beginning of this section the harmonic current through phase "b" is a result of the negative summation of eqns 3.28 and 3.41 for the odd harmonics and of eqns 3.29 and 3.42 for the even harmonics. These summations give respectively :

$$i_{bk} = - [I_{ck} \sin k(\theta - \phi_c) + I_{ak} \sin k(\theta + \phi_a + 120)]$$

for odd k (3.45)

where:

$$I_{ak} = I_{ck} = \frac{2I_{dc}}{k\pi} \sqrt{(\cos^2 k\phi_s - \cos^2 k\phi_d) + \sin^2 k\phi_d}$$

$$\phi_a = \phi_c = \frac{1}{k} \text{TAN}^{-1} \left(\frac{\sin k\phi_d \cos k\phi_s}{1 - \cos k\phi_d \cos k\phi_s} \right)$$

and

$$i_{bk} = - [I_{ck} \cos k(\theta + \phi_d) + I_{ak} \cos k(\theta - \phi_a + 120)]$$

for even k (3.46)

where

$$I_{ak} = I_{ck} = -\frac{2I_{dc}}{k\pi} \sin k\phi_s .$$

$$\phi_a = \phi_d .$$

Eqn 3.45 can be transformed into a sum of sines, i.e. :

$$i_{bk} = -I_{ck}[\sin k(\theta - \phi_c) + \sin k(\theta + \phi_c + 120)] \qquad (3.47)$$

Through the identity

$$\sin A + \sin B = 2 \sin \tfrac{1}{2}(a+B)\cos \tfrac{1}{2}(A-B)$$

eqn 3.47 can be reduced to

$$i_{bk} = -I_{ck}[2\sin k(\theta + 60)\cos k(\phi_c + 60)] \qquad (3.48)$$

which can be simplified into :

$$i_{bk} = I_{bk} \sin k(\theta + 60) \qquad (3.49)$$

where

$$I_{bk} = -2I_{ck} \cos k(\phi_c + 60) . \qquad (3.50)$$

Similarly, eqn 3.46 can be transformed into a sum of cosines, i.e.:

$$i_{bk} = -I_{ck}[\cos k(\theta + \phi_d) + \cos k(\theta + 120 - \phi_d)] . \qquad (3.51)$$

Through the identity

$$\cos A + \cos B = 2 \cos\tfrac{1}{2}(A+B)\cos\tfrac{1}{2}(A-B)$$

eqn 3.51 can be reduced to :

$$i_{bk} = - I_{ck}\, 2[\cos k(\theta + 60)\cos(\phi_d - 60)] \qquad (3.52)$$

which can be simplified into:

$$i_{bk} = I_{bk} \cos k(\theta + 60) \quad \text{for even } k \qquad (3.53)$$

where

$$I_{bk} = -2I_{ck} \cos(\phi_d - 60). \qquad (3.54)$$

Tables 3.6 and 3.7 summarise the equations for odd and even harmonics, respectively.

3.6.4 Cases of particular interest

Some cases of particular interest for the harmonic minimization method presented in Chapter 5 are highlighted below.

TABLE 3.6

A.C. SIDE ODD HARMONIC CURRENTS DUE TO A 50Hz M.S.

$$i_{ak} = A_k \sin k(\theta + \phi_c + 120)$$

$$i_{bk} = B_k \sin k(\theta + 60)$$

$$i_{ck} = A_k \sin k(\theta - \phi_c)$$

$$A_k = \frac{2I_{dc}}{k\pi} \sqrt{(\cos k\phi_s) - \cos k\phi_d)^2 + \sin^2 k\phi_d}$$

$$B_k = A_k[-2 \cos k(\phi_c + 60)]$$

$$k\phi_c = \text{Tan}^{-1}\left(\frac{\sin k\phi_d \cos k\phi_s}{1 - \cos k\phi_d \cos k\phi_s} \right)$$

$$\phi_s = \frac{\Delta\alpha_2 + \Delta\alpha_2}{2}$$

$$\phi_d = \frac{\Delta\alpha_1 - \Delta\alpha_2}{2}$$

TABLE 3.7

A.C. SIDE EVEN HARMONIC CURRENTS DUE TO A 50Hz M.S.

$i_{ak} = A_k \cos k(\theta - \phi_d + 120)$ $i_{bk} = B_k \cos k(\theta + 60)$ $i_{ck} = A_k \cos k(\theta + \phi_d)$
$A_k = -\frac{2I_{dc}}{k\pi} \sin k\phi_s$ $B_k = A_k[-2 \cos k(60 - \phi_d)]$
$\phi_s = \frac{\Delta\alpha_1 + \Delta\alpha_2}{2}$ $\phi_d = \frac{\Delta\alpha_1 - \Delta\alpha_2}{2}$

a) Second harmonic current (k = 2).

For k = 2, the equations in Table 3.7 becomes :

$$i_{c2} = I_{a2} \cos(2\theta - 2\phi_d + 240) \qquad (3.55)$$

$$i_{b2} = I_{b2} \cos (2\theta + 120) \qquad (3.56)$$

$$i_{c2} = I_{c2} \cos(2\theta + 2\phi_d) \qquad (3.57)$$

where:

$$I_{a2} = I_{c2} = -\frac{2I_{dc}}{\pi} \sin 2\phi_s$$

$$I_{b2} = \frac{2I_{dc}}{\pi} \sin 2\phi_s \cos(2\phi_d - 120).$$

If ϕ_d is negligible, equations 3.55 to 3.57 reduce to

$$i_{a2} = I_2 \cos(2\theta + 240) \qquad (3.58)$$

$$i_{b2} = I_2 \cos(2\theta + 120) \qquad (3.59)$$

$$i_{c2} = I_2 \cos(2\theta) \qquad (3.60)$$

where:

$$I_2 = I_{a2} = I_{b2} = I_{c2} = -\frac{I_{dc}}{\pi} \sin 2\phi_s.$$

Eqns 3.58 to 3.60 can be recognized as a balanced set of 3-phase second harmonic currents of positive sequence.

b) Modulating signal phase shifting.

Fig. 3.8 shows the effect of a 50Hz m.s. on the incremental line current of a 6-pulse converter. The negative going crossover of this m.s. coincides with the firing to valve 2 rather than valve 1 as previously. If the angle reference is shifted 60° as in Fig. 3.8, the incremental currents in this figure are related to those of Fig. 3.7 as follows :

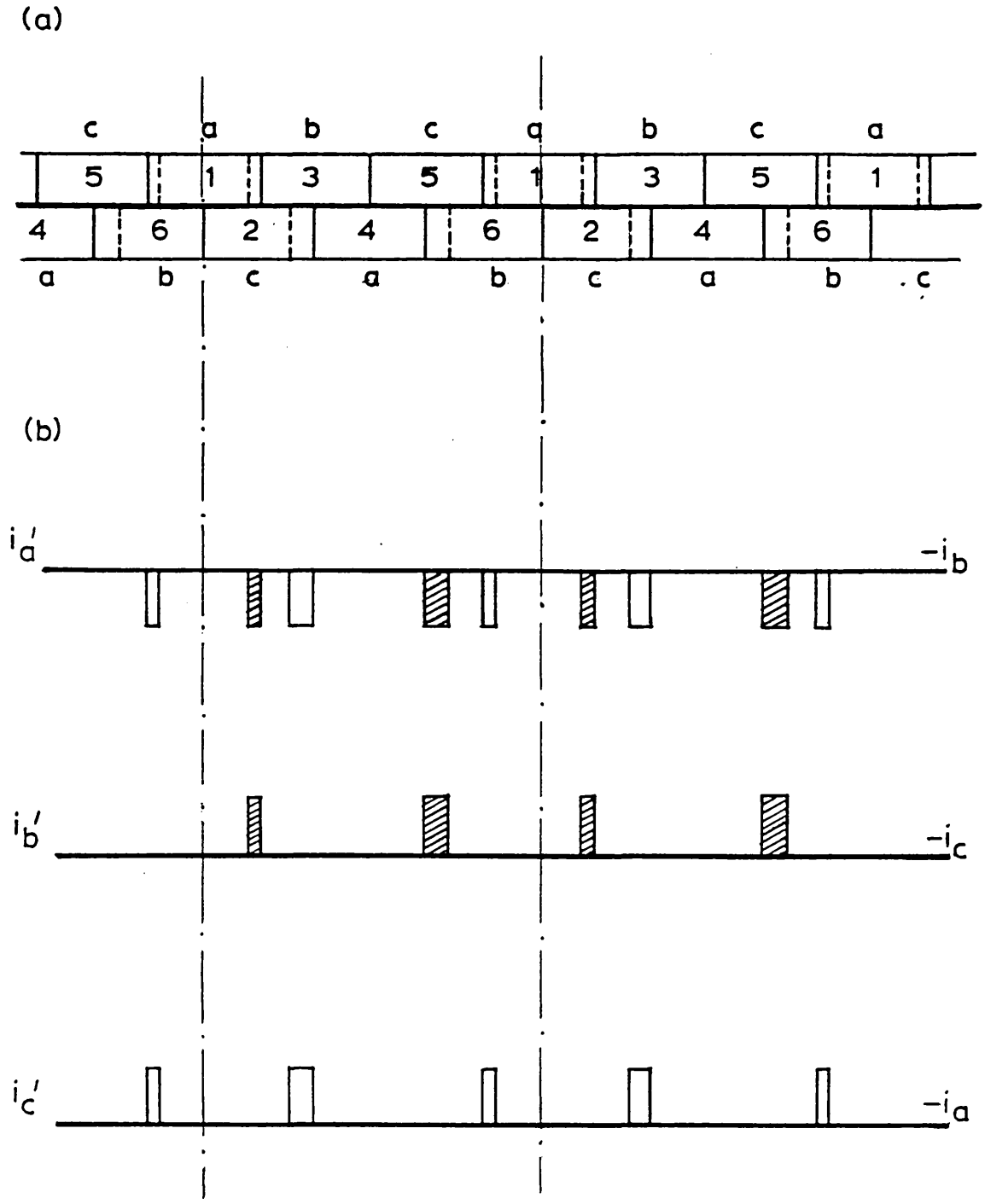

Fig. 3.8 - NEGATIVE GOING CROSSOVER OF A 50Hz m.s. COINCIDING WITH FIRING PULSE TO VALVE 2

(a) Line Currents
(b) Incremental Line Currents

$$i'_{ak} = i_{bk}$$

$$i'_{bk} = -i_{ck}$$

$$i_{ck} = -i_{ak}$$

Consequently, if θ is replaced by $\theta - 60$, the currents i'_{ak}, i'_{bk} and i'_{ck} can be expressed in terms of the equations in Tables 3.6 and 3.7.

$$i'_{ak} = - I_{bk} \cos k\theta$$

$$i'_{bk} = - I_{ck} \cos k(\theta + \phi_d - 60)$$

$$i'_{ck} = - I_{ak} \cos k(\theta - \phi_d + 60).$$

For k = 2, these equations can be rewritten as in Table 3.7

$$i_{a2} = I_2 \cos(2\theta + 180) \qquad (3.61)$$

$$i_{b2} = I_2 \cos(2\theta + 2\phi_d + 60) \qquad (3.62)$$

$$i_{c2} = I_2 \cos(2\theta - 2\phi_d + 300) \qquad (3.63)$$

For negligible ϕ_d, eqns 3.61 to 3.63 form a balanced set of 3-phase positive sequence second harmonic currents.

A similar analysis can be pursued for the case in which the negative-going crossover of the 50Hz m.s. coincides with the firing to valve 3. From analogy with the previous case, if θ is replaced by

$\theta - 120^{o}$, the equations of Tables 3.6 and 3.7 can be used again to express the incremental currents of Fig. 3.9.

$$i''_{ak} = i_{ck}$$

$$i''_{bk} = i_{ak}$$

$$i''_{ck} = i_{bk}$$

which lead to:

$$i''_{ak} = I_{ck} \cos k(\theta + \phi_d - 120) \tag{3.64}$$

$$i''_{bk} = I_{ak} \cos k(\theta - \phi_d) \tag{3.65}$$

$$i''_{ck} = I_{bk} \cos k(\theta - 60) \quad . \tag{3.66}$$

If ϕ_d is negligible and k = 2 in eqn 3.64 to 3.66, results

$$i''_{a2} = I_2 \cos(2\theta + 120) \tag{3.67}$$

$$i''_{b2} = I_2 \cos 2\theta \tag{3.68}$$

$$i''_{c2} = I_2 \cos(2\theta + 240) \quad . \tag{3.69}$$

It is possible to conclude that the phase of the second harmonic positive sequence changes according to the m.s. phase shift. That is, if the m.s. is shifted by 60^{o} in fundamental terms, the a.c. line second harmonic current also shifts by 60^{o} in second harmonic terms. This effect is further discussed later on in this chapter.

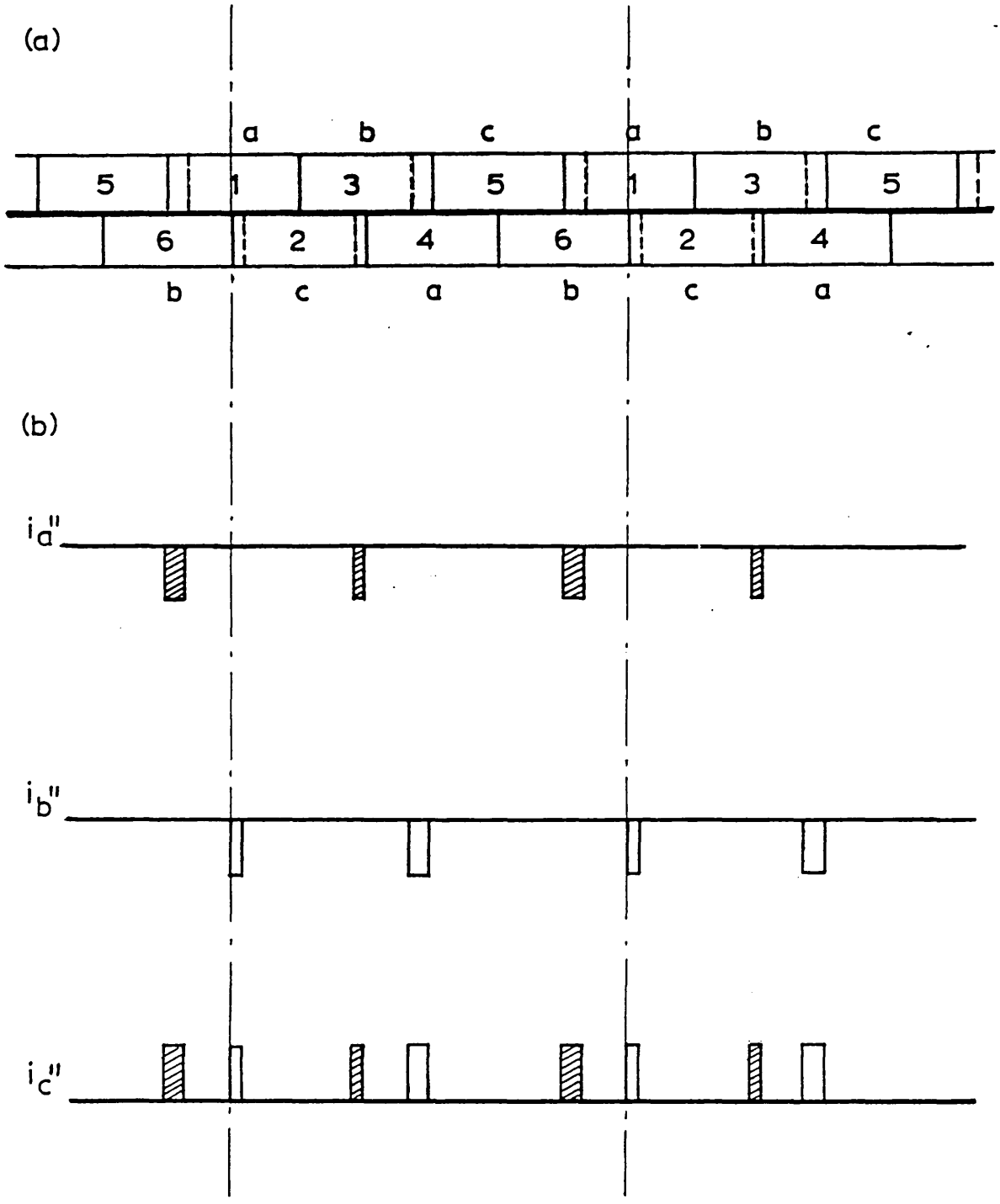

Fig. 3.9 - NEGATIVE GOING CROSSOVER OF A 50Hz m.s. COINCIDING WITH FIRING PULSE TO VALVE 3

(a) Line Currents
(b) Incremental Line currents

3.7 Effect of a 100Hz m.s. on the a.c. Line Harmonic Currents

The effect of a 100 Hz m.s. whose positive going crossover coincides with the firing pulse to valve 1, is shown in Fig. 3.10. The firing pulse distribution caused by this m.s. is such that the two valves connected to the same phase are both $\Delta\alpha$ degrees early or later. The magnitude of $\Delta\alpha$ depends on the m.s. phase and amplitude, as demonstrated in Section 3.3. The phase currents are now no longer made up of 120^{o} wide blocks but, of alternately shorter or longer blocks. The harmonic analysis that follows shows that such blocks of current generate triplen harmonics.

Figs 3.11 shows the incremental variation of valve current with respect to the base case when a 100 Hz m.s. is superimposed onto the control voltage as in Fig. 3.10. The following observations can now be made.

a) Phase "a" and phase "b" currents consist of alternate negative and positive pulse of width $\Delta\alpha$ spaced by 180^{o};

b) Phase "c" current leads phase "a" current by approximately 120^{o};

c) Phase "b" current is a combination of phase "a" and phase "c" currents;

d) There is no d.c. current through any of the phases.

Table 3.8 shows the variation in firing angle for the six valves with respect to the base case. The incremental current through phase "c" is again analysed first.

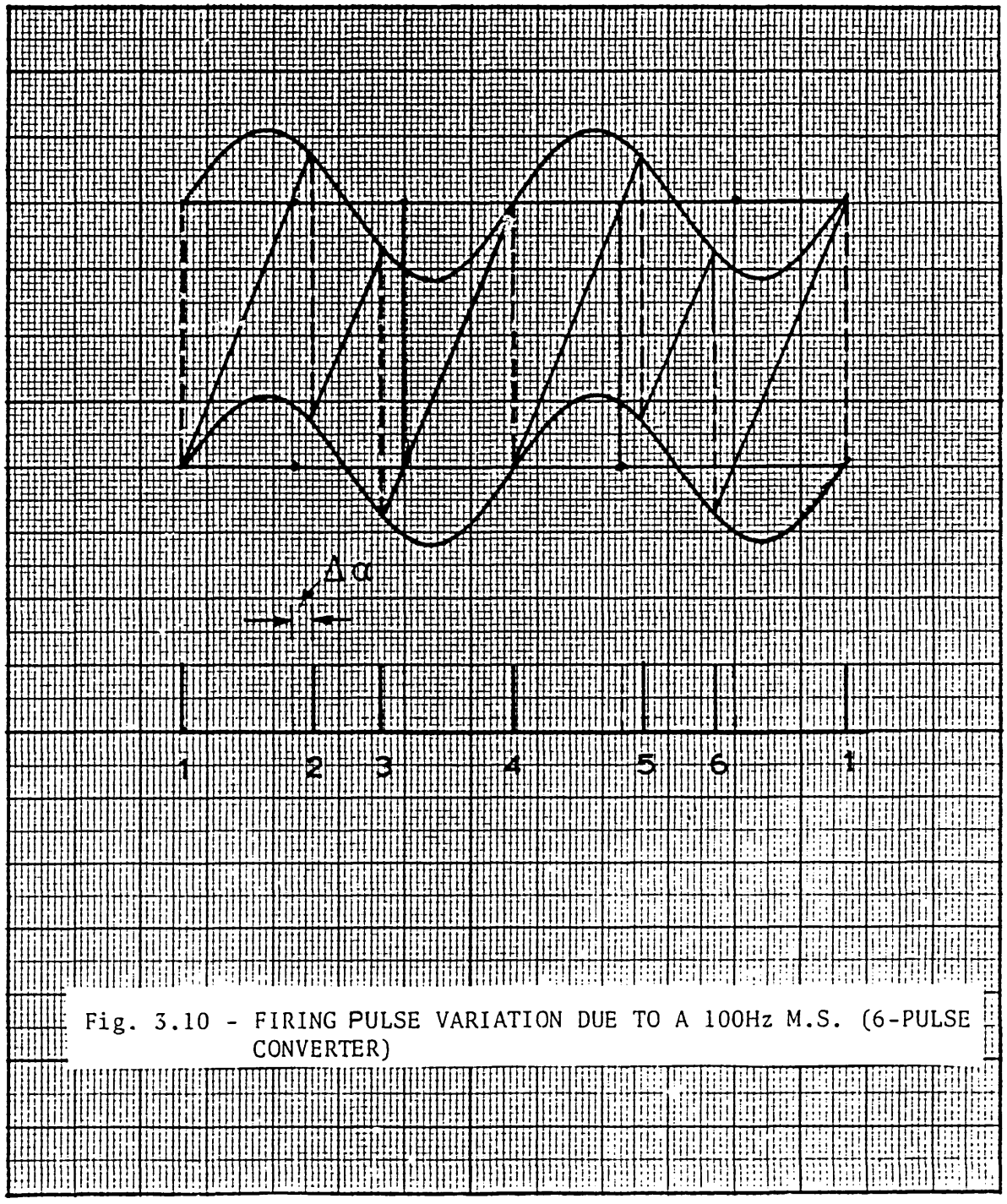

Fig. 3.10 - FIRING PULSE VARIATION DUE TO A 100Hz M.S. (6-PULSE CONVERTER)

TABLE 3.8

FIRING PULSE VARIATION DUE TO A 100 Hz M.S.

VALVE	$\Delta\alpha$
1	0
2	$\Delta\alpha$
3	$-\Delta\alpha$
4	0
5	$\Delta\alpha$
6	$-\Delta\alpha$

3.7.1 Harmonic Analysis of Phase "c"

The generic summation term given in eqn 3.23 is used to obtain a single expression to combine the series of positive and negative pulses of current.

Phase changing and sign reversing are used in connection with eqn 3.23 to obtain Fourier components of the incremental current through phase "c". This current can be split up into two types of pulse trains:

1) positive pulses

2) negative pulses.

Table 3.9 shows the values of "a" and "θ" to represent the harmonic currents through phase "c" according to the generic term of eqn 3.23. This table is compiled with values obtained from Fig. 3.11.

TABLE 3.9

PHASE "C" PULSE TRAIN PARAMETERS (100Hz M.S.)

TRAIN OF PULSES	a	θ
POS.	$\Delta\alpha$	$\theta - \frac{\Delta\alpha}{2}$
NEG.	$\Delta\alpha$	$\theta - \frac{\Delta\alpha}{2} - 180$

The generic term for the positive and negative pulses is given, respectively by

$$i'_{ck} = \frac{2I_{dc}}{\pi k} \sin\frac{k\Delta\alpha}{2} \cos k(\theta - \frac{\Delta\alpha}{2}) \qquad (3.70)$$

and

$$i''_{ck} = -\frac{2I_{dc}}{\pi k} \sin\frac{k\Delta\alpha}{2} \cos k(\theta - \frac{\Delta\alpha}{2} - 180). \qquad (3.71)$$

A single expression for the harmonic currents through phase "c" is obtained by adding together eqns 3.70 and 3.71.

$$i_{ck} = \frac{2I_{dc}}{\pi k} \sin\frac{k\Delta\alpha}{2} [\cos k(\theta - \frac{\Delta\alpha}{2}) - \cos k(\theta - \frac{\Delta\alpha}{2} - 180)]. \qquad \ldots (3.72)$$

For odd and even k's, eqn 3.72 reduces respectively to:

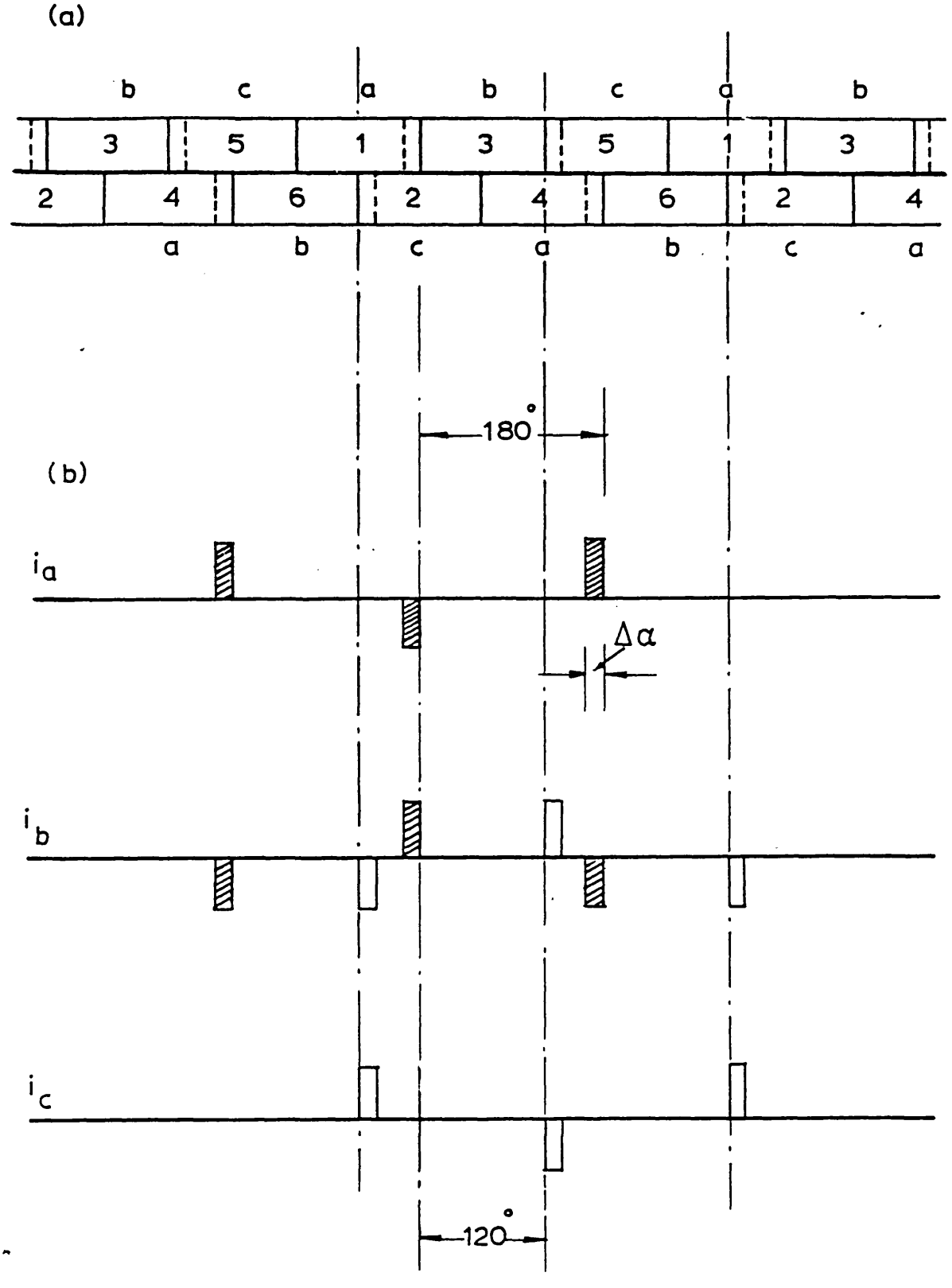

Fig. 3.11 - INCREMENTAL LINE CURRENT CAUSES BY A 100Hz m.s.

(a) Line Currents
(b) Incremental Line currents

$$i_{ck} = \frac{4 I_{dc}}{\pi k} \sin \frac{k\Delta\alpha}{2} \cos k(\theta - \frac{\Delta\alpha}{2}) \qquad (3.73)$$

$$i_{ck} = 0. \qquad (3.74)$$

3.7.2 Harmonic analysis of phase "a"

Table 3.10 gives the values of "a" and "θ" to be used in eqn 3.73 so that the current of phase "a" in Fig. 3.11 is derived.

TABLE 3.10

PHASE "a" PULSE TRAIN PARAMETERS

TRAIN OF PULSE	a	θ
+	$\Delta\alpha$	$\theta + \frac{\Delta\alpha}{2} - 240$
−	$\Delta\alpha$	$\theta + \frac{\Delta\alpha}{2} - 60$

As previously, the harmonic current of order k through phase "a" can be expressed by

$$i_{ak} = \frac{2I_{dc}}{\pi k} \sin \frac{k\Delta\alpha}{2} [\cos k(\theta + \frac{\Delta\alpha}{2} - 240) - \cos(\theta + \frac{\Delta\alpha}{2} - 60)] . \qquad \ldots (3.75)$$

In order to simplify the analysis, let $\theta_1 = \theta + 120$, so that:

$$i_{ak} = \frac{2I_{dc}}{\pi k} \sin \frac{k\Delta\alpha}{2} [\cos k(\theta_1 + \frac{\Delta\alpha}{2}) - \cos k(\theta_1 + \frac{\Delta\alpha}{2} - 180)] \qquad \ldots (3.76)$$

Eqn 3.7.6 can express odd and even harmonics separately as follows:

$$i_{ak} = \frac{4I_{dc}}{\pi k} \sin \frac{k\Delta\alpha}{2} \cos k(\theta + \frac{\Delta\alpha}{2})$$

for odd k's (3.77)

$$i_{ak} = 0 \qquad \text{for even k's} \quad . \tag{3.78}$$

3.7.3 Harmonic analysis of phase "b"

In Fig. 3.11, the harmonic currents through phase "b" are the negative summation of the harmonic currents through phase "a" (eqn 3.7.6) and phase "c" (eqn 3.7.2). No even harmonics are present. The odd harmonic currents in phase "b" are given by:

$$i_{bk} = - \frac{4I_{dc}}{\pi k} \sin \frac{k\Delta\alpha}{2} [\cos k(\theta - \frac{\Delta\alpha}{2}) + \cos k(\theta + \frac{\Delta\alpha}{2} + 120)] \tag{3.79}$$

Though the trigonometric identity

$$\cos A + \cos B = 2 \cos \frac{A+B}{2} \cos \frac{A-B}{2}$$

eqn 3.79 is simplified to read:

$$i_{bk} = - \frac{8I_{dc}}{k\pi} \sin \frac{k\Delta\alpha}{2} \cos k(60 + \frac{\Delta\alpha}{2}) \cos(\theta + 60)$$

(odd k's) (3.80)

3.7.4 Cases of particular interest

a) Harmonic currents of the 3rd and 9th order caused by 100Hz m.s. on the control voltage, are of particular interest because:

i) the fundamental (k = 1) is always present;

ii) no even harmonics are predicted;

iii) characteristic harmonics (k = 5, 7, 11, 13, etc.) are minimized by filters and/or 12-pulse operation.

Eqns 3.73, 3.77 and 3.80 for triplen harmonics are reduced to:

$$i_{ak} = \frac{4I_{dc}}{\pi k} \sin \frac{k\Delta\alpha}{2} \cos k(\theta + \frac{\Delta\alpha}{2}) \qquad (3.81)$$

$$i_{bk} = -\frac{4I_{dc}}{k\pi} \sin k\Delta\alpha \cos k\theta \qquad (3.82)$$

$$i_{ck} = \frac{4I_{dc}}{k\pi} \sin \frac{k\Delta\alpha}{2} \cos k(\theta - \frac{\Delta\alpha}{2}) \quad . \qquad (3.83)$$

For small values of $\Delta\alpha$, currents i_{ak} and i_{ck} are approximately in phase and both are in approximate phase opposition with i_{bk}.

b) The harmonic amplitude in eqns 3.81 and 3.83 is given by

$$A = \frac{4}{\pi k} \sin \frac{k\Delta\alpha}{2} \quad . \qquad (3.84)$$

Expanding the sine factor through

$$\sin \frac{k\Delta\alpha}{2} = \frac{k\Delta\alpha}{2} - \left(\frac{k\Delta\alpha}{3!2} \right)^3 + \left(\frac{k\Delta\alpha}{5!2} \right)^5 - \ldots \qquad (3.85)$$

Hence for small values of $\Delta\alpha$,

$$A \simeq \frac{2\Delta\alpha}{\pi} \quad .$$

It can be concluded that the amplitude of odd harmonics caused by a 100Hz m.s. are approximately proportional to $\Delta\alpha$. The same conclusion may be drawn for eqn 3.82.

c) Modulating signal phase effects.

Fig 3.12 shows the phase effects of a 100Hz m.s. on the incremental currents of a 6-pulse converter. The positive going crossover of this m.s. coincides with the firing to valve 2 rather than valve 1, as in Fig. 3.11. In figure 3.12, if the angle reference is shifted by 60 degrees, the incremental currents i'_a, i'_b and i'_c are related to the incremental currents i_a, i_b and i_c of Fig 3.11 through the expressions

$$i'_{ak} = -i_{bk}$$

$$i'_{bk} = -i_{ck}$$

$$i'_{ck} = -i_{ak}$$

Phase currents i'_{ak}, i'_{bk} and i'_{ck} can be expressed by the eqns 3.73, 3.77 and 3.80 if θ is replaced by $\theta - 60$. This gives

$$i'_{ak} = \frac{8I_{dc}}{k\pi} \sin\frac{k\Delta\alpha}{2} \cos k(60 + \frac{\Delta\alpha}{2}) \cos k\theta \qquad (3.86)$$

$$i'_{bk} = -\frac{4I_{dc}}{k\pi} \sin\frac{k\Delta\alpha}{2} \cos k(\theta - \frac{\Delta\alpha}{2} - 60) \qquad (3.87)$$

$$i'_{ck} = -\frac{4I_{dc}}{k\pi} \sin\frac{k\Delta\alpha}{2} \cos k(\theta + \frac{\Delta\alpha}{2} + 60) \qquad (3.88)$$

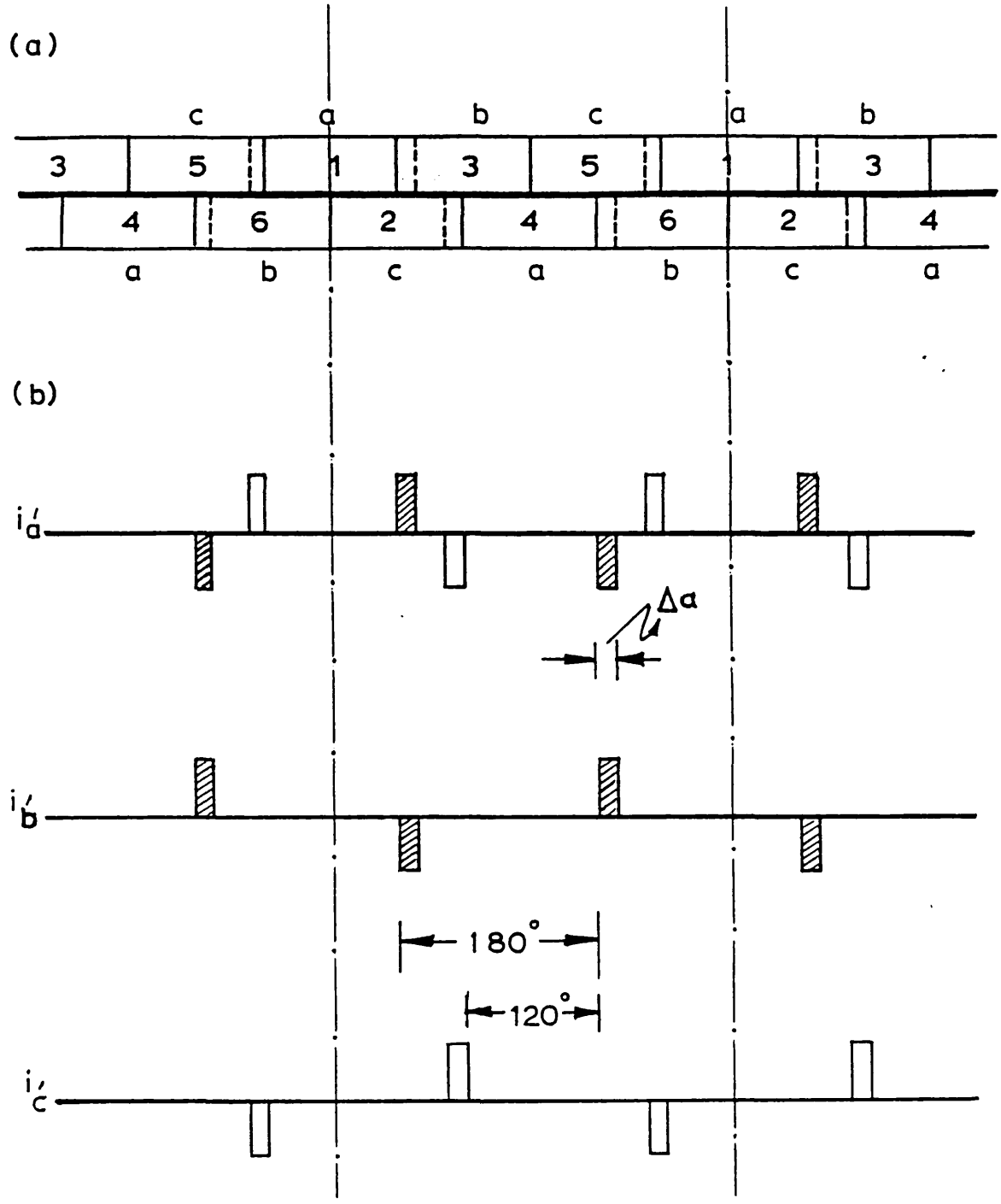

Fig. 3.12 - POSITIVE GOING CROSSOVER OF A 100Hz m.s. WITH FIRING PULSE TO VALVE 2

For triplen harmonics, eqns 3.86 to 3.88 are reduced to

$$i'_{ak} = -\frac{4I_{dc}}{k\pi} \sin k\Delta\alpha \cos k\theta \tag{3.89}$$

$$i'_{bk} = \frac{4I_{dc}}{k\pi} \sin \frac{k\Delta\alpha}{2} \cos k(\theta - \frac{\Delta\alpha}{2}) \tag{3.90}$$

$$i'_{ck} = \frac{4I_{dc}}{k\pi} \sin \frac{k\Delta\alpha}{2} \cos k(\theta + \frac{\Delta\alpha}{2}) \tag{3.91}$$

For small values of $\Delta\alpha$, harmonic currents i'_{bk} and i'_{ck} are approximatcly in phase with each other and in antiphase with respect to i'_{ak}.

Similar remarks can be made for phase shifts of the m.s coinciding with other firing pulses.

3.8 Effect of a 150Hz m.s. on the a.c. line harmonic currents

If a 150Hz m.s. is imposed on the control voltage of a 6-pulse converter, the firing pulses to the valves will be alternatively advanced and delayed, as shown in Fig. 3.13. The harmonic analysis below assumes that the odd-numbered valves are fired $\Delta\alpha$ degrees early and the even-numbered valves are fired on time, as indicated in Table 3.11. The current pulses corresponding to the difference between the base case and the case in which the firing pulse distribution is modified by a 150Hz m.s., are shown in Fig. 3.13. It can be observed in the following

a.) Phases "a", "b" and "c" consist of identical train of pulses phase shifted successively by 120°;

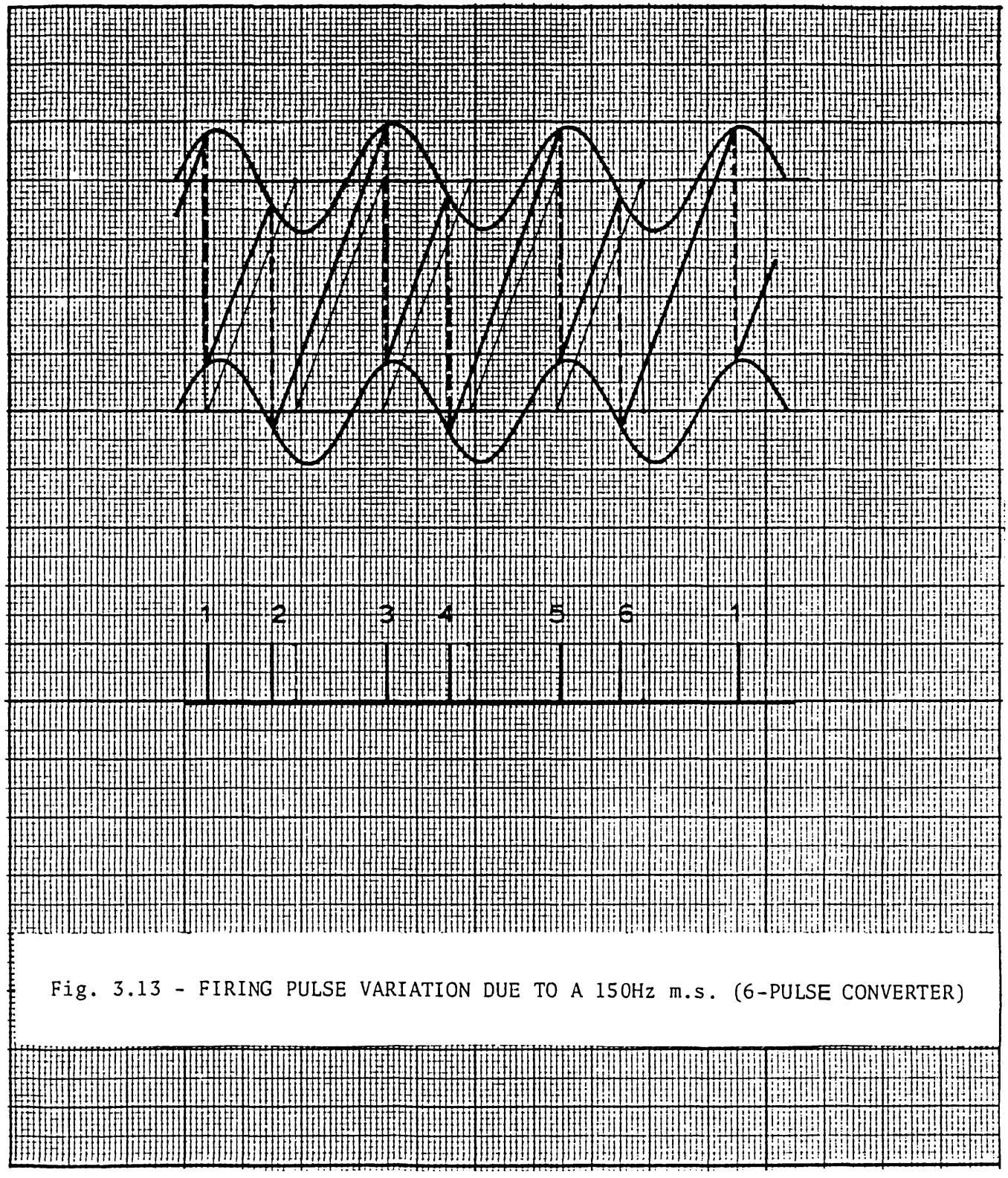

Fig. 3.13 - FIRING PULSE VARIATION DUE TO A 150Hz m.s. (6-PULSE CONVERTER)

TABLE 3.1.1

FIRING PULSE VARIATION DUE TO A 150Hz M.S.

VALVE	$\Delta\alpha$
1	$\Delta\alpha$
2	0
3	$\Delta\alpha$
4	0
5	$\Delta\alpha$
6	0

b) There is no d.c. current component

The harmonic analysis is started with phase "b".

3.8.1 Harmonic analysis of phase "b"

Table 3.12 gives the values of "a" and "θ" that should be introduced in eqn 3.23 to represent the "b" phase currents in Fig. 3.14.

TABLE 3.12

PHASE "b" PULSE TRAIN PARAMETERS (150Hz M.S.)

SERIES OF PULSES	a	θ
+	$\Delta\alpha$	$\theta + \frac{\Delta\alpha}{2}$
-	$\Delta\alpha$	$\theta - 240 + \frac{\Delta\alpha}{2}$

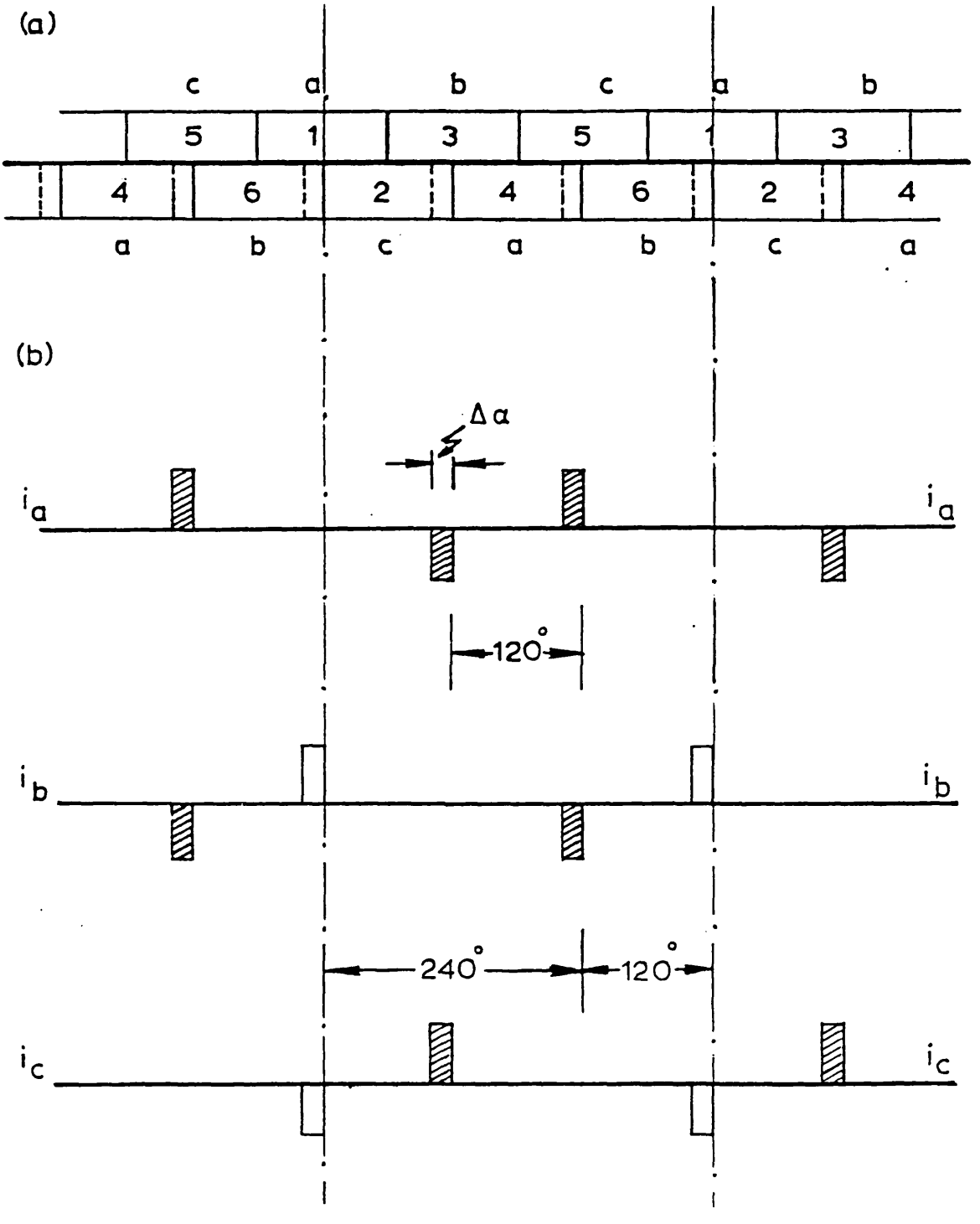

Fig. 3.14 - INCREMENTAL LINE CURRENT CAUSED BY A 150Hz m.s.

The train of positive and negative pulses is given, respectively by:

$$i'_{bk} = \frac{2I_{dc}}{k\pi} \sin \frac{k\Delta\alpha}{2} \cos k(\theta + \frac{\Delta\alpha}{2}) \qquad (3.92)$$

$$i''_{bk} = \frac{2I_{dc}}{k\pi} \sin \frac{k\Delta\alpha}{2} \cos k(\theta + \frac{\Delta\alpha}{2} - 240) \quad . \qquad (3.93)$$

To combine the trains of positive and negative pulses, eqn 3.93 is substracted from 3.92.

$$i_{bk} = \frac{2I_{dc}}{k\pi} \sin \frac{k\Delta\alpha}{2} [\cos k(\theta + \frac{\Delta\alpha}{2}) - \cos k(\theta + \frac{\Delta\alpha}{2} - 240)] \; . \qquad (3.94)$$

Eqn 3.94 can be simplified to:

$$i_{bk} = - \frac{4I_{dc}}{k\pi} \sin \frac{k\Delta\alpha}{2} \sin k\,120 \sin k(\theta + \frac{\Delta\alpha}{2} - 120) \quad . \qquad (3.95)$$

Harmonic currents expressed by eqn 3.95 can be classified into three categories:

a) Harmonics of order $k = 3q - 1$

Here the following form obtains

$$i_{bk} = \frac{2\sqrt{3}I_{dc}}{k\pi} \sin \frac{k\Delta\alpha}{2} \sin k(\theta + \frac{\Delta\alpha}{2} - 120) \qquad (3.96)$$

b) Harmonics of order $k = 3q + 1$

Here the form is

$$i_{bk} = - \frac{2\sqrt{3}I_{dc}}{k\pi} \sin \frac{k\Delta\alpha}{2} \sin k(\theta + \frac{\Delta\alpha}{2} - 120) \qquad (3.97)$$

c) Harmonics of order k = 3q

$$i_{bk} = 0.$$

3.8.2 Harmonic analysis of phase "a"

From Fig. 3.14 it is clear that phase current "a" can be obtained directly from eqns 3.96 and 3.97 through the substitution $\theta \rightarrow \theta + 120^{o}$

$$i_{ak} = - \frac{4I_{dc}}{k\pi} \sin \frac{k\Delta\alpha}{2} \sin k\,120 \sin k(\theta + \frac{\Delta\alpha}{2}) \qquad (3.98)$$

as the general form and

$$i_{ak} = \frac{2\sqrt{3}I_{dc}}{k\pi} \sin \frac{k\Delta\alpha}{2} \sin k(\theta + \frac{\Delta\alpha}{2}) \qquad (3.99)$$

for k = 3q - 1

$$i_{ak} = - \frac{2\sqrt{3}I_{dc}}{k\pi} \sin \frac{k\Delta\alpha}{2} \sin k(\theta + \frac{\Delta\alpha}{2}) \qquad (3.100)$$

for k = 3q + 1 .

3.8.3 Harmonic analysis of phase "c"

In this case the substitution $\theta \rightarrow \theta + 240$ gives :

$$i_{ck} = \frac{2\sqrt{3}I_{dc}}{k\pi} \sin \frac{k\Delta\alpha}{2} \sin k(\theta + \frac{\Delta\alpha}{2} - 240)$$

for k = 3q - 1 (3.101)

$$i_{ck} = -\frac{2\sqrt{3}I_{dc}}{k\pi} \sin\frac{k\Delta\alpha}{2} \sin k(\theta + \frac{\Delta\alpha}{2} - 240)$$

$$\text{for } k = 3q + 1 \ . \qquad (3.102)$$

Clearly harmonics of order $k = 3q - 1$ are of negative sequence and those of order $3q + 1$ are of positive sequence. There are no zero sequence currents.

3.8.4 General comments

a) Proportionality between $\Delta\alpha$ and a.c. line harmonic currents

The amplitude of the harmonic currents of order k given by equations 3.96 through 3.102 is

$$A_k = \frac{2\sqrt{3}I_{dc}}{k\pi} \sin\frac{k\Delta\alpha}{2} \ . \qquad (3.103)$$

Using a truncated Taylor series expressed for the sine factor results

$$A_k \cong \frac{\sqrt{3}\Delta\alpha I_{dc}}{\pi} \ .$$

It can be concluded that for small $\Delta\alpha$ the harmonic currents caused by a 150Hz m.s. on the control voltage, is proportional to $\Delta\alpha$.

b) Harmonics of even order.

For $k = 2$, eqns 3.96, 3.99 and 3.101 become :

$$i_{a2} = A_2 \sin(2\theta + \Delta\alpha) \qquad (3.104)$$

$$i_{b2} = A_2 \sin (2\theta + \Delta\alpha - 240) \qquad (3.105)$$

$$i_{c2} = A_2 \sin(2\theta + \Delta\alpha - 120) \qquad (3.106)$$

where A_2 is obtained from eqn 3.103.

Eqns 3.104 to 3.106 are recognized as a set of balanced 3-pulse second harmonic currents of negative sequence.

The 4th, 8th and 10th harmonic currents are close to the cut-off frequency of harmonic filters (turned at 5th, 7th, 11th) and a reduction in their magnitude should be expected.

c) Modulating signal phase shift

The incremental phase current in a 6-phase converter whose control voltage is modulated by a 150Hz m.s., is shown in Fig. 3.15. The m.s. here is delayed by 60 degrees with respect to the case illustrated in Fig. 3.14. The incremental harmonic currents i'_{ak}, i'_{bk} and i'_{ck} are described by eqns 3.96, 3.99 and 3.101 with a negative sign for harmonics of order $k = 3q - 1$ and by eqns 3.97, 3.100 and 3.102 with a negative sign for harmonics of order $k = 3q + 1$. The angle reference θ must also be replaced by θ-60. The incremental harmonic currents are then given by

a) for $k = 3q-1$

$$i'_{ak} = -A_k \sin k(\theta + \frac{\Delta\alpha}{2} + 300) \qquad (3.107)$$

$$i'_{bk} = -A_k \sin k(\theta + \frac{\Delta\alpha}{2} + 180) \qquad (3.108)$$

$$i'_{ck} = - A_k \sin k(\theta + \frac{\Delta\alpha}{2} + 60) \qquad (3.109)$$

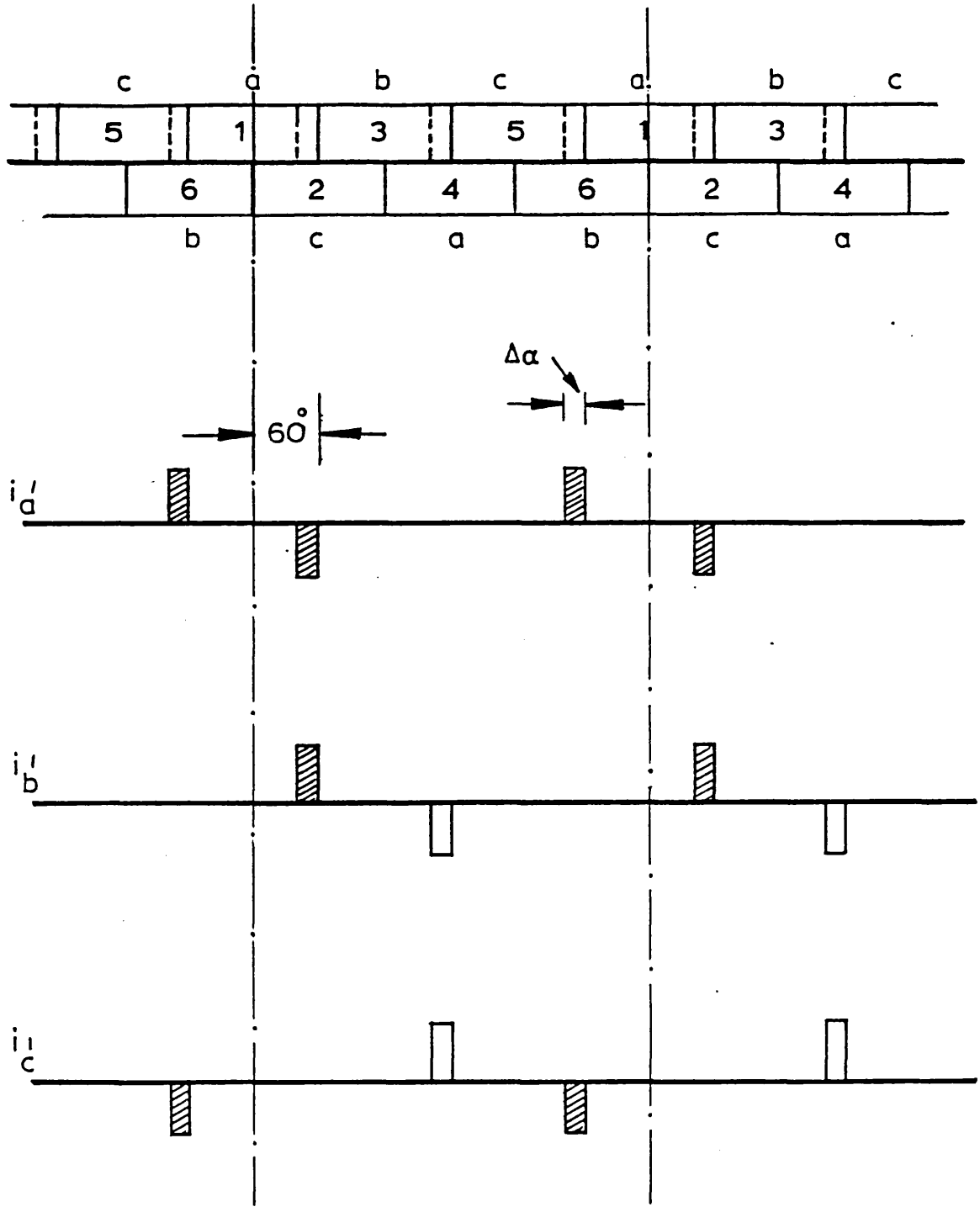

Fig. 3.15 - POSITIVE GOING CROSSOVER OF A 150Hz M.S. COINCIDING WITH FIRING PULSE TO VALVE 2

b) for $k = 3q + 1$

$$i'_{ak} = A_k \sin k(\theta + \frac{\Delta\alpha}{2} + 300) \quad (3.110)$$

$$i'_{bk} = A_k \sin k(\theta + \frac{\Delta\alpha}{2} + 180) \quad (3.111)$$

$$i'_{ck} = A_k \sin k(\theta + \frac{\Delta\alpha}{2} + 60) \; . \quad (3.112)$$

If $k = 2$, eqns 3.107 and 3.109 become

$$i'_{a2} = A_2 \sin(2\theta + \Delta\alpha + 60) \quad (3.113)$$

$$i'_{b2} = A_2 \sin(2\theta + \Delta\alpha + 180) \quad (3.114)$$

$$i'_{c2} = A_2 \sin(2\theta + \Delta\alpha + 300) \; . \quad (3.115)$$

Comparing eqns 3.113 to 3.115 with eqns 3.104 to 3.106 it is concluded that a second harmonic of negative sequence caused by a 150Hz m.s., changes its phase according to the phase of the m.s. . That is, if the m.s. is shifted by 60 degrees in fundamental terms, the a.c. line second harmonic current becomes also shifted 60 degrees but, in second harmonic terms. The implications of this are discussed later on in this chapter.

3.9 Effect of a 50 Hz m.s. on the d.c. voltage

A m.s. on the control voltage of a converter causes not only harmonic distortion on the a.c. current but also, on the d.c. current voltage. The heavy line in Fig. 3.16(a), represents the base case for which equally spaced firing pulses and a balanced sinusoidal a.c. supply

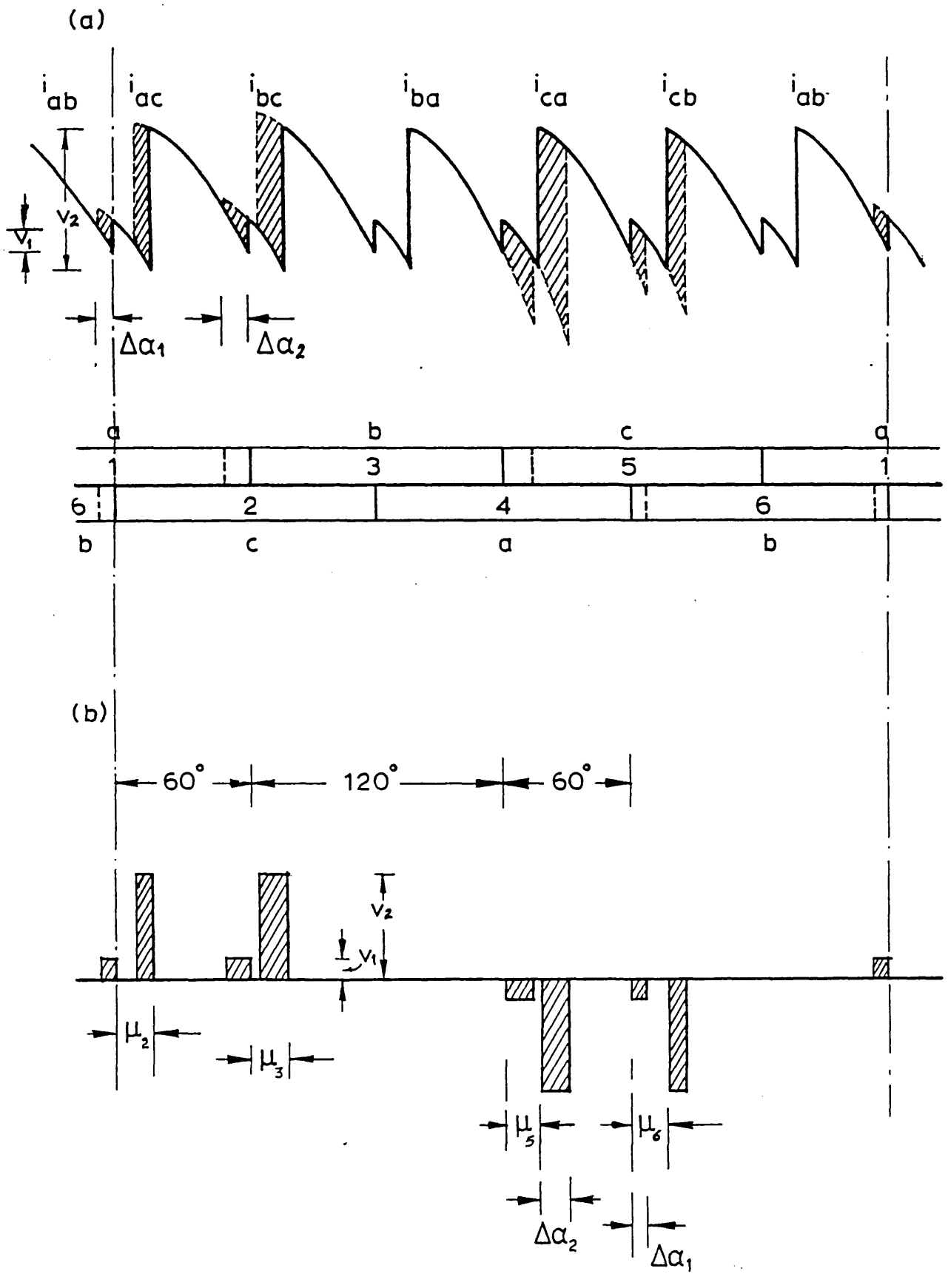

Fig. 3.16 - INCREMENTAL D.C. LINE VOLTAGE TO A 50Hz M.S. WHOSE POSITIVE GOING CROSSOVER COINCIDES WITH FIRING TO VALVE 1

(a) D.C. Voltage Ripple
(b) Incremental D.C. Voltage

are assumed. The shaded areas in the figure represent the incremental blocks of d.c. line voltage resulting from the difference between the base case and the case with a 50Hz m.s. superimposed on the control voltage.

In Fig. 3.16(b) it is assumed that the incremental d.c. voltage is approximated by rectangular pulses of voltage. It is also assumed that the overlap angles remain unaltered from their balanced steady-state value, μ .

a) The incremental d.c. line voltage consists of alternate pulses of amplitudes V_1 and V_2 and corresponding widths $\Delta\alpha_1$ and $\Delta\alpha_2$;

b) The phase difference between the series of pulses of amplitudes V_1 and V_2 is the overlap angle, μ;

c) There is no average incremental voltage level.

3.9.1. Harmonic analysis of the incremental d.c. voltage

Initially, only pulses of amplitude V_1 are considered. These pulses can be classified into four different types :

1) positive pulses of width $\Delta\alpha_1$ labelled $(+, \Delta\alpha_1)$;

2) negative pulses of width $\Delta\alpha_1$ labelled $(-, \Delta\alpha_1)$;

3) positive pulses of width $\Delta\alpha_2$ labelled $(+, \Delta\alpha_2)$;

4) negative pulses of width $\Delta\alpha_2$ labelled $(-, \Delta\alpha_2)$.

The generic summation term of eqn 3.23 is used again in the harmonic analysis of the incremental d.c. voltage shown in Fig. 3.16. Values of "a" and "θ" to represent the train of pulses of amplitude V_1 according to eqn 3.23 are given in Table 3.13.

TABLE 3.13

D.C. VOLTAGE PULSE TRAIN PARAMETERS (50Hz M.S.)

PULSE TYPE	a	θ
$(+, \Delta\alpha_1)$	$\Delta\alpha_1$	$\theta + \frac{\Delta\alpha_1}{2}$
$(-, \Delta\alpha_1)$	$\Delta\alpha_1$	$\theta - \frac{\Delta\alpha_1}{2} - 240$
$(+, \Delta\alpha_2)$	$\Delta\alpha_2$	$\theta \frac{\Delta\alpha_2}{2} - 60$
$(-, \Delta\alpha_2)$	$\Delta\alpha_2$	$\theta - 180 - \frac{\Delta\alpha_2}{2}$

The general equation corresponding to the summation of the series described in Table 3.13 is:

$$v'_{dk} = \frac{2V_1}{k\pi}\left[\sin\frac{k\Delta\alpha_1}{2}\left[\cos k\left(\theta + \frac{\Delta\alpha_1}{2}\right) - \cos k\left(\theta - 240 - \frac{\Delta\alpha_1}{2}\right)\right] + \sin\frac{\Delta\alpha_2}{2}\left[\cos k\left(\theta - 60 + \frac{\Delta\alpha_2}{2}\right) - \cos k\left(\theta - 180 - \frac{\Delta\alpha_2}{2}\right)\right]\right] \quad \ldots\ (3.116)$$

Eqn 3.116 can be simplified using the trigonometric identity

$$\cos A - \cos B = 2 \sin\frac{A+B}{2} \sin\frac{B-A}{2}$$

to become

$$v'_{dk} = -\frac{4V_1}{k\pi} \sin k(\theta - 120)\left[\cos k\,120 - \cos k(120 + \phi_s)\cos k\phi_d\right] \quad \ldots\ (3.117)$$

where V_1 is given by eqn 3.21 and ϕ_s and ϕ_d are defined by eqns 3.33 and 3.34, respectively.

The series of pulses of amplitude V_2 can be obtained from eqn 3.117 by replacing θ by $\theta-\mu$ and V_1 by V_2, i.e.

$$v''_{dk} = -\frac{4V_2}{k\pi}\sin k(\theta-\mu-120)[\cos k\,120 - \cos k(120 + \phi_s)\cos k\phi_d]. \quad (3.118)$$

The total incremental d.c. line harmonic voltage of order k is obtained by combining eqns 3.117 and 3.118 :

$$v_{dk} = -\frac{4}{k\pi}[V_1 \sin k(\theta + 120) + V_2 \sin k(\theta - \mu - 120)] \times [\cos k\,120 - \cos k(120 + \phi_s)\cos k\phi_d]. \quad (3.119)$$

If the overlap angle is neglected, then $V_1 = 0$ and $\mu = 0$.

3.9.2 Cases of particular interest

a) if k = 1 and for a negligible ϕ_d, eqn 3.119 becomes :

$$v_{d1} = \frac{4}{\pi}[V_1 \sin(\theta - 120) + V_2 \sin(\theta - \mu - 120)] \times [\cos 120 - \cos(120 + \phi_s)] . \quad (3.120)$$

In Appendix B eqn B.48 shows that the cosine difference in eqn 3.120 can be approximated by

$$\cos 120 - \cos(120 + \phi_s) \cong \phi_s \sin(120 + \frac{\phi_s}{2}) .$$

It can be concluded that the amplitude of the incremental d.c. line 50Hz harmonic voltage caused by a 50Hz m.s. is approximately proportional to the average of the firing angle variation ϕ_s

b) Modulating signal phase shifting

If the m.s. positive going crossover coincides with the firing to valve 2, then the incremental voltage pulses will be identical to the ones presented in Fig. 3.16 but with a 60 degree shift. So, θ in eqn 3.120 has to be replaced by $\theta - 60^o$. This phase shift results in

$$v_{d1} = \frac{4}{\pi}[V_1 \sin\theta + V_2 \sin(\theta-\mu)][\cos 120 - \cos(120 + \phi_s)]$$

It can be concluded that, a 60 degree phase shift in the m.s. corresponds to an identical phase shift in the incremental d.c. line 50Hz harmonic voltage.

3.10 Effect of a 100Hz m.s. on the d.c. line voltage

Fig. 3.17 represents the incremental d.c. line blocks of voltage between the base case and the case in which a 100Hz m.s. is superimposed on the control voltage. The following observation followed from Fig. 3.17.

a) The incremental d.c. line voltage consists of pulses alternately of amplitude V_1 and V_2.

b) The phase difference between the train of pulses of amplitude V_1 and those of amplitude V_2 is one overlap angle, μ.

c) All voltage pulses have the same width. $\Delta\alpha$.

d) There are two identical train of pulses 180 degrees apart therefore, the lowest harmonic order is the second.

e) There is no average incremental d.c. voltage.

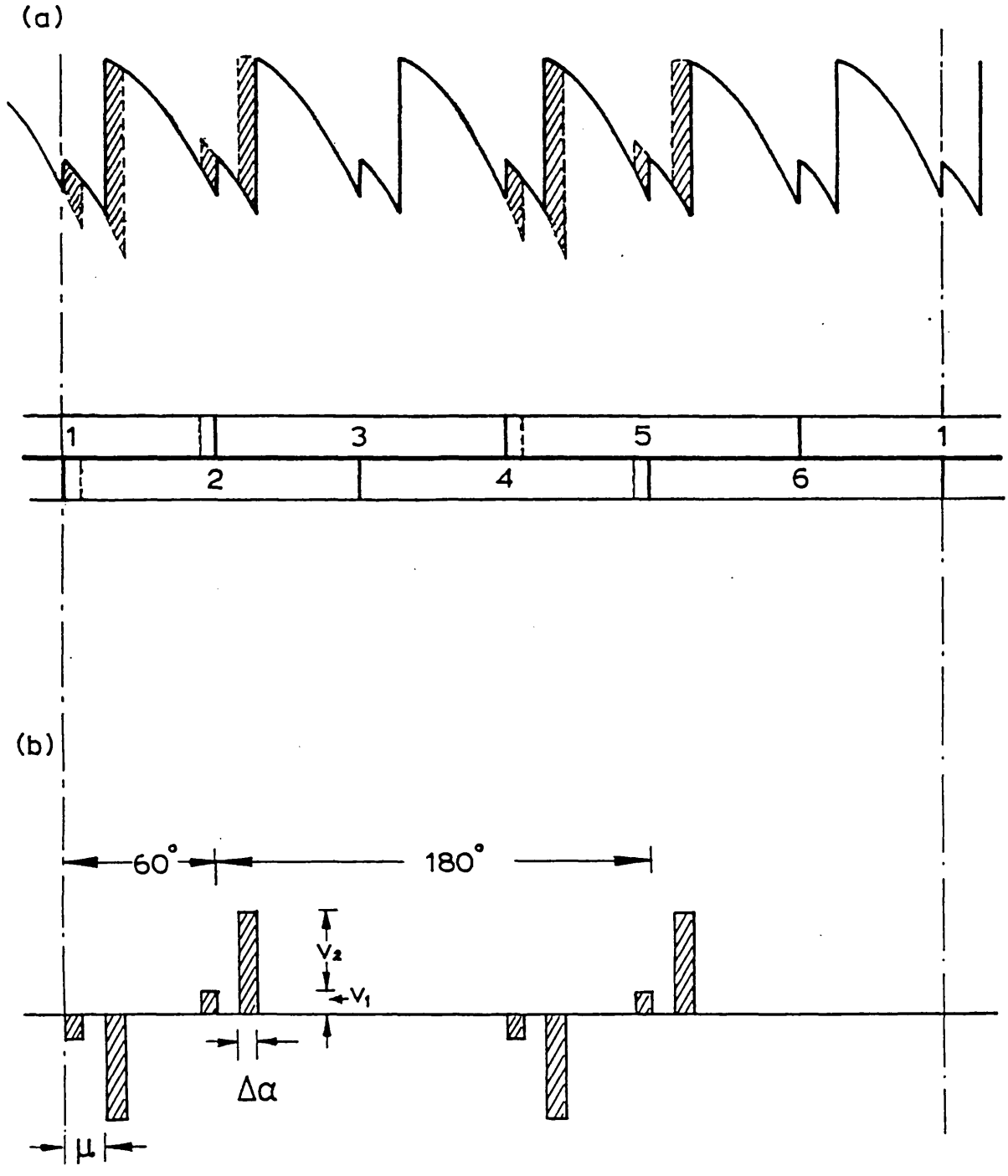

Fig. 3.17 - INCREMENTAL D.C. LINE VOLTAGE DUE TO A 100Hz M.S. WHOSE POSITIVE GOING CROSSOVER COINCIDES WITH FIRING PULSE TO VALVE 1

(a) d.c. Voltage Ripple
(b) Incremental D.C. Voltage

3.10.1 Harmonic analysis of the d.c. line voltage

The harmonic analysis follows the same lines as for the 50Hz m.s. case. Table 3.14 gives the values of "a" and "θ" to be used in eqn 3.23 to obtain the harmonic contribution of each train of pulses

TABLE 3.14

D.C. VOLTAGE PULSE TRAIN PARAMETERS(100Hz M.S.)

PULSE TRAIN	a	θ
+	$\Delta\alpha$	$\theta - 60 + \frac{\Delta\alpha}{2}$
-	$\Delta\alpha$	$\theta - \frac{\Delta\alpha}{2}$
+	$\Delta\alpha$	$\theta - 60 + \frac{\Delta\alpha}{2} - 180$
-	$\Delta\alpha$	$\theta - \frac{\Delta\alpha}{2} - 180$

The train of pulses of amplitude V_1 can be combined according to eqn 3.23 to give

$$v'_{dk} = \frac{2V_1}{k\pi} \sin \frac{k\Delta\alpha}{2}[\cos k(\theta-60+\frac{\Delta\alpha}{2}) - \cos k(\theta-\frac{\Delta\alpha}{2}) +$$

$$\cos k(\theta-60+\frac{\Delta\alpha}{2} - 180) - \cos k(\theta-\frac{\Delta\alpha}{2} - 180)]. \qquad (3.122)$$

For odd k's eqn 3.122 is equal to zero. For even k's and after algebraic manipulation yields

$$v'_{dk} = \frac{-8V_1}{k\pi} \sin\frac{k\Delta\alpha}{2} \sin k\left(\frac{\Delta\alpha}{2} - 30\right)\sin k(\theta - 30) \quad . \qquad (3.123)$$

The series of pulses of amplitude V_2 can be obtained directly from eqn 3.123 if θ is replaced by $\theta-\mu$ and V_1 by V_2 :

$$v''_{dk} = \frac{-8V_2}{k\pi} \sin\frac{k\Delta\alpha}{2} \sin k\left(\frac{\Delta\alpha}{2} - 30\right)\sin k(\theta-\mu-30)$$

$$\text{for even k's} \quad . \qquad (3.124)$$

The total incremental harmonic voltage is the summation of eqns 3.123 and 3.124 :

$$v_{dk} = -\frac{8}{k\pi} \sin\frac{k\Delta\alpha}{2}\sin k\left(\frac{\Delta\alpha}{2} - 30\right)[V_1 \sin k(\theta - 30) +$$

$$+ \sin k(\theta - \mu - 30)] \quad \text{for even k's} \; . \qquad (3.125)$$

For small values of $k\Delta\alpha$, the following approximations can be made:

a) $\sin\frac{k\Delta\alpha}{2} \cong \frac{k\Delta\alpha}{2}$

b) $\sin k\left(30 - \frac{\Delta\alpha}{2}\right) \cong \sin k\ 30$.

So, the amplitude of eqn 3.125 becomes

$$A \cong \frac{4\Delta\alpha}{\pi} \sin k\ 30 \quad . \qquad (3.126)$$

From eqn 3.126 can be concluded that the d.c. line harmonic due to a 100Hz m.s. is approximately proportional to $\Delta\alpha$.

3.10.2 Cases of particular interest

a) if k = 2 eqn. 3.125 becomes:

$$v_{d2} = \frac{4}{\pi} \sin \Delta\alpha \sin(60 - \Delta\alpha)[V_1 \sin(2\theta - 60) + V_2 \sin(2\theta - 2\mu - 60)] \quad (3.127)$$

b) Modulating signal phase shifting

If the m.s. positive-going crossover coincides with the firing to valve 2, the incremental pulses will be identical to the ones in Fig. 3.17 but delayed by 60°. If θ is replaced by θ-60 in eqn 3.125, it now expresses the incremental d.c. line voltage corresponding to the new phase of the m.s.:

$$v_{dk} = -\frac{8}{k\pi} \sin \frac{k\Delta\alpha}{2} \sin k\left(\frac{\Delta\alpha}{2} - 30\right)[V_1 \sin k(\theta - 90) + V_2 \sin k(\theta - \mu - 90)] \quad \text{for even k's} \quad . \quad (3.128)$$

In the particular case of a 2nd harmonic :

$$v_{d2} = \frac{+4}{\pi} \sin \Delta\alpha \sin(\Delta\alpha - 60)[V_1 \sin(2\theta) + V_2 \sin(2\theta - 2\mu)] \quad (3.129)$$

It can be concluded that a 60 degree phase shift of the m.s., in fundamental terms corresponds to an equivalent phase shift in the incremental d.c. line harmonic voltage.

3.11 Effect of a 150Hz m.s. on the d.c. line voltage

The incremental d.c. line voltage due to a 150Hz m.s. on the

control voltage of a 6- pulse converter, is presented in Fig. 3.18. The harmonic analysis follows the procedure used in the 100Hz m.s. case.

The following observations can be made on Fig. 3.18(b) :

a) The incremental d.c. line voltage consists of alternate pulses of amplitude V_1 and V_2;

b) The phase difference between the train of pulses of amplitude V_1 and the train of pulses of amplitude V_2 is exactly one overlap angle, μ ;

c) All voltage pulses have the same width, $\Delta\alpha$;

d) There are three identical sets of pulses 120°apart from each other and so, the 3rd harmonic is the lowest possible harmonic order in the Fourier Analysis;

e) There is no average incremental d.c. voltage.

3.11.1 Harmonic analysis of the d.c. line voltage

This analysis is based on eqn 3.23 and on the series of pulses of amplitude V_1. Values of "a" and "θ" corresponding to the train of pulses in Fig. 3.18, are shown in Table 3.15.

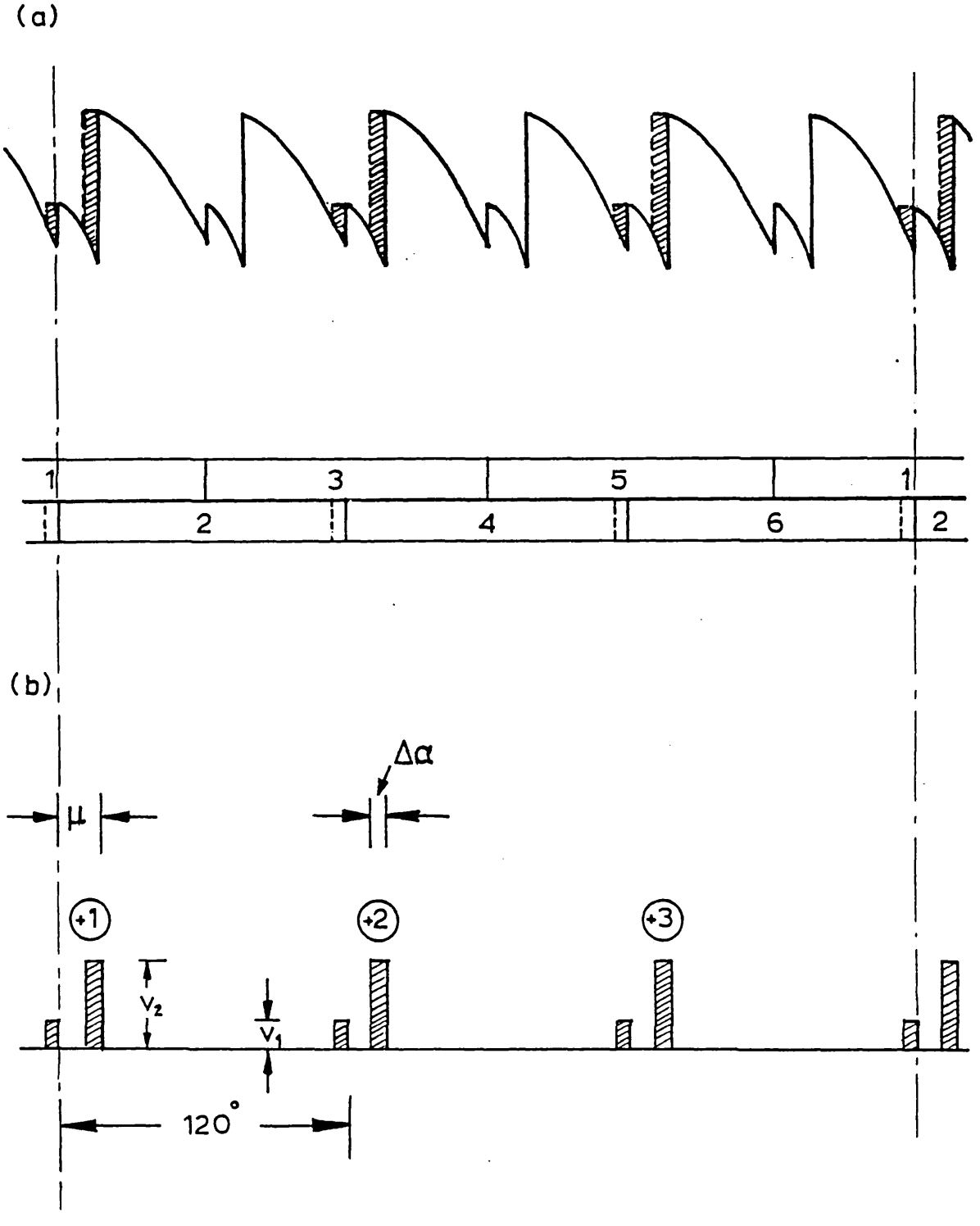

Fig. 3.18 - INCREMENTAL d.c. LINE VOLTAGE DUE TO THE 150Hz m.s. SHOWN IN Fig. 3.13

TABLE 3.15

D.C. VOLTAGE PULSE TRAIN PARAMETERS (150Hz M.S.)

TYPE OF TRAIN	a	θ
+1	$\Delta\alpha$	$\theta + \frac{\Delta\alpha}{2}$
+2	$\Delta\alpha$	$\theta - 120 + \frac{\Delta\alpha}{2}$
+3	$\Delta\alpha$	$\theta - 240 + \frac{\Delta\alpha}{2}$

The combination of the three types of pulses in Table 3.15 gives

$$v'_{dk} = \frac{2V_1}{k\pi} \sin \frac{k\Delta\alpha}{2} \left[\cos k(\theta+\frac{\Delta\alpha}{2}) + \cos k(\theta - 120 + \frac{\Delta\alpha}{2}) + \right.$$

$$\left. \cos k(\theta - 240 + \frac{\Delta\alpha}{2})\right]. \qquad (3.130)$$

This equation is equal to zero for all k's which are not multiples of three. The triplen harmonic, eqn 3.130 becomes :

$$v'_{dk} = \frac{6V_1}{k\pi} \sin \frac{k\Delta\alpha}{2} \cos k(\theta + \frac{\Delta\alpha}{2}). \qquad (3.131)$$

If V_1 is replaced by V_2 and θ by $\theta-\mu$, eqn 3.131 can be used to obtain the incremental harmonic voltage corresponding to the train of pulses of amplitude V_2:

$$v''_{dk} = \frac{6V_2}{k\pi} \sin \frac{k\Delta\alpha}{2} \cos k(\theta + \frac{\Delta\alpha}{2} - \mu) . \qquad (3.132)$$

The total incremental voltage due to a 150Hz m.s. is obtained

by adding eqns 3.131 and 3.132

$$v_{dk} = \frac{6}{k\pi} \sin\frac{k\Delta\alpha}{2} \left[V_1 \cos k(\theta + \frac{\Delta\alpha}{2}) + V_2 \cos k(\theta + \frac{\Delta\alpha}{2} - \mu)\right]$$

(for k multiple of 3) . (3.133)

For small values of $\Delta\alpha$, the sine factor outside brackets of eqn 3.133 can be approximated by $k\Delta\alpha/2$ therefore, the equation becomes:

$$v_{dk} \cong \frac{3\Delta\alpha}{\pi} \left[V_1 \cos k(\theta + \frac{\Delta\alpha}{2}) + V_2 \cos k(\theta + \frac{\Delta\alpha}{2} - \mu)\right]$$

(for k multiple of 3) . (3.134)

It can be concluded that for small values of $\Delta\alpha$ the d.c. line voltage due to a 150Hz m.s. is approximately proportional to $\Delta\alpha$.

Furthermore, a 60 degree m.s. phase shift, corresponds to a 60k degree phase shift of the incremental harmonic voltage of order k.

3.12 Relationship between $\Delta\alpha$ and d.c. line harmonic currents

Eqns 3.119, 3.125 and 3.133 give the approximate incremental harmonic components of the d.c. line voltage due to a 50Hz, 100Hz and 150Hz m.s., respectively. These equations can be used to obtain the incremental d.c. line harmonic currents, as explained below.

Let the d.c. line input impedance be represented by an equivalent impedance Z_{dk}, as shown in Fig. 3.19. For any harmonic voltage, V_{dk}, the d.c. line harmonic current is :

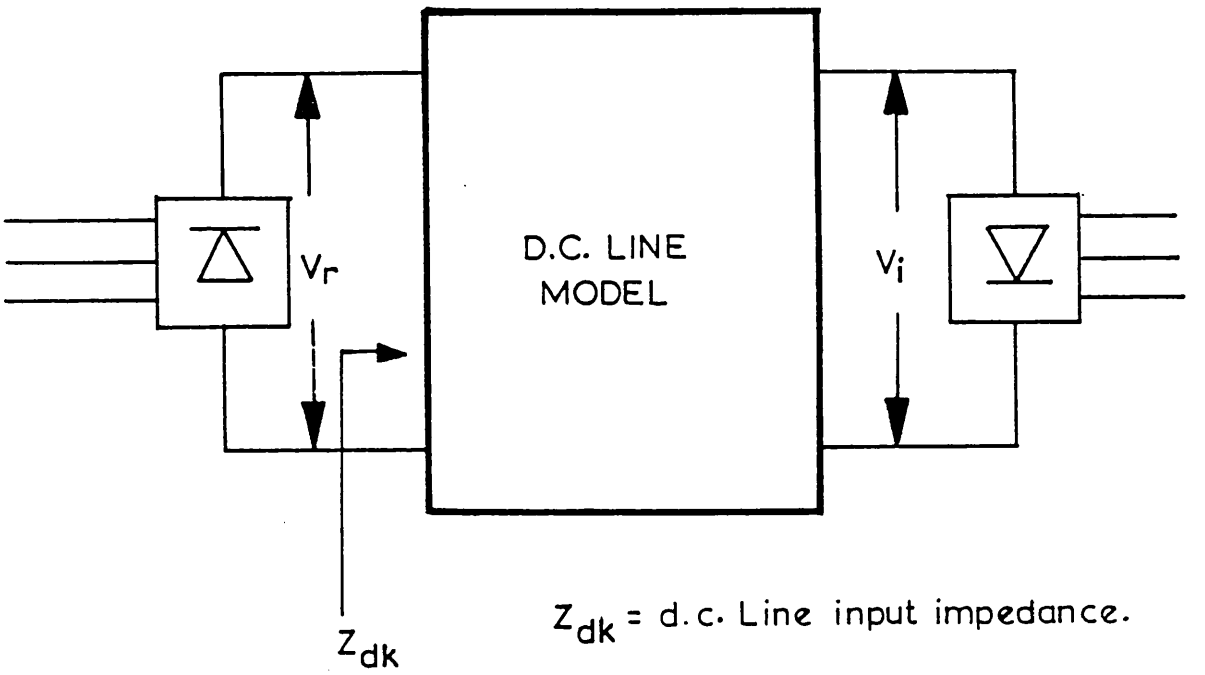

Fig. 3.19 - D.C.-SIDE REPRESENTATION

$$I_{dk} = \frac{V_{dk}}{Z_{dk}} \quad . \tag{3.135}$$

Hence, it may be concluded that I_{dk} is also proportional to $\Delta\alpha$.

Approximate expression of the d.f. for a balanced a.c. system can be derived from eqns 3.135 and 2.4 as follows

$$D.F. \cong \frac{I_{dk}\angle\theta_{dk}}{V_m\angle\theta_k} \tag{3.136}$$

3.13 Relationship between a.c.-side and d.c.-side harmonic voltage

Assuming at the outset no overlap angle and ideal a.c. conditions, the d.c. line voltage is given by the difference between any two generic phases, "m" and "n", as below:

$$V_{nm} = V_n - V_m \quad . \tag{3.137}$$

where

$$V_n = |V_n|\cos(\theta + \phi_n) \tag{3.138}$$

$$V_m = |V_m|\cos(\theta + \phi_m) \tag{3.139}$$

ϕ_m, ϕ_n are, respectively, the phase angle of phase "m" and phase "n" (with respect to an arbitrary common reference).

$\theta = \omega_0 t$

ω_0 = fundamental angular frequency.

V_m, V_n amplitude of phase "m" and phase "n", respectively, on the valve side of the converter transformer.

In order to simplify the harmonic analysis of the d.c. line ripple due to a.c. harmonic distortions, it is assumed that this distortion consists of sets of 3-phase harmonic voltages, predominantly of positive or negative sequence. The harmonic phase voltage during each interfiring period, is then added to the fundamental voltage to give the total d.c. side voltage. The harmonic phase voltage "difference" of order "ℓ" is given by:

$$V_\ell = V_{n\ell} - V_{m\ell} \tag{3.140}$$

where

$$V_{n\ell} = V \cos(\ell\theta + \ell\phi_n) \tag{3.141}$$

$$V_m = V \cos(\ell\theta + \ell\phi_m) \tag{3.142}$$

$|V|$ = voltage amplitude of the phase sequence.

Substituting eqns 3.141 and 3.142 into eqn 3.140 and simplifying through trigonometry, results

$$V_\ell = |V_\ell| \sin \ell(\theta + \phi_\ell) \tag{3.143}$$

where:

$$|V_\ell| = 2|V| \sin \ell\left(\frac{\phi_m - \phi_n}{2}\right) \quad \text{and}$$

$$\phi_\ell = \frac{\phi_m + \phi_n}{2} \ .$$

The primary harmonic voltage, V_ℓ, gives rise to uncharacteristic harmonic voltages in the d.c. voltage. These uncharacteristic harmonics can be obtained by Fourier Analysis through

$$V_d = \frac{A_0}{2} + \sum_{k=1}^{\infty} (A_k \cos k\theta + B_k \sin k\theta) \tag{3.144}$$

where :

$$A_0 = \frac{1}{2\pi}\int_0^{2\pi} V_d \, d\theta \tag{3.145}$$

$$A_k = \frac{1}{\pi}\int_0^{2\pi} V_d \cos k\theta \, d\theta \tag{3.146}$$

$$B_k = \frac{1}{\pi}\int_0^{2\pi} V_d \sin k\theta \, d\theta \tag{3.147}$$

To synthesize the d.c. voltage, the fundamental cycle can be subdivided into six parts each corresponding to one of the six interfiring periods. Therefore, to calculate A_k and B_k, the integrals of eqns 3.146 and 3.147 are split into six sections and the partial results added to obtain the total solution. If the general limits of each interfiring period are given as θ_i and θ_{i+1}, then A_k and B_k for that specific period are:

$$A_k = \frac{1}{2\pi}|V_\ell|\left[\cos \ell\phi_\ell \left(- \frac{\cos(\ell+k)\theta}{\ell+k} - \frac{\cos(\ell-k)\theta}{\ell-k} \right)_{\theta_i}^{\theta_{i+1}} + \right.$$
$$\left. \sin \ell\phi_\ell \left(+ \frac{\sin(\ell+k)\theta}{\ell+k} + \frac{\sin(\ell-k)\theta}{\ell-k} \right)_{\theta_i}^{\theta_{i+1}} \right] \tag{3.148}$$

$$B_k = \frac{1}{2\pi}|V_\ell|\left[\cos \ell\phi_\ell \left(- \frac{\sin(\ell+k)\theta}{\ell+k} + \frac{\sin(\ell-k)\theta}{\ell-k} \right)_{i}^{\theta_{i+1}} + \right.$$
$$\left. \sin \ell\phi_\ell \left(- \frac{\cos(\ell+k)\theta}{\ell+k} + \frac{\cos(\ell-k)\theta}{\ell-k} \right)_{\theta_i}^{\theta_{i+1}} \right] \tag{3.149}$$

Eqns 3.148 and 3.149 can be used to calculate approximately the d.c. side harmonic voltage caused by a particular a.c. side harmonic content. If more than one frequency is present on the a.c. side, the results can be

combined by superposition [3].

In order to appreciate the influence of eqns 3.148 and 3.149 on the d.c. line harmonics, let:

$$A_1 = \left[-\frac{\cos(\ell+k)\theta}{\ell+k} - \frac{\cos(\ell-k)\theta}{\ell-k} \right]_{\theta_i}^{\theta_{i+1}} \tag{3.150}$$

$$A_2 = \left[\frac{\sin(\ell+k)\theta}{\ell+k} + \frac{\sin(\ell-k)\theta}{\ell-k} \right]_{\theta_i}^{\theta_{i+1}} \tag{3.151}$$

$$B_1 = \left[-\frac{\sin(\ell+k)\theta}{\ell+k} + \frac{\sin(\ell-k)\theta}{\ell-k} \right]_{\theta_i}^{\theta_{i+1}} \tag{3.152}$$

$$B_2 = \left[-\frac{\cos(\ell+k)\theta}{\ell+k} + \frac{\cos(\ell-k)\theta}{\ell-k} \right]_{\theta_i}^{\theta_{i+1}} \tag{3.153}$$

Eqns 3.148 and 3.149 can now be written in terms of A_1, A_2, B_1 and B_2 :

$$A_k = \frac{1}{4\pi}|V_\ell| \left[A_1 \cos \ell\phi_\ell + A_2 \sin \ell\phi_\ell \right]_{\theta_i}^{\theta_{i+1}} \tag{3.154}$$

$$B_k = \frac{1}{4\pi}|V_\ell| \left[B_1 \cos \ell\phi_\ell + B_2 \sin \ell\phi_\ell \right]_{\theta_i}^{\theta_{i+1}} \tag{3.155}$$

For each interfiring period limited by θ_i and θ_{i+1}, A_1, A_2, B_1 and B_2 are constants and ϕ_ℓ changes according to the phase of the primary harmonic voltage of order ℓ. The overall effect of $|V_\ell|$ and ϕ_ℓ on the d.c. line harmonics can be better appreciated if eqns 3.154 and 3.155 are introduced into eqn 3.144:

$$V_d = \frac{A_0}{2} + \frac{1}{2\pi}|V_\ell| \sum_{k=1}^{\infty}\Big[(A_1 \cos \ell\phi_\ell + A_2 \sin \ell\phi_\ell)\cos k\theta +$$

$$(B_1 \cos \ell\phi_\ell + B_2 \sin \ell\phi_\ell)\sin k\theta\Big] . \qquad (3.156)$$

Rearranging eqn 3.156 results:

$$V_d = \frac{A_0}{2} + \frac{1}{2\pi}|V_\ell| \sum_{k=1}^{\infty}\Big[\cos \ell\phi_\ell(A_1 \cos k\theta + B_1 \sin k\theta) +$$

$$\sin \ell\phi_\ell(A_2 \cos k\theta + B_2 \sin k\theta)\Big]. \qquad (3.157)$$

Letting now

$$A_{\ell k} \sin k\phi = A_1 \cos k\theta + B_1 \sin k\theta \qquad (3.158)$$

$$A_{\ell k} \cos k\phi = A_2 \cos k\theta + B_2 \sin k\theta \qquad (3.159)$$

eqn 3.157 can be reduced to

$$V_d = \frac{A_0}{2} + \frac{1}{2\pi}|V_\ell| \sum_{k=1}^{\infty}\Big[A_{\ell k} \sin(\ell\phi + k\phi)\Big] \qquad (3.160)$$

which express the d.c. line harmonic voltage of order k as :

$$V_{dk} = \left|\frac{V_\ell}{2\pi}\right| A_{\ell k} \sin(\ell\phi_\ell + k\phi) . \qquad (3.161)$$

It can now be concluded that

a) The k-th harmonic voltage V_{dk}, is proportional to the amplitude of the primary symmetrical component, $|V_\ell|$.

b) The phase of V_{dk} depends on $\ell\phi_\ell$ which is the phase of the primary harmonic voltage of order ℓ.

For example, the contribution of a primary second harmonic ($\ell = 2$) to the d.c. line 50Hz harmonic voltage (k=1) is given by

$$V_{d1} = \frac{|V_2|}{2\pi} A_{21} \sin(2\phi_2 + \phi) \quad . \qquad (3.162)$$

Eqn 3.162 explains how a 30 degree phase shift (= 60 degree in second harmonic terms) in the primary second harmonic voltage causes a 60 degree phase shift in the d.c. side 50Hz harmonic voltage.

3.14 Fundamental a.c.-side imbalance and generation of d.c.-side even harmonics

Let the line voltage of the converter busbar be:

$$V_a\angle\theta_a \quad ; \quad V_b\angle\theta_b \quad ; \quad V_c\angle\theta_c \quad .$$

By definition, the a.c. source is balanced if:

$$V_a = V_b = V_c = V$$

$$\theta_a = \theta$$

$$\theta_b = \theta - 120$$

$$\theta_c = \theta - 240 \quad .$$

An imbalance in one of the phases can be represented by

$$\Delta V/\Delta\theta = V'/\theta' - V/\theta \qquad (3.163)$$

where V'/θ' is an unbalanced phase voltage relative to V/θ the balanced value. Using Euler's formula :

$$\Delta V/\Delta\theta = V'(\cos\theta' + j\sin\theta') - V(\cos\theta + j\sin\theta) \; . \qquad \ldots(3.164)$$

Wherefrom

$$\Delta V = \sqrt{(V')^2 + V^2 - 2V'V\cos(\theta' - \theta)} \qquad (3.165)$$

$$\Delta\theta = TAN^{-1}\left(\frac{V'\sin\theta' - V\sin\theta}{V'\cos\theta' - V\cos\theta}\right) \; . \qquad (3.166)$$

In what follows, the three possible alternatives are considered

a) $V' = V$

$\theta' = \theta$

$$\Delta V = \sqrt{2}\,V\sqrt{1 - \cos(\theta' - \theta)} \qquad (3.167)$$

$$\Delta\theta = TAN^{-1}\left(\frac{\sin\theta' - \sin\theta}{\cos\theta' - \cos\theta}\right) \; . \qquad (3.168)$$

Simplifying eqn 3.167 through the trigonometric identity

$$1 - \cos A = 2\sin^2 A$$

results

$$\Delta V = 2V\sin\left(\frac{\theta' - \theta}{2}\right)$$

and for small values of $\left(\frac{\theta' - \theta}{2}\right)$,

$$\Delta V \cong V \cdot (\theta' - \theta) \quad . \tag{3.169}$$

It may be concluded that the amplitude imbalance ΔV is proportional to the phase imbalance.

b) $V' \neq V$

$\theta' = \theta$

$$\Delta V = (V' - V) \tag{3.170}$$

$$\Delta\theta = \theta \quad . \tag{3.171}$$

It may be concluded that the imbalance ΔV is proportional to the amplitude difference between balanced and unbalanced voltage amplitudes.

c) $V' \neq V$

$\theta' \neq V$.

This case is a combination of a) and b).

It can be concluded that a fundamental imbalance may be represented by a balanced 3-phase set plus a superimposed voltage of the same frequency and of amplitude and phase given by equations 3.165 and 3.166 respectively.

Assuming that superposition is obeyed, the imbalance vector $\Delta V/\Delta\theta$ will be rectified by the converter and will contribute to the d.c.-side 2nd harmonic. However in practice, second order effects will be present. For example, other harmonics will be generated due to the shift of the a.c.-side zero crossing points and changes in overlap angles. Such effects should be much smaller compared to the 2nd harmonic presence. The effect of the 2nd harmonic on the d.f. for a m.s. at 100Hz is illustrated in Fig. 2.19 for phase imbalance of 0%, 1% and 2% of the fundamental.

3.15 Uncharacteristic harmonics in 12-pulse converters

Twelve-pulse operation is achieved from two identical 6-pulse converters connected to the a.c. supply through star-star(YY) and star-delta (YΔ) transformers. The phase shift between primary and secondary (here "primary" is assumed to indicate the a.c.-side and "secondary" the valve side winding of the transformer) currents of same harmonic order in any one of the bridges depend on the transformer connection. Under steady-state and balanced conditions, the phase shift introduced by the star-star connection is equal to zero for harmonics of all orders. But with star-delta connection, a phase shift between primary and secondary currents is introduced. This phase shift depends on the harmonic order and on the harmonic phase sequence. Generally, the harmonic phase shift in the primary currents can be grouped into two types :

I) Secondary phase shift, θ_1, because the rectangular blocks of current are already shifted by 30^o, as represented in Fig. 3.20(a).

II) Secondary-to-primary phase shift, θ_2, because the secondary 3-phase harmonic current sets of positive and negative sequence are referred to the primary as shown in Fig 3.20(b).

The phase shifts of the first type depend on the harmonic order, k, and on the sign of the phase shift introduced by the converter transformer on the fundamental zero crossings. For a positive fundamental 30 degree phase shift, yields

$$\theta_1 = k30 \quad . \tag{3.172}$$

The second type of phase shift, is a result of the difference between any two vectors which are 120 degrees from each other. The sign

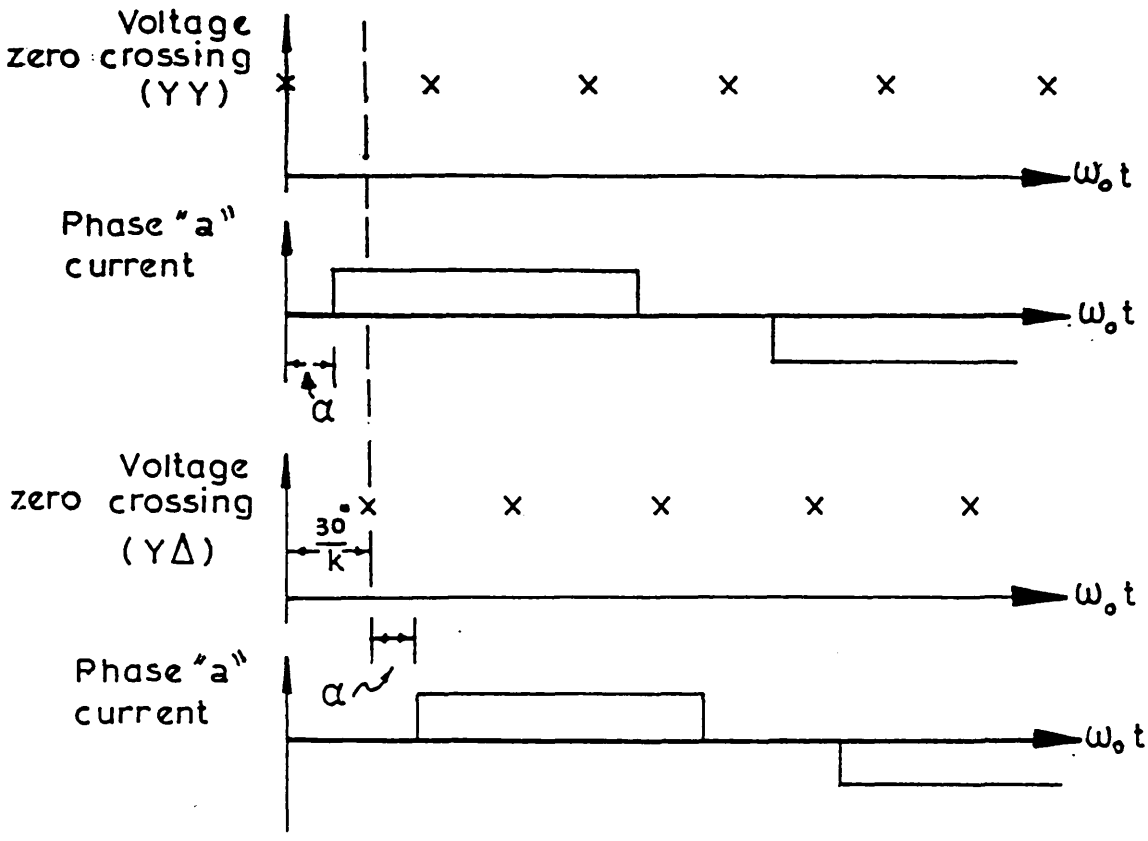

(a) Secondary phase shift between YY and YΔ transformers.

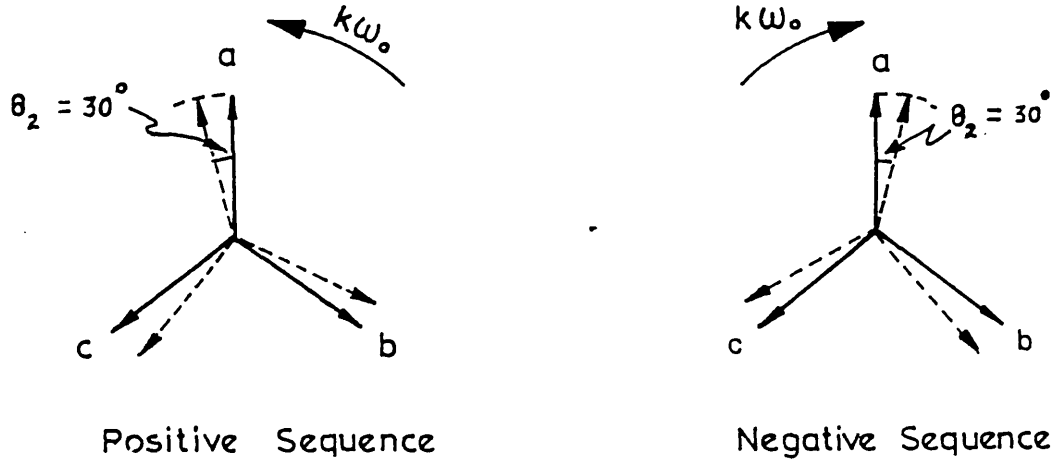

(b) Secondary to primary phase shift.

Fig. 3.20 - COMPOSITION OF THE PRIMARY PHASE SHIFT

of this difference changes according to the harmonic phase sequence as follows:

$$\begin{aligned} \theta_2 &= -30 \qquad \text{for positive sequence} \\ \theta_2 &= +30 \qquad \text{for negative sequence .} \end{aligned} \tag{3.173}$$

The phase shift between primary and secondary harmonic currents, can be classified by the harmonic symmetrical component as presented in Table 3.16. These values were obtained assuming a sinusoidal a.c. supply and secondary currents represented by series of rectangles 120 degrees from each other.

TABLE 3.16

HARMONIC PHASE SHIFT IN A YΔ TRANSFORMER

k	θ_1=k30	θ_2=±30	TOTAL SHIFT
3q-1	90q-30	+30	90q
3q	90q	0	90q
3q+1	90q+30	-30	90q

With no harmonic voltage imposed on the primary busbar, Table 3.16 indicates that the total phase shift between primary and secondary harmonic is always equal to 90q (q is an integer which depends on the harmonic order) as shown in the first column of Table 3.16).

Table 3.17 gives the total phase shift obtained from Table 3.16 as a function of the integer q.

TABLE 3.17

HARMONIC PHASE SHIFT AS A FUNCTION OF "q"

q MULTIPLE OF	TOTAL PHASE SHIFT
1	90
2	180
3	270
4	0

If the sign of the fundamental phase shift in the star-delta transformer is reversed, all signs in Tables 3.16 and 3.17 have to be reversed.

Table 3.18 gives the theoretical values of the primary current through the star-star and star-delta transformers of a 12-pulse converter. The phasor $I/\underline{\theta}$ represents the current contribution from each bridge. The fourth column in the Table gives the total theoretical a.c. current of the 12-pulse bridge.

The harmonic currents predicted in Tables 3.16, 3.17 and 3.18 assume :

a) balanced and sinusoidal a.c. supply

b) equally spaced firing pulses.

If these assumptions are not met, harmonic components of any sequence may be generated. A non-equidistant firing pulse case is discussed below in connection with 50Hz m.s. superimposed on the control voltage of 6-pulse converters.

Fig. 3.21 shows a comparison of how the firing pulses may be affected by a 50Hz m.s. according to the type of transformer connection. It is assumed that the positive going crossover of the m.s. is coinciding

TABLE 3.18

COMPOSITION OF THE PRIMARY HARMONIC CURRENT OF A 12-PULSE CONVERTER

k	SECONDARY HARMONIC CURRENT REFERRED TO THE PRIMARY OF THE TRANSFORMER		PRIMARY HARMONIC COMPOSITION (YY & YΔ)
	YY	YΔ	
1	I/θ	I/θ	$2I/\theta$
2	I/θ	$I/\theta+90$	$\sqrt{2}I/\theta+45$
3	I/θ	$I/\theta+90$	$\sqrt{2}I/\theta+45$
4	I/θ	$I/\theta+90$	$\sqrt{2}I/\theta+45$
5	I/θ	$I/\theta+180$	0
6	I/θ	$I/\theta+180$	0
7	I/θ	$I/\theta+180$	0
8	I/θ	$I/\theta+270$	$\sqrt{2}I/\theta-45$
9	I/θ	$I/\theta+270$	$\sqrt{2}I/\theta-45$
10	I/θ	$I/\theta+270$	$\sqrt{2}I/\theta-45$
11	I/θ	I/θ	$2I/\theta$
12	I/θ	I/θ	$2I/\theta$
13	I/θ	I/θ	$2I/\theta$

with the firing pulse to valve 1 either of the YY- or of the YΔ- connected bridges. In Fig. 3.21(a), the continuous line represents the m.s. for a YY- connected bridge. The corresponding firing pulse distribution is also shown on the same diagram.

In the case of a YΔ- connected bridge, it is necessary to shift the m.s. by 30^{o} to make its positive going crossover coincide with the firing pulse to valve 1. This is represented by the dotted line superimposed on the m.s. of the YY- connected bridge. The results for YY- and YΔ- connected bridges are overlapped so that, the interfiring period differences can be appreciated.

Fig. 3.21 (b) represents the firing pulse distribution of a 12-pulse bridge when a 50Hz m.s. is superimposed on the control voltage. The positive going crossover also coincides with the firing pulse to valve 1. If Figs 3.21(a) and 3.21(b) are compared to each other for small amplitudes of m.s., it can be concluded that the firing pulse distribution of a 12-pulse converter is approximately identical to the firing pulse distribution of a YY- connected bridge superimposed by the firing pulse distribution of a YΔ- connected bridge whose m.s. is 30^{o} shifted. This conclusion is important in terms of harmonic cancellation interbridges in 12-pulse converters.

3.16 Conclusions

In this Chapter, the relationships necessary to derive a method of harmonic minimization based on control voltage modulation are established.

Firstly, a transfer function to relate control voltage ripple

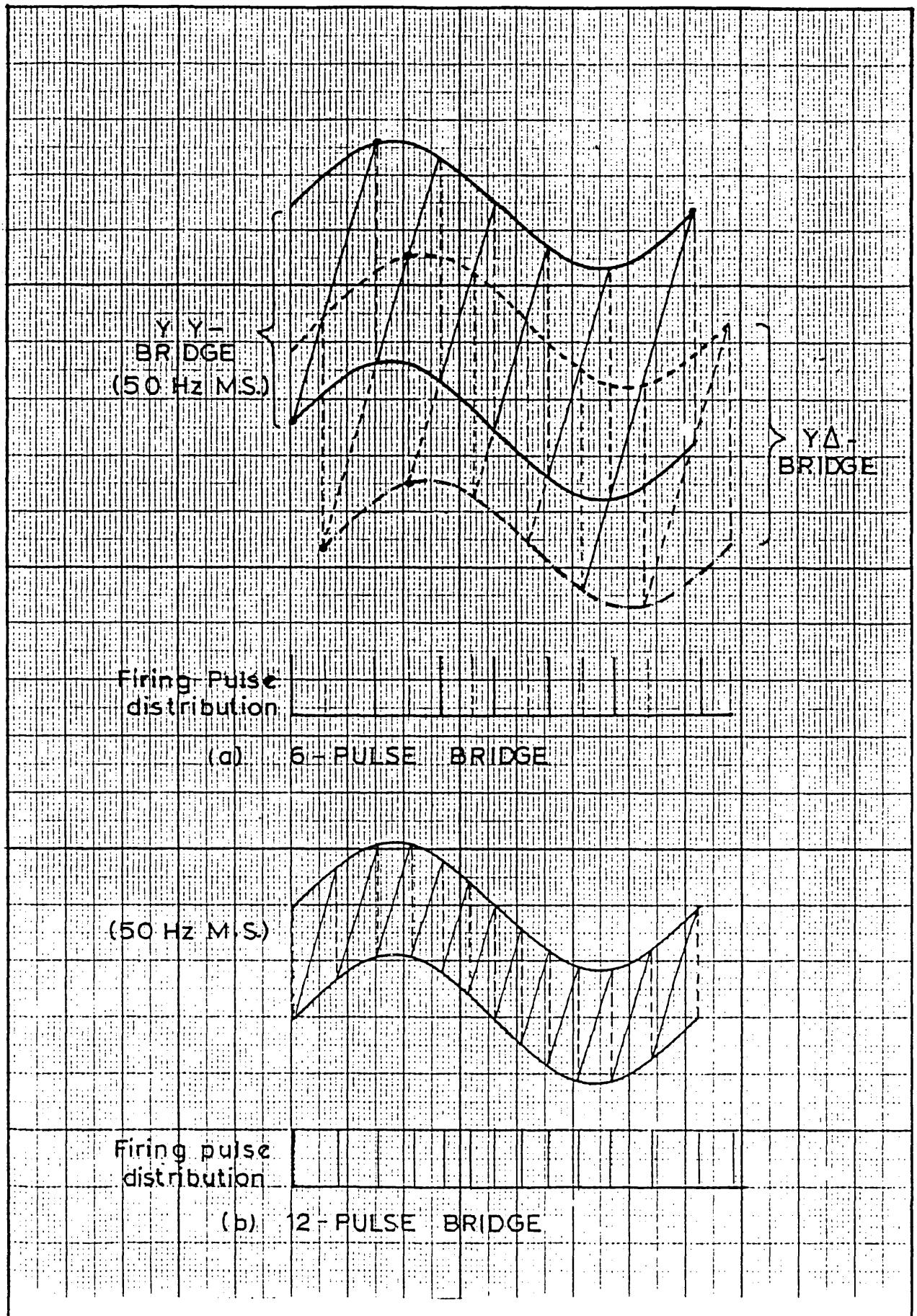

Fig. 3.21 - FIRING PULSE DISTRIBUTION OF 6-PULSE AND 12-PULSE BRIDGES

to d.c. current ripple is obtained. Such transfer functions have a low pass characteristic whose cut-off frequency is determined by a compromise between fast control response and negligible control voltage ripple. It is also established that there is an approximate linear relationship between small amplitudes of the modulating signal and the corresponding firing pulse variation, $\Delta\alpha$. This relationship can be used to obtain analytically the interfiring periods.

The magnitude and phase of a.c.- and d.c.-side uncharacteristic harmonic voltages and currents were shown to be approximately proportionally related to the m.s. amplitude and phase. Special attention was given to the effect on uncharacteristic harmonics of 50Hz, 100Hz and 150Hz m.s. . The results are summarized below :

a) On the a.c.-side :

1) a 50Hz m.s. gives rise to predominantly second harmonic currents of positive sequence and causes odd harmonics of very small amplitudes only;

2) a 100Hz m.s. causes triplen harmonic currents only;

3) a 150Hz m.s. causes second harmonic current of negative sequence only.

b) On the d.c.-side:

1) For the m.s. frequencies studied, the lowest harmonic current present corresponds to that of the m.s. frequency.

2) For small amplitude of m.s., the d.c.-side harmonic voltages and currents are proportional to the amplitude of the harmonics present on the a.c.-side even when under open loop control.

An interesting outcome of this study is that a phase shift of the a.c.-side second harmonic current corresponds to one half of the phase shift of the d.c.-side 50Hz harmonic, irrespective of whether they were

caused by control voltage modulation or distortions on the a.c. busbar voltage.

Imbalances in the fundamental voltage may be represented by a balanced 3-phase set plus a superimposed incremental voltage of same frequency corresponding to the difference between the balanced and unbalanced cases. The incremental voltage is rectified by the converter and its contribution on the d.c.-side will result basically on the presence of a 2nd harmonic.

Finally, it was shown that a m.s. on the control voltage of a 12-pulse converter, causes uncharacteristic harmonic currents through the YΔ- transformer which are shifted by approximately 30 degrees with respect to the uncharacteristic harmonic currents of the same frequency through the YY- transformer. This fact explains why on the a.c.-side, 6th harmonic currents are virtually cancelled out at the primary of a 12-pulse converter while 2nd harmonic currents may be present.

CHAPTER 4

CIRCUITRY FOR IMPLEMENTATION OF CONTROL VOLTAGE MODULATION

4.1 Introduction

In h.v.d.c. transmission systems, the power flow is set to a desired level by means of closed-loop control. Such control is implemented through direct action onto the converter by advancing or delaying the firing instants of the individual valves, as explained in Chapter 2. Therefore, the controller should ensure fast and stable operation, free from oscillatory modes and a low level of abnormal harmonic currents and, as a consequence, acceptable a.c. system voltage distortion levels.

In Chapter 3, it is theoretically demonstrated how a.c.-side voltage distortion and control voltage ripple can be associated with a.c.-side side and d.c.-side harmonics. The control voltage ripple is related to the control time constant and may be virtually suppressed by imposing a large time constant in the controller. The drawback of such a large time constant is a slower dynamic response of the controller.

In this chapter, a circuit to select, adjust and inject a modulating signal (m.s.) into the control voltage is proposed and tested. A transient detector connected to the output of the injection circuit inhibits the m.s. injection during transients. This control feature is important for two reasons:

a) it allows fast transient response of the control;

b) it does not contribute to oscillatory behaviour.

In order to verify the theoretical predictions presented in Chapter 3, the Imperial College h.v.d.c. simulator was used. The experimental set-up includes the following :

a) a.c.-side harmonic injection

b) a.c.-side and d.c.-side harmonic measurement

c) injection of the modulating signal.

Modulating signals of 50Hz, 100Hz and 150Hz were used in the tests.

4.2 A.c.-side harmonic injection

4.2.1 Second harmonic generation

The second harmonic generator used, consists of three single-phase fullwave rectifiers each one connected in series with one of the a.c. supply phases through isolating transformers, as shown in Fig. 4.1 for phase "a". One isolating transformer at least is necessary to avoid injection of d.c. current originated in the rectifying process, into the converter transformers. The d.c. power is dissipated in a variable resistor (R).

The type of second harmonic generator described above has four important characteristics.

1) it can be continuously adjusted from 0% to 100% of the a.c. supply voltage through the secondary of a 3-phase variac transformer;

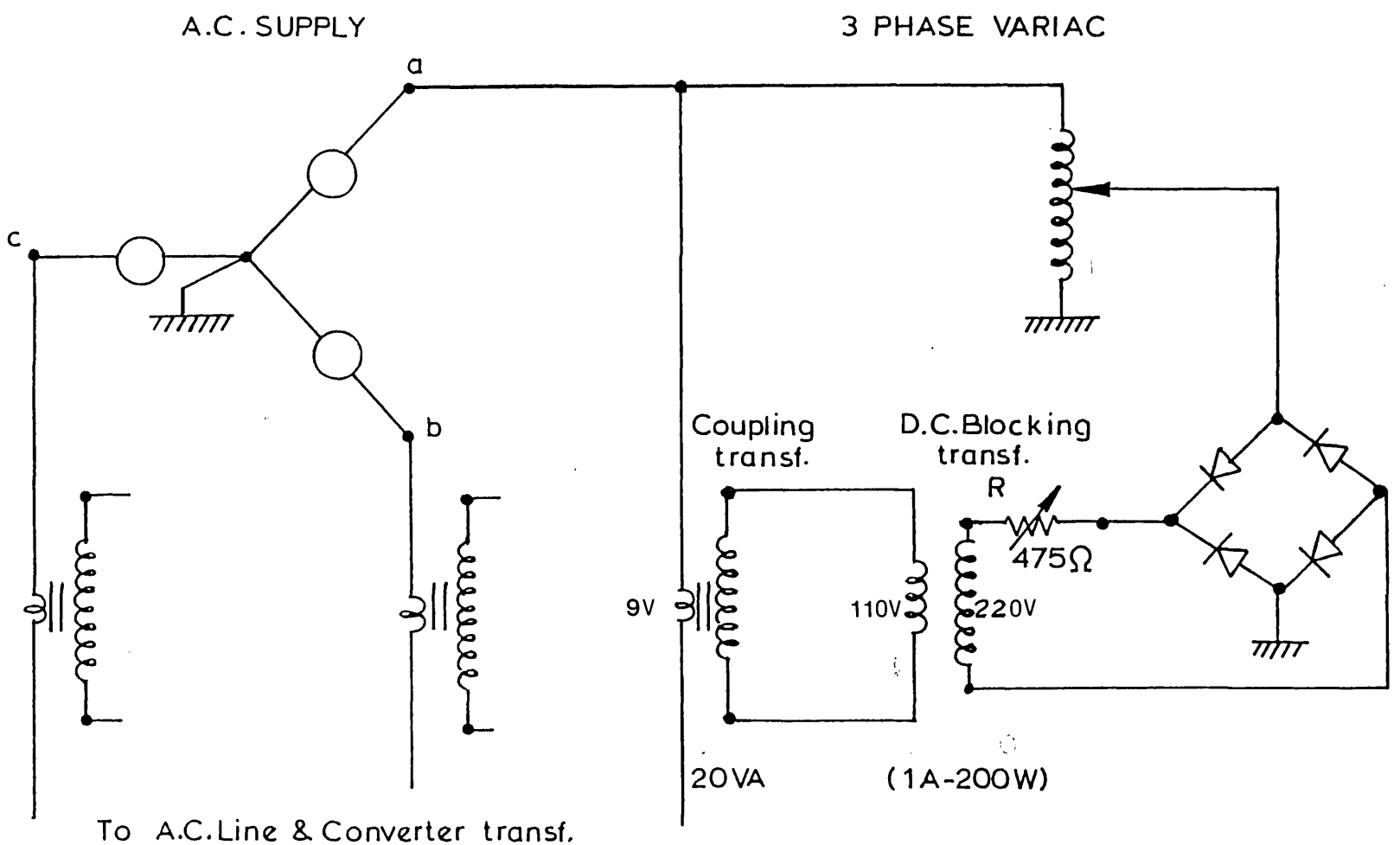

Fig. 4.1 - SECOND HARMONIC GENERATOR

2) the phase sequence can be changed by injecting harmonics from one phase into another;

3) the output impedance of the injection circuit is negligible due to the large turn ratio of the coupling transformer;

4) synchronization with the fundamental voltage is ensured.

4.2.2 Third harmonic generation

Third harmonic can be generated by using an unbalanced a.c. supply, the harmonic magnitude being dependent on the percentage of imbalance of the a.c. source.

4.3 Harmonic measurement

Five methods for measuring the a.c.—side and d.c.—side harmonics are listed below:

1) A digital storage oscilloscope with direct digital output to a computer;

2) A digital storage oscilloscope with analog output to a plotter;

3) A spectrum analyser capable of measuring harmonic amplitude and phase;

4) Implementation of the discrete Fourier transform (DFT) on a microcomputer whose A/D converter can be fed through active filters;

5) Implementation of the Fourier analysis on a computer system whose input data can be supplied through an auxiliary microcomputer capable of feeding on line data.

The first method is the most direct but requires the availability of an expensive digital storage oscilloscope. The second method is lengthy, tedious and of low accuracy, though it is the cheapest one. The third method can be lengthy, tedious and expensive. In the fourth method, filters may introduce phase shift which is not easily compensated. The fifth method gives good accuracy and it was the one chosen because of its easy availability.

The on-line data collection from the converter is made by a Texas Instruments microcomputer (model TM990/101) and fed to the ICCC-CDC computer system (CYBER 174 - Nos. 1.4). The link between these two computers is made through an intelligent terminal (CORVUS WORKSTATION - CORVUS SYSTEM CONCEPT) which controls the data acquisition in the TM 990/101 and also operates the ICCC-CDC link

Fig. 4.2 shows the block diagram of the computational arrangement for the FOURIER analysis of a.c.-side and d.c.-side voltages. A complete 50Hz cycle of each a.c.-phase voltage and d.c. line voltage is sampled at a rate of 80 times per cycle through four A/D converter channels (TEXAS 9900 FAMILY-RTY-1211). These values are stored in the microcomputer in hexadecimal form and then, transferred to the CDC - system. The hexadecimal data is transformed into decimal values on which Fourier analysis is performed. The block diagram of the Fourier program to execute these operations is presented in Fig. 4.3(a) and the program text is presented in Appendix C.

Fig. 4.3(b) shows the block diagram of the assembly program to execute channel multiplexing on the A/D converter. The program text is given in Appendix C.

An interface circuit between the measured quantities and the measuring equipment had to be implemented. Also in order to allow a

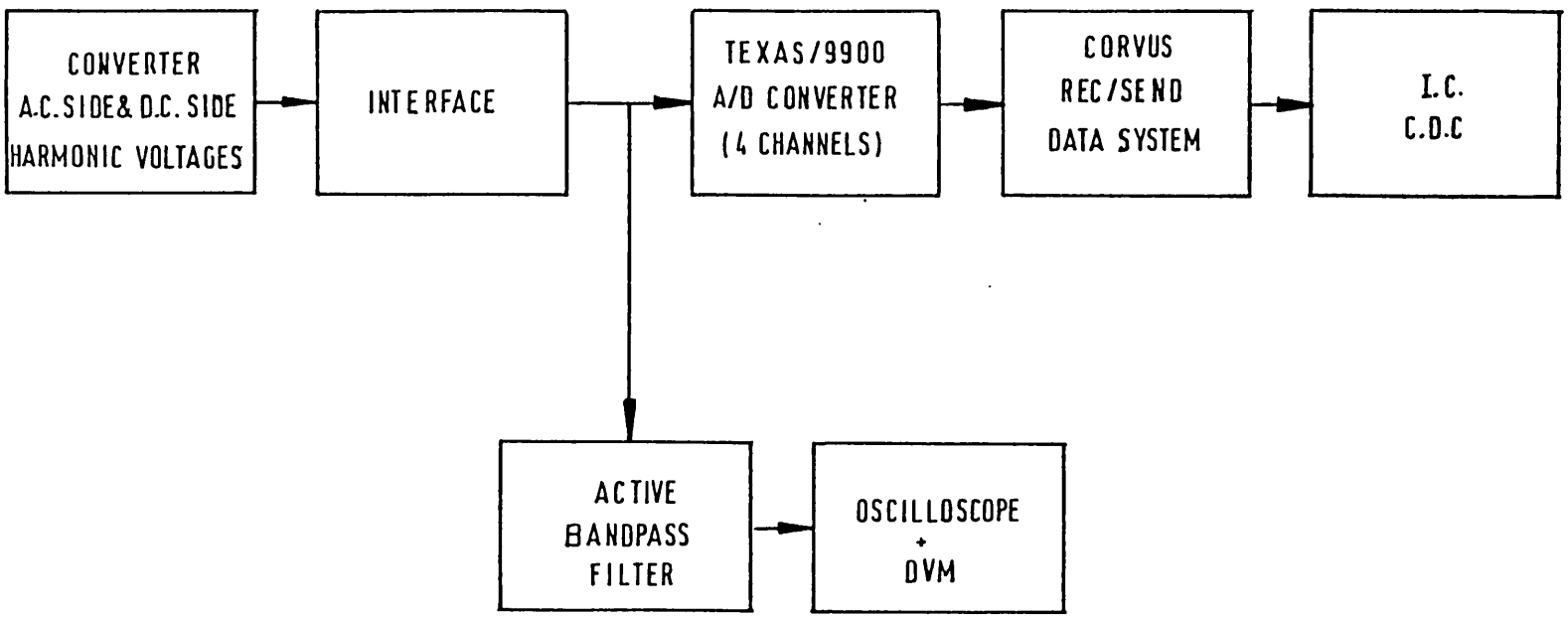

Fig. 4.2 - HARMONIC MEASUREMENT - MAIN BLOCK DIAGRAM

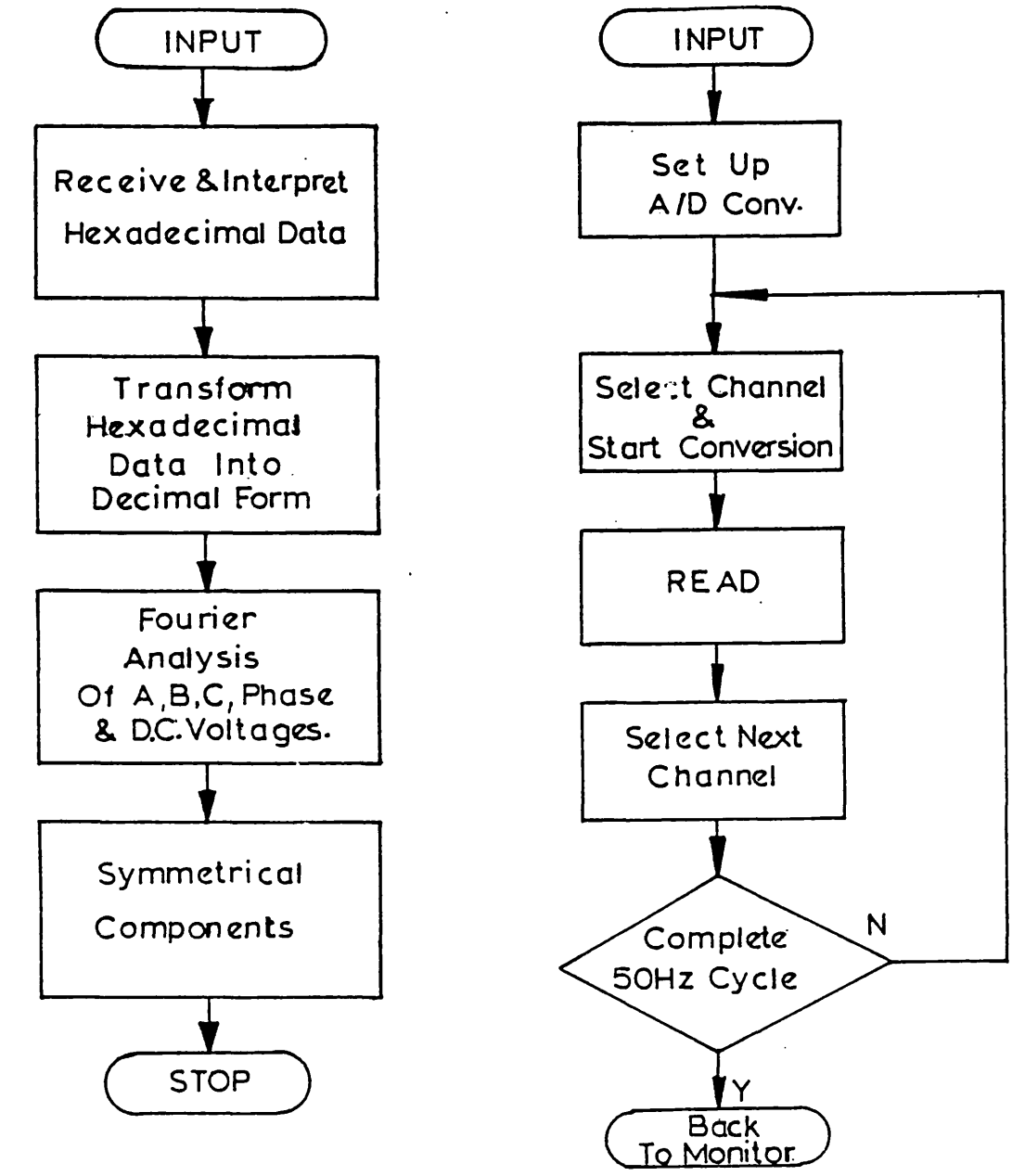

(a) ICCC-CDC Fortran Program (b) Texas 9900-Assembly Program

Fig. 4.3 - COMPUTER SOFTWARE FOR DATA INPUT AND FOURIER ANALYSIS

continuous monitoring of the frequency under analysis, it is convenient to install a filter tuned to that particular frequency. These circuits are described in the following sections.

4.3.1 Voltage interface

The 100:1 resistive potential divider used to render the high voltage under measurement compatible with the measuring equipment under low distortion levels, is shown in Fig. 4.4(a). Resistors of high value and solidly grounded, provide a reasonable insulation level between the high voltage terminals and the voltage dividing point. The signal from the potential divider is then buffered through an operational amplifier and transmitted to the A/D converter. Similar arrangement is repeated for each a.c. busbar phase and for the d.c.-side voltage.

The buffered output of each potential divider can be connected to an active filter whose output is connected to a digital voltmeter (DVM) and to an oscilloscope, as indicated in Fig. 4.4(b) for phase "a". The DVM gives the instantaneous effective harmonic voltage and the oscilloscope gives the phase angle relatively to some arbitrary reference. The input of the active filter can be selectively connected either to any a.c.-phase or to the d.c.-side voltage signals.

4.3.2 Active filter

The amplitude of the selected a.c.-side harmonic can be very small compared to the fundamental. Therefore, in order to use a minimum number

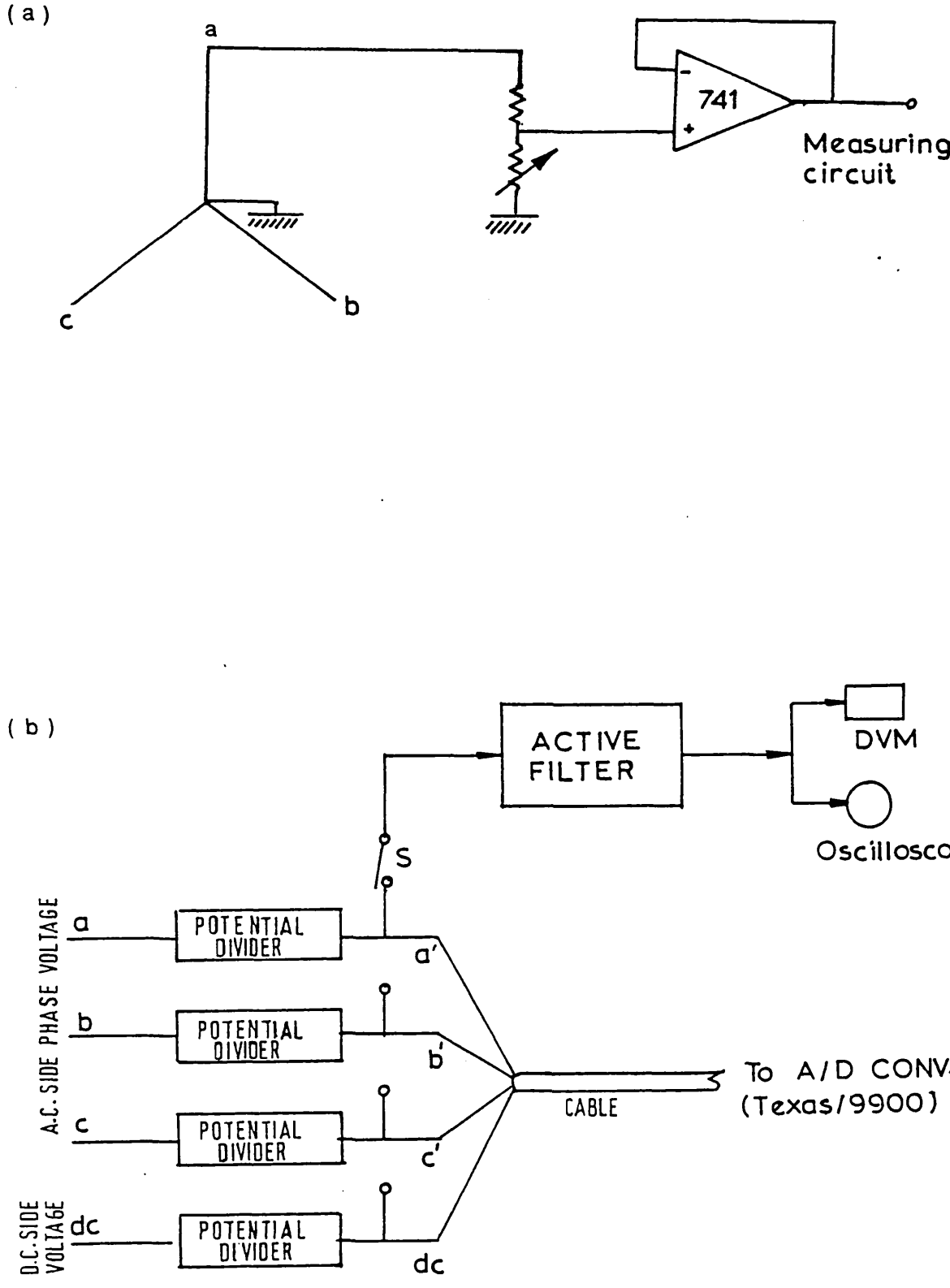

Fig. 4.4 - MEASUREMENT INTERFACE

(a) Phase potential Divider
(b) Harmonic Measurement

of filtering stages and, at the same time, to have a good signal fidelity, a 50Hz suppressor connected to a bandpass filter, is implemented as shown in Fig. 4.5(a).

4.3.3 The 50Hz suppressor

The 50Hz suppressor consists of an active bandpass filter tuned to 50Hz in series with a phase shifter circuit, as shown in Fig. 4.5. The output of the phase snifter is adjusted to be in phase opposition with the 50Hz input. The whole circuit is then adjusted to allow passage of any harmonic frequency except 50Hz. This output is connected to a bandpass filter.

4.3.4 Bandpass filter

There are several possible configurations of bandpass filters[42], i.e. gyrators, inductor-capacitor, infinite-gain multiple feedback, controlled source (VCVS), infinite-gain state variable and negative immitance converter (INIC). The last configuration (INIC) was chosen for its low sensitivity to component value changes as compared with other realizations and for the moderate number and size of the components used. However, the INIC realization does not have a low output impedance and isolating circuits must be used between the cascaded stages.

The voltage transfer function of a second order bandpass filter is given by :

a) ACTIVE FILTER

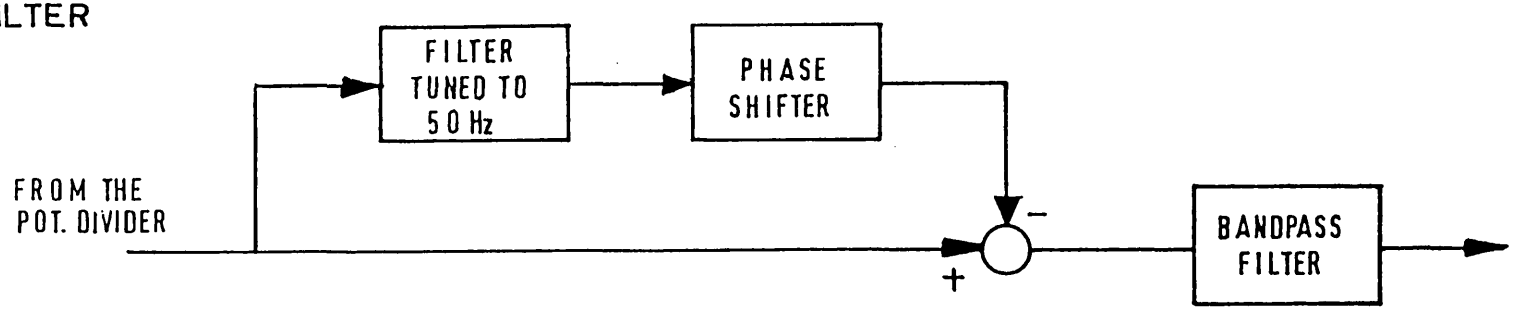

b) 50 Hz SUPPRESSOR

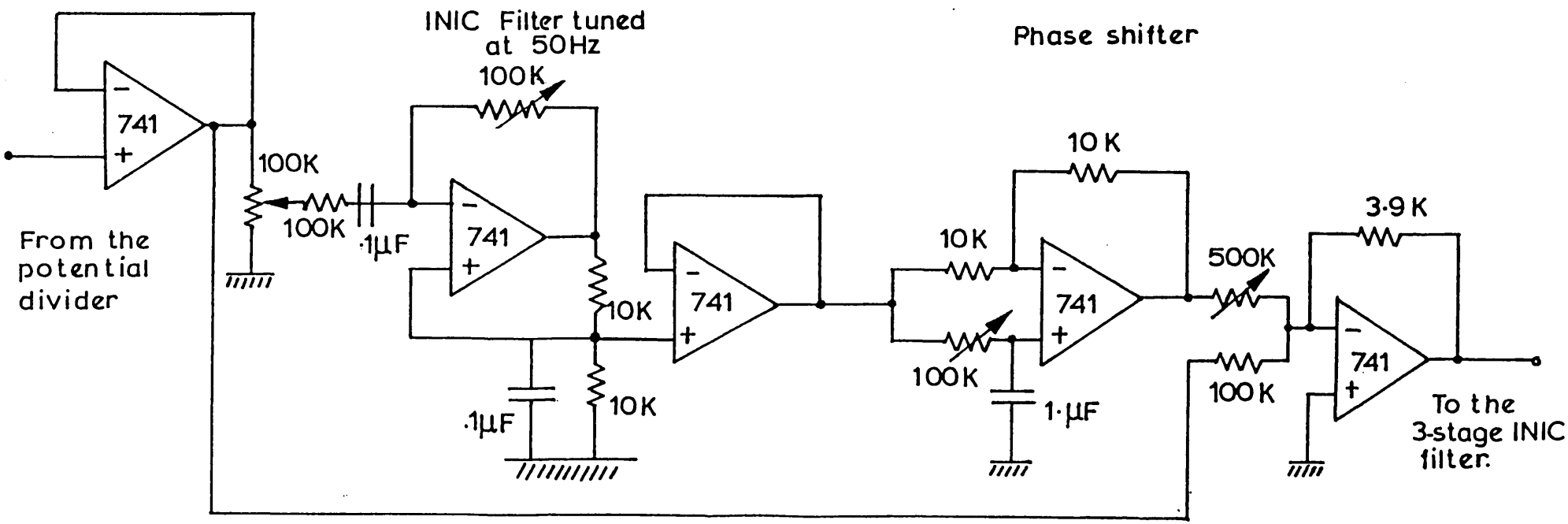

Fig. 4.5 - THE ACTIVE FILTER

The network parameters are :

$$H_0 = \frac{K}{\frac{C_2}{C_1} + \frac{R_1}{R_2} - K} \qquad (4.3)$$

$$\omega_0 = \frac{1}{\sqrt{R_1 C_1 R_2 C_2}} \qquad (4.4)$$

This filter configuration has a very high gain and a gain reduction between stages becomes necessary. The input resistor of the gain reducer has to be high enough to avoid interstage loading.

Fig. 4.6(b) shows the 3-stage adjustable filter used to select injection of harmonic voltage back into the control voltage. The gain reducer is used as a means of controlling the harmonic amplitude. The values of the filter components are selected in such a way that :

a) 50Hz, 100Hz and 150Hz are easily tuned ;

b) Q and ζ are adjustable

c) The overall gain is controllable

The tuning of components values was carried out by defining two auxiliary factors as follows:

$$k' = \frac{R_2}{R_1} \qquad (4.5)$$

$$k'' = \frac{C_2}{C_1} = 1 \qquad (4.6)$$

In order to allow leakage current compensation between C_1 and C_2, factor k'' was chosen equal to one.

$$H(s) = \frac{e_0}{e_i} = \frac{H_0 \zeta \omega_0 s}{s^2 + \zeta \omega_0 s + \omega_0^2} \qquad (4.1)$$

where

$$Q = \frac{f_0}{\Delta f} = \frac{1}{\zeta}$$

Q : quality factor

f_0 : resonant frequency of middle range

Δf : bandpass (3dB)

ζ : damping factor

$\omega_0 = 2\pi f_0$.

Figs. 4.6(a) and 4.6(b) present the INIC realization of a bandpass filter. The INIC voltage transfer function is given by:

$$\frac{E_0}{E_i}(s) = \frac{-Ks/R_1C_2}{s^2 + s\left(\frac{1}{R_1C_1} + \frac{1}{R_2C_2} - \frac{R}{R_1C_2}\right) + \frac{1}{R_1C_1R_2C_2}} \qquad (4.2)$$

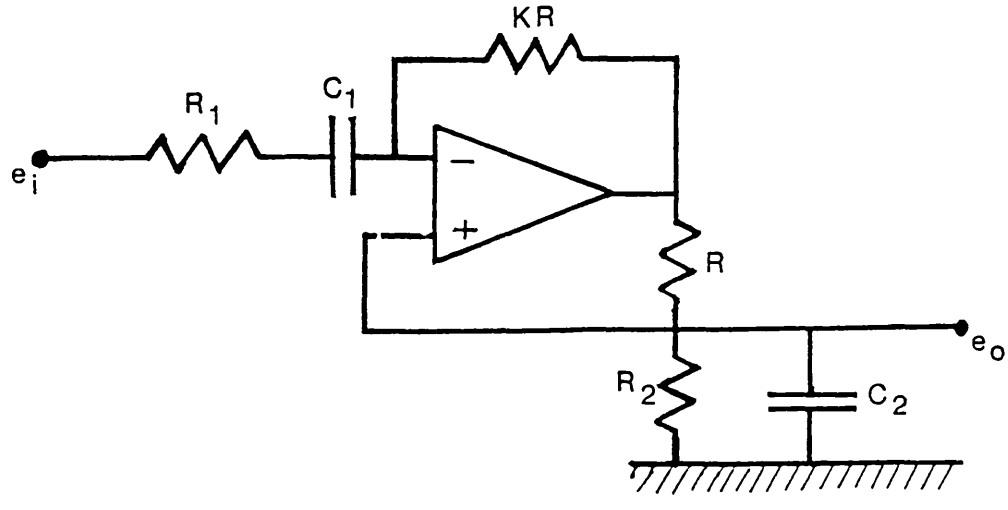

Fig. 4.6(a) - INIC FILTER STAGE

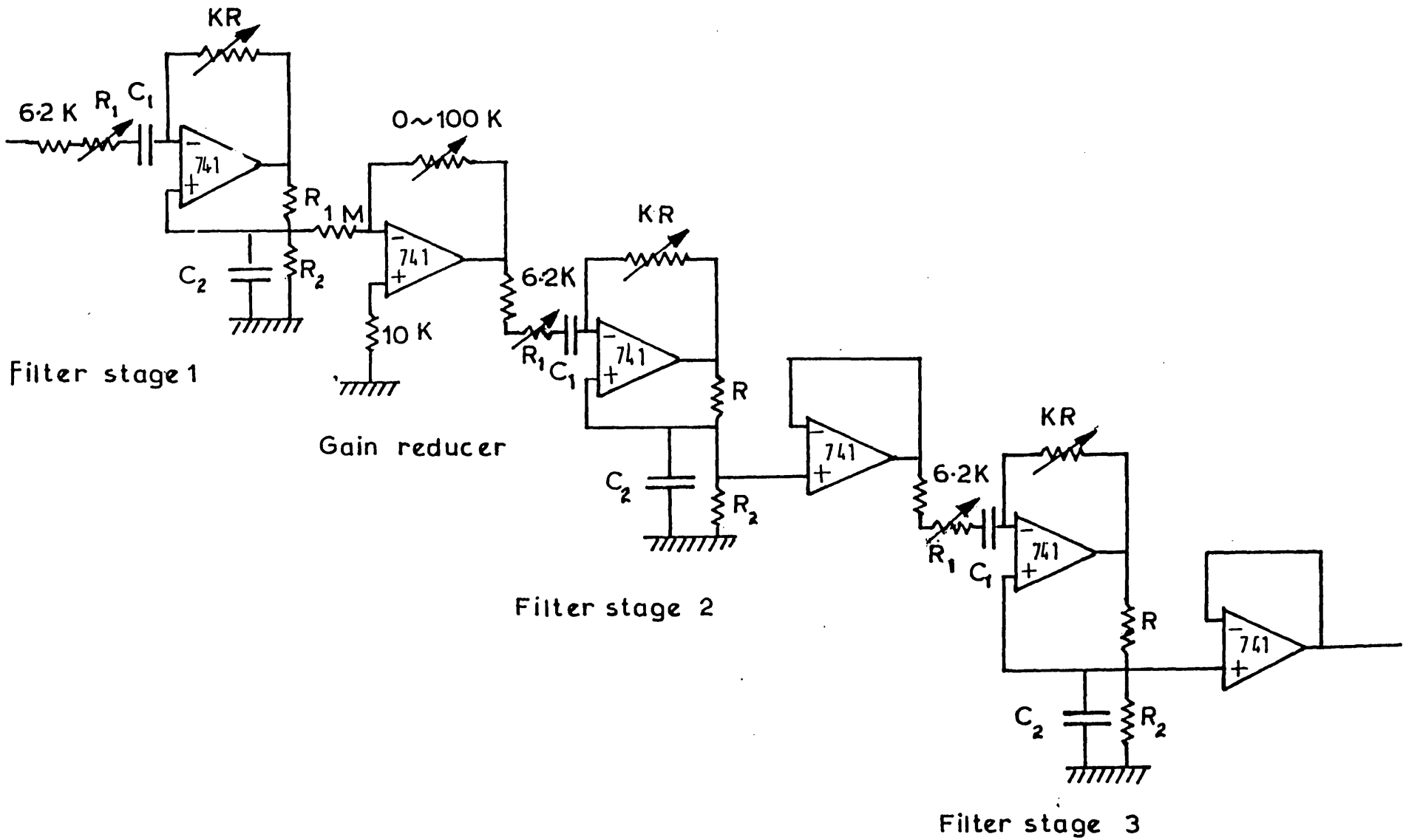

Fig. 4.6(b) - INIC ADJUSTABLE FILTER (3-STAGE)

Replacing ω_0 by $k\omega_0$ and combining eqns 4.4 to 4.6 results in :

$$k' = k^2(\omega_0 R_2 C_1)^2 \quad . \tag{4.7}$$

Equating numerator and denominator of eqns 4.1 and 4.2 respectively results in

$$\zeta\omega_0 = \frac{1}{R_1 C_1} + \frac{1}{R_2 C_2} - \frac{K}{R_1 C_2} \tag{4.8}$$

$$H_0 = - \frac{K}{\zeta\omega_0 R_1 C_2} \quad . \tag{4.9}$$

Combining eqns 4.7 and 4.8 and rearranging yields

$$K = 1 + \frac{1}{k'} - \frac{\zeta}{\sqrt{k'}} \quad . \tag{4.10}$$

Equating 4.3 and 4.4 and using again 4.7 results in :

$$H_0 = \frac{1}{\zeta}[\sqrt{k'} + \frac{1}{\sqrt{k'}}] - 1 \quad . \tag{4.11}$$

Fig. 4.7 shows the frequency response of the INIC filter for 1 and 3 stages. The INIC one-stage frequency response is rather poor and 3 cascaded stages had to be used.

Table 4.1 gives the component values of the circuit presented in Fig. 4.6. The input resistors, R_1's, are used for frequency tuning and the feedback resistors, R's, are used for Q-α adjustments.

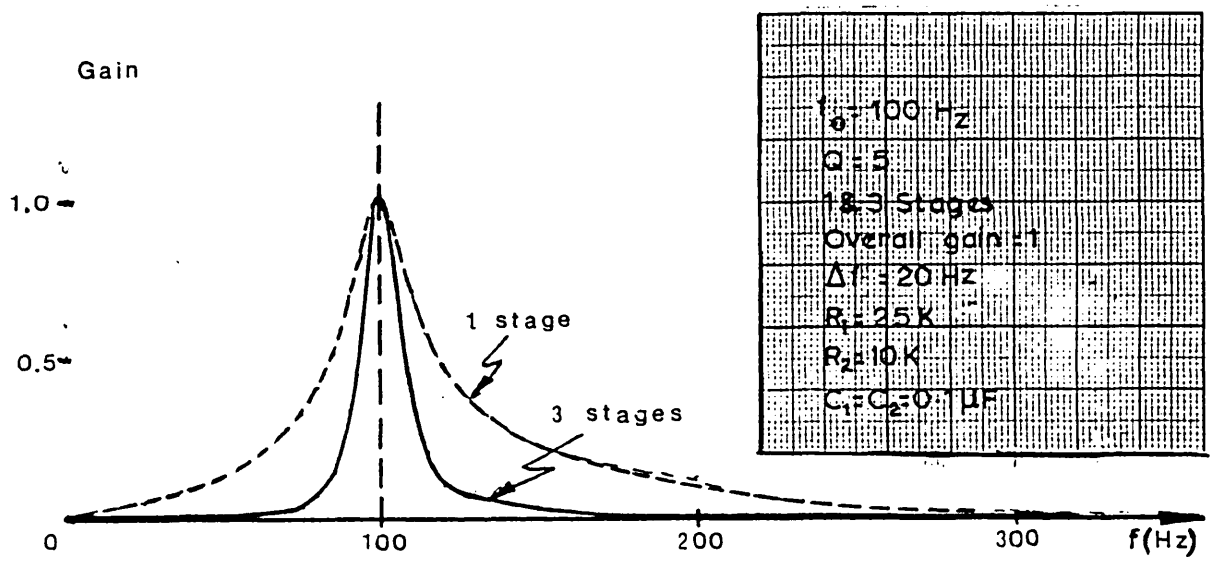

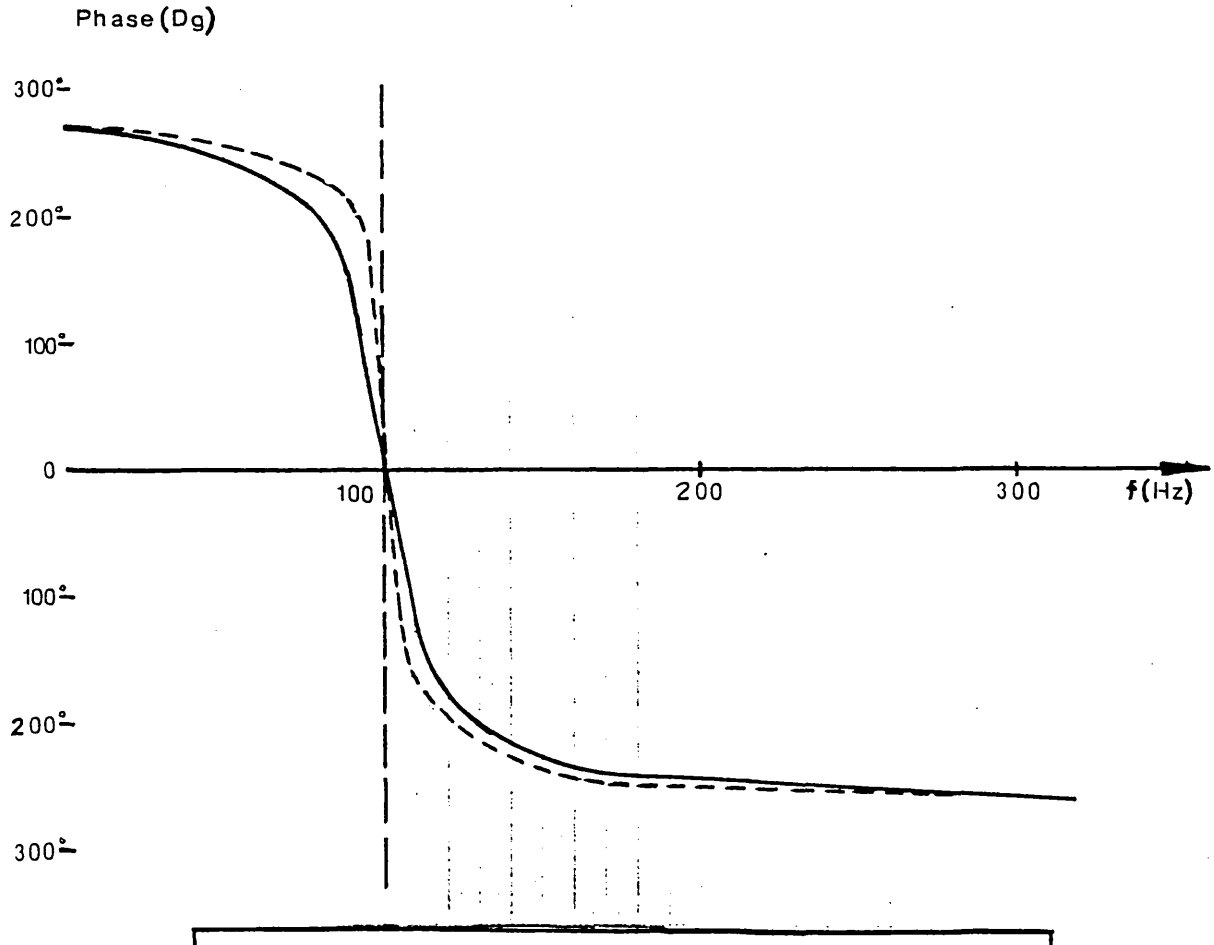

Fig. 4.7 - FREQUENCY RESPONSE OF THE INIC FILTER

TABLE 4.1

COMPONENT VALUES OF THE INIC FILTER PRESENTED IN FIG. 4.6

FREQ	C_1	C_2	R_1	R_2	k'	k''
(HZ)	μF	μF	kΩ	kΩ	-	-
50	0.1	0.1	100	10	0.1	1
100	0.1	0.1	25	10	0.4	1
150	0.1	0.1	10	10	0.9	1
k.50	0.1	0.1	$\frac{100}{k^2}$	10	$0.1k^2$	1

4.4 Principle of the Analogue Injection

The basic principle of analogue injection is diagramatically presented in Fig. 4.8. A d.c. current transducer provides a signal compatible with the reference current, I_{ref}. The error processing unit produces an error signal by comparing I_{dc} with I_{ref}. The error signal is produced to give the control voltage, V_c', which is then fed into three different circuits as follows :

a) Directly to the summing point;

b) To a highpass or bandpass set of filters in order to select the frequency or frequencies to be injected. The filtered output is fed into the injection circuit whose output is also directly connected to the summing point. The output signal from the injection circuit is referred

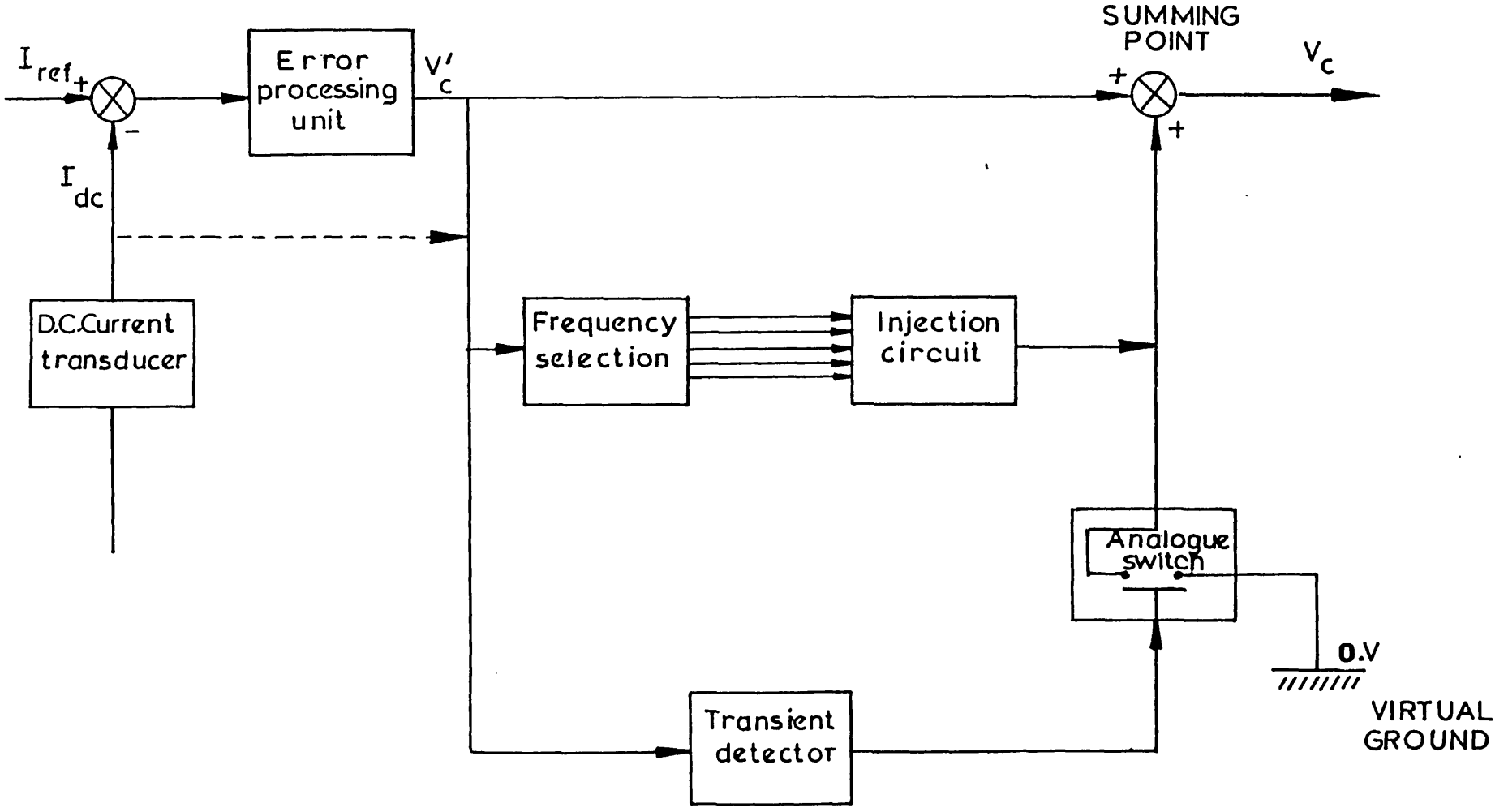

Fig. 4.8 - BLOCK DIAGRAM OF THE INJECTION CONTROLLER.

to as the modulating signal (m.s.). The amplitude and phase of the m.s. can be adjusted continuously from zero up to maximum value. The multiple arrows at the input of the injection circuit indicate the possibility of injecting more than one signal at a time. The output of the injection circuit is also fed to an analogue controlled switch connected to ground which is operated by a transient detector.

c) To a transient detector: this circuit triggers a monostable as soon any appreciable change in the d.c.-line current level is detected. The monostable in its ON state closes the analogue switch which grounds the injection signal.

The overall effect of the analogue injection as proposed here, is to select one or more harmonics present in the control voltage, shift them, adjust their amplitude and finally, add them back to the control voltage in such a way that their presence in V_c is controllable. The dashed line in Fig 4.8 indicates that the m.s. can be selected either from I_{dc} or from V'_c.

All blocks in the diagram of Fig. 4.8 are fully explained in the following sections.

4.5 Injection Circuit

The signal injection circuit and its transfer function are presented in Fig. 4.9. This injection circuit allows full range adjustment of amplitude (0. ~ ± 12V) and of angle (0^o ~ 360^o). The signal injection is enabled or disabled by an analogue switch connected across input and output of the inverting stage.

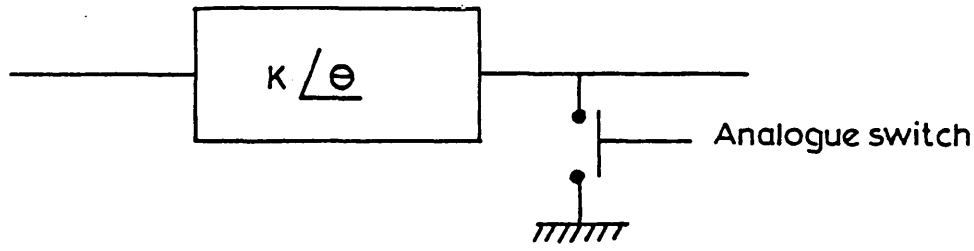

a) Transfer function of the signal injection circuit

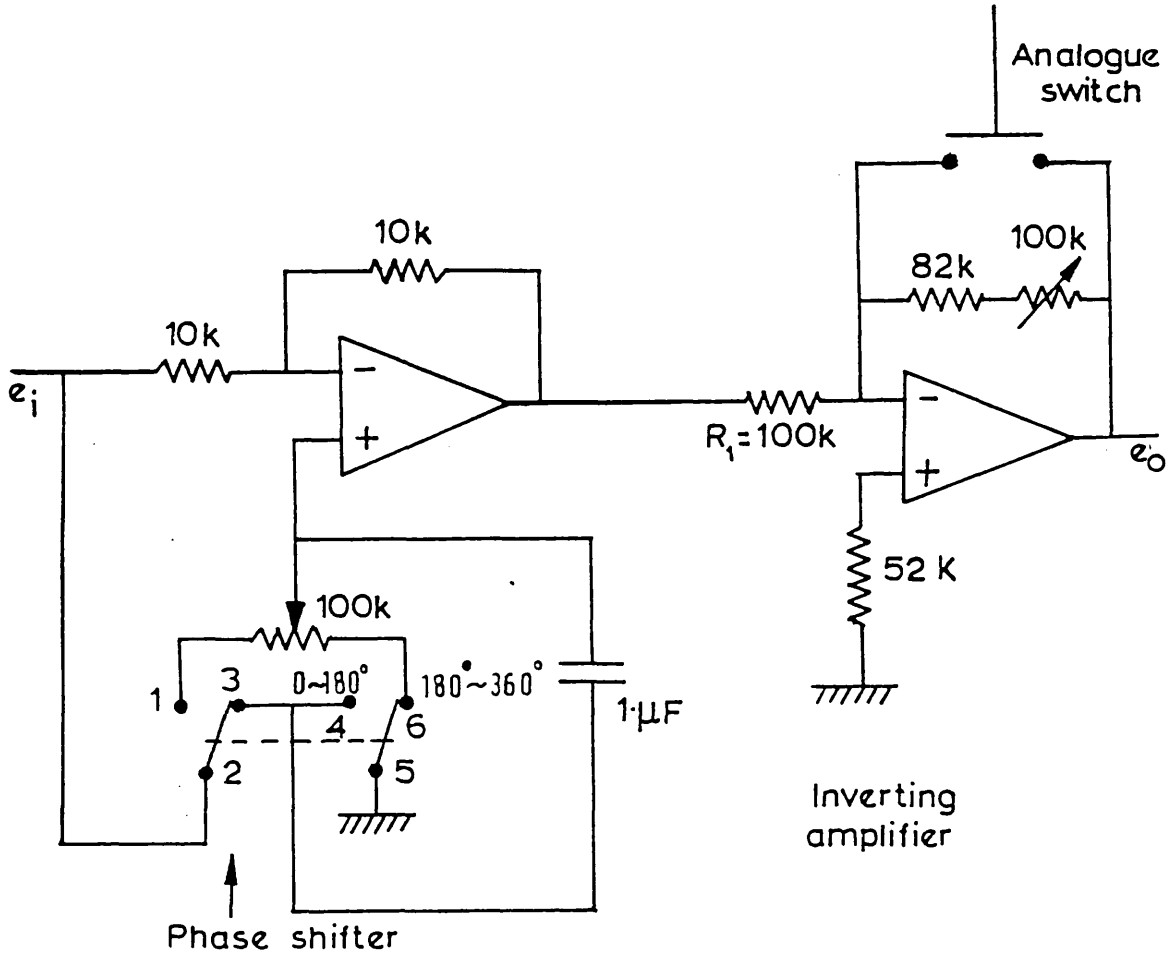

b) Injection signal circuitry

Fig. 4.9 - THE INJECTION CIRCUIT

The drain-source ON resistance of the analogue switch has a low value (typically, 70Ω) but it is not zero. So, the input resistor, R_i, of the inverting stage was chosen high enough (R_i = 100KΩ) to minimize the amplifier gain when the analogue switch is closed.

4.6 Frequency selection

The main reason for using only highpass or bandpass filters in the harmonic selection circuit is to block the d.c. component of the control voltage. The main features of these filters in connection with injection signal are outlined below.

a) The use of a highpass filter smooths out the control voltage by injecting back all its own ripple with negative signal. The simplest version of a highpass filter is the one presented in Fig. 4.10. The buffer amplifier is included to avoid interaction between the filter and the next amplifier stage.

The step response of an RC-filter is given by

$$i(t) = \frac{u(t)}{R} e^{-\frac{t}{RC}} \qquad u(t) = \begin{cases} V \rightarrow t > 0 \\ 0 \rightarrow t \leq 0 \end{cases} .$$

The transfer function of the RC injection circuit is obtained from Fig. 4.11 and given below :

$$\frac{V_c}{V'_c} = 1 + \frac{sK_2K_1/\theta}{1+sT_2} \qquad (4.12)$$

where: $T_2 = K_2 = CR.$

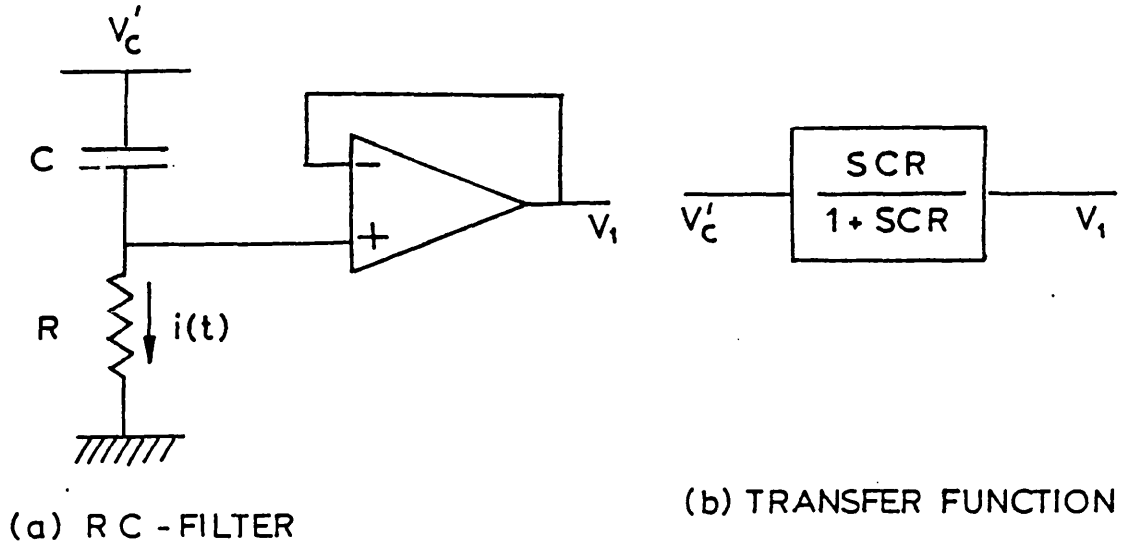

Fig. 4.10 - HIGH PASS FILTER

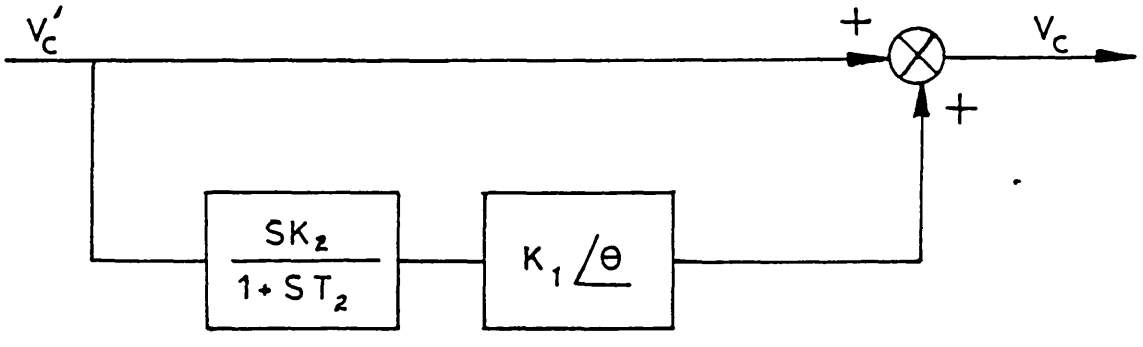

Fig. 4.11 - THE HIGHPASS FILTER INJECTION

The highpass filter injection can act as a low pass filter if $K_1 = -1$ and $\theta = 0°$. In this case, eqn 4.12 becomes

$$\frac{V_c}{V_c'} = \frac{1}{1+sT_2} \tag{4.13}$$

b) Bandpass filters permit selection of one or a group of frequencies from the control voltage ripple. The circuit of this filter is presented in Fig. 4.6 and is the same one used for measurement, as described in subsection 4.3.4.

To summarize, the adjustment of the injection signal can be realized as explained in Table 4.2.

TABLE 4.2

INJECTION SIGNAL ADJUSTMENT (f, V_m, θ)

QUANTITY	CIRCUIT ADJUSTED
(f) frequency →	High pass or bandpass filter
(V_m) amplitude →	Gain reducer of the INIC filter
(θ) phase →	Phase shifter of the injection circuit

4.7 The transient detector

Fig. 4.12 shows the block diagram of the transient detector. Transient detection is based on the presence of d.c. current through the resistor of an RC-filter. Such current arises whenever the control voltage level is changed. The transient d.c. current signal is fed into an absolute value amplifier.

A high-gain absolute value amplifier is necessary in order to cope with small or large control voltage variations of positive or negative slope. Also, an adjustable level detector must be used to eliminate from the transient detector feedback loop, variation in the current that should not trigger the detector. The output signal of the level detector triggers a monostable circuit which in turn, operates the analogue switch.

The blocks of Fig. 4.12 are described below.

a) Transient detection:

A low time constant RC-filter may be used as transient detector. Such a filter is connected to the output of the control voltage circuit as shown in Fig. 4.13.

The RC time constant is chosen to be much lower than the time response of the error processing unit circuit. In such circumstances, the steady-state oscillations of the control voltage cannot appear across the filter resistor and only variation of the control d.c. component will be detected.

The first few microseconds of transient on the control voltage can be approximated by a ramp voltage whose slope k may be positive or negative. Fig. 4.14 depicts such a transient state which may be expressed as follows:

$$R_i + \frac{1}{c}\int_{t_0}^{t_+} idt = V_{co} + k(t - t_0) \qquad (4.14)$$

where :

i : is the current through the filter resistor

k : approximate initial slope of the control voltage variation

V_{co} : initial control voltage level

t_0 : initial time of the transient.

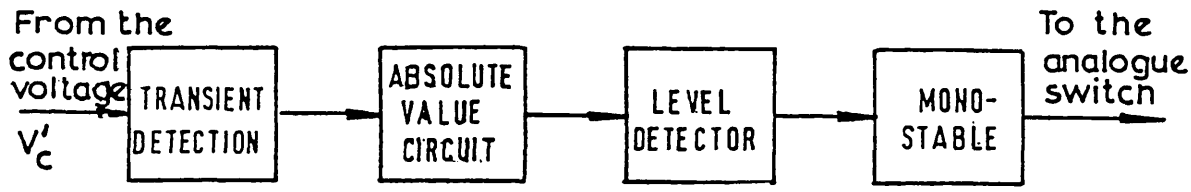

Fig. 4.12 - THE TRANSIENT DETECTOR

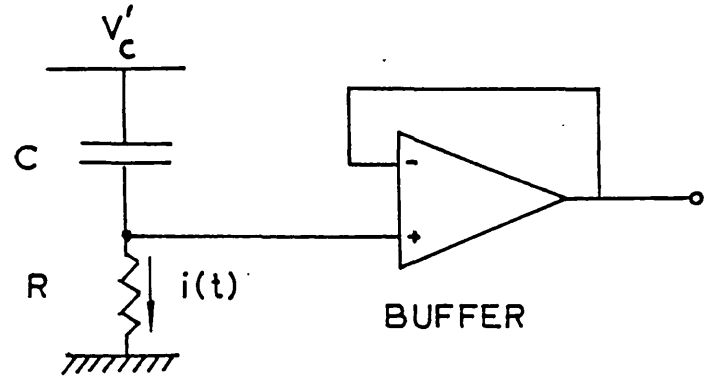

Fig. 4.13 - INDEPENDENT RC FILTER

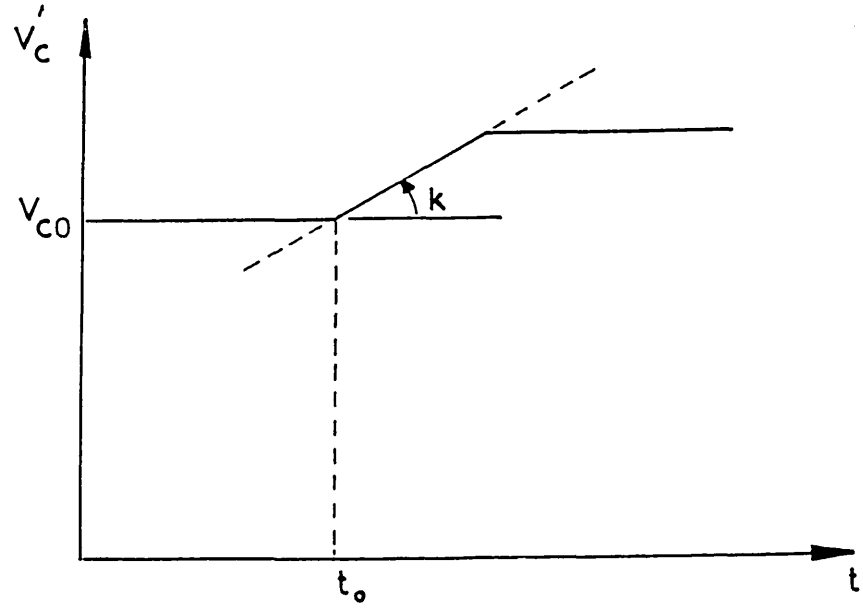

Fig. 4.14 - REPRESENTATION OF A TRANSIENT ON THE CONTROL VOLTAGE

Eqn 4.14 can be solved in terms of i(t) :

$$i(t) = kC(1 - e^{-\frac{t}{RC}}) \quad . \qquad (4.15)$$

It can be seen from eqn 4.15 that the current through the first resistor is proportional to the ramp slope, k. A small response delay should be expected due to the time elapsed between the beginning of the slope and the time when i(t) has a level sufficient to trigger the monostable.

b) Absolute value circuit and amplification

The signal coming from the transient detection is fed into a fullwave rectifier in order to obtain its absolute value (Fig. 4.15). A high gain amplifier is used at the rectifier output in order to improve the transient detector sensitivity to very small surges.

c) Level detector

The output of the level detector is designed to feed TTL level of voltage directly to the monostable. The circuit is represented in Fig. 4.16.

d) Monostable

The IC-TTL SN74121 was used as the monostable circuit and its connection is shown in Fig. 4.17.

The ON time of the monostable is determined by : $t_{\omega} = 0.7\ (C_{EXT}R_T)$. This time can be adjusted from approximately 8mS up to 180mS, that is from half a cycle up to 9.0 cycles (50Hz), approximately.

e) Analogue switch

The IC-MOS DG308 was used as the analogue switch, its connection is shown in Fig. 4.18.

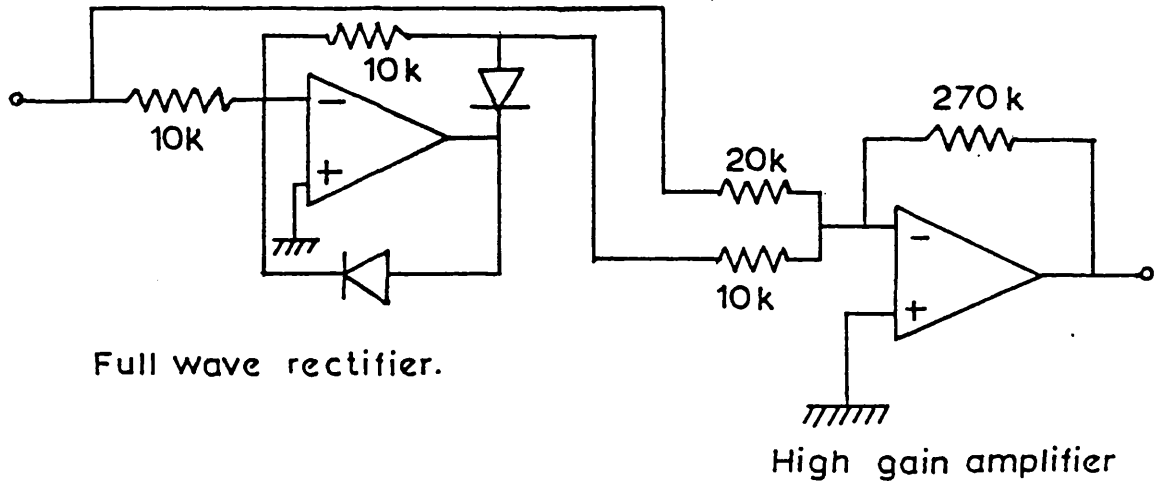

Fig. 4.15 - ABSOLUTE VALUE CIRCUIT

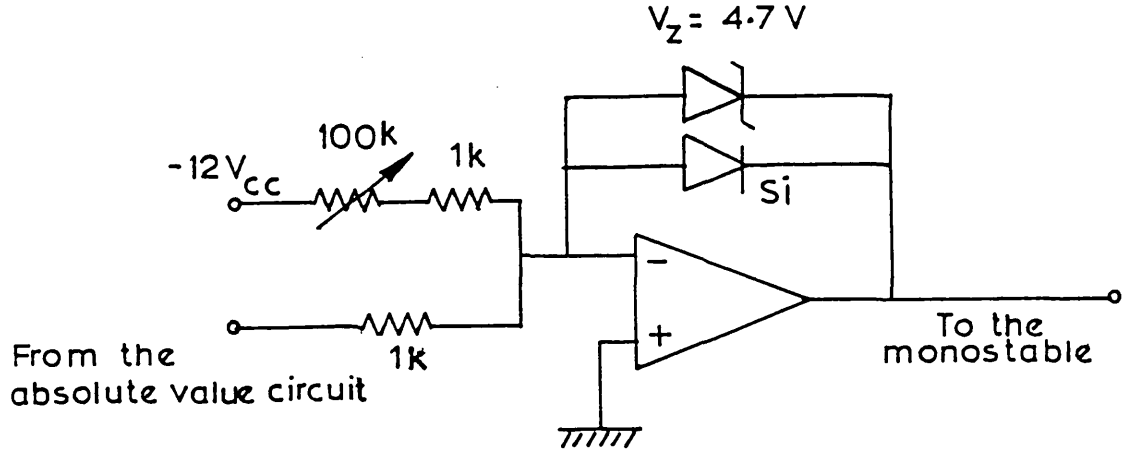

Fig. 4.16 - LEVEL DETECTOR

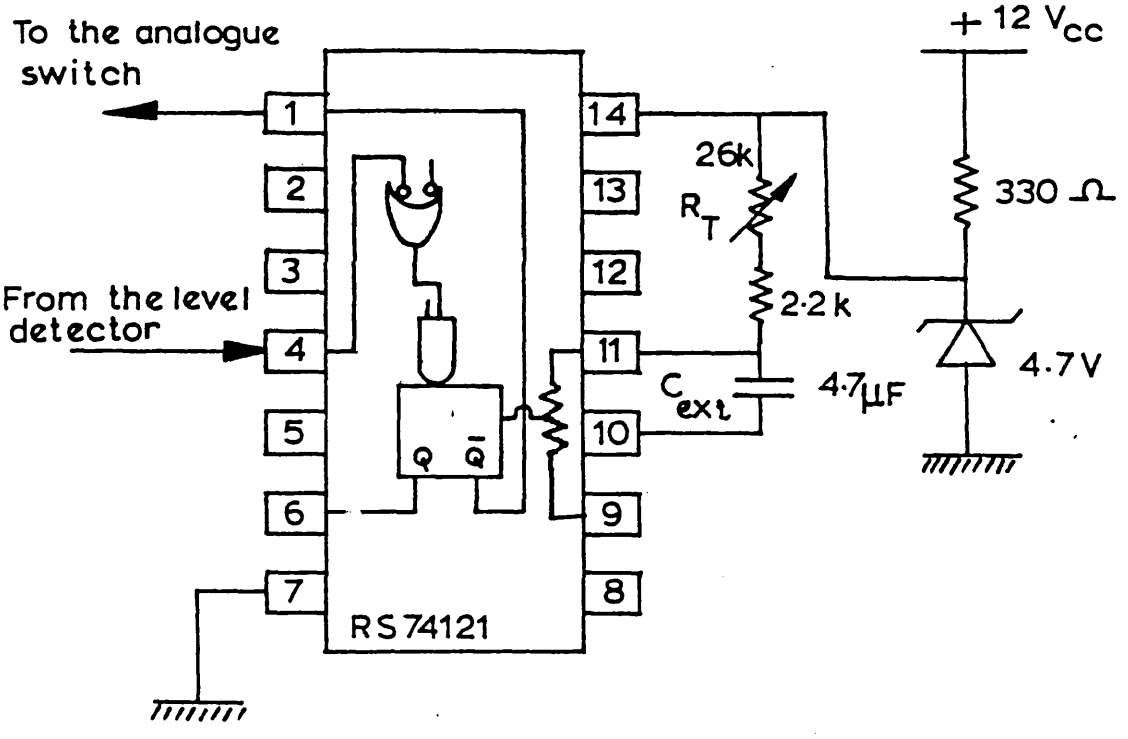

Fig. 4.17 - THE MONOSTABLE CONNECTION

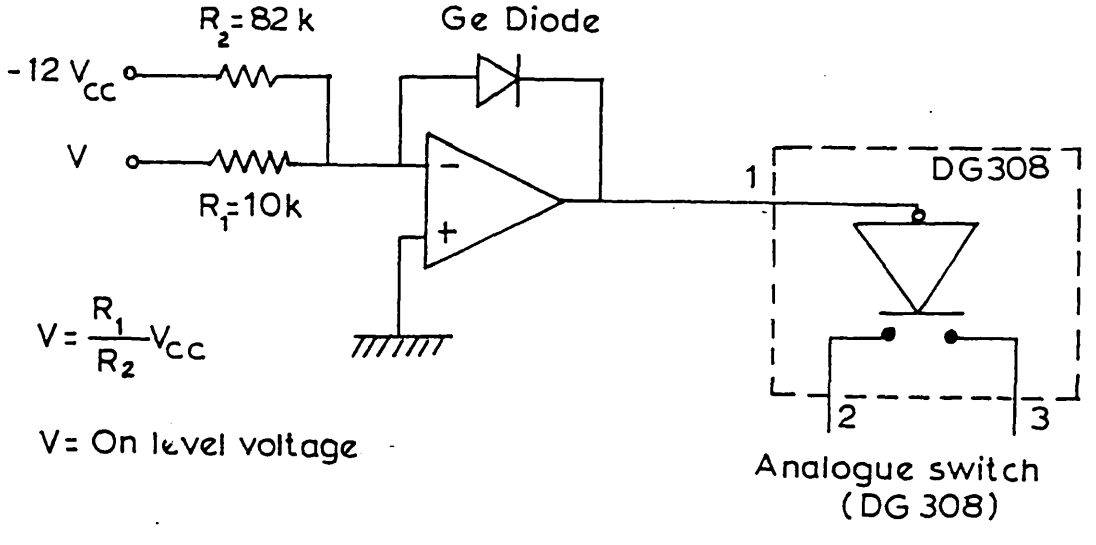

Fig. 4.18 - ANALOGUE SWITCH CONNECTION

4.8 Off-line tests

4.8.1 Test of the injection circuit

The circuit to simulate signal injection was set up as shown in Fig. 4.19. Signal frequencies, ω, from 15Hz up to 4kHz were tested with amplitude range from 0.0 Volt up to 10.0 Volts. The results were the straightforward verification of the lowpass filter response given in eqn 4.13. For example, the presence of a 300Hz oscillation at V_c, is reduced to about 1/40 of its original value if R_1C_1 = 20m sec. With the same time constant and a 50Hz signal, the reduction was about 1/6 whilst with 20Hz signal V_c' and V_c were virtually identical.

4.8.2 Test of the transient detector

The circuit used to test the transient detector is shown in Fig. 4.20.

Switching surges were simulated by using a square wave generator so that the control voltage, V_c', is given by:

$$V_c' = V_{co} + V_m \sin \omega t + V_{sq}$$

where

V_{co} : simulates the d.c. component of the control voltage

V_m : is the magnitude of an imposed oscillation

ω : is the frequency of the imposed oscillation

V_{sq} : square wave voltage representing sudden changes on the control voltage, V_c'.

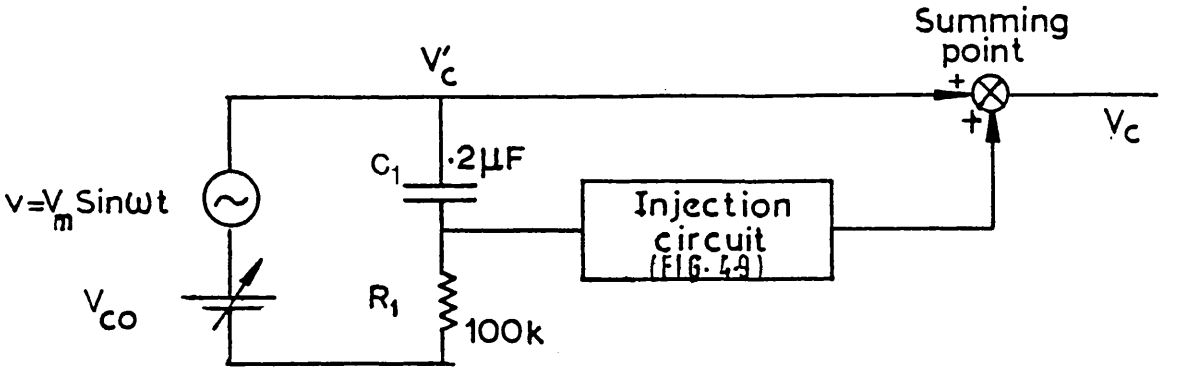

Fig. 4.19 - TEST OF THE INJECTION SIGNAL

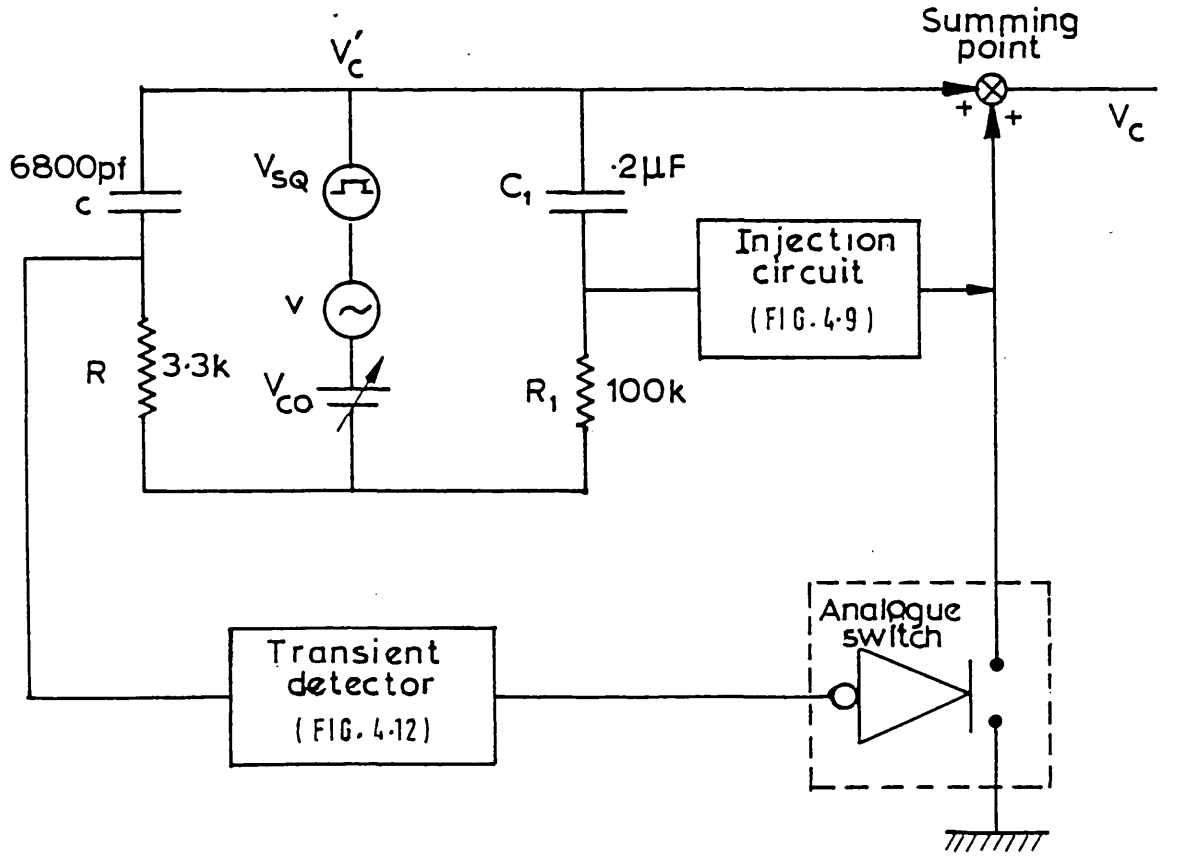

R_1C_1 = Time constant of the injection filter.
RC = Time constant of the transient detector.

Fig. 4.20 - TEST OF THE TRANSIENT DETECTOR

Fig. 4.21 shows a typical output of the control voltage before and after the summing point of Fig. 4.20.

The square wave amplitude simulating transient surges was varied within 0.2V to 5V, the range of values used in the IC-h.v.d.c. model controller. It was confirmed that different levels of V_{co} do not affect the output ripple. Only when V_m is large enough to cause triggering of the monostable does the output control voltage, V_c, become the replica of V_c'. In this case, the replication of the input is only interrupted for short periods when the monostable changes its state from ON to OFF and to ON again. Otherwise, Fig. 4.21 is a typical input-output pattern shape of signal injection irrespective to the V_{co} level used.

Numerical results are not presented because they are the straightforward verification of the RC-circuit switching principles. The time elapsed between the square wave step and the analogue switch closure was not more than 100 μsec for the cases studied.

4.9 Tests on the d.c. transmission model

The general condition under which these tests were performed, are:

SCR = ∞

line voltage = 160V

I_{dc} = 1.5A

α = 15°

Controller gain = 100

t_{OFF} = 150msec (7.5 fundamental cycles)

Closed-loop tests

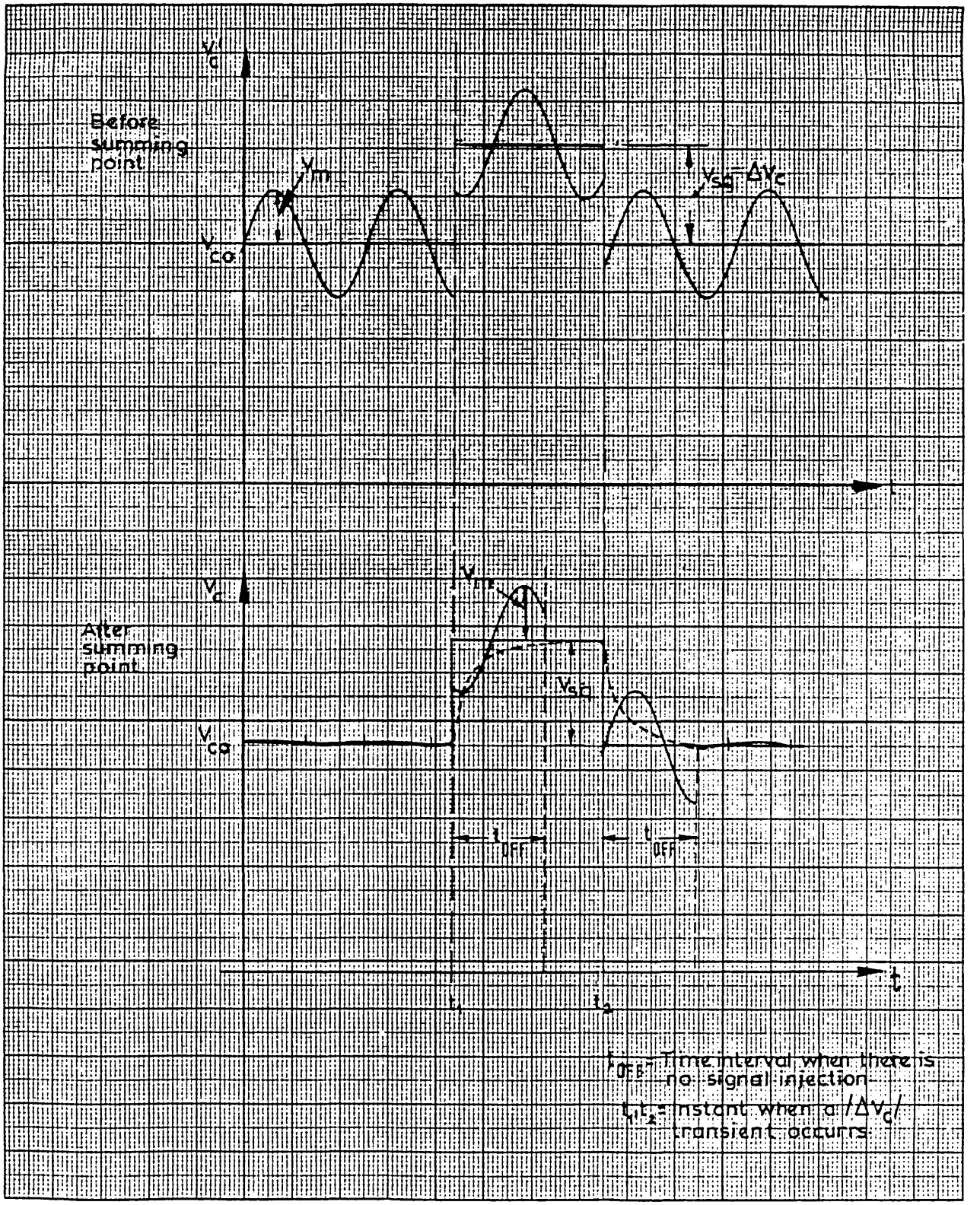

Fig. 4.21 - CONTROL VOLTAGE

4.9.1 Frequency selection

All tests presented in Chapter 5, use selection of only one frequency from the control voltage ripple and, for this reason, no examples of the bandpass filter selection are presented here. Fig. 4.22 shows how the control voltage can be smoothed out by injecting back its own ripple, as explained in Section 4.6.

4.9.2 Transient detector

Operation of the transient detector was tested under several a.c.- and d.c.-side conditions of the converter. Fig. 4.23 illustrates the case in which a square wave is superimposed on the reference current I_{ref} which, due to the high gain of the controller, causes a ±5 Volt amplitude perturbation on V_c. This severe test shows that:

1) From practical point of view, the transient detector operates instantly after the surge has occurred even under very severe conditions.

2) V_c is a good replica of V_c' outside the t_{OFF} interval. During t_{OFF}, the controller is able to react freely to any surge condition under its own time constant which can be much smaller than that of the injection circuit. After t_{OFF} has elapsed, the injection circuit switches on again causing a damped oscillation on V_c. This small amplitude oscillation has little effect on the d.c. current ripple.

3) Comparison between the transients started at instants t_1 and t_2 shows that the transient detector reacts satisfactorily for either positive or negative ΔV_c.

4) Due to the large time constant of the m.s. selection circuit, a decaying d.c. voltage remains across the injection circuit output

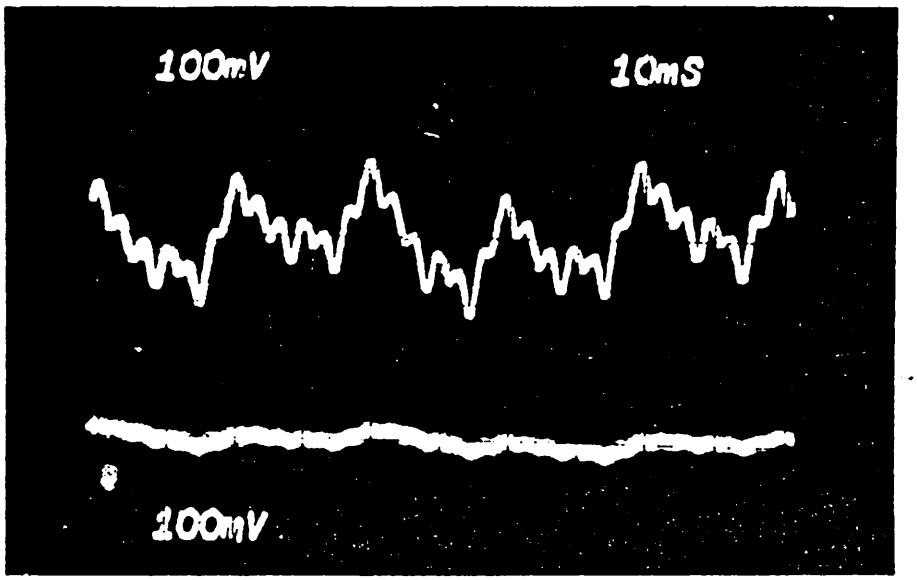

a

b

Fig. 4.22 - CONTROL VOLTAGE RIPPLE

(a) Before Summing Point (V_c')
(b) After Summing point (V_c)

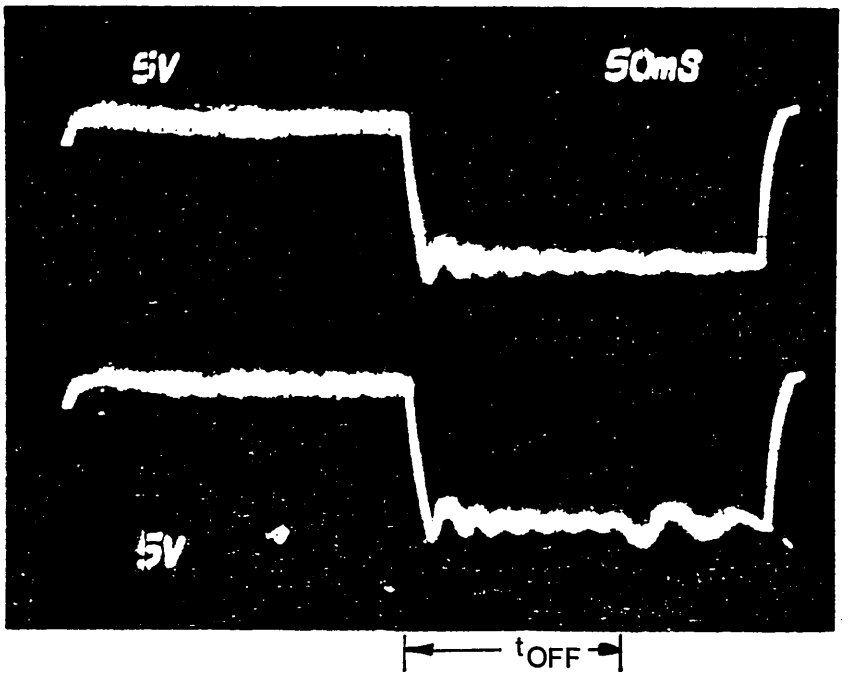

a

b

Fig. 4.23 - CONTROL VOLTAGE DURING A TRANSIENT

(a) Before Summing Point (V_c')
(b) After Summing Point (V_c)

terminals after each transient. To prevent this from affecting the control voltage, t_{OFF} has to be long enough so that the longest expected transient has decayed. Nevertheless, if the transient condition still persists after t_{OFF} has elasped, the transient detector will restart the t_{OFF} period.

Tests with small system disturbances, e.g. a 10% change in the d.c.-line resistance were sufficient to activate the transient detector.

4.9.3 Effects on the d.c.-side voltage

Injection of a closed-loop m.s. into the control voltage has a very pronounced effect on the d.c. line voltage. This is experimentally confirmed by the minimization of 50Hz and 100Hz harmonics clearly present on the d.c. voltage ripple shown in Fig. 4.24 and virtually eliminated in Fig. 4.25.

4.10 Conclusions

This chapter deals with the circuitry necessary to implement the generation, control and modification of the a.c.-side harmonic content dealt with in Chapter 5.

Presence of second harmonic is obtained from an adjustable 3-phase second harmonic generator based on the effects of fullwave rectifiers on the phase current. The third harmonic is obtained from a.c. supply imbalances.

The a.c. busbar harmonics are continuously measurable and observable

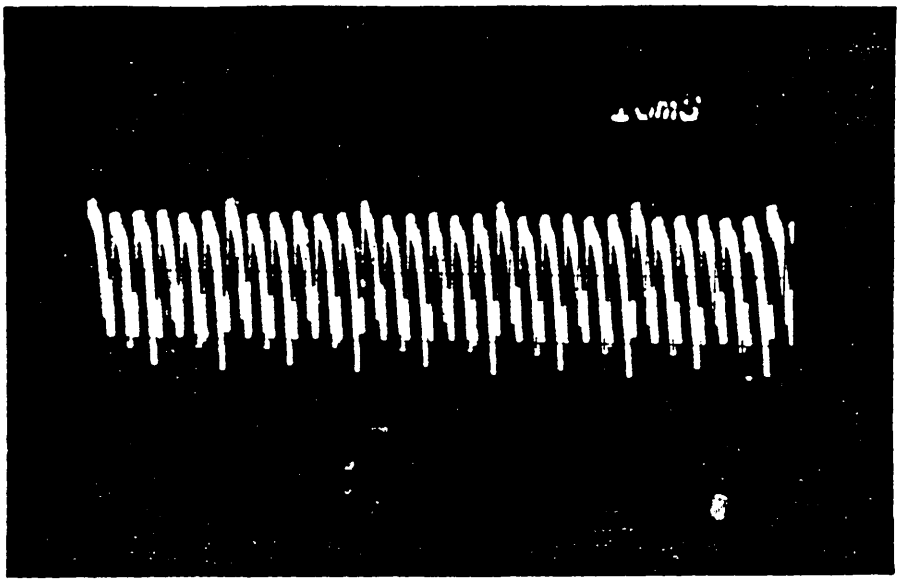

Fig. 4.24 - d.c. VOLTAGE RIPPLE WITHOUT CONTROL m.s.

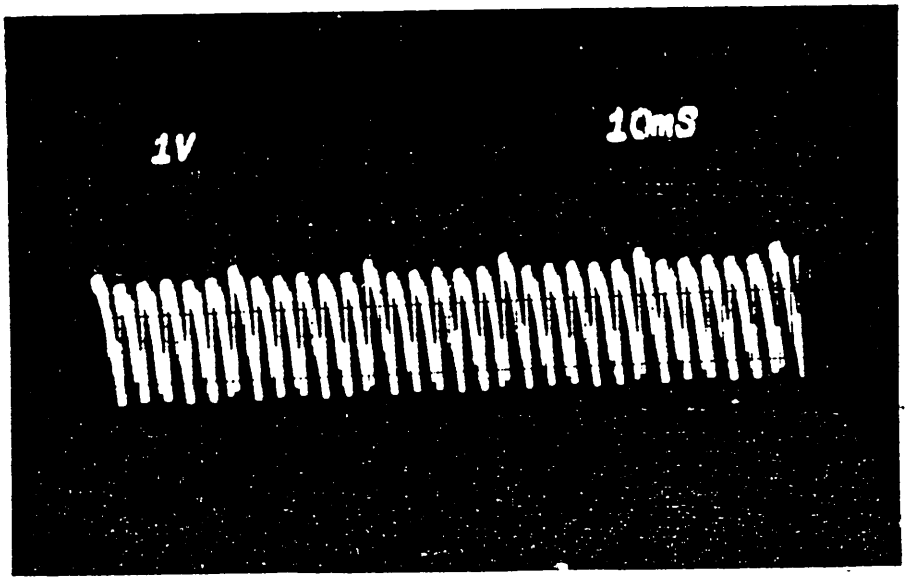

Fig. 4.25 - d.c. VOLTAGE RIPPLE WITH CONTROL VOLTAGE RIPPLE

on a conventional oscilloscope and on a DVM by using a purpose built bandpass filter. The frequency spectrum of each phase and of the d.c. voltage are simultaneously obtained from an on-line computational arrangement which can perform Fourier analysis and phase sequence decomposition.

It is shown how the control voltage ripple can be modified by introducing in the frequency selection circuit, an RC-filter with large time constant. A transient detector ensures that the control time constant is temporarily restored to its conventional value so that transients in the d.c.-side current are treated as usual. These transients always leave some residual d.c. voltage across the output of the injection circuit which can have undesired effects on the control voltage. To prevent this the off-time of the injection circuit, t_{OFF}, has to be adjusted to a value equivalent to the time constant of the high-pass or bandpass filters.

Tests on the d.c. simulator using closed-loop m.s. have shown that the d.c. voltage ripple is mostly dependent on the control voltage ripple. It was also shown that this m.s. can be obtained from the control voltage ripple and that its amplitude and phase are controllable and locked to the d.c. line current.

CHAPTER 5

HARMONIC MINIMIZATION METHOD AND EXPERIMENTAL RESULTS

5.1 Introduction

The use of the d.f. technique to predict limit cycle oscillations synchronized with the a.c. system was discussed in Chapter 2. The d.f. results were obtained from the steady-state control voltage modulation by a signal of known amplitude, frequency and phase and from measurements of the d.c.-side harmonic of the same frequency. Uncharacteristic harmonics were experienced on the a.c.-side and d.c.-side as a result of a m.s. on the control voltage. In Chapter 3, approximate relationships between these uncharacteristic harmonics and the m.s. as well as the relationships between d.c.-side uncharacteristic harmonics due to a.c.-side harmonic distortion, were obtained. A circuitry to implement the m.s. injection into the control voltage was described in Chapter 4.

In this chapter, a general description of the harmonic minimization method based on control voltage modulation, is presented. Experimental confirmation of the method and of the approximate relationships obtained in Chapter 3 are also presented.

In order to show how the m.s. remains locked to the minimized a.c.-side harmonic and to compare converter operation with and without m.s. on the control voltage, the Fourier analysis of the a.c.-side and d.c.-side voltage of the h.v.d.c. simulator, were carried out and the results are discussed for 50Hz, 100Hz and 150Hz m.s.

In all tests, the m.s. is always derived from the d.c.-side current ripple.

5.2 Harmonic minimization by control voltage modulation

The harmonic content of the converter busbar voltage is a combination of harmonics caused a) by the converter station itself and b) by other loads also connected to the converter busbar. As suggested in Chapter 2 and discussed in Chapter 3, there is a virtual independence between harmonics caused by a) control voltage modulation and b) a.c.-side voltage distortion.

In strong systems (high SCR) uncharacteristic harmonics are fairly low, except in the case of a non-sinusoidal a.c.-supply. In weak systems (low SCR), the harmonics present in the converter busbar may be of considerable amplitude. If the harmonics generated by the converter could be varied by firing angle modulation (as explained in Chapter 3) and if they were adjusted to be in approximate phase opposition with the harmonics originated in the a.c. system itself, then the overall level of harmonic presence on the converter busbar is minimized.

The converter busbar harmonics change according to the operating conditions of the a.c./d.c. system and the m.s. must be corrected whenever a variation occurs in amplitude and/or phase of the harmonic being minimized. In a practical operation, such correction must be continuous, i.e. the m.s. has to be locked to the minimized harmonic.

The relations developed in Chapter 3, show that a given m.s.

has an approximate relation with some a.c.-side harmonic frequencies, so that, within certain limits, the m.s. amplitude and phase can be locked, to the a.c.-side harmonic. The locking mechanism can be understood with the help of Fig. 3.1 as follows. The a.c.-side harmonic distortion is transferred to the d.c.-side through the converter bridge (as demonstrated in Section 3.13) causing d.c.-side harmonic currents defined by the d.c.-line input impedance (Section 3.12). These harmonic currents are transferred to the converter through the d.c. current transducer (Section 3.2). Due to the lowpass characteristic of the d.c. current transducer and of the controller itself, the control voltage will contain harmonics of low orders only, which will be fed into the injection circuit whose output is the modulating signal (Section 4.4). These relationships were experimentally verified for the small amplitudes of m.s. ($\Delta\alpha<6°$) and the results are discussed in the next sections.

5.3 Relation between m.s. and uncharacteristic harmonics

As discussed in Chapter 3, a.c.-side harmonics of several orders are excited by the presence of a m.s. . The tests performed on the IC-h.v.d.c. simulator were designed to show that the amplitude of these harmonics are approximately proportional to the m.s. for small amplitudes as examplified for a 50Hz m.s. in Fig. 5.1. The m.s. amplitude was varied from 0.0 to 0.5 volts ($\Delta\alpha\cong0°\sim10°$) and the a.c.-side harmonic amplitude were monitored on a spectrum analyser (model hp No. 3 5 8 0 A). The computer program (described in Section 2.7)

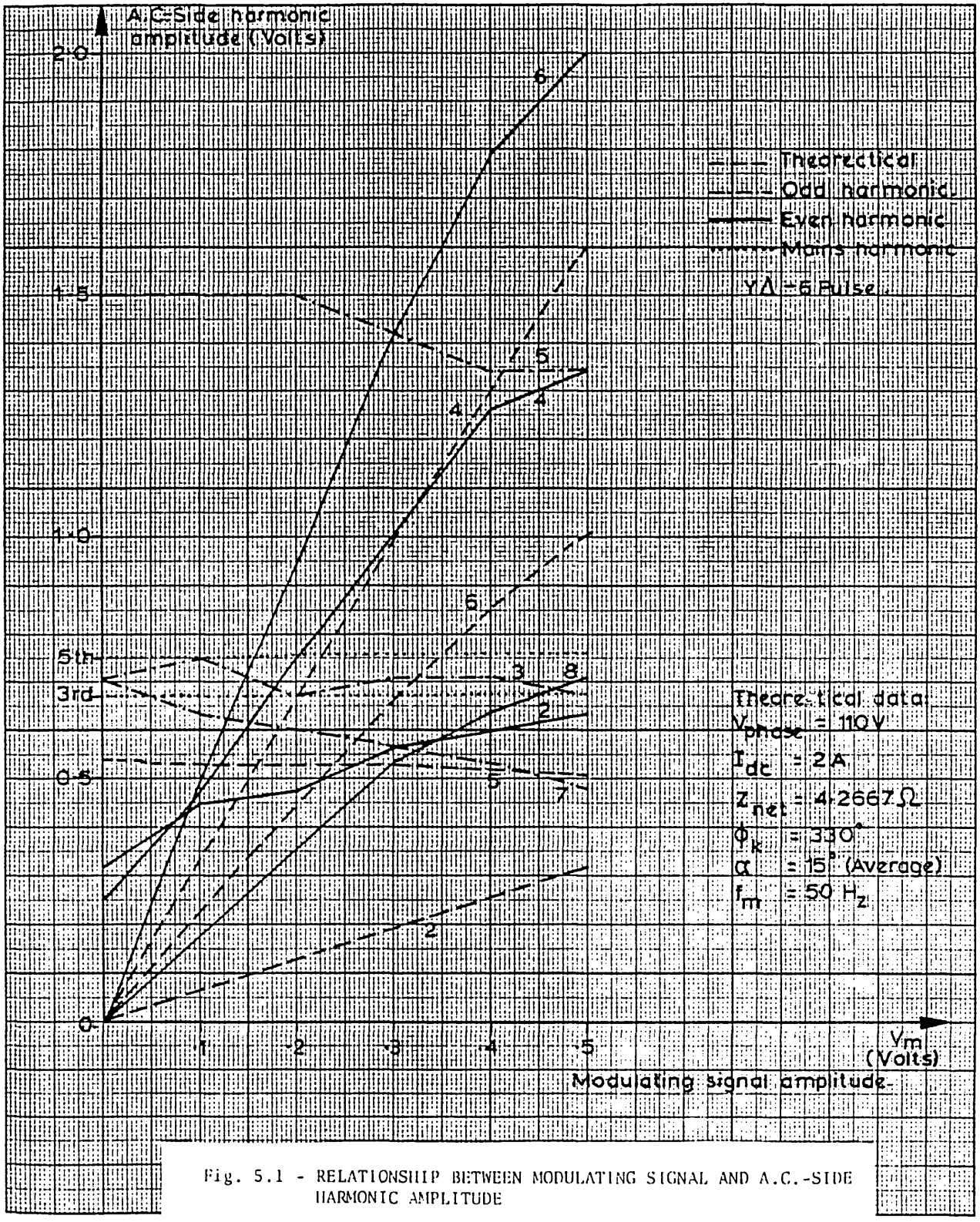

Fig. 5.1 - RELATIONSHIP BETWEEN MODULATING SIGNAL AND A.C.-SIDE HARMONIC AMPLITUDE

was, also run with the system parameters of Table 5.1. Unless otherwise indicated, all uncharacteristic harmonics present at the converter busbar for V_m = 0. have their origin in the network itself and were not artificially injected in any way.

As shown in Fig. 5.1, an increase in the amplitude of a 50Hz m.s. causes a proportional increase in the a.c.-side even harmonics whilst odd harmonics are minimally affected. This proportionality is good up to V_m = 0.3 Volts ($\Delta\alpha = 6°$). Beyond that point the relationship becomes non-linear.

Included in Fig. 5.1 are also the a.c.-side harmonics predicted theoretically by harmonic analysis from the computer program for similar conditions except that the a.c. power supply is assumed to be purely sinusoidal, a situation clearly not obtained in a power systems laboratory.

Fig. 5.2 shows the effect of the m.s. phase ϕ_k, on the a.c.-side harmonics when a fixed m.s. amplitude V_m = 0.3 Volts is used. Again, even rather than odd harmonics are mainly affected. The irregularities on the curves in Figs 5.1 and 5.2 are believed to be due to the unavoidable interaction between harmonics generated by the m.s. and the harmonics naturally present in the a.c. system. This results in harmonic magnification or reduction according to relative phase differences. For example, in Fig. 5.3 the m.s. phase was set at 225° to give at the same time minimum second and fourth harmonics (see vertical line in Fig. 5.2). The m.s. amplitude was then varied from 0.0 to 0.15 Volts. A minimum second harmonic is achieved for V_m = 0.08 Volts but at the expenses of a drastic increase in the 6-th harmonic. In Fig. 5.4, the m.s. was adjusted to give a minimum 6-th harmonic (approximately zero) and reduced 2nd

TABLE 5.1

SYSTEM DATA

Converter rated output	
d.c. voltage	
rectifier side	70.4V
inverter side	42.5V
d.c. current	2. A
SCR for z = (1.94+j60.7)/phase	3.5
Converter transformer	220W
rating	$100\sqrt{3}/63$V
reactance	0.77pu
resistance	0.877pu
turns ratio	2.75
Control setting	
nominal firing angle	15°
nominal estinction angle	20°
gain	8.
Smoothing reactor (per station)	
resistance	1.6Ω
inductance	0.3H
D.c. transmission line (T-model)	
resistance	14Ω
inductance	0.2H
capacitance	0.

(Relevant differences from the system data above are indicated in the diagrams)

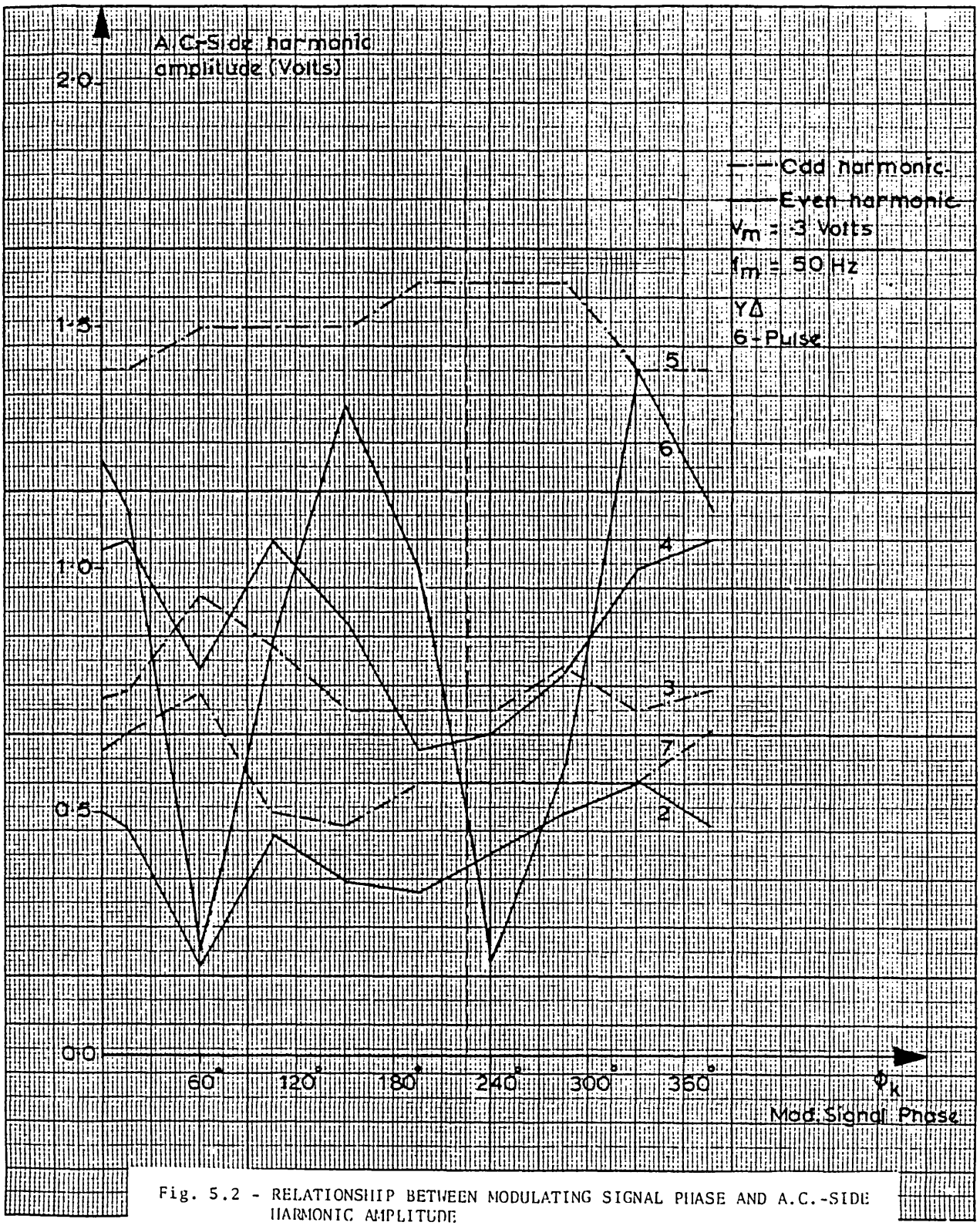

Fig. 5.2 - RELATIONSHIP BETWEEN MODULATING SIGNAL PHASE AND A.C.-SIDE HARMONIC AMPLITUDE

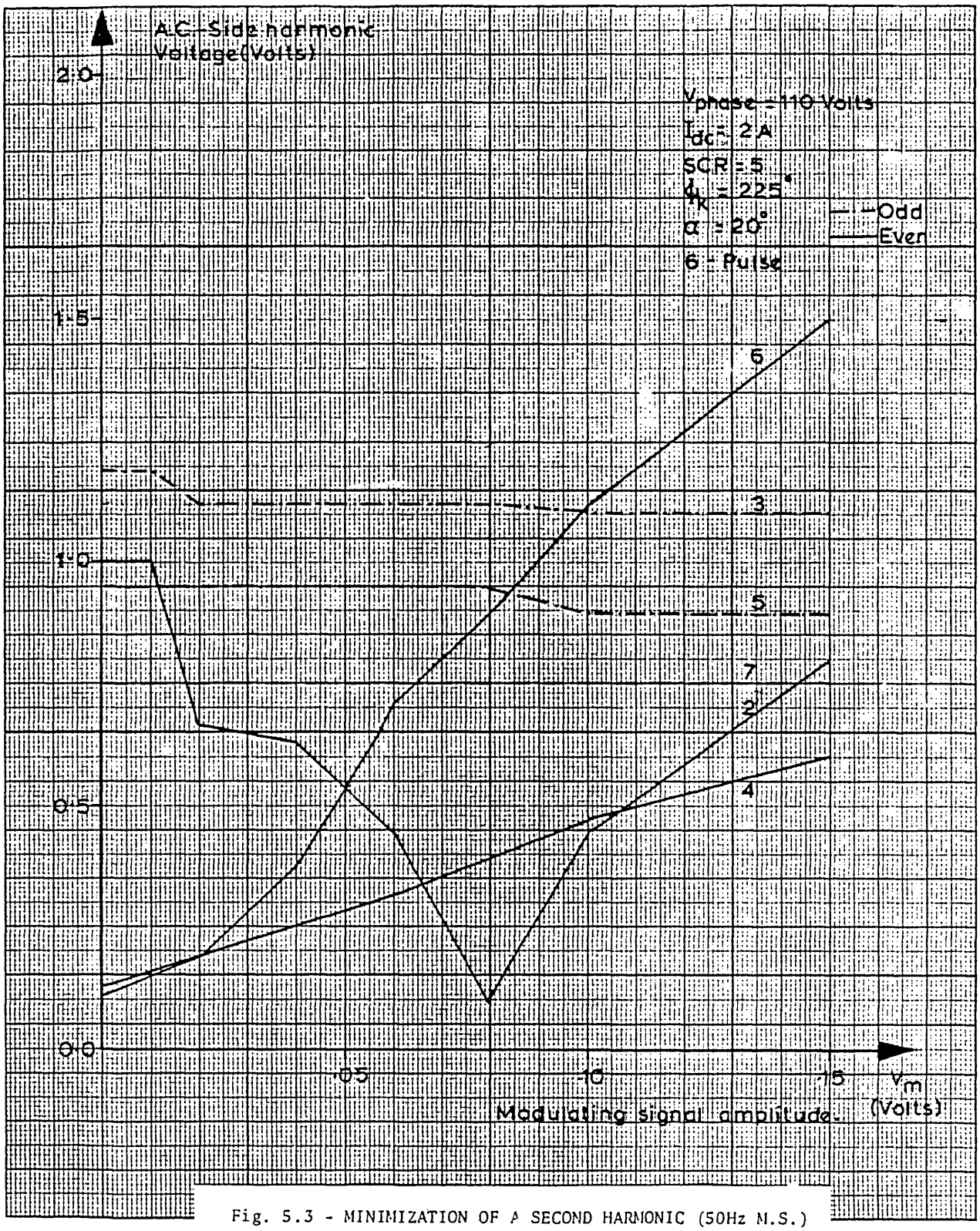

Fig. 5.3 - MINIMIZATION OF A SECOND HARMONIC (50Hz M.S.)

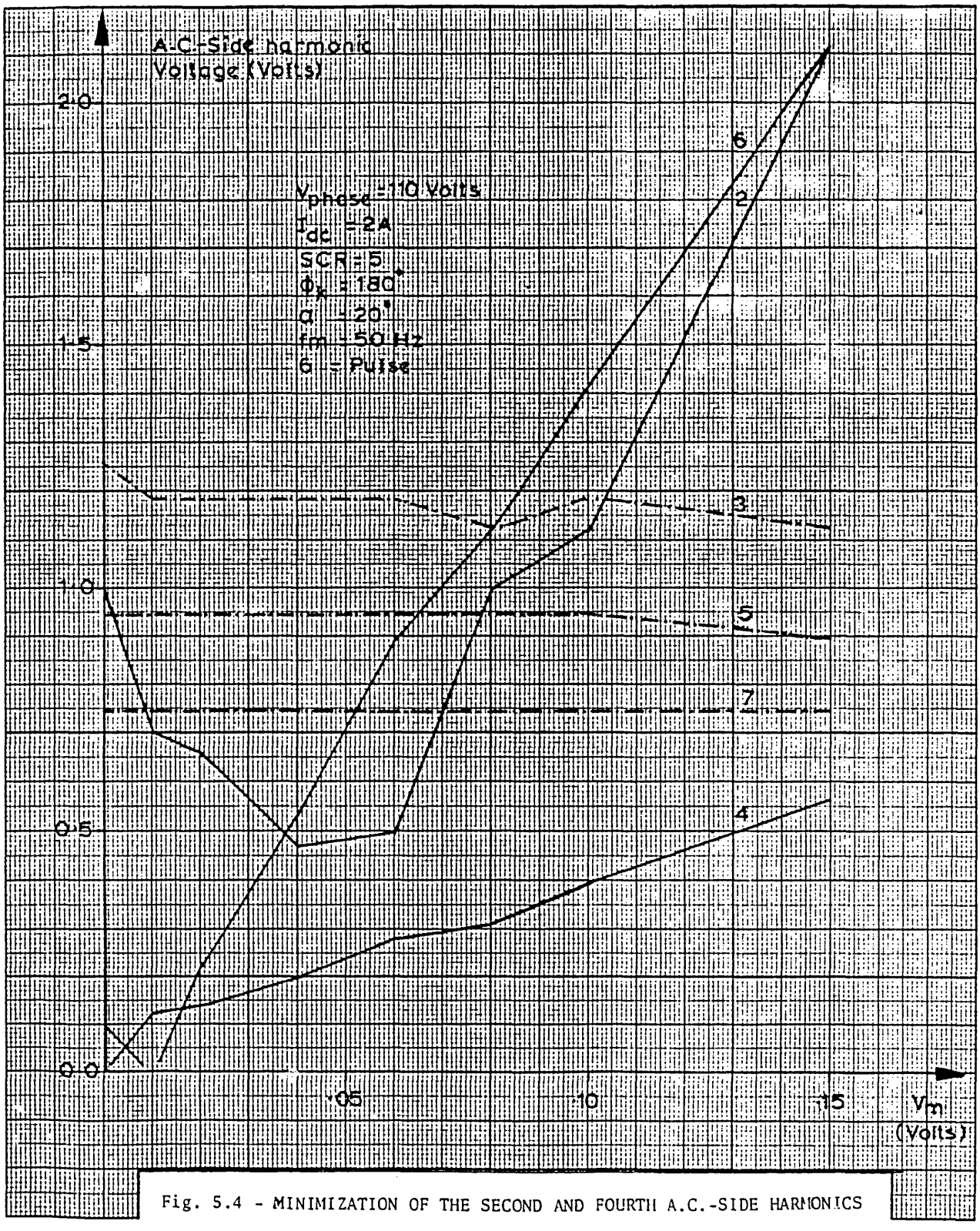

Fig. 5.4 - MINIMIZATION OF THE SECOND AND FOURTH A.C.-SIDE HARMONICS

and 4-th harmonics. The 2nd harmonic reduction in this case is about 30% only. Obviously this ad hoc procedure is not a convenient way of selecting and adjusting a m.s. to obtain harmonic minimization. An alternative procedure is described later.

For small amplitudes, the a.c.-side harmonics are moderately locked to the m.s. . This is demonstrated for an a.c.-side second harmonic of positive sequence which was minimized by a 50Hz m.s. . In order to reduce the negative sequence level from the a.c. system, a positive sequence from the second harmonic generator was injected into the d.c. simulator converter busbar. The 50Hz m.s. was then varied in amplitude and phase. To monitor the results, a four-trace oscilloscope was used to display simultaneously :

a) d.c.-side voltage ripple;

b) 50Hz m.s.;

c) a.c.-side second harmonic obtained from the output of the INIC filter (described in Section 4.3);

d) firing pulse to valve 1.

The amplitude and phase of the signals shown in Figs 5.5(ii) and (iii) are relative to the amplitude and phase of the signal in Fig. 5.5(i). Figs. 5.5(i) and (ii) show that doubling the m.s. amplitude, doubles the a.c.-side second harmonic without affecting appreciably the relative phase shift. Also, a 180° phase shift in the m.s., cause a 90° phase shift in the a.c.-side second harmonic (or 180° in second harmonic terms) without noticeable variation on the relative amplitude. This was theoretically predicted in Section 3.6.

To show the effects of a.c.-side harmonics on d.c.-side harmonics, the following experiment was carried out. The a.c.-side negative sequence second harmonic was gradually increased through

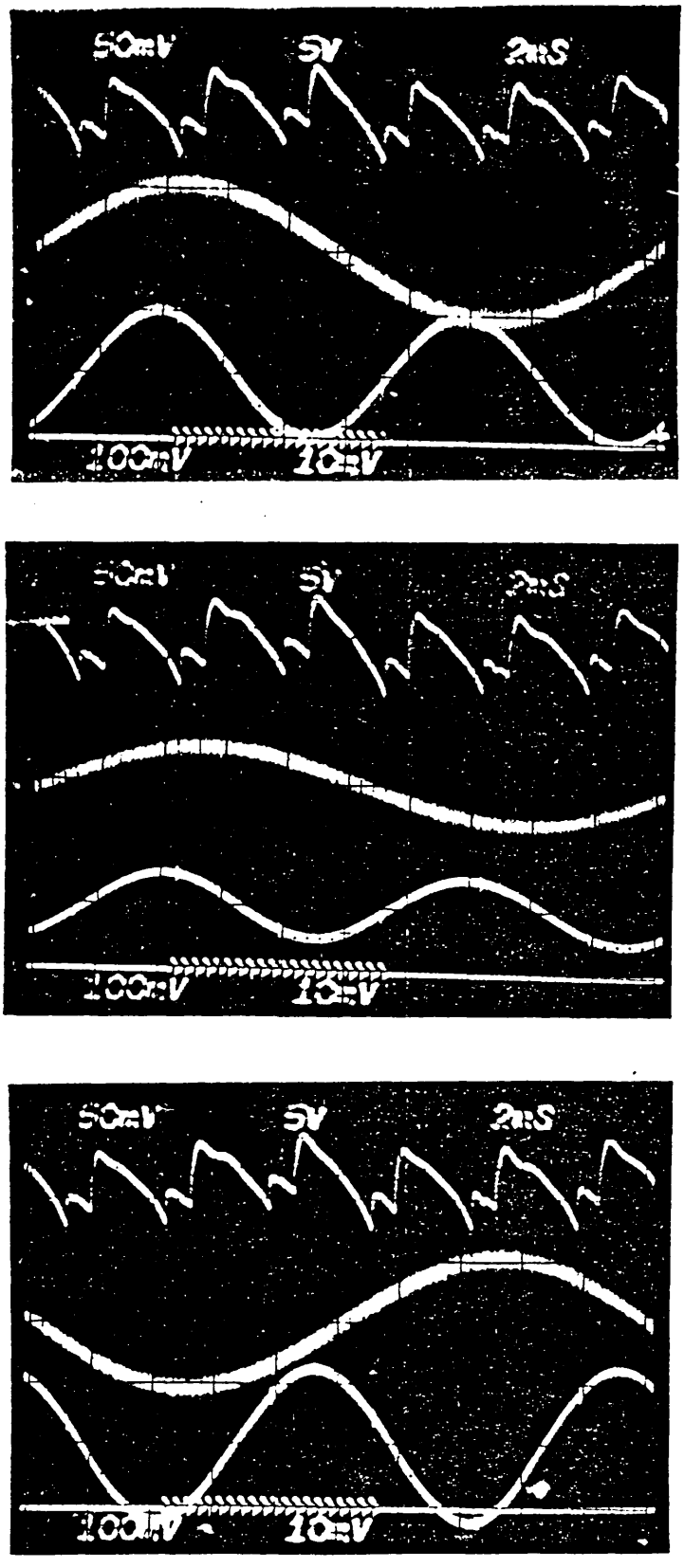

Fig. 5.5 - LINEARITY BETWEEN A 50Hz M.S. AND THE A.C.-SIDE 2nd HARMONIC

(a) D.c. Voltage Ripple
(b) Modulating Signal (50Hz)
(c) A.c.-side 2nd Harmonic
(f) Firing Pulse to Valve 1

the second harmonic generator up to about 20% of the fundamental amplitude. As a result, the d.c.-side 150Hz harmonic voltage increased proportionally. Similarly, the second harmonic of positive sequence gave rise to a proportional d.c.-side, 50Hz. These effects are illustrated in Figs. 5.6(I) to (III). Fig. 5.6(I) shows the relative d.c.-voltage ripple and its corresponding a.c.-side second harmonic of predominantly positive sequence which was naturally present in the converter busbar. Figs. 5.6(II) and (III) shows the d.c.-voltage ripple affected respectively by a negative and a positive sequence second harmonic.

5.4 Selection and adjustment of a m.s.

Most of the harmonics excited by control voltage modulation are not injected into the a.c. system because:

a) tuned filters are provided for characteristic harmonics of low orders, and highpass filters (low Q) are usually provided for harmonic orders higher than the 12-th[9];

b) harmonics close to the cut off frequency of the filters are also drastically reduced;

c) of harmonic cancellation in 12-pulse converters.

For these reasons, the second, third and ninth a.c.-side harmonics are of special importance when using m.s.'s.

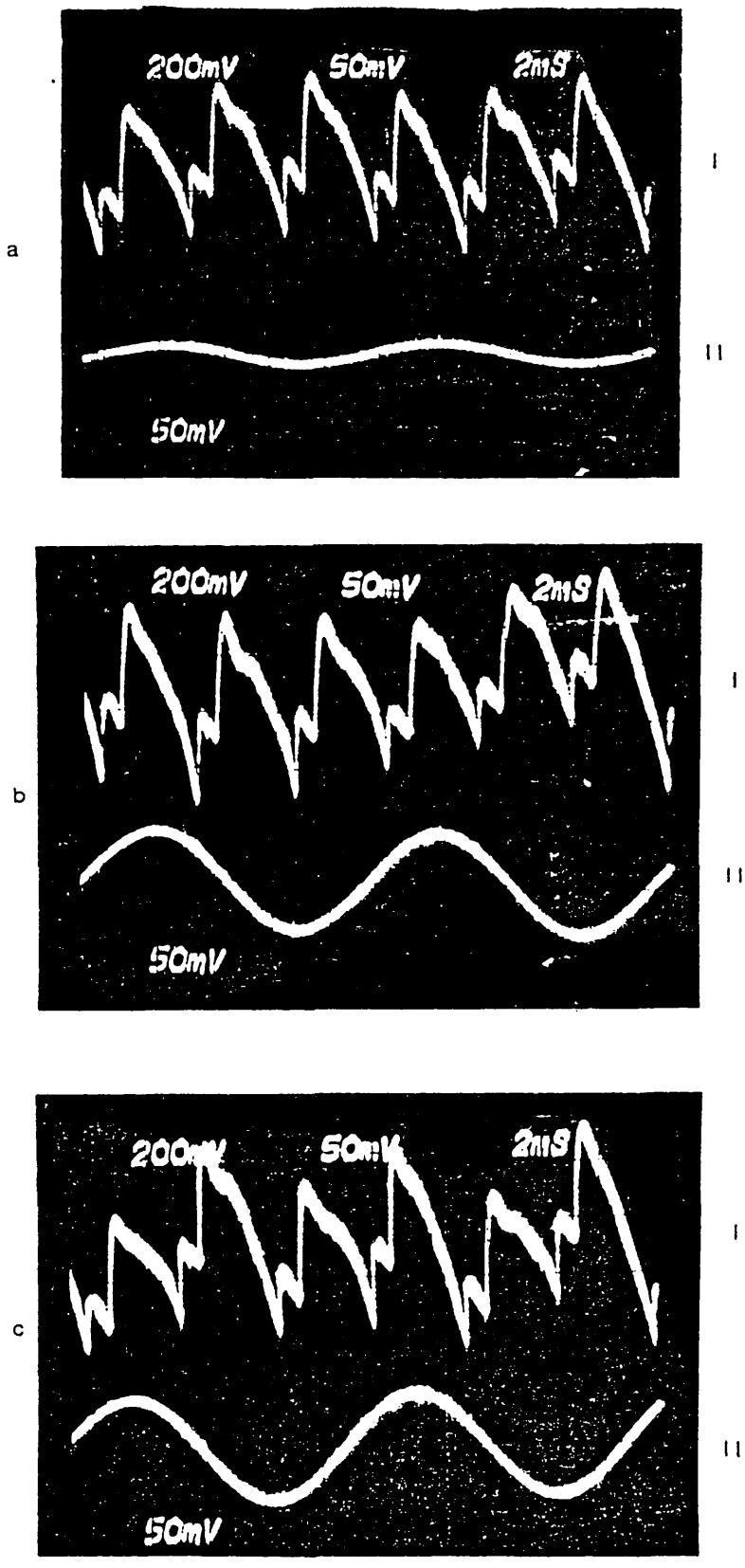

Fig. 5.6 - EFFECTS OF THE A.C.-SIDE 2nd HARMONIC ON THE D.C. VOLTAGE RIPPLE

(a) No a.c.-side 2nd Harmonic Injected (reference)
(b) Positive Sequence 2nd Harmonic
(c) Negative Sequence 2nd Harmonic

(I) D.c. Voltage Ripple
(II) A.c.-side 2nd Harmonic

Selection of the appropriate m.s. involve three tasks:

1) Identification of the frequency and phase sequence of the a.c.-side harmonic to be minimized;
2) incremental analysis of the m.s. effects on the a.c.-side voltage (as explained in Chapter 3);
3) adjustment of the m.s. amplitude and phase in such a way that the selected a.c.-side harmonic is reduced to a minimum value in all three phases.

Table 5.2 gives the m.s. required for minimization of second and the third order harmonics. Note the correspondence between Tables 5.2 and 2.1.

TABLE 5.2

M.S.'s to minimize a.c.-side harmonics

M.S. FREQ.	HARM. ORDER	PHASE SEQUENCE
50Hz	2nd	+
100Hz	3rd	.
150Hz	2nd	-

Wrong selection of m.s. could result in :

1) harmonic minimization in one phase with harmonic magnification in the other phases;

2) harmonic minimization in the three phases but with harmonic magnification of other orders.

In practice, the correct adjustment of the m.s. amplitude and phase could be made through four steps:

1) injection into the control voltage of a very small amplitude of the selected m.s. (e.g. $V_m \tilde{=} 0.1$ Volts);
2) tuning of the m.s. phase to minimize the selected a.c.-side harmonic;
3) increasing of the m.s. amplitude until the a.c.-side harmonic has reached its minimum value;
4) convergence to an optimum reached through successive applications of steps 2) and 3).

Examples of harmonic minimization are given in the next sections

5.5 Examples of harmonic minimization

The a.c.-side and d.c.-side harmonics presented in this section were obtained from the computer program described in the Section 2.7 with the data given in Section 5.4 for 50Hz, 100Hz and 150Hz m.s. . The practical tests were performed on the I.C.-d.c. simulator using similar parameters and quantities as for the theoretical studies. In this section, the practical tests for 100Hz and 150Hz m.s. are only briefly presented whilst in the next section, an example using a 50Hz m.s. is described in greater detail.

5.5.1 Positive sequence second harmonic

A 50Hz m.s. is used here to minimize the a.c.-side positive sequence second harmonic. Amplitudes of the a.c.-side 2nd harmonic and d.c.-side 50Hz harmonic are shown in Fig. 5.7(a) for several values of m.s. phase, ϕ_k, between 0° and 360° and a constant m.s. amplitude V_m = 0.1 Volts. The approximate sinusoidal shape of the curves is due to the relative difference between the variable m.s. phase and the constant a.c.-side harmonic phase. The minimum content is reached for ϕ_k = 108°.

Fig. 5.7(b) shows the same two harmonics as above except that now the m.s. phase is kept constant (ϕ_k = 108°) and the m.s. amplitude is varied from 0.0 to 0.7 Volts. A minimum a.c.-side 2nd harmonic is obtained for $V_m \cong$ 0.4 Volts.

The approximate linear decrease in the d.c.-side 50Hz is explained by the phase opposition between the d.c.-side 50Hz caused by converter busbar voltage distortion and the 50Hz caused by firing angle modulation. It can be concluded that a minimum d.c.-side 50Hz harmonic voltage does not necessarily coincide with a minimum a.c.-side 100Hz. Therefore, for a V_m higher than 0.4 Volts, the second harmonic injected by the converter into the a.c. system becomes increasingly imbalanced due to an increase in $\Delta\alpha$, as predicted in Section 3.6. For example, if V_m = 0.4 Volts, the harmonic imbalance in terms of second harmonic is ± 16° (=2 * 0.4 Volts * 20 deg/Volt), that is the phase imbalance may be of 32° (=2×16°).

The 3rd and 9-th a.c.-side harmonics are not shown in Fig. 5.7 because their values were lower than the minimum value the optimized computer program is able to produce, that is they are less than about 1/15 of the highest harmonic order present on the spectrum[1].

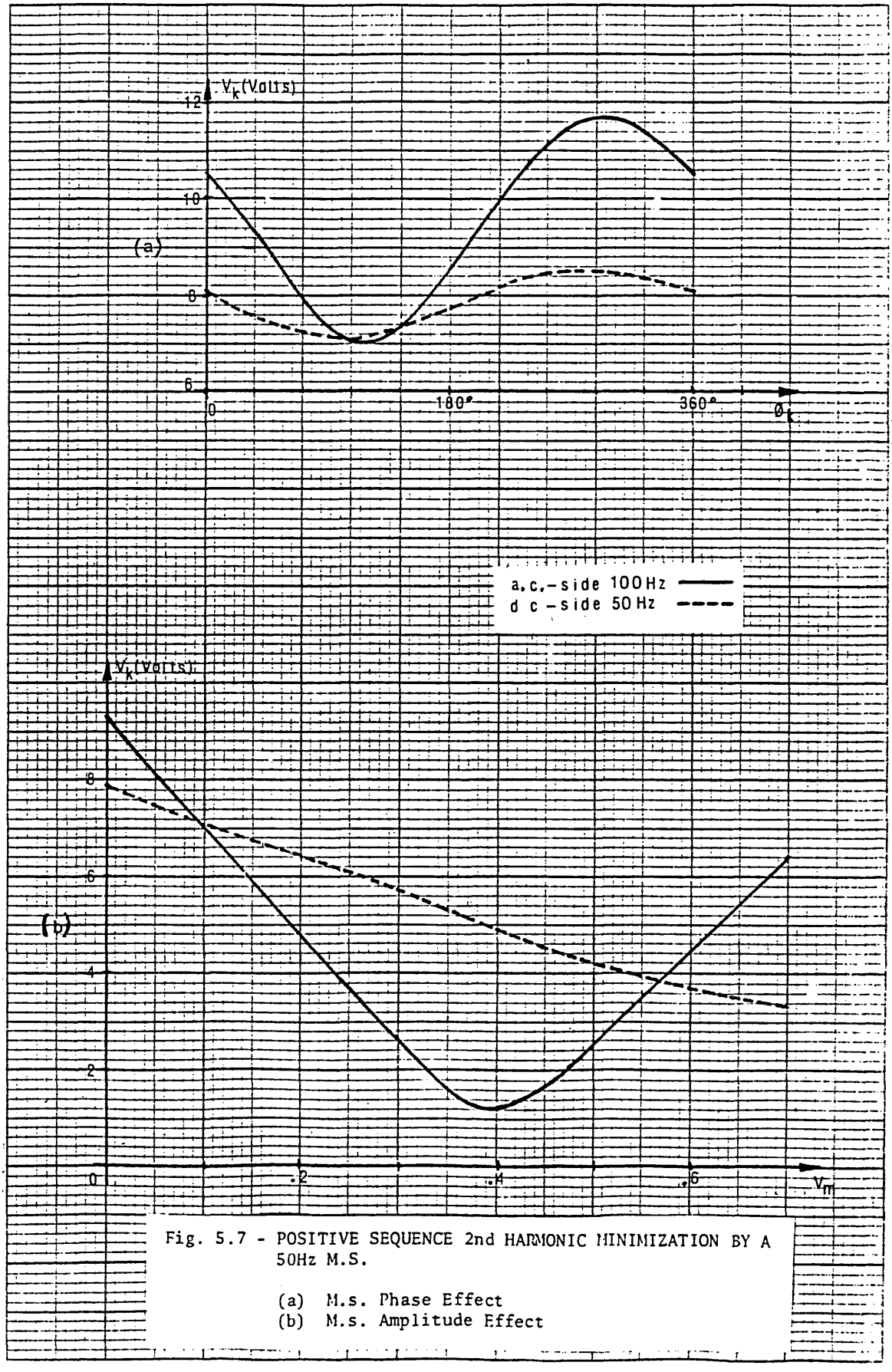

Fig. 5.7 - POSITIVE SEQUENCE 2nd HARMONIC MINIMIZATION BY A 50Hz M.S.

(a) M.s. Phase Effect
(b) M.s. Amplitude Effect

5.5.2 Negative sequence second harmonic

Here a 150Hz m.s. is used to minimize the a.c.-side negative sequence second harmonic. The a.c.-side 100Hz and d.c.-side 150Hz harmonics are plotted in Fig. 5.8(a) as a function of the m.s. phase for V_m = 0.1 Volts. The minimum amplitude of the a.c.-side 100Hz is for $\phi_k \cong 36°$. In Fig 5.8(b) the same harmonics are plotted for $\phi_k = 36°$ and values of V_m from 0.0 to 0.3 Volts. The m.s. amplitude for a minimum a.c.-side 100Hz is about V_m = 0.12 Volts. In this case, the choice of ϕ_k did not produce a.c.-side phase opposition between the 150Hz caused by busbar voltage distortion and the 150Hz caused by firing angle modulation and as a consequence, for $V_m > 0.12$ Volts the d.c.-side 150Hz voltage increases approximately linearly with V_m. The reasons why phase opposition was not kept for $V_m > 0.12$ Volts was not well understood.

The oscilloscope displays obtained from a d.c. simulator are shown in Fig. 5.9, and provide a comparison between the a.c.-side 2nd harmonic when the control voltage is subject to a 150Hz m.s. and when the conventional control voltage is used.

5.5.3 Third harmomic

A 100Hz m.s. may be used to minimize the a.c.-side 3rd harmonic present on the converter busbar. In this case the converter transformer deserves especial consideration.

Third harmonic is usually of zero sequence, and therefore it should be blocked by YΔ-transformers and practically ,

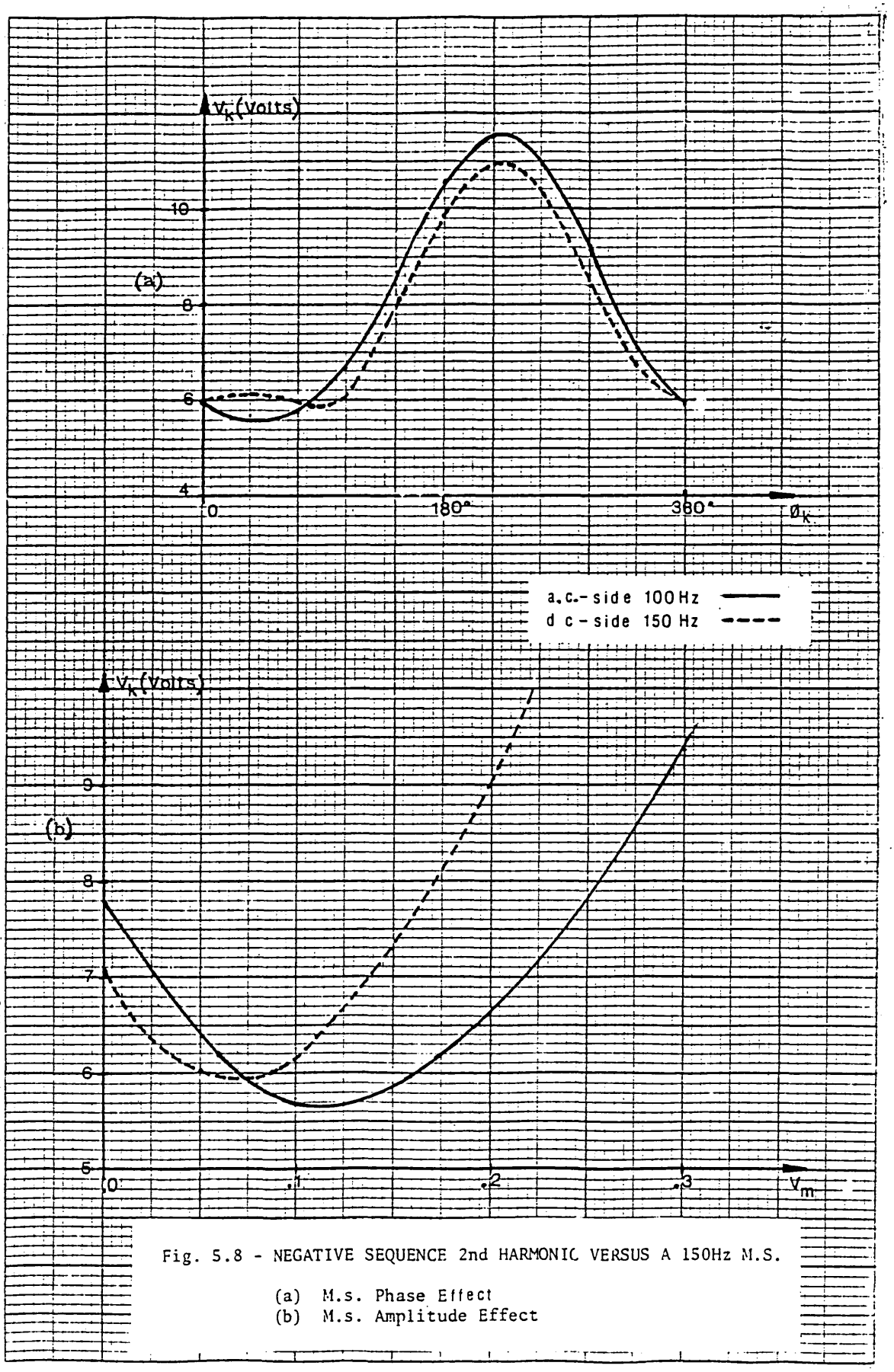

Fig. 5.8 - NEGATIVE SEQUENCE 2nd HARMONIC VERSUS A 150Hz M.S.

(a) M.s. Phase Effect
(b) M.s. Amplitude Effect

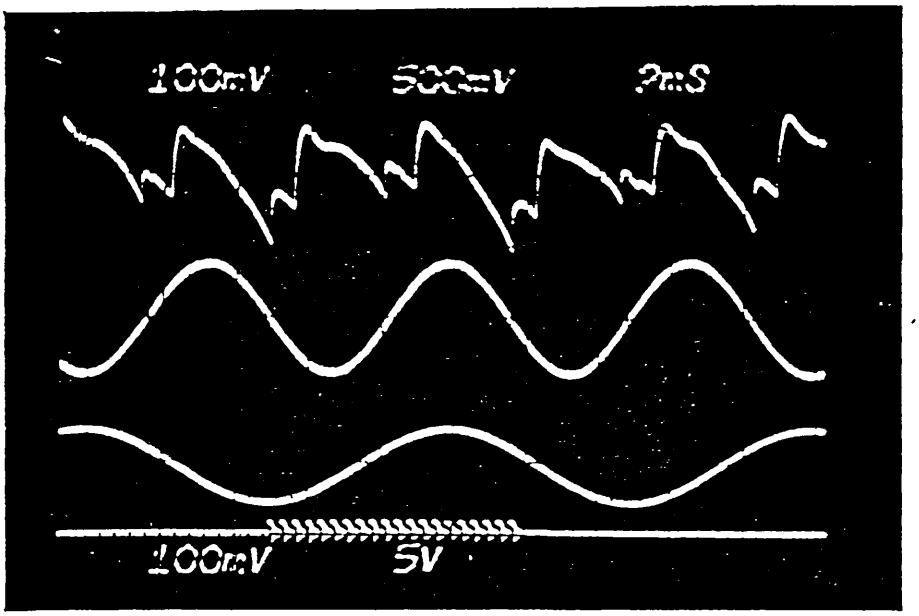

with m. s.

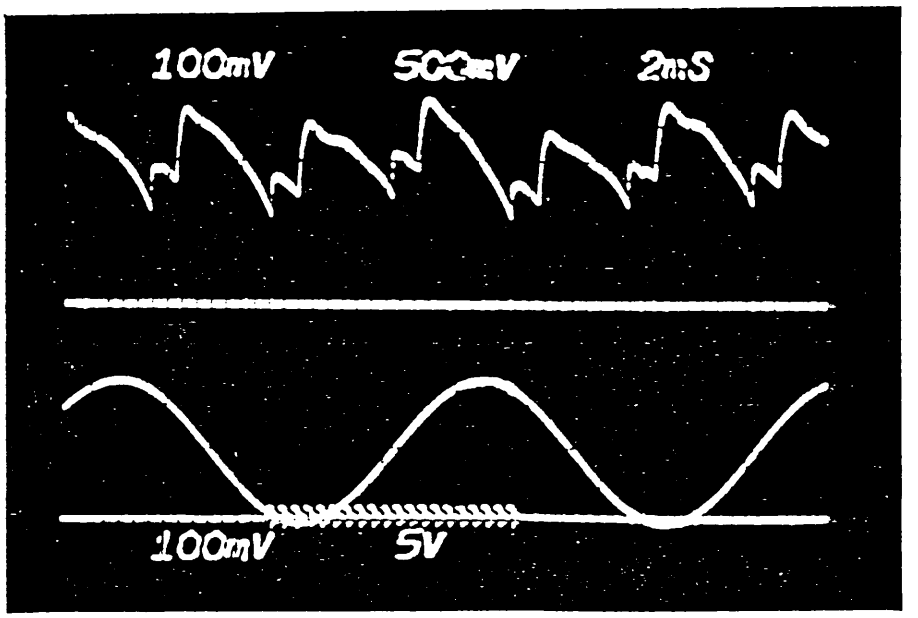

without m. s.

Fig. 5.9 - PRACTICAL EXAMPLE OF A.C.-SIDE 2nd HARMONIC MINIMIZATION BY A 150Hz M.S.

(a) D.c. Voltage Ripple
(b) Modulating Signal (150Hz)
(c) Negative Sequence 2nd Harmonic
(d) Firing Pulse to Valve 1

blocked by YY-transformers[11,12]. However, as shown in reference [13], the a.c.-side 150Hz is mostly dependent on the relative 3rd harmonic current distribution through the secondary windings. For this reason, the 3rd harmonic may not be very sensitive to a 100Hz m.s. amplitude although sensitive to the m.s. phase or vice-versa, as can be observed on the Fourier analysis plots presented in Figs 5.10 and 5.11 (for $\phi_k = 180°$). This fact diminishes the possibility of 3rd harmonic minimization by a 100Hz m.s. . However, this modulating signal may still be useful for other situations such as :

a) 3-phase third harmonic minimization when a specific primary current distribution for which there is some ϕ_k such that the 3rd harmonic produced by the converter can oppose the 3rd harmonic already existing in the converter busbar;

b) Amplitude equalization in the three phases by redistribution of the harmonic levels.

A practical example of amplitude equalization is presented in the Fig. 5.12. The m.s. phase is set to $\phi_k \cong 324°$ ($V_m = 0.4$ Volts) for which an equivalent 3rd harmonic amplitude is obtained for the three phases (Fig. 5.12(a)). The m.s. amplitude was varied from 0.0 to 0.2 Volts and plotted with the third harmonic in Fig. 5.12(b). For $V_m = 0.12$ Volts, the 3rd, harmonic relative phase and amplitude were, for phases "a", "b" and "c", respectively :

$$V_{3a} = 0.26\underline{/0°}$$
$$V_{3b} = 0.23\underline{/266.4}$$
$$V_{3c} = 0.26\underline{/302.4} \quad .$$

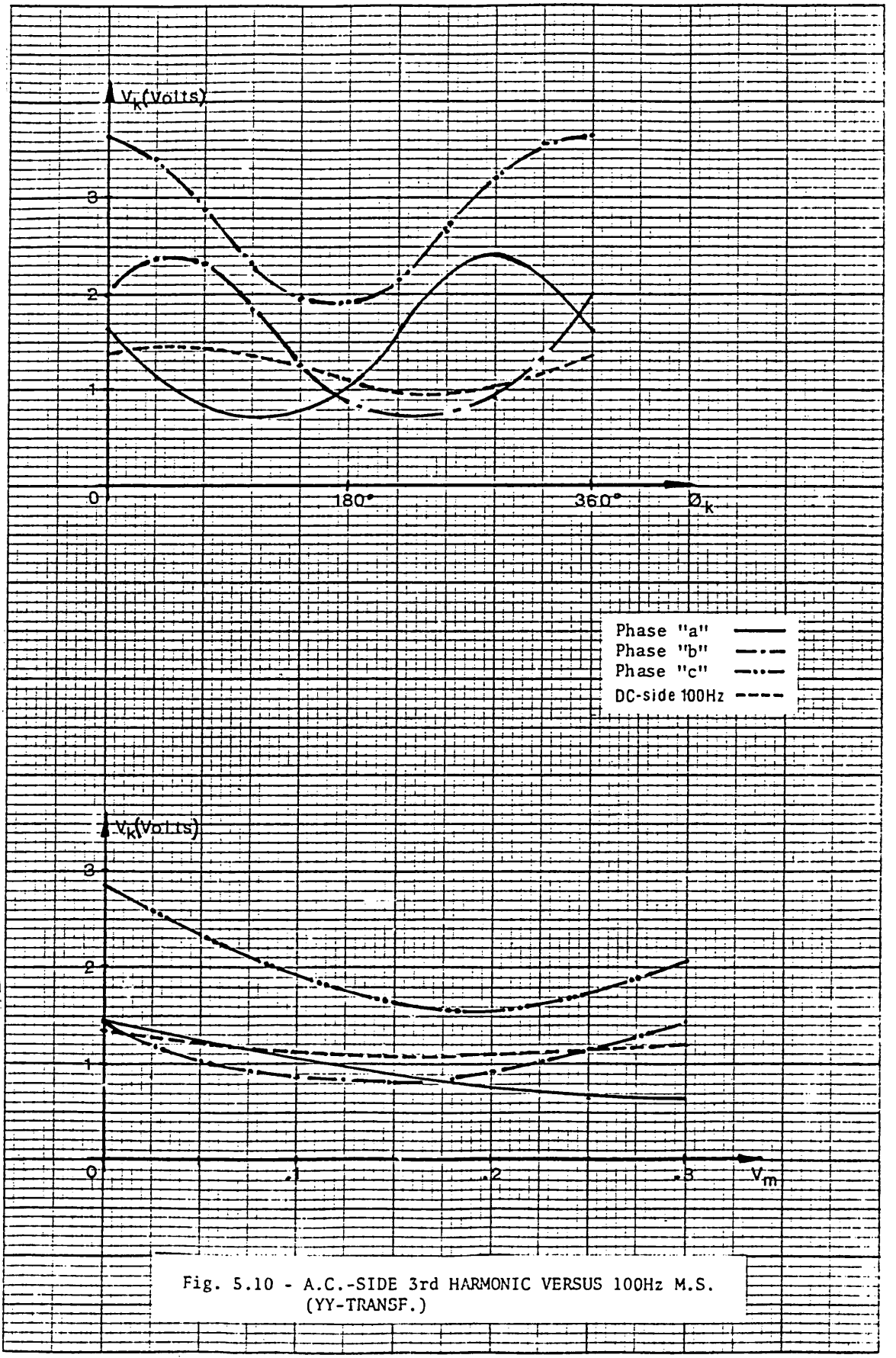

Fig. 5.10 - A.C.-SIDE 3rd HARMONIC VERSUS 100Hz M.S.
(YY-TRANSF.)

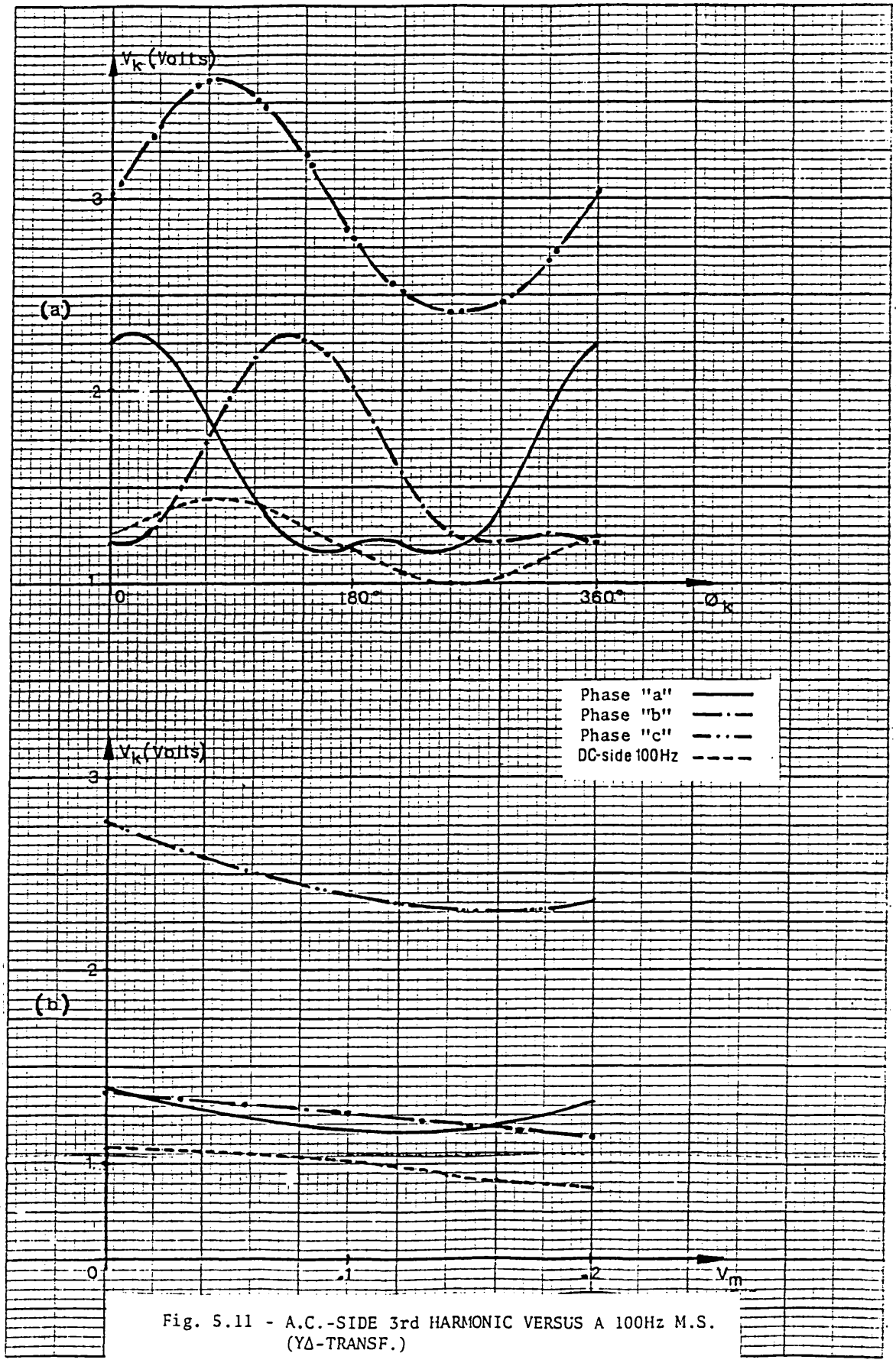

Fig. 5.11 - A.C.-SIDE 3rd HARMONIC VERSUS A 100Hz M.S. (YΔ-TRANSF.)

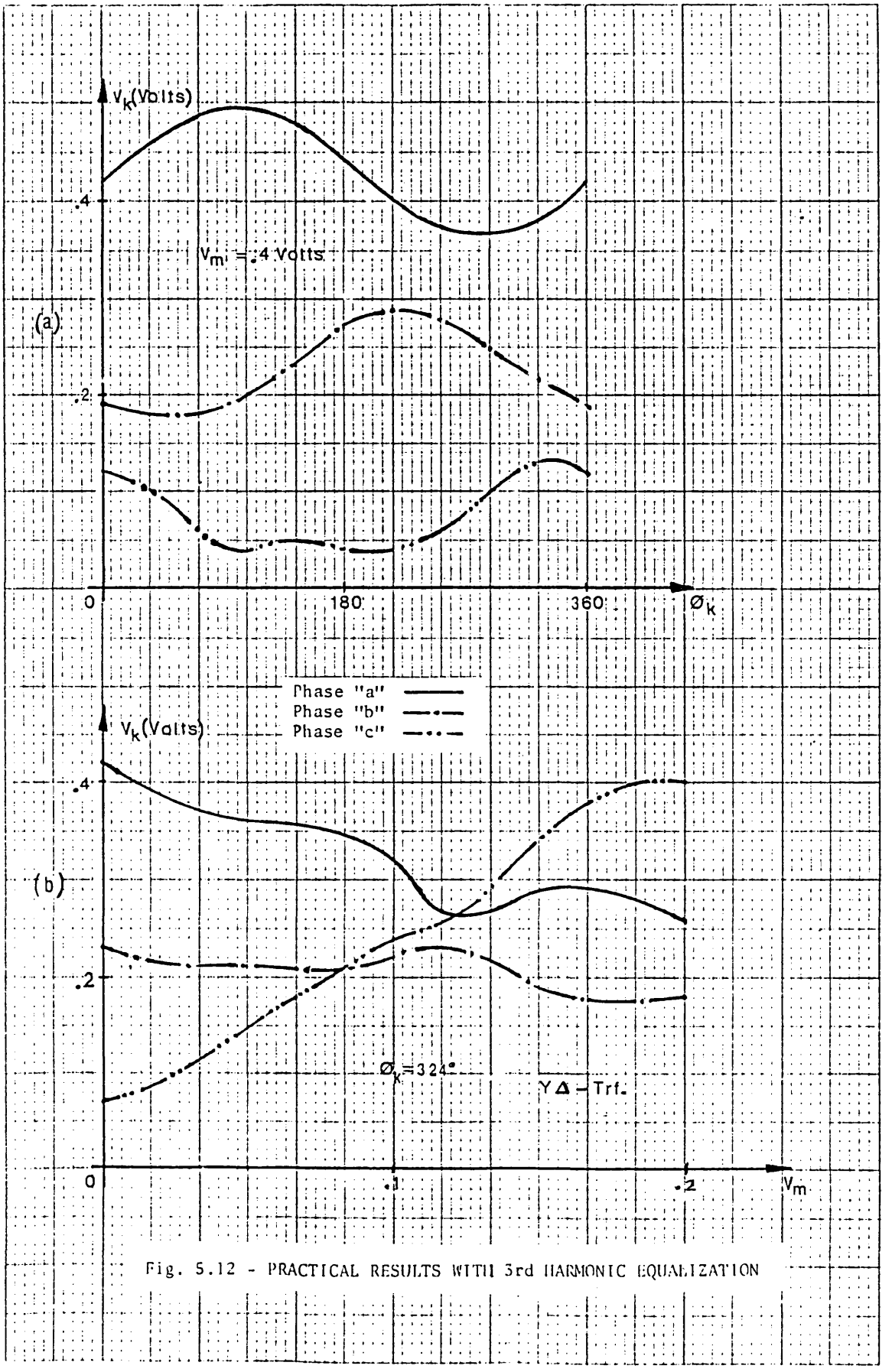

Fig. 5.12 - PRACTICAL RESULTS WITH 3rd HARMONIC EQUALIZATION

An appreciable reduction of the high level of 3rd harmonic in phase "a" was thus achieved at the expense of a moderate increase in phase "c" harmonic level. It can be considered that under certain circumstances of imbalanced third harmonic presence in the a.c. supply, m.s. injection could equalize the harmonic levels.

5.6 Example of m.s. locking onto an a.c.-side harmonic

The example described in this section shows that the m.s. adjusts itself to compensate variations in the harmonic source. A 50Hz m.s. is used to minimize an a.c.-side second harmonic of positive sequence. The d.c. simulator was set up as described in Table 5.1. The results presented in Table 5.3(a) are for no m.s. and a 2nd harmonic level about 5.47% of the fundamental. With m.s. optimally adjusted, the second harmonic of the positive sequence was reduced to about 1.68% as shown in Table 5.3(b). A general amplitude reduction in several other a.c.-side harmonics is also noticed although there is a slight overall increase on the d.c.-side harmonics. The m.s. amplitude for this case is V_m = 0.12 Volts.

Table 5.4(a) shows the Fourier analysis result with a reduction of 44.7% in the 2nd harmonic level. The m.s. loop was subsequently energized without modifying its setting, and it was noted that the m.s. amplitude was $V_m \cong 0.03$ Volts. Fourier analysis for this case is presented in Table 5.4(b) where it can be seen that the 2nd harmonic of positive sequence is still attenuated.

M00H060

HARM. ORDER	SEQ. POS. AMPLITUDE	ANGLE	SEQ. NEG. AMPLITUDE	ANGLE	SEQ. ZERO AMPLITUDE	ANGLE
1	102.8692	-.4627	.4304	-34.7253	3.3946	161.5221
2	5.4691	86.3738	.7236	166.3064	.1224	-31.2273
3	1.6775	-176.4160	1.3461	-150.6948	1.0211	178.7376
4	.5531	36.4679	.4925	53.1683	.2399	177.9361
5	.4809	-141.2732	.4495	50.0025	.7183	4.5513
6	.6825	50.3478	.6711	138.6076	.1413	-55 5342
7	.5922	20.7810	.2886	-47.0679	.3855	-139.9781
8	.2975	156.5488	.0557	97.6882	.0848	-172.7531
9	.3884	-74.7343	.2133	25.2246	.1884	15.0175
10	.1760	92.3610	.1832	171.6095	.1053	-98.9534
11	.2604	-41.8001	.3750	-41.4057	.1531	136.2949
12	.1692	80.1394	.1661	152.8818	.0509	-44.5686
13	.4188	-63.1041	.0668	21.7422	.0782	-52.9768
14	.1229	-173.4039	.2032	-131.1472	.0419	-35.3396
15	.1171	48.3867	.1260	66.3793	.1593	106.2272

D.C.-SIDE HARMONIC VOLTAGES

FOURIER COMPONENTS

	AMPLITUDE	PHASE
1	.7045	195.58
2	.2047	277.50
3	.1629	134.73
4	.1091	123.31
5	.1131	342.03
6	.8446	210.44
7	.1587	260.80
8	.0496	43.67
9	.0159	313.00
10	.0692	4.86
11	.0797	166.67
12	.1852	59.68
13	.0172	18.58
14	.0108	177.68
15	.0224	354.41

DC COMPONENT = 70.4000

TABLE 5.3(a) - A.C.-SIDE AND D.C.-SIDE FOURIER ANALYSIS WITHOUT M.S. (V_m = 0.0)

M11H060

HARM. ORDER	SEQ. POS. AMPLITUDE	ANGLE	SEQ. NEG. AMPLITUDE	ANGLE	SEQ. ZERO AMPLITUDE	ANGLE
1	101.8194	-1.3401	2.1152	12.1113	4.3187	153.3442
2	1.6842	106.9985	1.2011	-177.4137	.4124	36.8900
3	.3943	50.9418	1.2322	-171.9135	1.7221	150.1799
4	.6831	106.5403	.6761	-13.2282	.1293	69.9102
5	.5808	-173.8147	1.0178	49.3841	.8865	-26.0570
6	.9899	6.4455	.7733	153.2064	.1400	-102.1322
7	1.0850	22.9023	.1126	166.1964	.4036	-141.5512
8	.6614	-143.7984	.2755	-87.6151	.1341	43.6628
9	.1650	-179.5470	.3581	10.3014	.2430	-44.0297
10	.2750	-71.4456	.1612	-73.7772	.2027	-60.8487
11	.3295	-15.0247	.2811	-88.1766	.1150	21.4764
12	.1258	-8.1811	.1097	-139.8997	.0505	35.8898
13	.5663	-118.9689	.1417	-28.9948	.2456	-123.3561
14	.1231	-134.9814	.0866	94.0425	.1975	-117.1675
15	.0758	7.0944	.1378	-169.3889	.0818	-1.3274

D.C.-SIDE HARMONIC VOLTAGES

FOURIER COMPONENTS

	AMPLITUDE	PHASE
1	.7983	171.97
2	.2101	280.13
3	.3388	144.68
4	.1122	57.67
5	.1163	263.58
6	.9416	198.54
7	.0709	23.10
8	.0298	198.22
9	.0465	1.11
10	.0228	221.30
11	.1027	129.31
12	.1983	26.55
13	.0237	316.35
14	.0154	251.13
15	.0333	51.13

DC COMPONENT = 70.4000

TABLE 5.3(b) - A.C.-SIDE AND D.C.-SIDE FOURIER ANALYSIS WITH M.S. (V_m = 0.12 Volts)

SYMMETRICAL COMPONENTS

HARM. ORDER	SEQ. POS. AMPLITUDE	SEQ. POS. ANGLE	SEQ. NEG. AMPLITUDE	SEQ. NEG. ANGLE	SEQ. ZERO AMPLITUDE	SEQ. ZERO ANGLE
1	101.8660	-1.1387	1.5468	34.4340	3.3266	159.7824
2	3.0245	105.3405	1.0332	175.9802	.0929	-135.4355
3	1.0115	124.6137	.6634	-140.0708	1.4591	147.7619
4	.3911	16.6836	.2985	-55.5138	.0566	53.1938
5	.1827	-22.3964	.4799	80.0871	.7170	-2.3723
6	.1695	-25.8176	.5217	164.1423	.0949	-70.5303
7	.4410	20.7461	.1208	104.4003	.3435	-138.1550
8	.5266	-173.4906	.1916	34.3612	.0250	-77.7035
9	.1959	87.0694	.3648	44.1737	.1235	-171.0494
10	.2392	57.9732	.2629	-49.7052	.0236	17.5564
11	.3187	7.3400	.3576	-64.6177	.0337	98.9774
12	.2400	-35.2922	.1222	-166.7872	.0839	-13.8116
13	.5038	-93.5229	.1191	175.2063	.1823	-79.9673
14	.0226	87.1220	.0953	105.8566	.0618	16.3449
15	.0556	-175.2156	.1834	39.9449	.0526	-79.5568

D.C.-SIDE HARMONIC VOLTAGES

FOURIER COMPONENTS

	AMPLITUDE	PHASE
1	.4538	176.48
2	.2136	274.67
3	.2831	122.17
4	.0485	79.35
5	.1314	299.50
6	.8555	205.16
7	.1276	296.05
8	.0298	229.94
9	.0325	309.79
10	.0271	195.08
11	.0834	125.76
12	.1719	50.74
13	.0392	141.14
14	.0391	37.64
15	.0574	276.56

DC COMPONENT = 70.4000

TABLE 5.4(a) - A.C.-SIDE AND D.C.-SIDE FOURIER ANALYSIS WITH LOWER A.C.-SIDE 2nd HARMONIC LEVEL WITHOUT M.S. (V_m = 0.0)

M03H020

SYMMETRICAL COMPONENTS

HARM. ORDER	SEQ. POS. AMPLITUDE	SEQ. POS. ANGLE	SEQ. NEG. AMPLITUDE	SEQ. NEG. ANGLE	SEQ. ZERO AMPLITUDE	SEQ. ZERO ANGLE
1	102.6453	-.7732	.8385	-41.1034	3.7983	149.3507
2	1.4343	172.3152	1.3935	-131.8895	.0835	42.0759
3	1.2896	-144.7391	.6091	-132.4763	2.0480	139.7527
4	.6632	-79.3747	.6122	18.4040	.1343	-10.2912
5	.3616	-29.9920	.9801	60.1299	.8566	-18.2512
6	.6136	24.6422	.3023	127.7171	.2645	173.4623
7	.9619	33.3730	.2532	54.0468	.5055	-153.0619
8	.2198	-140.7254	.1350	148.0400	.1120	69.1789
9	.2210	62.0662	.2575	119.6288	.1226	-142.7445
10	.2520	135.6143	.2051	-104.3584	.0535	-159.2974
11	.0884	-169.7131	.3298	-80.7366	.0877	109.8510
12	.1090	-153.9783	.1918	-152.5632	.0203	-47.8987
13	.4916	-101.5096	.1875	-60.7524	.1791	-63.7008
14	.0639	-147.2024	.0951	22.1170	.0347	115.7088
15	.0549	-45.5106	.1572	15.4111	.0756	29.7121

D.C.-SIDE HARMONIC VOLTAGES

FOURIER COMPONENTS

	AMPLITUDE	PHASE
1	.4949	162.97
2	.1662	293.23
3	.4261	134.98
4	.0995	116.88
5	.1012	279.30
6	.8820	205.24
7	.0794	33.54
8	.0481	40.00
9	.0149	313.75
10	.0277	33.63
11	.0582	117.84
12	.1722	49.52
13	.0585	274.04
14	.0591	273.05
15	.0581	235.23

DC COMPONENT = 70.4000

TABLE 5.4(b) - A.C.-SIDE AND D.C.-SIDE FOURIER ANALYSIS WITh LOWER A.C.-SIDE 2nd HARMONIC LEVEL WITH M.S. (V_m = 0.03 Volts)

The following factors should be kept in mind when assessing these test results:

1) The IC-d.c. simulator is supplied from the laboratory mains whose harmonic content changes from instant to instant according to the vagaries of the other laboratory experimenters. To minimize such extraneous effects some tests were performed at night. In any case there was no guarantee that the a.c. system conditions for the successive test were identical;

2) The second harmonic generator used does not provide a pure sinusoidal output therefore the level of other harmonics may be affected by the output level of the generator;

3) The Fourier analysis is based on data sampled within one 50Hz cycle only, therefore spurious noise could affect the results;

4) No lowpass filters were used to reduced the effect of high on low frequency orders ("foldover effect").

5.7 Conclusions

It was confirmed experimentally that, within limits the a.c.-side harmonics are related in phase and amplitude to the m.s. and that there is a frequency relation between a.c.-side and d.c.-side harmonics of specific orders and phase sequence. These conclusions were used to establish a harmonic minimization method based on control voltage

modulation.

Injection of a selected m.s. onto the control voltage can minimize specific a.c.-side harmonic voltages without appreciably increasing other harmonics. The m.s. selection is based on the phase sequence and order of the a.c.-side harmonic to be minimized. As the d.c. current ripple is related to the a.c.-side harmonics, the m.s. adjusts itself in phase and amplitude to compensate any steady-state changes in the a.c. system condition so that the selected a.c.-side harmonic is still attenuated.

Third harmonics are not amenable to suppression through m.s. because of the blocking properties of ungrounded transformer secondaries.

Nevertheless, it is possible to obtain a more balanced distribution of harmonic voltages in the three phases.

CHAPTER 6

CONCLUSIONS

6.1 Conclusions

The constant current closed-loop control invariably used in the rectifying converter in h.v.d.c. links, leads to a number of topics examined in this thesis, namely:

1) System stability;
2) Selection and adjustment of an appropriate m.s. for the purpose of uncharacteristic harmonic minimization;
3) m.s. locking mechanism related to the minimized a.c.-side harmonic.

The first topic was dealt with in Chapter 2 where a non-linear technique for stability analysis based on the describing function technique (d.f.) was used for the study of oscillations synchronized with the a.c. system voltage. The d.f. was defined for a particular frequency as the complex ratio of the output d.c.-side harmonic to the input control voltage harmonic. The condition for a limit cycle oscillation was obtained for a particular control gain and frequency from the intersection of the control linear locus, $G(jw)$, with the non-linear locus, $-1/N(x,w)$. As a consequence, modification of the d.f. locus according to a.c.-side and/or d.c.-side conditions, assume a particular importance as they affect stability margins. Studies of such conditions led to some interesting observations on converter d.f.'s.

It was established that d.f. for both, 6- or 12-pulse converters under similar operating conditions exhibit only slight differences. It was established that the most important cause of variations on the d.f. locus are the d.c.-side and a.c.-side conditions of resonance and antiresonance. The d.c.-line input impedance has the most pronounced effects.

Continuity of the d.f. loci is limited by a maximum m.s. amplitude defined by K/k, where K is the ramp slope of the sawtooth voltage generator and k is the m.s. harmonic order.

Periodicity of the d.f. was established for balanced a.c.-systems. This fact allows appreciable reduction on the lengthy d.f. computation time which, in some cases, could be reduced to less than 10% of the original computing time.

Possibility of decomposition of the d.f. into three vectors was surmised from the d.f. studies and from theoretical studies of m.s. injection on the control voltage. Such a decomposition is based on the approximate independence of effects on the d.c.-line harmonic currents caused by :

1) Harmonics on the a.c. system
2) m.s. imposed on the control voltage.

Another less important cause of d.f. locus distortion is transformer saturation. The d.c. current through the secondary winding of the converter transformer alters the d.f. locus especially when the m.s. is 50Hz. The alterations are proportional to the secondary winding d.c.-level. In general, transformer saturation has negligible effects on the d.f. loci for m.s. frequencies of order

higher than one when compared with other causes, e.g. the presence of a negative sequence 100Hz on the supply.

The second topic of control voltage modulation is related to selection and adjustment of the m.s. . With this in mind, the incremental analysis of uncharacteristic harmonics in d.c. converters due to control voltage modulation was carried out. In this study, it was found that the magnitude and phase of a.c.-side and d.c.-side uncharacteristic harmonic voltages are, within limits, proportionally related to the m.s. amplitude and phase. On the a.c.-side, a 50Hz m.s. gives rise to second harmonic of positive sequence; a 100Hz m.s. causes triplen harmonics only; and a 150Hz m.s. causes second harmonic of negative sequence. In particular, a phase shift on the a.c.-side second harmonic current corresponds to a half of the phase shift of the d.c.-side 50Hz harmonic, irrespective of whether this is caused by control voltage modulation or distortion on the a.c. busbar voltage. It was also shown that imbalances on the fundamental, cause a second harmonic on the d.c.-side which is the result of the rectification of a fundamental imbalance.

On the d.c.-side, the lowest uncharacteristic harmonic caused by a m.s. corresponds to that of the m.s. frequency. The d.c.-side harmonics are nearly proportional to the amplitude of the harmonics present on the a.c.-side even under open loop control.

In a 12-pulse converter, a m.s. in the control voltage causes uncharacteristic harmonic currents through the secondary of the YΔ-transformer which are shifted by approximately 30° with respect to the uncharacteristic harmonics of the same frequency through secondary of the YY-transformer. The approximate total primary phase shift between YY- and YΔ-transformers is given by 90q,

where "q" is related to the harmonic order.

Locking of the m.s. onto the a.c.-side harmonic to be minimized can be made through the current closed loop control. The approximate linear relationships between m.s. and uncharacteristic harmonics have shown that the d.c. voltage ripple is mostly dependent on the control voltage ripple. Therefore, the approximate m.s. can be obtained from the control voltage ripple. The m.s. amplitude and phase has to be adjusted for optimal reduction of the selected harmonic.

All practical tests were carried out using an injection circuit capable of selecting, adjusting and injecting the locked m.s. into the control voltage. Time constant of the control was modifiable by bypassing the large time constant of the injection circuit through a transient detector. This device inhibits the m.s. injection during transients and restores the control time constant to its conventional value.

6.2 Original Contributions

The author believes that the following contributions are original :

1) Extension of a computer program to obtain the describing function of 12-pulse converters;

2) Describing function studies of 6- and 12 - pulse converters with transformer saturation;

3) Studies of the properties of converter d.f.'s with the view of reducing the time of computer program to evaluate the d.f.'s;

4) Analytical prediction of the firing pulse instants when the control voltage is subject to a modulating signal;

5) Incremental analysis of the effects of a m.s. on the a.c.-side and d.c.-side harmonics;

6) Approximate relationships between m.s. and uncharacteristic harmonics with regard to an a.c.-side harmonic minimization method based on control voltage modulation;

7) Implementation of circuitry to select, adjust and inject a m.s. into the control voltage so that the m.s. is kept locked to the d.c.-side current. A transient detector modifies the control time constant during transients;

8) Test results of a harmonic minimization method using closed loop injection of a m.s. into the control voltage.

6.3 Suggestions for further work

1) Optimized computer program to obtain the d.f. using an approximate vectorial representation;

2) Stability analysis of an optimal injection circuit;

3) Digital injection circuit using the software flexibility of microcomputers. This flexibility should allow several combination of $\Delta\alpha$ modulations;

4) Use of m.s. frequencies of higher orders especially with 12-pulse converters;

5) Optimization of the harmonic injection circuit by using non-sinusoidal m.s.'s, e.g. square waves;

6) Automatic selection of the m.s. frequency, amplitude and phase to be always suppressing the most predominant harmonics on the a.c.-side.

REFERENCES

1. J.M.D. Ferreira de Jesus, "D.C. transmission system harmonic analysis and stability using describing functions", Ph.D. thesis, University of London, 1982.

2. E.W. Kimbark, "Direct Current Transmission - Vol I", Book, Wiley Interscience, 1971.

3. J.C. de Oliveira, "Multiple converter harmonic calculations with non-ideal conditions", Ph.D. Thesis, University of Manchester, Institute of Science and Technology, 1978.

4. J.D. Ainsworth, "The phase-locked oscillator - a new control method for controlled static converters", IEEE Trans., Vol PAS-87, pp. 857-865, 1968.

5. A.B. Turner, "Modelling techniques for the study of h.v.d.c. infeeds to weak a.c. systems", IEEE PAS-100, No. 7, July 1981.

6. E. Ullman, "Power Transmission by Direct Current", Book, Springer-Verlag, Berlin/Heidelberg, 1975.

7. J.P. Sucena Paiva, R. Hernandez and L.L. Freris, "Stability study of controlled rectifiers using a new discrete model", Proc. IEE, Vol. 119, No. 9, pp.1285-1293, Sept. 1972.

8. R. Hernandez Millan, J.P. Sucena Paiva and L.L. Freris, "Modelling of controlled rectifiers in feedback systems", IEEE Transactions, Vol. PAS-93, pp. 167-175, Jan/Feb. 1974.

9. J. Arrillaga, "Harmonic Elimination", paper, Power Systems Engineering Series 81, U.M.I.S.T., Manchester, pp. 37-75, Sept. 1981.

10. A. Gelb, W.E. Vander Velde, "Multiple-input Describing Functions and Nonlinear System Design, McGraw-Hill, 1968

11. O.I. Elgerd, "Electric Energy System Theory:An Introduction", Book, TATA-McGraw-Hill Publishing Co. Ltd., 1971.

12. L. Gyu yi, E.R. Taylor, Jr., "Characteristic of static thyristor-controlled shunt compensators for power transmission system applications", IEEE-PES Winter Meeting, New York, N.Y. Feb. 3-8, 1980.

13. A.B. Gieswer, J. Arrilaga, "Behaviour of h.v.d.c. links under unbalanced a.c.-fault conditions", Proc. IEE, Vol. 119, No.2, Feb. 1972.

14. P.G. Kendall, "Harmonic in Power Systems", Power System Engineering Series, U.M.I.S.T., Manchester, pp. 2-14, Sept. 1981.

15. J.A. Orr, A.E. Emanuel, "Harmonic sources and effects on Communications",An International Conference on harmonic in Power Systems, Paper, U.M.I.S.T., Manchester, Sept. 1981.

16. H. Sasaki, T. Machida, "A new method to eliminate a.c. harmonics currents by magnetic flux compensation - consideration on basic design", IEEE - Winter Power Meeting, N.Y. pp. 2009-2019, Jan/Feb 1971. (April 1971- PAS 90).

17. B.M. Bird , J.F. Marsh, P.R. McLellan, "Harmonic reduction in multiple converters by triple-frequency current injection", Proc. IEE, Vol. 116, No. 10, 1969.

18. A. Ametani, "Generalized method harmonic reduction in a.c.-d.c. converters by harmonic current injection", Proc. IEE, Vol. 119, No. 7. 1972.

19. J.F. Baird and J. Arrillaga, "Harmonic reduction in d.c.-ripple reinjection, Proc. IEE, Vol. 127, Pt. C., No. 5, Sept. 1980.

20. L.L. Freris and J. Nunes de Carvalho, "An electromechanical harmonic filter", IEE Conference Publication 107, 1973.

21. N. Mohan et al, "Active filters for a.c. harmonic suppression", Trans. IEEE Winter Power Meeting, 1977.

22. S.A. Mahmoud, M. El-Harony, "Reduction of a.c. harmonics in thyristor power converter using injection technique", UPEC-18

23. P. Mehta, T. Thomas, A.J. Fernandes, "Switched-capacitor technique for elimination of harmonics in power electronics equipment", UPEC-18, 1983.

24. M.E. Masoud, "Reduction of harmonics generated by reactive power static compensator in electrical power system", UPEC-19, Universites Power Engineering Conference-19, Universities of Aberdeen and Dundee, Apr. 1984.

25. D.G.T. Lewis, W.M. Ritchie, B. Hall, "The reduction of harmonic pollution and application of power factor correction", UPEC 19, Universities Power Engineering Conference 19, Universities of Aberdeen and Dundee, Apr. 1984.

26. A.E. Emanuel, N. Harish Chandra, E.M. Gulachenski, "Thyristorized harmonics cancellation device", IEE Power Engineering Society, PES, Winter Meeting, N.Y., Feb. 1979.

27. J.D. Ainsworth, "Harmonic instability between controlled static converters and a.c. networks", Proc. IEE, Vol. 114, No. 7, July 1967.

28. J.D. Ainsworth, "The phased-locked oscillator - a new control system for controlled static converters", IEEE PAS-87, No.3, pp. 859-865, Mar. 1968.

29. F. Busemann, "h.v.d.c. transmission hunting of rectifiers with marked compounding", ERA Report, No. B/T104, 1951.

30. F. Busemann, "The theory of the control problem of h.v.d.c. transmission with rectifiers and invertors in bridge circuit", ERA Report, No. 7/T74, 1948.

31. N.A. Bjaresten, "The static converter as a high-speed power amplifier", Direct Current, Vol. 8, pp. 154-165, 1963.

32. F. Fallside, A.R. Farmer, "Ripple instability on closed loop control system with thyristor amplifiers", Proc. IEE, Vol. 114, pp. 139-152, 1967.

33. F. Fallside, C.J. Goodman and R.D. Jackson, "Stability of order sampling and thyristor systems", Electrical Letters, Vol. 50, pp. 566-567, 1969.

34. J.P. Sucena Paiva and L.L. Freris, "Stability of a d.c. transmission between a.c. system", Proc. IEE, Vol. 121, No. 6, pp. 515, Jun. 1974.

35. D.J. Pileggi, A.E. Emanuel, "Field experience with overcurrent relay tripping caused by parallel resonance at the fourth harmonic", An International Conference on Harmonic in Power System, U.M.I.S.T., Manchester, Sept. 1981.

36. J.P. Sucena Paiva, "A steady state stability study of converters and high voltage a.c. transmission systems", Ph.D. Thesis, University of London, 1972.

37. J.D. Ainsworth, "Non-characteristic frequencies in a.c./d.c. converters", Power Systems Engineering series, International Conference on Harmonics in Power Systems, pp. 76-84, Sept. 1981.

38. M.A. Slonin et al, "Steady-state stability of controlled rectifiers", IEEE IA582-196, pp. 388-393, 1982.

39. C.R. Fitton et al, "Analysis of a h.v.d.c. transmission link with finite resistance and inductance values, "Loughborough, University of Technology, England, UPEC-18, 1983.

40. E. Lekatsas, G. Georcantzis, "Problem in the determination of the specification for an h.v.d.c. back-to-back converter station", Mediteranean Electromechanical Conference, Proc. Vol. I, Edited by E.N. Protonotarios et al, May 1983.

41. K.W. Kanngiesser et al, "Commissioning of the Cabora Bassa-Appollo h.v.d.c. scheme", CICRE paper 14-13, 1978.

42. J.G. Graeme, G.E. Tobey, L.P. Huelsman, "Operational Amplifiers, Design and Applications", Book, McGraw-Hill Kogakisha Ltd., 1971.

43. P. Mehta, T. Thompson, C. Murouchoso, "Harmonic elimination by current injection using switched capacitor technique", paper, an International Conference on Harmonics in Power Systems, U.M.I.S.T., Manchester, Sept. 1981.

44. LABORELEC, "Comparison between recommendations in various countries for the connection of industrial equipment generating harmonics", Translation of original french report LABORELEC" Section 1-AR/1300/802, Dec. 1979.

45. R.M. Mathur, A.M. Sharp, "Harmonics on the d.c.-side in h.v.d.c. conversion", IEEE, PAS-96, No. 5, Sept/Oct. 1977.

46. A.C. Williamson, "The effects of system harmonics upon machines", International C nference on Harmonics in Power Systems", U.M.I.S.T., Manchester, pp. 85-101, Sept. 1981.

47. J. Reeve, "Harmonic d.c. line voltage arising from h.v.d.c. power converters", IEEE, PAD-89, No. 7, pp. 1679-1627, Sept/ Oct. 1970.

48. B. Delfino et al, "A contribution to the evaluation of converter harmonics in Power Systems", UPEC 14, Universites Power Engineering Conference, Universities of Aberdeen and Dundee, April, 1984.

49. R. Jötten et al, "Control in h.v.d.c. systems", CIGRÉ, Conference on Power Systems paper 14-10, 1978.

50. J. Arrillaga, "Harmonics monitoring", International Conference on Harmonics in Power Systems", U.M.I.S.T., Manchester, pp. 159-174, Sept. 1981.

51. R.H. Kitchin, "Computer simulation of resonance effects in power systems with a.c./d.c. converters". IEE, International Conference on Thyristor and Variable Static Equipment for a.c. and d.c. Transmission", London, Nov/Dec, 1981.

52. G.L. Brewer et al, "Harmonic filters for the 2000 MW cross channel line", IEE, International Conference on Thyristor and variable static equipment for a.c. and d.c. transmission, London, Nov/Oct 1981.

53. C.A.O. Peixoto et al, "Engineering studies for Itaipu converter station design ", IEE, International Conference on Thyristor and Variable Static Equipment for a.c. and d.c. Transmission", London, Nov/Dec. 1981.

54. A.E. Emanuel, "The need for standards limiting power system disturbance caused by phase-burst modulation control", paper, An International Conference on Harmonic in Power Systems, U.M.I.S.T. , Manchester, Sept. 1981.

55. S.A. Morais et al, "Harmonic current calculations for the ITAIPU h.v.d.c. transmission system", paper, An International conference on Harmonic in Power System, U.M.I.S.T., Manchester, Sept. 1981.

56. T. Sakurai et al, "A study of a certain a.c. oscillation of h.v.d.c. system", paper A79-100-9, IEEE Power Engineering Society Winter Meeting, New York, Feb. 1979.

APPENDIX A

A.1 Definition of Short-Circuit Ratio (SCR)

Fig. A.1 is the Thevenin's equivalent of an a.c. source, V_{ϕ} :

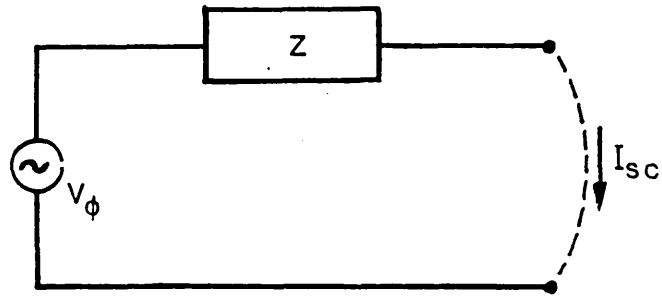

Fig. A.1 - Thevenin's Equivalent

The short-circuit of this equivalent is given by

$$I_{sc} = \frac{V_{\phi}}{Z} \qquad (A.1)$$

For this current, the power supplied by the source is given by:

$$P_{\phi} = \frac{V_{\phi}^2}{Z} \; . \qquad (A.2)$$

The short-circuit power, P_{ϕ}, is known as short-circuit capacity (SCC).

In the case of a 3-phase balanced source, the S.C.C. is given by:

$$SCC = 3P_{\phi} = P_{3\phi} \quad . \tag{A.3}$$

In h.v.d.c., short-circuit ratio (SCR) is defined as :

$$SCR = \frac{SCC}{P_{dc}} \tag{A.4}$$

where P_{dc} is the d.c. power.

Without losses [2] :

$$P_{dc} = P_{ac} \tag{A.5}$$

where P_{ac} is the 3-phase active power.

An a.c. system is strong if SCR > 3, otherwise, it is considered a weak system.

Eqns A.2 to A.5 can be combined to give :

$$SCR = \frac{3V_{\phi}^{2}}{ZP_{ac}} \quad . \tag{A.6}$$

In terms of line voltage ($V_{\phi} = V_{\ell}/\sqrt{3}$) eqn A.6 becomes:

$$SCR = \frac{V_{\ell}^{2}}{ZP_{ac}} \quad . \tag{A.7}$$

A.2 A.c. busbar harmonic voltage

From Fig. 2.12 (Chapter 2) ;

$$V_n = E_n - I_{sn} Z_{sn} \tag{A.8}$$

$$V_n = (I_{sn} - I_n) Z_{fn} \quad . \tag{A.9}$$

Replacing eqn A.8 in terms of I_{sn} into eqn A.9 results

$$V_n = \left(\frac{E_n - V_n}{Z_{sn}} - I_n \right) Z_{fn} \quad . \tag{A.10}$$

Isolating V_n in eqn A.10 yields

$$V_n = Z_n \left(\frac{E_n}{Z_{sn}} - I_n \right) \tag{A.11}$$

where

$$Z_n = \frac{Z_{sn} Z_{fn}}{Z_{sn} + Z_{fn}} \quad .$$

A.3 D.c. - side impedance

Fig. A.2 is a simplified representation of a converter model connected to the d.c.-line representation given in Fig. 2.14. The overall input of the circuit is :

$$Z_i = Z_1 + \frac{Z_2 (Z_1 + Z_3)}{Z_1 + Z_2 + Z_3} \quad . \tag{A.12}$$

Assuming that :

$$Z_1 = j\omega L_1$$

$$Z_2 = \frac{1}{j\omega C}$$

$$Z_3 = R_3 + j\omega L_3$$

eqn A.12 becomes

$$Z_i = \frac{R_3 - \omega^2 R_3 C L_1 + j(-\omega^3 L_1^2 C + 2\omega L_1 - \omega^3 C L_1 L_3 + \omega L_3)}{-\omega^2 C(L_1 + L_3) + 1 + j\omega C R_3} \qquad (A.13)$$

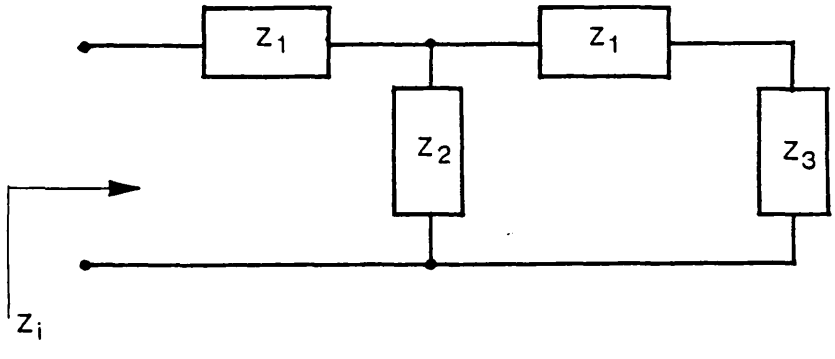

Z_1 = reactor + half d.c.-line series impedance

Z_2 = d.c.-line shunt impedance

Z_3 = inverter equiv. impedance

Fig. A.2 - d.c.-line impedance

If $R_3C \cong 0$ in eqn A.13, yields :

$$Z_1 = \frac{R_3 + j(-\omega^3 L_1^2 C + 2\omega L_1 - \omega^3 C L_1 L_3 + \omega L_3)}{1 - \omega^2 C(L_1+L_3)} \quad . \qquad (A.14)$$

A.2.1 Resonant frequency

From eqn A.14, the resonant frequency condition is given by :

$$-\omega^3 L_1^2 C + 2\omega L_1 - \omega^3 C L_1 L_3 + \omega L_3 = 0 \quad . \qquad (A.15)$$

Eqn A.15 can be rearranged as below

$$\omega(-\omega^2 L_1^2 C + 2L_1 - \omega^2 C L_1 L_3 + L_3) = 0 \quad . \qquad (A.16)$$

Solutions of eqn A.16 are

$$\omega_1 = 0$$

$$\omega_{2,3} = \pm \sqrt{\frac{(2L_1+L_3)}{L_1 C(L_1+L_3)}} = \pm\left(\frac{1}{C(L_1+L_3)} + \frac{1}{L_1 C}\right).$$

Eqn A.17 can be used to establish the resonant frequency, that is:

$$\omega_0 = \frac{1}{2\pi}\left(\frac{1}{C(L_1+L_3)} + \frac{1}{L_1 C}\right) \quad . \qquad (A.18)$$

A.2.2 Antisonant frequency

From eqn A.14 the antiresonant condition is established by :

$$1 - \omega_{\infty}^{2}C(L_1 + L_3) = 0 \ . \qquad (A.19)$$

Solution of eqn A.19 gives the antiresonant frequency :

$$\omega_{\infty} = \frac{1}{C(L_1+L_3)} = 2\pi f_{\infty} \ . \qquad (A.20)$$

If the reactance of the converter model at the receiving end is much smaller than d.c.-line impedance plus terminal reactors, then L_3 is negligible. In this case, eqns A.17 and A.20 can be given in terms of frequency, respectively, by :

$$f_0 = \frac{2}{\pi\sqrt{L_1 C}} \qquad (A.21)$$

$$f_{\infty} = f_0/2 \ . \qquad (A.22)$$

APPENDIX B

This appendix gives the most tedious demonstrations which are referred in Chapter 3.

B.1 Approximation of equation 3.30

The amplitude of equation 3.30 is given by:

$$I_{ck} = \frac{2I_{dc}}{k\pi} \sqrt{(\cos k\phi_s - \cos k\phi_d)^2 + \sin^2 k\phi_d} \quad . \qquad (B.1)$$

An approximation of equation B.1 for small values of k, $\Delta\alpha_1$ and $\Delta\alpha_2$ is obtained by:

$$\phi_d \cong 0 \qquad (B.2)$$

$$\sin k\phi_d \cong 0 \qquad (B.3)$$

$$\cos \phi_d \cong 1 \quad . \qquad (B.4)$$

Replacing in equation B.1 :

$$I_{ck} \cong \frac{2I_{dc}}{k\pi} \sqrt{(\cos k\phi_s - 1)^2} \quad . \qquad (B.5)$$

Term $\cos k\phi_s$ may be approximated by the first two terms of the cosine series :

$$\cos k\phi_s \cong 1 - \frac{(k\phi_s)^2}{2} \quad . \qquad (B.6)$$

Replacing B.6 in B.5 and simplifying, results :

$$I_{ck} \cong \frac{kI_{dc}}{2\pi} \phi_s^2 \quad . \tag{B.7}$$

By definition :

$$\phi_s = \frac{\Delta\alpha_1 + \Delta\alpha_2}{2}$$

which replaced in B.7 yields :

$$I_{ck} = \frac{kI_{dc}}{8\pi} (\Delta\alpha_1 + \Delta\alpha_2)^2 \quad . \tag{B.8}$$

The argument of eqn 3.32 is :

$$k\phi_c = TAN^{-1}\left\{\frac{\sin k\phi_d \cos k\phi_s}{1 - \cos k\phi_d \cos k\phi_s}\right\} \quad . \tag{B.9}$$

Replacing the approximations suggested by eqns B.2 to B.4, in B.9 results :

$$k\phi_c \cong 0 \quad . \tag{B.10}$$

B.2 Approximation of equation 3.31

The amplitude of eqn 3.31 is given by :

$$I_{ck} = -\frac{2I_{dc}}{k\pi} \sin k\phi_s \quad . \tag{B.11}$$

For small values of k, $\Delta\alpha_1$ and $\Delta\alpha_2$, the sine function in equation B.11 can be approximated by its arc value to give

$$I_{ck} \cong - \frac{2I_{dc}}{k\pi}(k\phi_s) \quad . \qquad (B.12)$$

Replacing ϕ_s and simplifying :

$$I_{ck} \cong \frac{I_{dc}}{\pi} (\Delta\alpha_1 + \Delta\alpha_2) \quad . \qquad (B.13)$$

The argument of eqn 3.29 is :

$$k\phi_d \cong 0 \ . \qquad (B.14)$$

B.3 Harmonic analysis of Phase "a" (50Hz m.s.)

Following the same procedure used in subsection 3.62, but now based on Table 3.5, the harmonic current of order "k" through phase "a" is given by :

$$i_{ak} = - \frac{2I_{dc}}{k\pi} \left[\sin \frac{k\Delta\alpha_1}{2} \cos k(\theta + 120 - \frac{\Delta\alpha_1}{2}) + \right.$$

$$\left. \sin \frac{k\Delta\alpha_2}{2} \cos k(\theta - 60 + \frac{\Delta\alpha_2}{2}) \right] \quad . \qquad (B.15)$$

Letting $\theta_1 = \theta + 120$ and using the identity

$$\cos(A \pm B) = \cos a \cos B \mp \sin A \sin B$$

eqn B.15 becomes :

$$i_{ak} = -\frac{2I_{dc}}{k\pi}\left[\sin\frac{k\Delta\alpha_1}{2}\left(\cos k\theta_1 \cos\frac{k\Delta\alpha_1}{2} + \sin k\theta_1 \sin k\frac{\Delta\alpha_1}{2}\right) + \right.$$

$$\left. \sin\frac{k\Delta\alpha_2}{2}\left(\cos k\theta_1 \cos k(\frac{\Delta\alpha_2}{2} - 180) - \sin k\theta_1 \sin k(\frac{\Delta\alpha_2}{2} - 180)\right)\right].$$

... (B.16)

Grouping together the terms containing $\sin k\theta_1$ and $\cos k\theta_1$ results

$$i_{ak} = -\frac{2I_{dc}}{k\pi}\left[\sin k\theta_1\left(\sin\frac{2k\Delta\alpha_1}{2} - \sin\frac{k\Delta\alpha_2}{2}\sin k(\frac{\Delta\alpha_2}{2} - 180)\right) + \right.$$

$$\left. \cos k\theta_1\left(\sin\frac{k\Delta\alpha_1}{2}\cos\frac{k\Delta\alpha_1}{2} + \sin k\frac{\Delta\alpha_2}{2}\cos k(\frac{\Delta\alpha_2}{2} - 180)\right)\right].$$

... (B.17)

Eqn B.17 can be further simplified if odd and even harmonics are considered separately.

a) Odd harmonics

For odd k's, equation B.17 becomes:

$$i_{ak} = -\frac{2I_{dc}}{k\pi}\left[\sin k\theta_1\left(\sin^2\left(\frac{k\Delta\alpha_1}{2}\right) + \sin^2\left(\frac{k\Delta\alpha_2}{2}\right)\right) + \right.$$

$$\left. \cos k\theta_1\left(\sin\frac{k\Delta\alpha_1}{2}\cos\frac{k\Delta\alpha_1}{2} - \sin\frac{k\Delta\alpha_2}{2}\cos\frac{k\Delta\alpha_2}{2}\right)\right].$$

... (B.18)

Equation B.18 can be written

$$i_{ak} = -\frac{2I_{dc}}{k\pi}\left[A \sin k\theta_1 \cos k\phi_a + A \cos k\theta_1 \sin k\phi_a\right]$$

... (B.19)

where:

$$A \sin k\phi_a = \sin \frac{k\Delta\alpha_1}{2} \cos \frac{k\Delta\alpha_1}{2} - \sin \frac{k\Delta\alpha_2}{2} \text{ as } \frac{k\Delta\alpha_2}{2}$$

$$A \cos k\phi_a = \sin^2 \left(\frac{k\Delta\alpha_1}{2}\right) + \sin^2 \left(\frac{k\Delta\alpha_2}{2}\right) .$$

From equation B.19 $k\phi_a$ is given by:

$$k\phi_a = \text{TAN}^{-1} \left(\frac{A \sin k\phi_a}{A \cos k\phi_a}\right) \qquad \text{(B.20)}$$

or

$$k\phi_a = \text{TAN}^{-1} \left(\frac{\sin \frac{k\Delta\alpha_1}{2} \cos \frac{k\Delta\alpha_1}{2} - \sin \frac{k\Delta\alpha_2}{2} \cos \frac{k\Delta\alpha_2}{2}}{\sin^2 \left(\frac{k\Delta\alpha_1}{2}\right) + \sin^2 \left(\frac{k\Delta\alpha_2}{2}\right)} \right)$$

... (B.21)

Using the trigonometric identities

$$\sin 2A = 2 \sin A \cos A$$

$$\sin A - \sin B = 2 \cos \tfrac{1}{2}(A+B) \sin \tfrac{1}{2}(A-B)$$

$$\sin^2 A = \tfrac{1}{2} - \tfrac{1}{2} \cos 2A$$

eqn A.21 becomes

$$k\phi_a = \text{TAN}^{-1} \left(\frac{\sin k\phi_d \cos k\phi_s}{1 - \cos k\phi_d \cos k\phi_s}\right) \qquad \text{(B.22)}$$

"A" in eqn B.19 can be determined from :

$$A^2 = \left[\sin \frac{k\Delta\alpha_1}{2} \cos \frac{k\Delta\alpha_1}{2} - \sin \frac{k\Delta\alpha_2}{2} \cos \frac{k\Delta\alpha_2}{2}\right]^2 +$$

$$\left[\sin^2\left(\frac{k\Delta\alpha_1}{2}\right) + \sin^2\left(\frac{k\Delta\alpha_2}{2}\right)\right]^2 . \qquad (B.23)$$

which after some trigonometric manipulations, becomes

$$A = \sqrt{(\cos k\phi_s - \cos k\phi_d)^2 + \sin^2 k\phi_d} \quad . \qquad (B.24)$$

Hence, replacing back $\theta_1 = \theta + 120$, the implicit form of equation B.19 becomes :

$$i_{ak} = I_{ak} \sin k(\theta + \phi_a + 120) \qquad (B.25)$$

where $k\phi_a$ is defined by eqn B.22 and I_{ak} is obtained by replacing eqn B.24 into equation B.19. The amplitude of equation B.25 is then :

$$I_{ak} = \frac{2I_{dc}}{k\pi} \sqrt{(\cos k\phi_s - \cos k\phi_d)^2 + \sin^2 k\phi_d} \quad . \qquad (B.26)$$

b) Even harmonics

For even k's, equation B.17 becomes

$$i_{ak} = -\frac{2I_{dc}}{k\pi}\left[\sin k\theta_1 \sin^2\left(\frac{k\Delta\alpha_1}{2}\right) - \sin^2\left(\frac{k\Delta\alpha_2}{2}\right)\right] +$$

$$\cos k\theta_1\left[\frac{\sin k\Delta\alpha_1 + \sin k\Delta\alpha_2}{2}\right] \quad . \qquad (B.27)$$

Equation B.27 can be put into a more compact form. Let

$$A \sin k\phi_a = \sin^2\left(\frac{k\Delta\alpha_1}{2}\right) - \sin^2\left(\frac{k\Delta\alpha_2}{2}\right) \qquad (B.28)$$

$$A \cos k\phi_a = \frac{\sin k\Delta\alpha_1 + \sin k\Delta\alpha_2}{2} \quad . \qquad (B.29)$$

The argument $k\phi_a$, can be obtained from the combination of equations B.28 and B.29

$$k\phi_a = \text{TAN}^{-1}\left[\frac{2\left(\sin\left(\frac{k\Delta\alpha_1}{2}\right) - \sin\left(\frac{k\Delta\alpha_2}{2}\right)\right)\left(\sin\left(\frac{k\Delta\alpha_1}{2}\right) + \sin\left(\frac{k\Delta\alpha_2}{2}\right)\right)}{\sin k\Delta\alpha_1 + \sin k\Delta\alpha_2}\right] \quad .$$

... (B.30)

After some trigonometric manipulations, eqn B.30 is simplified to:

$$k\phi_a = \text{TAN}^{-1}\left[\frac{\sin k\phi_d}{\cos k\phi_d}\right] \quad . \qquad (B.31)$$

From equation B.31

$$\phi_a = \phi_d \quad . \qquad (B.32)$$

The magnitude of A is also obtained from equations B.28 and B.29 by adding the square of these two equations and simplifying, that is :

$$A^2 = \sin^2\left(\frac{k\Delta\alpha_1}{2}\right) - \sin^2\left(\frac{k\Delta\alpha_2}{2}\right) + \left(\sin\frac{k\Delta\alpha_1}{2}\cos\frac{k\Delta\alpha_1}{2} + \cos\frac{k\Delta\alpha_2}{2}\sin\frac{k\Delta\alpha_2}{2}\right)^2 \quad . \qquad (B.33)$$

Taking into account that :

$$\sin^2 A = \tfrac{1}{2} - \tfrac{1}{2} \cos 2A$$

and

$$\sin 2A = 2 \sin A \cos A$$

equation B.33 can be simplified to:

$$A^2 = \left(\frac{\cos k\Delta\alpha_1 - \cos k\Delta\alpha_2}{2} \right)^2 + \left(\frac{\sin k\Delta\alpha_1 + \sin k\Delta a_2}{2} \right) \quad \ldots \quad (B.34)$$

Through trigonometric and algebraic manipulations eqn B.34 is reduced to

$$A = \sin k\phi_s \quad . \quad (B.35)$$

Eqns B.31 and B.35 can be used to obtain a more compact form of equation B.27

$$i_{ak} = I_{ak} \cos k(\theta - \phi_a + 120) \quad (B.36)$$

where

$$I_{ak} = - \frac{2I_{dc}}{k\pi} \sin k\phi_s \quad (B.37)$$

$$\phi_a = \phi_d = \frac{\Delta\alpha_1 - \Delta\alpha_2}{2} \quad (B.38)$$

B.4 Approximation of equation 3.120

The cosine difference in eqn 3.120 may be simplified as follows:

$$\cos 120 - \cos(120 + \phi_s) = \cos 120(1 - \cos \phi_s) + \sin 120 \sin\phi_s \quad \ldots. \quad (B.39)$$

Equation B.39 has a ϕ_s dependent factor which may be put as :

$$A \sin \phi = 1 - \cos \phi_s \quad (B.40)$$

$$A \cos \phi = \sin \phi_s \quad (B.41)$$

where

$$\phi = \text{TAN}^{-1} \left[\frac{1 - \cos \phi_s}{\sin \phi_s} \right] \quad (B.42)$$

$$A = \sqrt{(1 - \cos \phi_s)^2 + \sin^2 \phi_s} \quad . \quad (B.43)$$

Using the trigonomentric identity

$$1 - \cos X = 2 \sin^2 2X$$

eqns B.42 and B.43 can be simplified to

$$\phi = \text{TAN}^{-1} \left[\frac{2 \sin^2 \left(\frac{\phi_s}{2} \right)}{\sin \phi_s} \right] \quad (B.44)$$

$$A = 2 \sin \frac{\phi_s}{2} \quad . \quad (B.45)$$

For small arcs the sine and the tangent functions can be approximated by their arcs and equations B.44 and B.45 are approximated by :

$$\phi \cong \frac{\phi_s}{2} \tag{B.46}$$

$$A \cong \phi_s \tag{B.47}$$

Replacing eqns B.46 and B.47 in equation B.39 gives

$$\cos 120 - \cos(120 + \phi_s) \cong \phi_s \sin(120 + \frac{\phi_s}{2}) \tag{B.48}$$

APPENDIX C

In this appendix, the FORTRAN and ASSEMBLY programs used to interface the converter busbar with the ICCC-CDC computer system, are listed. The programs are selfexplanatory.

Phase correction due to delay time reading between two any channel of the A/D converter is PHREAD = 0.01872335882439 rd.

```
      PROGRAM ACHARM(INPUT,OUTPUT,TAPE5=INPUT,TAPE6=OUTPUT)
C: FOURIER ANALYSIS OF A.C. & D.C.-SIDE HARMONIC VOLTAGES OF CONVERTER
      DIMENSION Y(1500),CH(32),ANUM(16)
      DIMENSION A0(500),A1(500),A2(500)
      COMPLEX SEQ1,SEQ2,A0,A1,A2
      NPTS=82
      NH=15
      NCHANN=4
      PI=4.*ATAN(1.)
      DIFF=-1.000000000
      DCOFF=204175.0032
      DCVOLT=70.4
      DO100N=1,NH
      A0(N)=CMPLX(0.,0.)
      A1(N)=CMPLX(0.,0.)
      A2(N)=CMPLX(0.,0.)
  100 CONTINUE
      CALL HEXDEC(Y,NPTS,NCHANN)

C     FOURIER ANALYSIS OF PHASES 'A','B' AND 'C'

      SEQ1=CMPLX(1.,0.)
      SEQ2=CMPLX(1.,0.)
      WRITE(6,*)'                PHASE A'
      NB=1
      NE=NPTS
      CALL FOURIER(NB,NE,Y,NPTS,NH,YSCALE,PHREF,DIFF,DCOFF,SEQ1,SEQ2,
     +A0,A1,A2,PI)
      C=COS(2.*PI/3.)
      S=SIN(2.*PI/3.)
      SEQ1=CMPLX(C,S)
      SEQ2=CMPLX(C,-S)
      WRITE(6,*)'                PHASE B'
      NB=NPTS+1
      NE=2*NPTS
      CALL FOURIER(NB,NE,Y,NPTS,NH,YSCALE,PHREF,DIFF,DCOFF,SEQ1,SEQ2,
     +A0,A1,A2,PI)
      WRITE(6,*)'                PHASE C'
      NB=2*NPTS+1
      NE=3*NPTS
      CALL FOURIER(NB,NE,Y,NPTS,NH,YSCALE,PHREF,DIFF,DCOFF,SEQ2,SEQ1,
     +A0,A1,A2,PI)
      WRITE(6,*)'-'
      WRITE(6,*)'                                    SYMMETRICAL  COMPONENTS'
      WRITE(6,*)'-'
      WRITE(6,*)' HARM.         SEQ. POS.                SEQ. NEG.
     +       SEQ. ZERO'
      WRITE(6,*)' ORDER     AMPLITUDE  ANGLE        AMPLITUDE  ANGLE
     +   AMPLITUDE  ANGLE'
      WRITE(6,*)'------+-------------------------------------------------
     +--------------------'

C     DATA FOR THE SYMMETRICAL COMPONENTS ANALYSIS

      DO200N=1,15
      AMOD0=CABS(A0(N))/3.
      AMOD1=CABS(A1(N))/3.
      AMOD2=CABS(A2(N))/3.
      AA0=AIMAG(A0(N))
      AA1=AIMAG(A1(N))
      AA2=AIMAG(A2(N))
      IF(AA0.EQ.0.)GO TO 200
      IF(AA1.EQ.0.)GO TO 200
      IF(AA2.EQ.0.)GO TO 200
      ARG0=ATAN2(AIMAG(A0(N)),REAL(A0(N)))*180./PI
      ARG1=ATAN2(AIMAG(A1(N)),REAL(A1(N)))*180./PI
      ARG2=ATAN2(AIMAG(A2(N)),REAL(A2(N)))*180./PI
      WRITE(6,150)N,AMOD1,ARG1,AMOD2,ARG2,AMOD0,ARG0
  150 FORMAT(1H ,I2,3X,3(F10.4,2X,F10.4,2X))
  200 CONTINUE
      WRITE(6,*)','
      WRITE(6,*)','
      WRITE(6,*)','

C     FOURIER ANALYSIS OF THE DC VOLTAGE

      WRITE(6,*)'    D.C.-SIDE HARMONIC VOLTAGES'
      NB=3*NPTS+1
      NE=4*NPTS
      CALL FOURIER(NB,NE,Y,NPTS,NH,YSCALE,PHREF,DIFF,DCVOLT,SEQ1,SEQ2,
     +A0,A1,A2,PI)
      STOP
      END
```

```
      SUBROUTINE HEXDEC(Y,NPTS,NCHANN)
C     READ AND INTERPRET HEXADECIMAL DATA FROM THE TEXAS 990
      DIMENSION CH(32),ANUM(16),Y(1500)
C     READ HEXADECIMAL DATA
      DATA ANUM/1H0,1H1,1H2,1H3,1H4,1H5,1H6,1H7,1H8,1H9,
     +          1HA,1HB,1HC,1HD,1HE,1HF/
      JJ=1
      LINES=1+NCHANN*NPTS/8
      DO500K=1,LINES
      READ(5,10) CH
   10 FORMAT(5X,4(4A1,2X),4(2X,4A1))
      DO400N=1,8
      VAL=0.
      NE=4*N
      NS=NE-3
      DO30J=NS,NE
      DO 2 I=1,16
      IF (CH(J).EQ.ANUM(I)) GOTO 3
    2 CONTINUE
C     TRANSFORM HEXADECIMAL INTO DECIMAL VALUES
    3 VAL=VAL*16+I-1
   30 CONTINUE
      Y(JJ)=VAL
C     WRITE(6,*)VAL
      JJ=JJ+1
  400 CONTINUE
  500 CONTINUE
      RETURN
      END
/
```

```
      SUBROUTINE FOURIER(NB,NE,Y,NPTS,NH,YSCALE,PHREF,DIFF,DCOFF,SEQ1,
     +SEQ2,A0,A1,A2,PI)
      DIMENSION A0(500),A1(500),A2(500)
      DIMENSION Y(1500),A(500),B(500)
      COMPLEX AA,A0,A1,A2,SEQ1,SEQ2
      TETA=0.
      A0=0.
      DO10N=1,NH
      A(N)=0.
   10 B(N)=0.
      PHREAD=1.872335882439E-2
      PIX2=PI*2.
      DELTA=PIX2/NPTS
      DO30I=NB,NE
      TETA=TETA+DELTA
      A0=A0+Y(I)
      DO20N=1,NH
      A(N)=A(N)+Y(I)*COS(N*TETA)
   20 B(N)=B(N)+Y(I)*SIN(N*TETA)
   30 CONTINUE
      WRITE(6,40)
   40 FORMAT(1H ,//,9X,'FOURIER COMPONENTS',//,7X,'AMPLITUDE',7X,
     +'PHASE',//)
      IF(NE.NE.NPTS)GO TO 80
      YSCALE=(PI*100.)/(SQRT(A(1)*A(1)+B(1)*B(1))*DELTA)
      PHREF=ATAN2(A(1),B(1))
      GO TO 81
   80 IF(NE.NE.4*NPTS)GO TO 81
      A0=A0*DELTA/PIX2
      YSCALE=DCOFF/A0
      A0=A0*YSCALE
      GO TO 82
   81 A0=((A0-DCOFF)*DELTA*YSCALE)/(PIX2)
   82 DIFF=DIFF+1.000000000
      DO60N=1,NH
      AN=A(N)
      A(N)=SQRT(A(N)*A(N)+B(N)*B(N))*DELTA/PI
      IF(A(N).LT.1.E-6)GO TO 60
      B(N)=ATAN2(AN,B(N))-N*(PHREF+DIFF*PHREAD)
      A(N)=A(N)*YSCALE
  110 IF(B(N).GE.0.)GO TO 100
      B(N)=B(N)+PIX2
      GO TO 110
  100 IF(B(N).LE.PIX2)GO TO 90
      B(N)=B(N)-PIX2
      GO TO 100
   90 BN=B(N)*180./PI
      WRITE(6,50)N,A(N),BN
   50 FORMAT(1H ,I3,2X,F10.4,4X,F10.2)
      IF(NE.EQ.4*NPTS)GO TO 60
      AREAL=A(N)*COS(B(N))
      AIMGN=A(N)*SIN(B(N))
      AA=CMPLX(AREAL,AIMGN)
      A0(N)=A0(N)+AA
      A1(N)=A1(N)+SEQ1*AA
      A2(N)=A2(N)+SEQ2*AA
   60 CONTINUE
      WRITE(6,70)A0
   70 FORMAT(1H ,//,3X,'DC COMPONENT = ',F9.4,////)
      RETURN
      END
/
```

ASSEMBLY PROGRAM TO INTERFACE CDC TO TEXAS

```
F404 02E0  LWPI >4D0
F402 04D0
F406 1002  JMP >40C          starting
F408 0420  BLWP a>E000       procedure
F40A E000
F40C 04C4  CLR R4
F40E C804  MOV R4,a>AFF4
F410 AFF4
F412 C804  MOV R4,a>AFF8
F414 AFF8
F416 0720  SETO a>AFFA
F418 AFFA                     read R5
F41A 0560  INV a >AFFC
F41C AFFC
F41E 11FD  JLT >41A
F420 C160  MOV a>AFFA,R5
F422 AFFE
F424 0285  CI R5,>7B0        compare with
F426 07B0                   average  value
F428 1301  JEQ >42C
F42A 10F1  JMP >40E
F42C C804  MOV R4,a>AFF4
F42E AFF4
F430 C804  MOV R4,a>AFF8      read R5
F432 AFF8
F434 0720  SETO a>AFFA
F436 AFFA
F438 0560  INV a>AFFC
F43A AFFC
F43C 11FD  JLT >438
F43E C160  MOV a>AFFE,R5
F440 AFFE
F442 0285  CI R5,>7B0
F444 07B0
F446 1501  JGT >44A
F448 10F1  JMP >42C
F44A 02E0  LWPI >4D0
F44C 04D0
F44E 1002  JMP >454
F450 0420  BLWPI a>E000
F452 E000
F454 0201  LI R1,>1
F456 0001
F458 0202  LI R2,>2
F45A 0002                        A/D
F45C F203  LI R3,>3     (channels 0,1,2 & 3)
F45E 0003
F460 0204  LI R4,>0
F462 0000
F464 0205  LI R5,>500
```

(PTO)

(Continued)

```
F466 0500
F468 0206  LI,R6,>5A2
F46A 05A2                    first addresses
F46C 0207  LI,R7,>644       of phases a,b & c
F46E 0644                   and of DC-voltage
F470 0208  LI R8,>6E6
F472 06E6
F474 C804  MOV R4,a>AFF4       set up A/D
F476 AFF4
F478 C804  MOV R4,a>AFF8     select channel 0
F47A AFF8
F47C 0720  SETO a>AFFA       trigger channel 0
F47E AFFA                      (start conv.)
F480 0560  INV a>AFFC          check if conv.
F482 AFFC                        is ready
F484 11FD  JLT >480
F486 CD60  MOV a>AFFE,*R5+       read  and
F488 AFFE                      increment  R5
F48A C801  MOV R1,a>AFF8
F48C AFF8
F48E 0720  SETO a>AFFA
F490 AFFA                    idem channel  1
F492 0560  INV a>AFFC
F494 AFFC
F496 11FD  JLT >492
F498 CDA0  MOV a>AFFE,*R6+
F49A AFFE
F49C C802  MOV R2,a>AFF8
F49E AFF8
F4A0 0720  SETO a>AFFA
F4A2 AFFA                    idem channel  1
F4A4 0560  INV a>AFFC
F4A6 AFFC
F4A8 11FD  JLT >4A4
F4AA CDE0  MOV a>AFFE,*R7+
F4AC AFFE
F4AE C803  MOV R3,a>AFF8
F4B0 AFF8
F4B2 0720  SETO a>AFFA
F4B4 AFFA                    idem channel  1
F4B6 0560  INV a>AFFC
F4B8 AFFC
F4BA 11FD  JLT >4B6
F4BC CE20  MOV a>AFFE,*R8+
F4BE AFFE
F4C0 0288  CI R8,>788        last address ?
F4C2 0790
F4C4 11D9  JLT >478
F4C6 0460  B a>450           link back
F4C8 0450                    to monitor
```